

STUDIES TOWARDS THE SYNTHESIS OF BIELSCHOWSKYSIN AND TOTAL
SYNTHESIS OF DAROBACTIN A

BY

MARKO NESIC

DISSERTATION

Submitted in partial fulfillment of the requirements
for the degree of Doctor of Philosophy in Chemistry
in the Graduate College of the
University of Illinois Urbana-Champaign, 2023

Urbana, Illinois

Doctoral Committee:

Associate Professor David Sarlah, Chair
Professor Scott E. Denmark
Professor Scott K. Silverman
Professor Douglas A. Mitchell

ABSTRACT

The isolation of evermore complex natural products has been continuously inspiring chemists to achieve total syntheses of such targets, while pushing the frontiers of the field of organic synthesis. The intellectual challenges encountered in these endeavors have tested the limits of our current knowledge and resulted in development of novel methodologies, thereby providing significant advancements in the field. Moreover, total synthesis of natural products that have promising bioactivity has had great merit in identifying novel pharmacophores and leads, thereby directly impacting the field of medicinal chemistry.

The first chapter of the dissertation describes our approach towards the total synthesis of beilschowskysin, a marine furanocembranoid diterpenoid with impressive antimalarial and cytotoxic activity. The daunting structure of this natural product has posed a great challenge for the synthetic community, making it one of the most intractable natural products ever discovered. While most of the past approaches towards this molecule relied on a [2+2] cycloaddition to form the strained core, our study was based on a different paradigm, accessing this unprecedented molecular framework via a Norrish-Yang photocyclization. Herein, we describe our successful synthesis of the macrocyclic precursor for the aforementioned photocyclization and further investigation of this key step.

The second chapter will focus on our total synthesis of darobactin A, a bismacrocyclic heptapeptide, that was recently isolated from a bacterial symbiont of entomopathogenic nematodes. This natural product has shown remarkable antibacterial activity, selectively targeting gram-negative pathogens via a novel mechanism of action. We have developed a concise and convergent synthesis of this antibiotic, via sequential halogen-selective Larock indole syntheses.

ACKNOWLEDGMENTS

I would like to thank:

-My advisor, Prof. David Sarlah, firstly for giving me the incredible opportunity to work in his lab over a summer as a visiting undergraduate student, then for accepting me as a graduate student in his group, and lastly for providing me with great support, encouragement, motivation and guidance throughout the entirety of my PhD;

-My committee members: Profs. Scott Denmark, Scott Silverman and Douglas Mitchell for giving me valuable feedback and setting high expectations, in doing so motivating me to always give my best;

-Senior students: Alex Shved, Yaroslav Boyko, Christopher Huck, Lucas Hernandez and Chad Ungarean who have helped me tremendously during my undergraduate visit and early years of graduate studies and have transferred their experience by either teaching me new lab skills or having insightful discussions with me;

-My coworkers: David Ryffel, Jonathan Maturano, Maegen Kincaon, Yianni Lysandrou, Siqu Dong, Pavle Kravljanac, Justin Ngai, Yushang Zhou and our collaborators from Merck for their tremendous work on our projects;

-My parents, for their love and support.

Dedicated to Natasa and Goran

TABLE OF CONTENTS

CHAPTER 1: STUDIES TOWARDS THE SYNTHESIS OF BIELSCHOWSKYSIN	1
1.1 Introduction.....	1
1.2 Previous synthetic studies	4
1.3 Retrosynthetic analysis	7
1.4 Synthetic studies	9
1.5 Conclusion	21
1.6 Experimental section.....	23
1.7 References.....	48
1.8 Acknowledgements and contributions	51
CHAPTER 2: TOTAL SYNTHESIS OF DAROBACTIN A	52
2.1 Introduction.....	52
2.2 Previous total syntheses of RiPPs.....	56
2.3 Initial retrosynthetic analysis	62
2.4 Synthetic studies	64
2.5 Revised retrosynthetic analysis.....	82
2.6 Forward synthesis	83
2.7 Conclusion	102
2.8 Experimental section.....	103
2.9 References.....	149
2.10 Acknowledgements and contributions	155

CHAPTER 1: STUDIES TOWARDS THE SYNTHESIS OF BIELSCHOWSKYSIN*

1.1 Introduction

For many years, marine organisms have been gifting chemists with a plethora of natural products with intricate structures and interesting bioactivities.¹ Molecules with novel skeletal frameworks are being continuously isolated from these organisms, providing synthetic chemists with new challenges for testing their skills and gauging the boundaries of what is currently achievable by known organic manipulations. Moreover, some of these natural products inspired the development of novel therapeutic treatments for a variety of conditions.²

Furanocembranoids (**1.1**) represent a diverse family of marine diterpenoids, most of which can be defined by having a furan ring and a butenolide embedded within a 14-membered macrocycle (Figure 1.1a).³⁻⁵ These molecules are produced in nature either by gorgonian corals which inhabit the northwestern Atlantic Ocean and the Caribbean Sea, or by soft corals which are indigenous to the Indo-Pacific reefs. The first furanocembranoid to be characterized was pukalide (**1.2**) in 1975 (Figure 1.1a).⁶ Since then, more than a hundred of natural products in this family

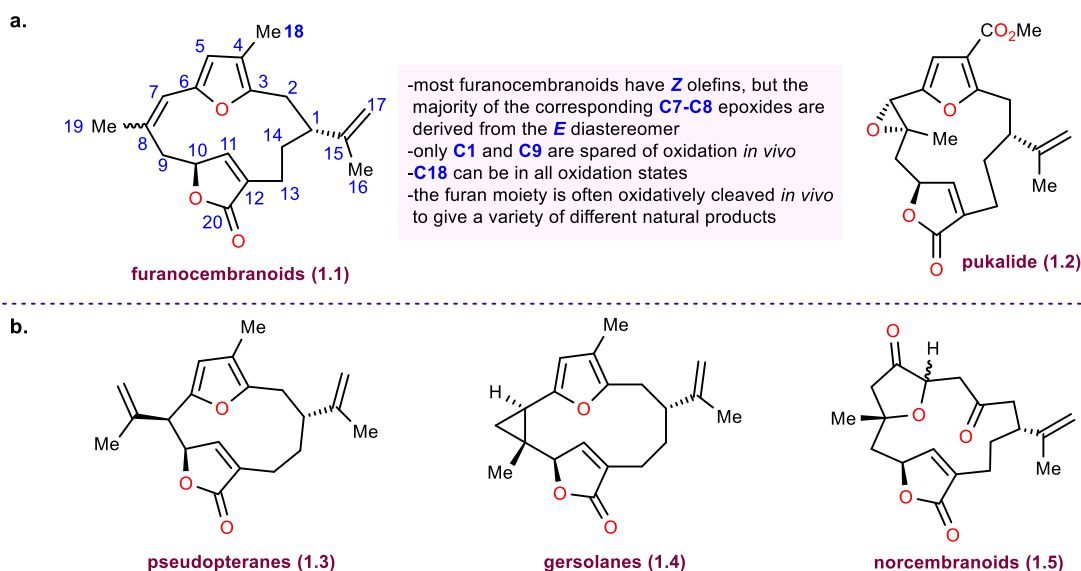


Figure 1.1: a. The generic structure of furanocembranoids with their numbering system (left), common structural features (middle) and the structure of pukalide (right); b. Generic structures of pseudopteranes, gersolanes and norcembranoids.

*Portions of the herein described work have been previously published: Nestic, M.; Kincanon, M. M.; Ryffel, D. B.; Sarlah, D. *Tetrahedron* **2020**, 76, 131318–131321.

have been isolated with varying degrees of structural complexity and diverse bioactivities. A vast number of these natural products had structures that varied considerably from the parent furanocembranoid skeleton. These molecules were categorized into new classes of furanocembranoid-derived diterpenoids, namely pseudopteranes (**1.3**), gersolanes (**1.4**) and the norcembranoids (**1.5**) which lack the C18 atom (Figure 1.1b).^{3,4} Amongst them, the “polycyclic furanobutenolide-derived” furanocembranoids (Figure 1.2a) and norcembranoids (Figure 1.2b) are the structurally most complex members.⁷ These natural products are derived from oxidative transformations of the furan and subsequent transannular interactions of the resulting highly unstable intermediates with the butenolide to afford these polycyclic motifs.⁵ Due to their structural complexity, many research groups have shown interest in synthesizing these compounds and in turn, have invested considerable efforts. However, most of these efforts proved futile, showcasing what a gargantuan challenge these molecules present to the synthetic community.⁷ Only in recent years, several members of this subcategory have succumbed to total synthesis. Three polycyclic furanobutenolide-derived cembranoids have been synthesized so far (Figure 1.2a). Intricarene (**1.9**) was synthesized first, independently by the Trauner (2006 and 2014)^{8,9} and

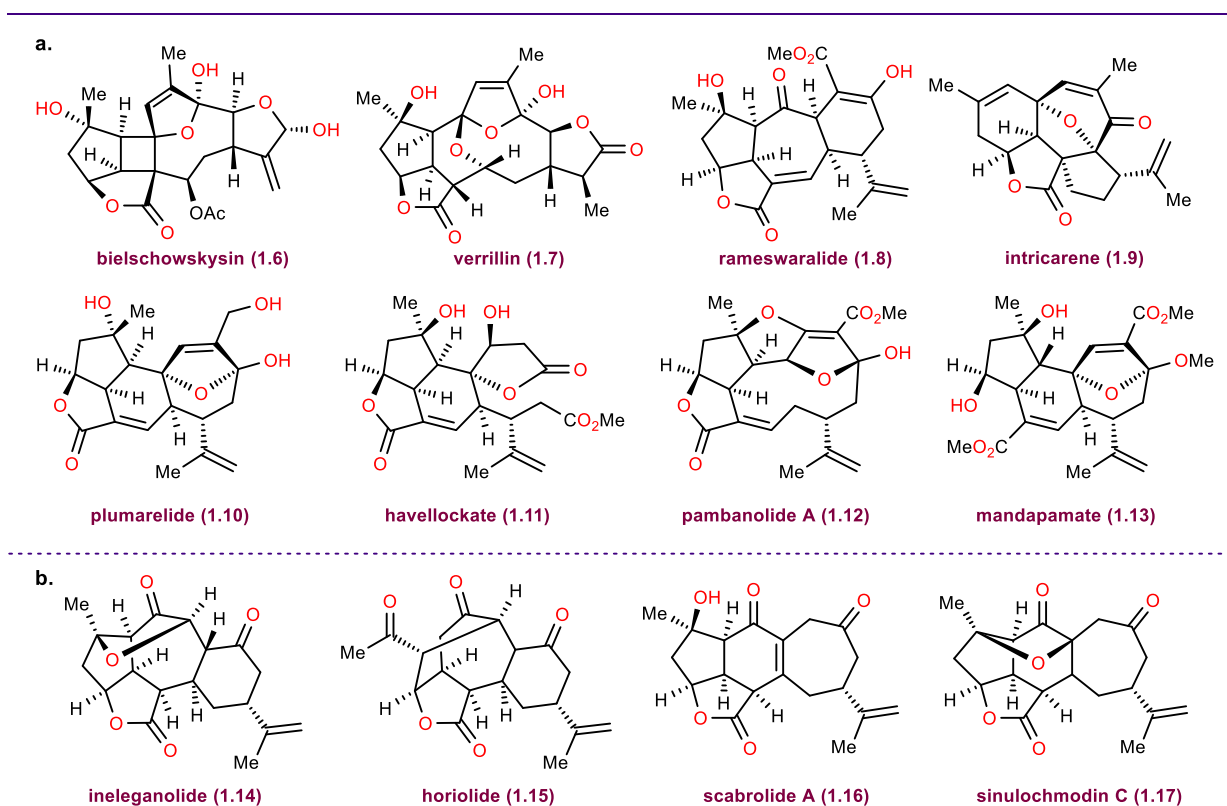
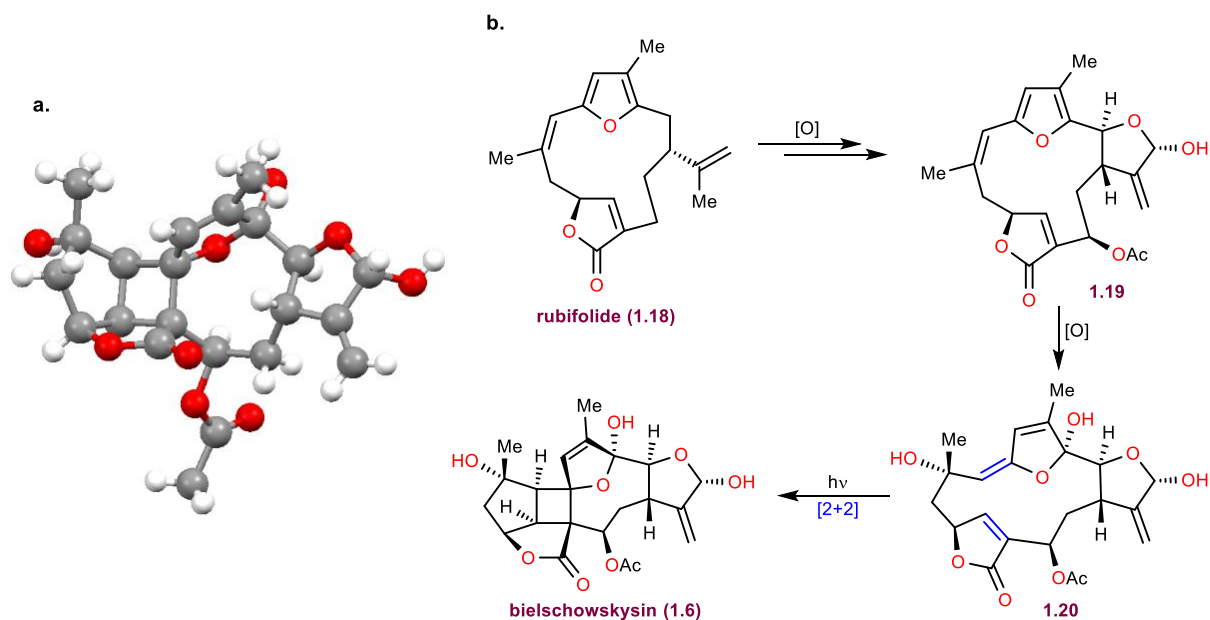


Figure 1.2: a. Representative examples of polycyclic furanobutenolide-derived cembranoids; b. Representative examples of polycyclic furanobutenolide-derived norcembranoids

Pattenden (2006)^{10,11} labs. Rameswaralide (**1.8**) succumbed to synthesis in 2022 by Romo's group¹² while the total synthesis of havellockate (**1.11**) was completed by the Stoltz lab in the same year.¹³ Regarding polycyclic furanobutenolide-derived norcembranoids, the first major breakthrough occurred in 2011 with Pattenden's semi-synthesis of ineleganolide (**1.14**).¹⁴ A decade later, this natural product and sinulochmodin C (**1.17**) were made *de novo* by the Wood lab in 2022,¹⁵ while scabrolide A (**1.16**) was synthesized by both the Stoltz (2020)¹⁶ and the Furstner (2022) group.¹⁷

The furanocembranoid that has attracted our interest was bielschowskysin (**1.6**, Figure 1.2a), which is regarded as the flagship member of the family. This molecule was isolated in 2004 from the gorgonian coral *Pseudopterogorgia kallos* that is native to the Southwestern Caribbean Sea.¹⁸ Bielschowskysin has a highly intricate structure: an extremely strained ring system with an unprecedented [5.4.9]-ring architecture and a hexasubstituted cyclobutane with two quaternary stereocenters (Scheme 1.1a). In addition to that, this natural product has impressive bioactivity, as well. It is cytotoxic against the EKVX nonsmall cell lung cancer ($GI_{50} < 0.01 \mu\text{M}$) and CAKI renal cancer ($GI_{50} = 0.51 \mu\text{M}$), but also exhibits antiplasmodial activity against *Plasmodium falciparum* ($IC_{50} = 10 \mu\text{g/mL}$). The absolute configuration of bielschowskysin has yet to be determined. All of the aforementioned properties combined, make this natural product a highly desirable target for a total synthesis campaign.



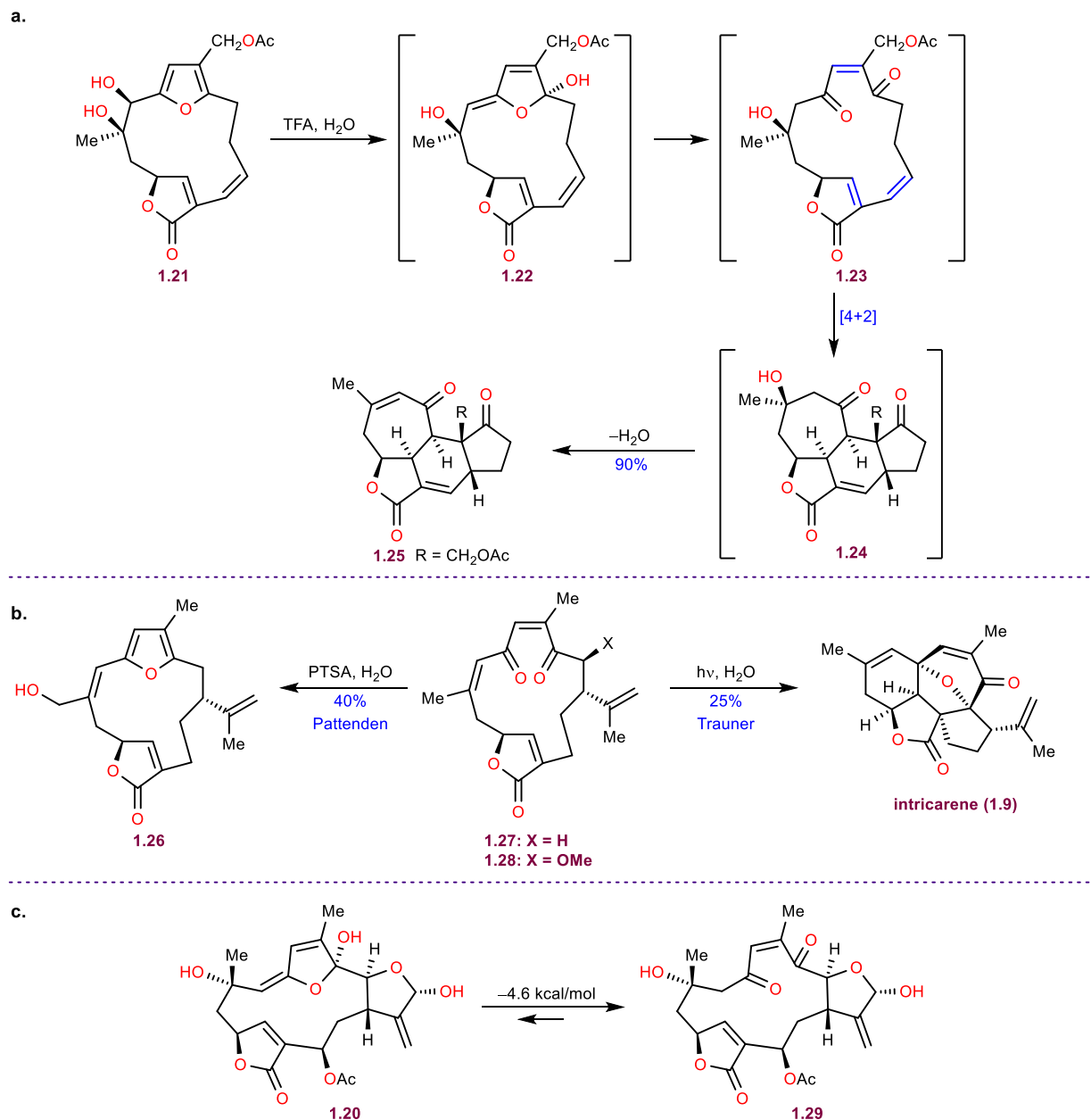
Scheme 1.1: a. X-Ray structure of bielschowskysin; b. Proposed biosynthetic pathway from rubifolide

It is believed that bielschowskysin is biosynthetically derived from rubifolide (**1.18**, Scheme 1.1b). Oxidation at various positions leads to macrocycle **1.19**. Further oxidation of the furan results in the formation of the enol hemiacetal intermediate **1.20**, which is suited to undergo a transannular [2+2] cycloaddition, resulting in the formation of the natural product.^{4,5}

1.2 Previous synthetic studies

Bielschowskysin (**1.6**) is regarded as one of the most intractable natural products ever discovered. A testimony to this is that more than 20 synthetic studies by numerous research groups have been published in the past, with no completed total synthesis to date.¹⁹⁻⁴⁰ Most of the synthetic studies have focused on the biomimetic synthesis of the cyclobutane core via a photochemical [2+2] cycloaddition.

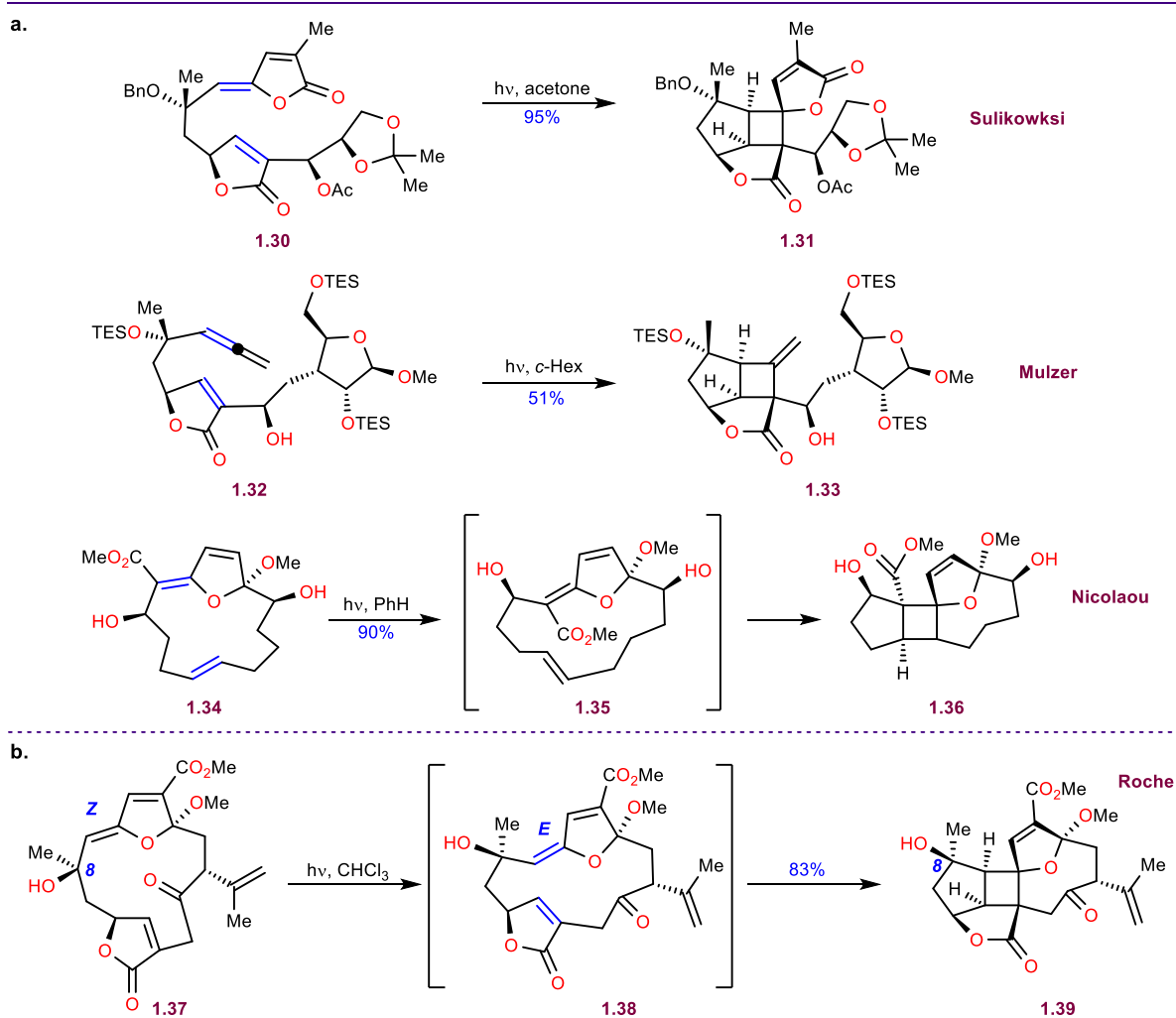
To test the biosynthetic hypothesis, the enol hemiacetal **1.20** had to be synthesized. Initial studies by Pattenden have revealed that this key intermediate is highly unstable (Scheme 1.2a).⁴¹ The study was performed on a model system **1.21** that upon exposure to acid, rapidly tautomerized to the ring-opened enedione tautomer **1.23**, likely through the intermediacy of the transient enol hemiacetal **1.22**. The enedione rapidly engaged in a transannular Diels-Alder reaction providing the tetracyclic product **1.25**. The elusive enol hemiacetal **1.22** couldn't be detected in the reaction mixture. In another study, Pattenden has shown that treatment of enedione **1.27** with PTSA leads to restoration of the furan ring, providing **1.26** (Scheme 1.2b).⁴² Realizing that the key enol hemiacetal intermediate **1.20** is not a stable compound, Trauner envisioned that irradiating an aqueous solution of enedione **1.28** would result in excitation of the fleeting enol hemiacetal tautomer which is expected to be in equilibrium with their substrate, resulting in a [2+2] cycloaddition thereby shifting the equilibrium towards the enol hemiacetal and providing the core structure of bielschowskysin. However, this wasn't the case, as enedione **1.28** got excited instead due to the existence of a strong chromophore. Fortunately, the excited state of this enedione engaged in a productive pathway, resulting in the formation of another furanocembranoid natural product – intricarene (**1.9**), hence establishing the biosynthesis of this molecule (Scheme 1.2b).⁹ Moreover, Paton has utilized DFT calculations to confirm that the ring-opened enedione intermediate **1.29** is thermodynamically more stable than the cyclic enol hemiacetal **1.20** by 4.6 kcal/mol (Scheme 1.2c).³⁸ This unfavorable equilibrium has deterred further attempts at the synthesis of the elusive enol hemiacetal **1.20**.



Scheme 1.2: a. Pattenden's trapping of the enedione tautomer; b. Pattenden's and Trauner's studies of the enedione; c. Paton's DFT calculations showcasing the instability of the enol hemiacetal

Accordingly, focus has shifted to the exploration of [2+2] photocycloadditions on stable intermediates that can be isolated, characterized and successfully engaged in this transformation, Resulting in the formation of various cyclobutane-containing advanced intermediates (Scheme 1.3a). In 2013, the Sulikowski lab has reported the preparation of intermediate **1.30** which efficiently participated in an intramolecular [2+2] cycloaddition providing advanced intermediate **1.31** in quantitative yield.²⁰ However, this intermediate couldn't be further elaborated into the macrocycle-embedded skeleton of bielschowskyisin. In the same year, the Mulzer group has

reported an analogous intramolecular [2+2] cycloaddition, this time engaging an allene **1.32** in the transformation.²⁷ Even though the strained western tricyclic fragment **1.33** was made, Mulzer had encountered the same challenge as Sulikowski, being unable to form the strained macrocycle. The first successful synthesis of the unique [5.4.9] ring architecture was performed by the Nicolaou lab.³¹ Their success was based on forming the macrocycle **1.34** first, and then performing the [2+2] cycloaddition in a transannular manner (**1.34**→**1.36**). Another key feature of their system is the presence of the methyl ester group on the dienol acetal, which makes this functionality a good chromophore. Upon excitation of **1.34**, the dienol acetal underwent double bond isomerization affording **1.35** before participating in the cycloaddition. Nevertheless, the final product **1.36** was a model system that lacked a number of functionality that is otherwise present in the natural product, and hence couldn't be elaborated into the target molecule. This study has inspired Roche's

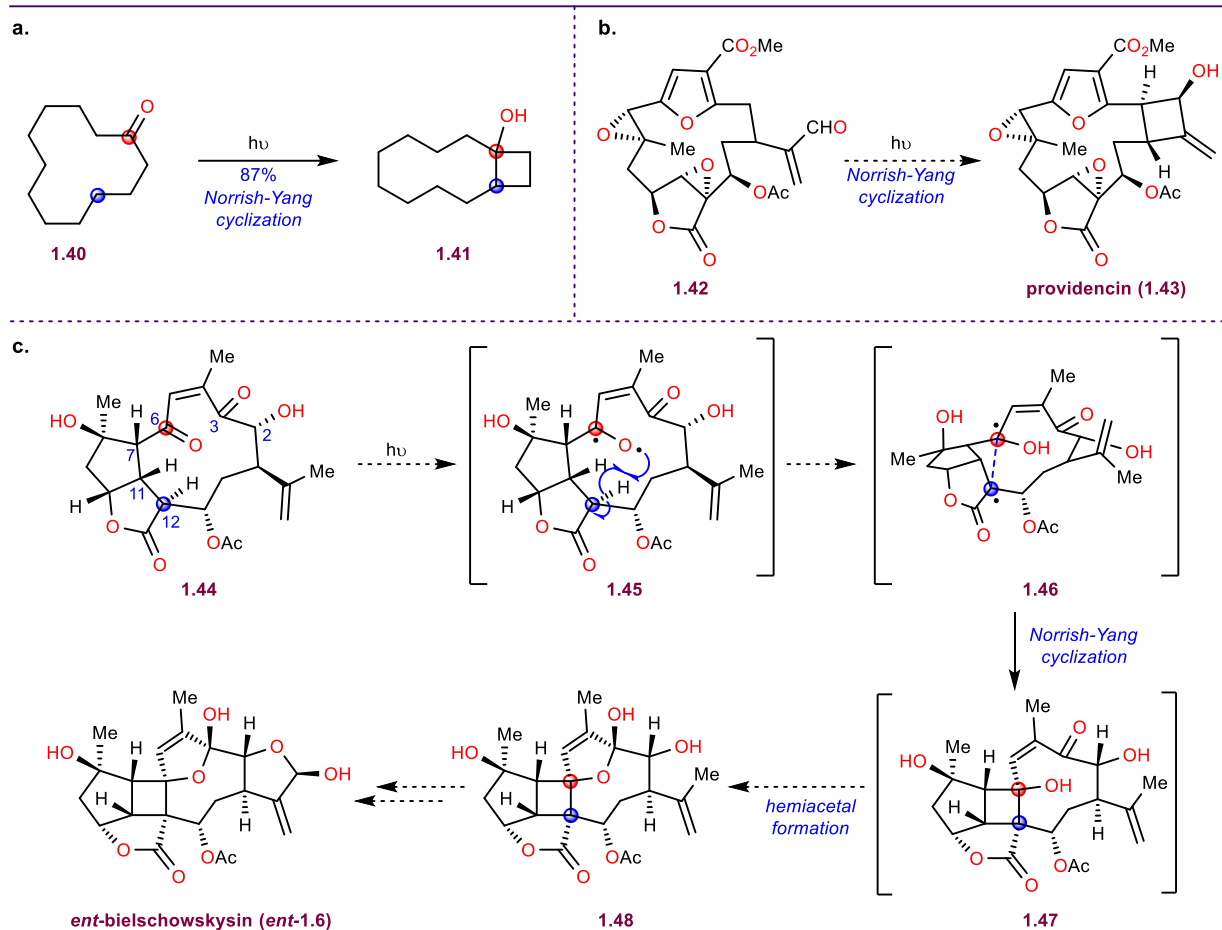


Scheme 1.3: a. Successful [2+2] photocycloadditions; b. Roche's study is the most significant advancement

semi-synthetic approach reported in 2018, which represents the most significant breakthrough towards the synthesis of bielschowskysin (Scheme 1.3b).³⁹ His group was able to form the enol acetal intermediate **1.37** in a kinetic dearomatization process, in contrast to the previously attempted thermodynamic dearomatization approach that were described in Scheme 1.2. This approach worked only if the starting furan contains an electron-withdrawing substituent ($-\text{CO}_2\text{Me}$). Besides stabilizing the enol acetal, another important role of the ester group is to facilitate photochemical isomerization of the starting (*Z*)-enol acetal **1.37** to the reactive (*E*)-diastereomer **1.38** by extending the conjugation of the π -system in a similar manner as previously reported by the Nicolaou lab. Concomitantly, the highly strained core of bielschowskysin **1.39** was formed with great efficiency, in 83% yield (Scheme 1.3b). Besides having the challenge of selective reduction of the methyl ester group at a late stage, the stereochemistry at C8 in the starting material **1.37** was incorrect. At the onset of our study, the desired diastereomer has still eluded synthesis.

1.3 Retrosynthetic analysis

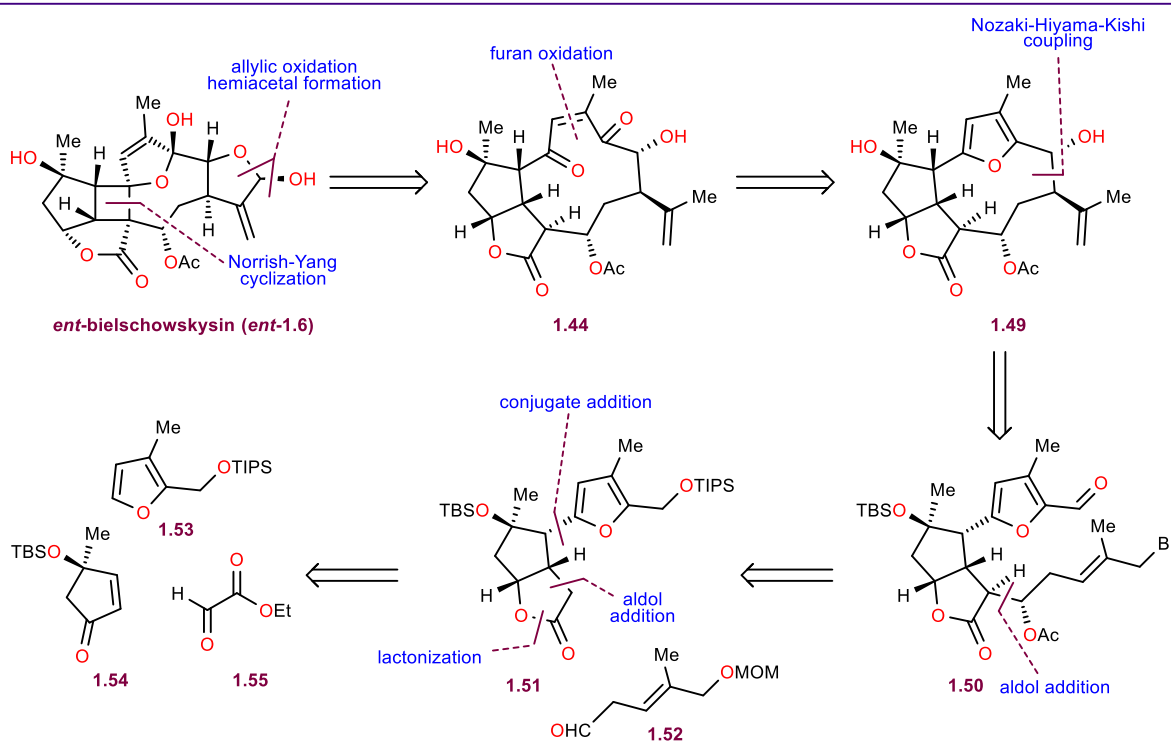
While the [2+2] cyclization strategy seems appealing, aforementioned attempts were met with significant challenges, as exemplified in Schemes 1.2 and 1.3. Therefore, we decided to pursue a completely different mechanistic paradigm for the construction of the cyclobutane core. Knowing from previous studies that oxidative dearomatization of electron-rich furans leads to enedione intermediates³⁸⁻⁴² instead of the desired enol hemiacetal, and taking inspiration from Trauner's synthesis of intricarene (Scheme 1.2b)⁹, we decided to employ a transannular Norrish-Yang photocyclization on the enedione as the key step for our synthesis of the strained cyclobutane core of the natural product.⁴³ An important precedent corroborating our proposal was reported by Wynberg in 1975 where irradiation of macrocyclic ketone **1.40** led to the formation of cyclobutanol **1.41** in excellent yield (Scheme 1.4a).⁴⁴ We were also encouraged by the proposed biosynthesis of providencin **1.43** where a Norrish-Yang photocyclization provides the cyclobutanol present in this natural product (**1.42**→**1.43**, Scheme 1.4b).⁴⁵ With this in mind, we envisioned the mechanistic paradigm presented in Scheme 1.4c (note that our study was based on the synthesis of *ent*-bielschowskysin *ent*-**1.6**). Irradiation of macrocyclic enedione **1.44** would lead to the excited state that can be represented by the reactive ketyl radical **1.45**. The oxygen atom at C6 should have a favorable orientation for a 1,5-hydrogen atom abstraction at C12 producing



Scheme 1.4: **a.** Precedence for transannular Norrish-Yang cyclization; **b.** Proposed biosynthesis of providencin; **c.** Our hypothesis biradical **1.46**. This highly reactive species is then posed to undergo a radical recombination step, providing the cyclobutane ring in **1.47**. This marks the conclusion of the Norrish-Yang cyclization cascade. Subsequently, attack of the hydroxyl group of the obtained cyclobutanol **1.47** onto the carbonyl group at C3 of the enone would provide hemiacetal **1.48**, which contains the complete carbon skeleton of bielschowskysin (*ent-1.6*). The proper orientation of the oxygen atom at C6 is provided by the presence of the C7-C11 bond as well as the stereochemistry at C7, C11 and C12 and should facilitate the hydrogen abstraction step. Intermediate **1.48** could then be elaborated into *ent*-bielschowskysin (*ent-1.6*) in a couple of steps.

Our retrosynthetic analysis, which is based on the previously described mechanistic paradigm, is depicted in Scheme 1.5. Firstly, *ent*-bielschowskysin (*ent-1.6*) could be traced back to enedione **1.44** via the aforementioned Norrish-Yang photocyclization and disconnection of the eastern hemiacetal via allylic oxidation/hemiacetal formation. Our plan was to obtain the enedione functionality in **1.44** through oxidative dearomatization of macrocyclic furan **1.49**. Furthermore,

this macrocycle could be disconnected through a Nozaki-Hiyama-Kishi coupling (**1.49**→**1.50**), which has proven to be a reliable method for the formation of macrocyclic furanocembranoids and is expected to provide us the desired *anti* stereochemistry, as established in previous literature reports.⁴⁶⁻⁴⁸ The revealed open-form precursor **1.50** could be assembled by employing an aldol addition between lactone **1.51** and the unstable β,γ -unsaturated aldehyde **1.52**. The challenge in synthesizing lactone **1.51** is that it possesses a furan substituent on the more sterically congested concave face of the bicyclic system. Notwithstanding, we envisioned that we can quickly access it from simple building blocks: TIPS-protected furan **1.53** and the highly versatile TBS-protected enone **1.54** via transition metal mediated conjugate addition, followed by enolate trapping with ethyl glyoxylate (**1.55**). As this one pot-three component transformation is expected to provide the incorrect stereochemistry at the α carbon atom of the enone, subsequent correction of the stereochemistry will be necessary.

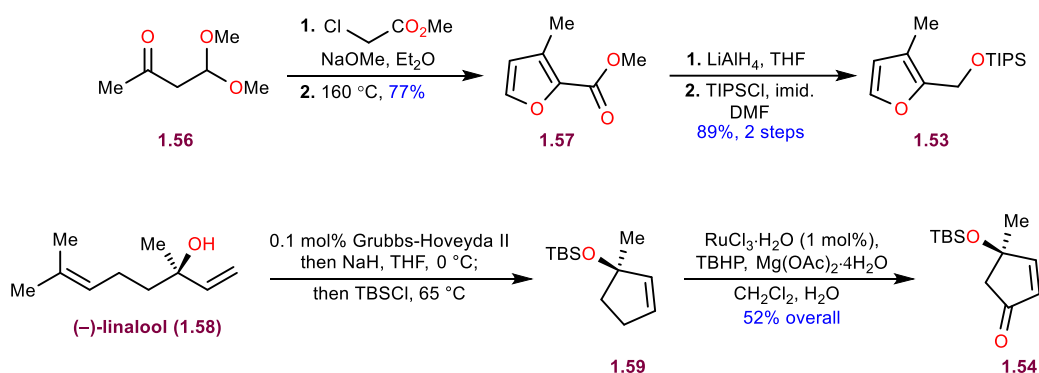


Scheme 1.5: Retrosynthetic analysis of *ent*-bielshowskysin

1.4 Synthetic studies

We commenced our synthetic campaign with the synthesis of building blocks **1.53** and **1.54** (Scheme 1.6). The synthesis of furan **1.53** starts with a known procedure: Darzens reaction of

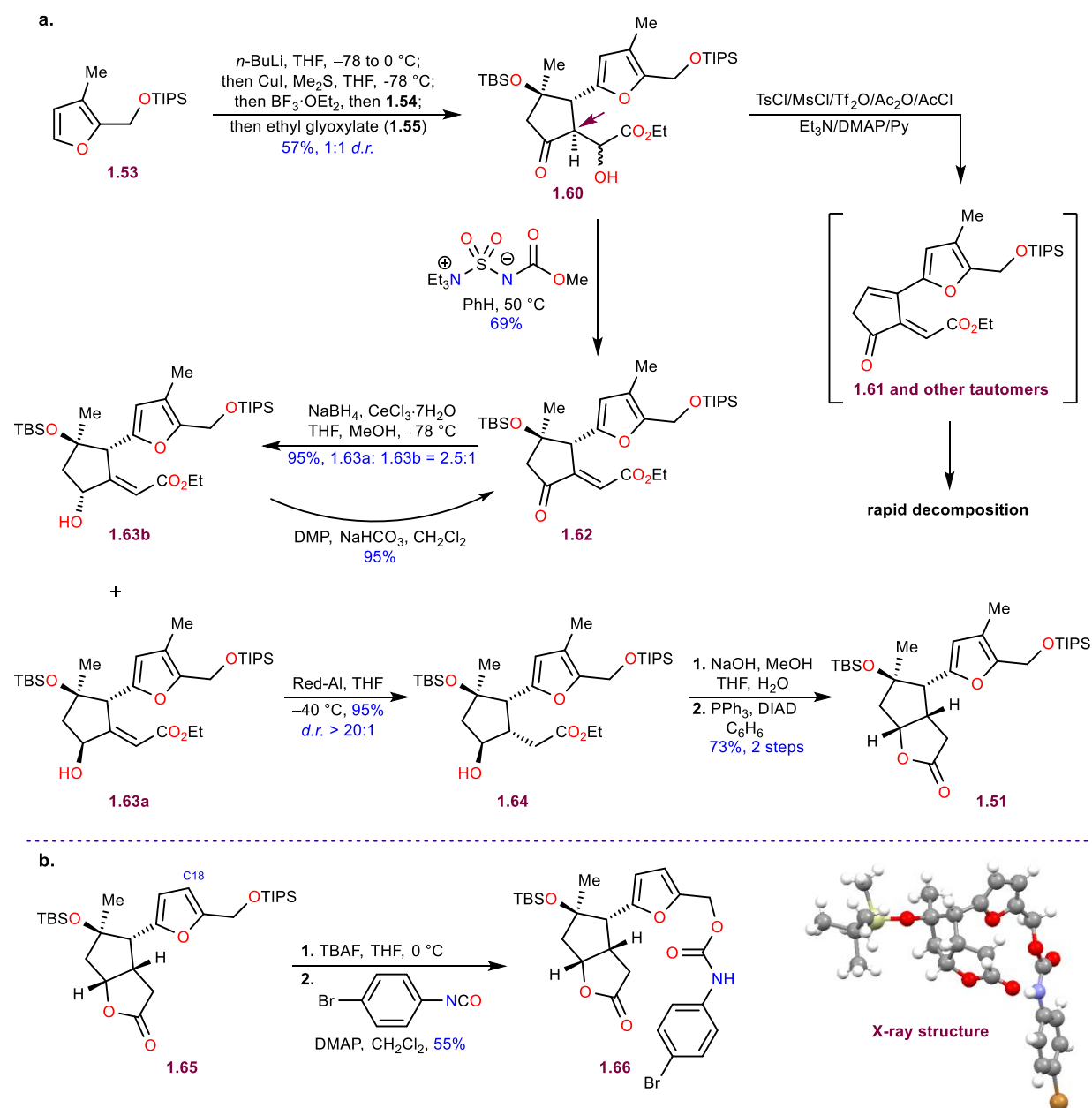
methylchloroacetate and ketone **1.56** which furnished the epoxide-acetal that was rearranged to furan **1.57** upon heating at 160 °C.⁴⁹ Subsequent reduction of the methyl ester with LAH afforded the corresponding alcohol that upon protection with TIPSCl resulted in the formation furan **1.53** on multidecagram scale.⁵⁰ Enone **1.54** was synthesized according to Maimone's protocol.⁵¹ (-)-Linalool (**1.58**) was subjected to a Grubbs metathesis reaction and the tertiary alcohol was protected with a TBS group affording **1.59**. Finally, allylic oxidation of cyclopentene **1.59** catalyzed by RuCl₃ in the presence of superstoichiometric quantities of oxidant TBHP, produced enone **1.54** on multigram scale.



Scheme 1.6: Syntheses of the starting building blocks

With the requisite building blocks at hand, the stage was set for their unification. After extensive experimentation, the optimal conditions for the three component conjugate addition/enolate trapping have been found (Scheme 1.7a). Furan **1.53** was α -lithiated with *n*-BuLi and the obtained furyllithium species was converted to the corresponding organocuprate with CuI. The organocuprate was furthermore reacted with enone **1.54** in the presence of BF₃•OEt₂. The enolate obtained by this conjugate addition was trapped with the highly unstable ethyl glyoxylate (**1.55**), to give product **1.60** in 57% yield, as a mixture of diastereomers (*d.r.* = 1:1 at the α -carbon of the ethyl ester). Other copper salts and organometallic species gave inferior yields, while in the absence of BF₃•OEt₂, the reaction wouldn't proceed at all.⁵² Notably, if the furan is protected with a TBS group instead of TIPS, the yield of the conjugate addition is significantly lower (ca 20%), likely due to removal of the TBS group with BF₃•OEt₂ and subsequent decomposition of the revealed furfuryl alcohol. Ethyl glyoxylate (**1.55**) is highly unstable and rapidly converts to hydrates and oligomers which are detrimental for the reaction, hence it had to be distilled over P₂O₅ and used immediately. The addition of glyoxylate occurred *anti* to the furan, as expected, providing us with the undesired diastereomer at the α -stereocenter of the ketone. At this point we

had to correct the stereochemistry at the α -carbon of the ketone, while also figuring out a way to deal with the diastereomeric mixture at the α -carbon of the ethyl ester. To obviate both of these challenges, we decided to eliminate the alcohol functionality. Dehydration of the obtained aldol diastereomeric mixture **1.60** wasn't as straightforward as we initially expected it to be. Upon conversion of the alcohol to a good leaving group (e.g. acetate or tosylate) in the presence of a mild organic base, very low and variable yields of the desired elimination product **1.62** were obtained. A significant amount of an unstable side product was forming. After a column on neutral

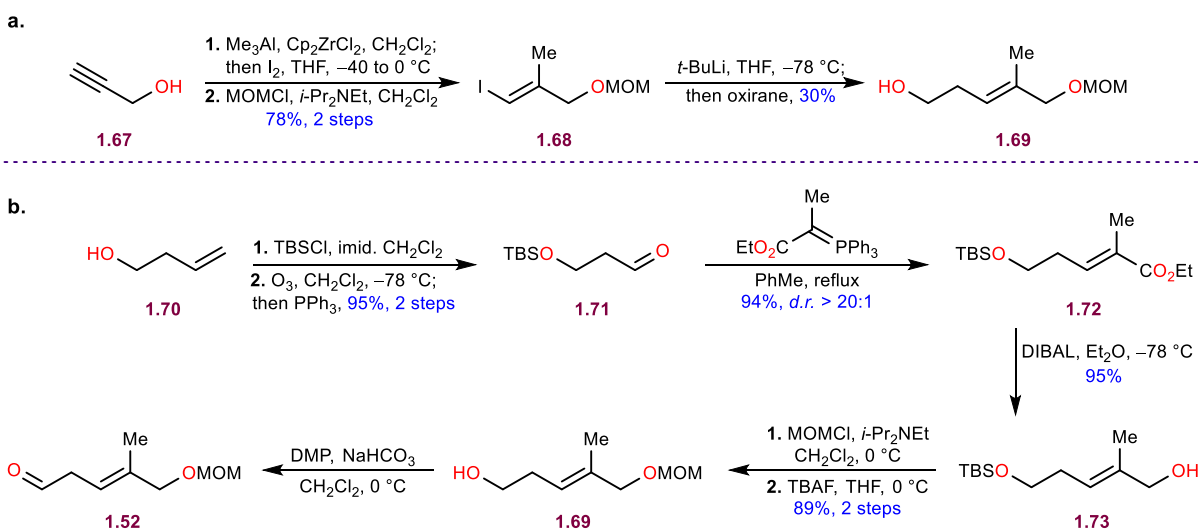


Scheme 1.7: a. Synthesis of lactone **19**; b. Confirmation of stereochemistry on a model system

alumina and NMR analysis, it was realized that the tertiary TBS protected alcohol got eliminated as well, resulting in the formation of the dienone **1.61** and related tautomers, which were highly unstable and prone to decomposition. Therefore, milder conditions for alcohol elimination were sought for. Ultimately, we found that reacting **1.60** with Burgess reagent at 50 °C, affords the desired elimination product **1.62** in reproducible 69% yield.⁵³ The double bond stereochemistry was inferred from ¹H-NMR chemical shift of the olefinic proton (6.65 ppm is in accordance with *E*- configuration). Due to low stability of ene-dicarbonyl **1.62**, we decided to perform reduction of the ketone next, to arrive at a more stable allylic alcohol. To this end, the ketone functionality was reduced under Luche conditions to provide the corresponding allylic alcohol as a mixture of diastereomers **1.63a**:**1.63b**. = 2.5:1 (the stereochemistry was determined at a later stage, see below).⁵⁴ The low temperature was beneficial for the yield, due to low stability of the furan in the presence of Lewis acids. While the diastereomeric ratio could not be improved, the diastereomers could be easily separated by column chromatography. Even though the major diastereomer **1.63a** has the opposite configuration at the alcohol when compared to bicyclic lactone **1.51**, we realized that we could utilize this hydroxyl group for a directed conjugate addition via internal hydride delivery. This would allow us to set up the correct stereochemistry at the troublesome stereocenter. Therefore, major diastereomer **1.63a** was subjected to directed conjugate reduction with Red-Al.⁵⁵ The saturated ester product **1.64** was formed in nearly quantitative yield (95%) as a single diastereomer. The minor diastereomer of the Luche reduction **1.63b** could be recycled by reoxidizing it back to ene-dicarbonyl **1.62** with DMP and resubjecting this compound to Luche reduction. Afterwards, the ethyl ester **1.64** was hydrolyzed with aqueous NaOH to produce the free carboxylic acid, which turned out to be somewhat unstable when heated, resulted in acid-initiated polymerization of the furan. Finally, an intramolecular Mitsunobu reaction on the revealed acid, resulted in the inversion of the stereochemistry of the alcohol with formation of bicyclic lactone **1.51** in 73% yield over two steps.⁵⁶ Considerable efforts have been invested in confirming the stereochemistry of lactone **1.51** by X-ray crystallography, but no derivatives would afford high quality single crystals. To our delight, the model system **1.65** that doesn't contain the C18 methyl group (made according to the same sequence as **1.51**) could be derivatized to compound **1.66** that formed crystals of good enough quality for X-ray diffraction (Scheme 1.7b). Firstly, the TIPS group on the primary alcohol of **1.65** was removed with TBAF and the revealed hydroxyl group was reacted with *p*-bromophenylisocyanate to afford the corresponding carbamate. This derivative

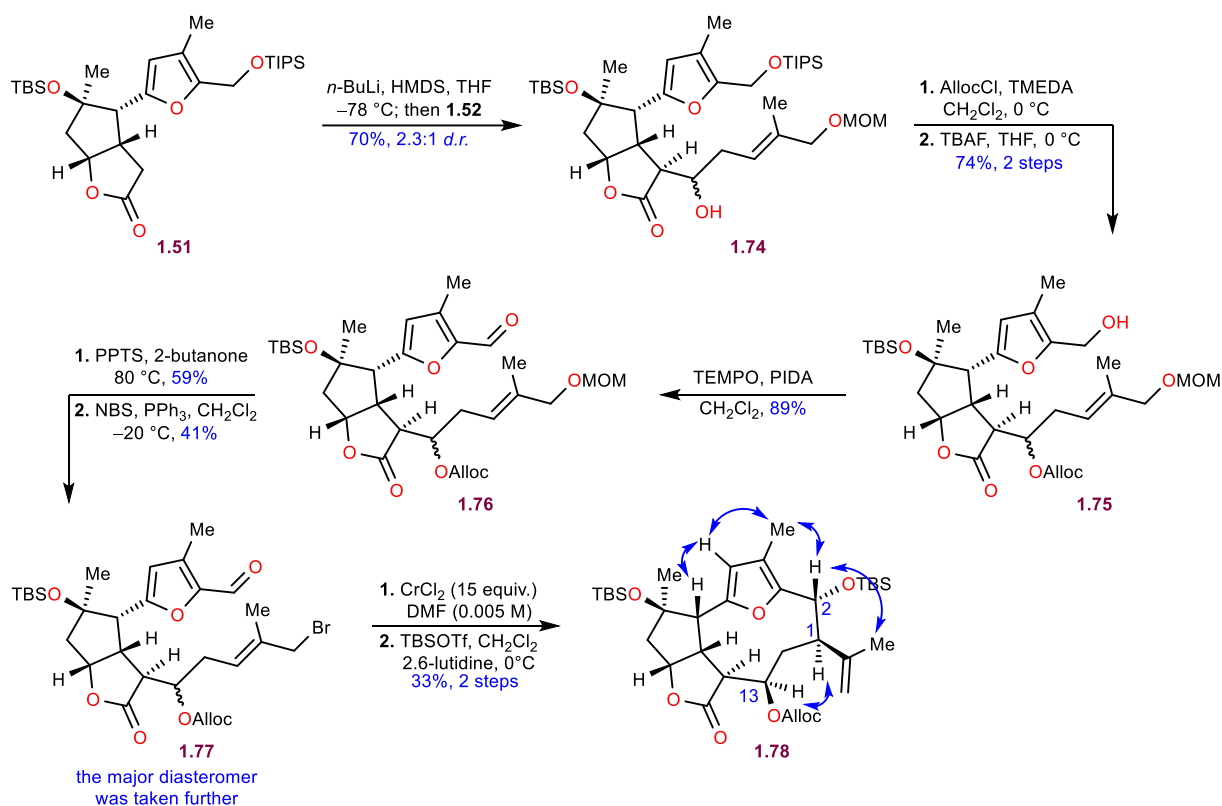
was crystallized from a pentane/ethyl acetate mixture and subjected to crystal lattice analysis by X-ray diffraction. This way, we were finally able to confirm the stereochemistry of all stereocenters in our advanced intermediate **1.51**.

The previously described route was highly scalable and could provide us with multigram quantities of lactone **1.51**. Our focus was now directed to designing a similarly scalable synthesis of aldehyde **1.52**. At first, we examined the shortest route we could envision towards this intermediate (Scheme 1.8a).⁵⁷ Propargyl alcohol (**1.67**) was subjected to methylalumination-iodination, followed by MOM protection of the alcohol to afford iodide **1.68** in 78% yield over two steps. Iodine-lithium exchange with *t*-BuLi, resulted in the formation of the organolithium species that was subsequently reacted with oxirane (prepared as a solution in THF), giving homoallylic alcohol **1.69** in only 30% yield. Even though this route produced aldehyde **1.52** in only four steps (after oxidation of **1.69** to **1.52**), the poor yield of the organolithium addition to oxirane, as well as low scalability, deterred us from pursuing this route any further. Instead we opted to establish a more practical solution (Scheme 1.8b). Starting from 3-buten-1-ol **1.70**, allylic alcohol **1.69** was obtained according to a known sequence.⁵⁸ Firstly, alcohol **1.70** was protected with a TBS group, and the olefin was oxidatively cleaved by ozonolysis to afford aldehyde **1.71**. A Horner-Wadsworth-Emmons reaction furnished unsaturated ester **1.72** as a single diastereomer. 1,2-Reduction of the ester was done selectively with DIBAL at cryogenic temperature to produce allylic alcohol **1.73**. Subsequent MOM protection of this alcohol was followed by TBS deprotection with TBAF to afford intermediate **1.69** in 89% yield, over two steps. This sequence,



Scheme 1.8: a. Shortest route towards aldehyde **1.52**; b. More scalable route towards aldehyde **1.52**

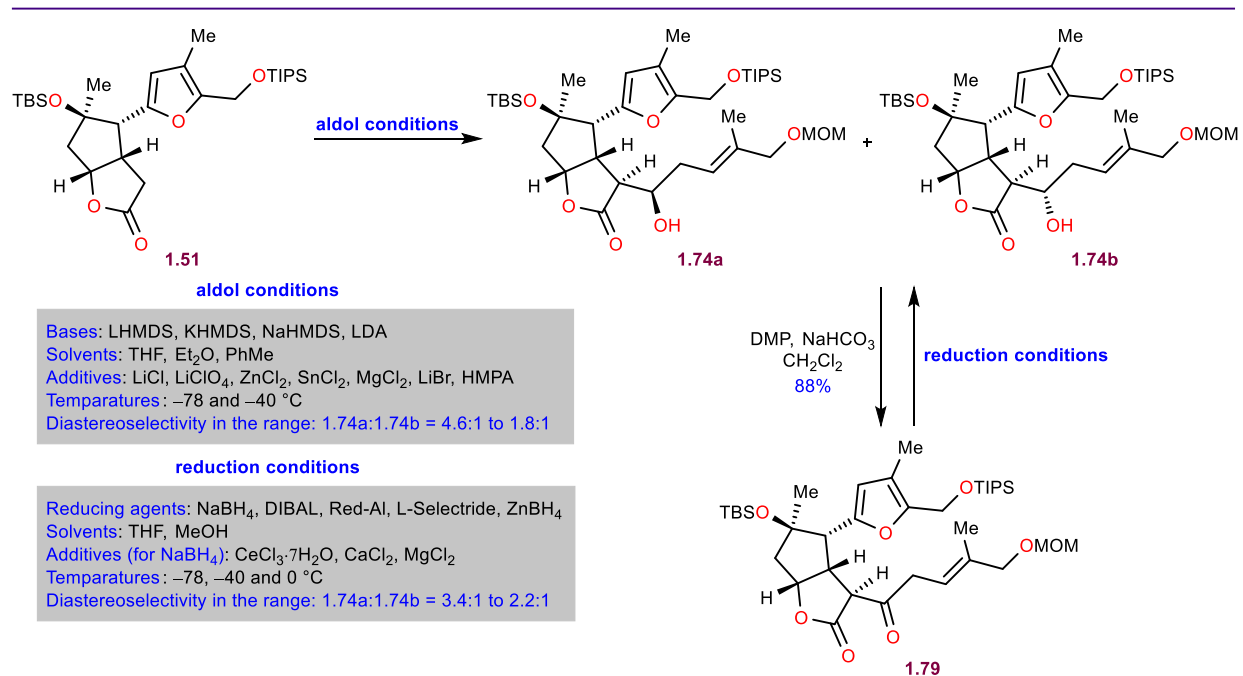
even though longer than the previous one, resulted in the production of **1.69** on multigram scale. Establishing a scalable route towards **1.69**, enabled us to produce significant quantities of aldehyde **1.52** through DMP oxidation. Expectedly, the deconjugated aldehyde proved to be quite unstable and it was best to prepare it and use it immediately and without purification in the following step - aldol addition (Scheme 1.9). Lactone **1.51** was treated with LHMDS, and the obtained lithium enolate was trapped with aldehyde **1.52**, affording the aldol product **1.74** in 63% yield as a mixture of diastereomers (*d.r.* = 2.3:1).⁵⁷ At this point we weren't able to determine which diastereomer is the desired one, so we decided to take the mixture forward and determine the stereochemistry after macrocyclization. Instead of converting the secondary alcohol to the acetate that is present in the natural product, we decided to attach a protecting group that could be easily deprotected after macrocyclization, giving us a chance of correcting the stereochemistry through oxidation/reduction if deemed necessary. Alloc group was chosen for this purpose, as it was orthogonal to the other protecting groups present in the molecule (TBS, TIPS and MOM). However, the protection was more challenging than we expected and only worked in the when TMEDA was employed as the base.⁵⁹ Then, the TIPS group on the primary alcohol was removed



Scheme 1.9: Synthesis of the macrocycle (key NOE correlations are marked by arrows)

selectively in the presence of the TBS group on the tertiary alcohol with 1 equiv. of TBAF revealing furfuryl-alcohol **1.75** in 74% yield, over two steps. The exact stoichiometry of TBAF is crucial for selective deprotection, since excess of TBAF leads to removal of the TBS group, too. Oxidation of alcohol **1.75** was done with TEMPO and PIDA and produced aldehyde **1.76** in 89% yield. The MOM group was removed under mild conditions with PPTS in 2-butanone at 80 °C (59%)⁶⁰ and the obtained allylic alcohol was converted to allylic bromide **1.77** under typical Appel reaction conditions (41%). The stage was now set for the challenging Nozaki-Hiyama-Kishi coupling. Subjecting the diastereomeric mixture of allylic bromides to macrocyclization led to a complex mixture of products. Therefore, we decided to separate the two diastereomers at this stage and attempt macrocyclization on the major one. The separation was very challenging and could only be achieved with a PhMe/EtOAc solvent system with normal phase silica column chromatography. The Nozaki-Hiyama-Kishi coupling was performed on the major diastereomer via dropwise addition of the substrate solution in DMF into a solution of CrCl₂ (15 equiv.) in DMF (2 mM with respect to the substrate). Even though the desired macrocyclization took place, the obtained macrocycle was inseparable from oligomeric side products. Extensive purification efforts were met with failure. Therefore, we decided to treat the crude reaction mixture with TBSOTf, thereby protecting the secondary alcohol. Now the major product **1.78** could be successfully purified and isolated in 33% yield, over two steps. NOE analysis has revealed a strong correlation between C13-H and C1-H (Scheme 1.9) proving that the major diastereomer from the aldol addition had the undesired stereochemistry. Other NOE correlations marked in Scheme 1.9 helped us confirm that the macrocyclization proceeded with the expected *anti* stereoselectivity.^{46-48,57} At this stage, we decided to return to the aldol addition and try to optimize it for the desired diastereomer, subsequently attaching an acetate group on the alcohol, since this group is present in the natural product and would shorten our synthetic sequence.

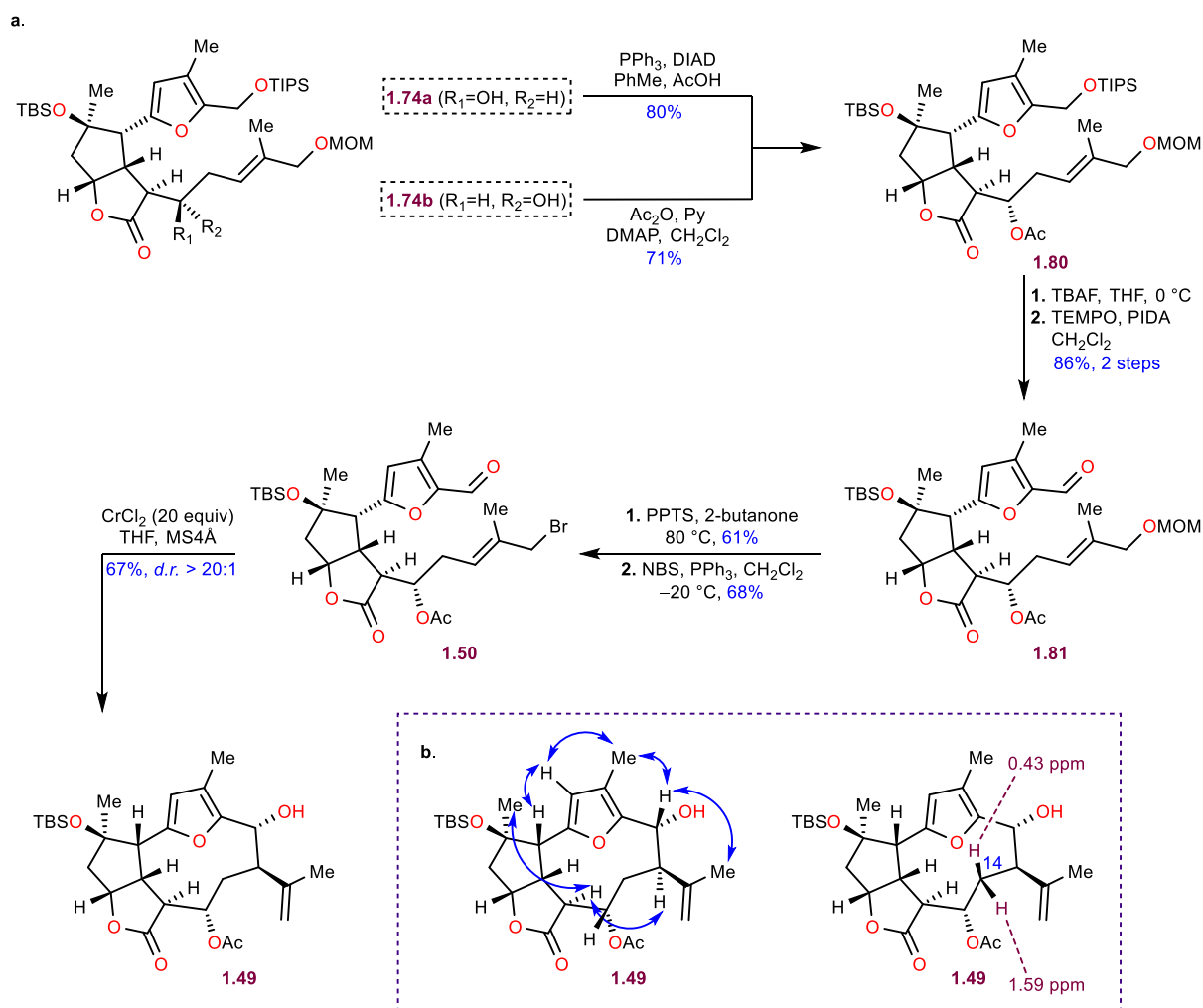
Results of extensive optimization of the aldol addition are shown in Scheme 1.10. Different bases, solvents and additives were examined. In all cases, the undesired diastereomer **1.74a** was formed preferentially. Being unable to reverse the selectivity of the aldol addition, we decided to oxidize the mixture of aldol products **1.74a/1.74b** with DMP (88%) and do stereoselective reduction of the corresponding ketone **1.79**. To our dismay, most examined reducing agents either favored diastereomer **1.74a** or led to decomposition. At this point we decided to separate the aldol



Scheme 1.10: Attempts at correcting the stereochemistry of the aldol product

diastereomers **1.74a/1.74b** by column chromatography and converge them both to the same acetylated product **1.80** (Scheme 1.11a). This was successfully achieved in the following manner: the major diastereomer was subjected to a Mitsunobu reaction with acetic acid to provide acetylated product **1.80** in 80% yield, while the minor diastereomer **1.74b** was reacted with acetic anhydride in the presence of pyridine and DMAP to yield the same acetylated product in 71% yield. From here onwards, the same synthetic sequence as the one described in Scheme 1.9, was utilized to arrive at bromide **1.50**. With good quantities of the correct diastereomer of the bromide, we were ready to reinvestigate the macrocyclization. After some optimization, we found that THF as the solvent instead of DMF had a beneficial effect on the reaction outcome. The Nozaki-Hiyama-Kishi coupling afforded the corresponding macrocycle **1.49** in 67% yield showcasing that the stereochemistry at C13 has an important effect on the efficiency of the macrocyclization event. The stereochemistry of this macrocycle was confirmed by careful NOE analysis (Scheme 1.11b). Notably there was no correlation between the C13-H and C1-H, assuring us that this time, we have indeed obtained the macrocycle with the correct stereochemistry. We have also noticed an interesting phenomenon in the ¹H NMR of this system. More specifically, the diastereotopic methylene protons at C14 have significantly distinct chemical shifts (Scheme 1.11b). The proton that is pointing towards the center of the macrocycle experiences transannular shielding by the

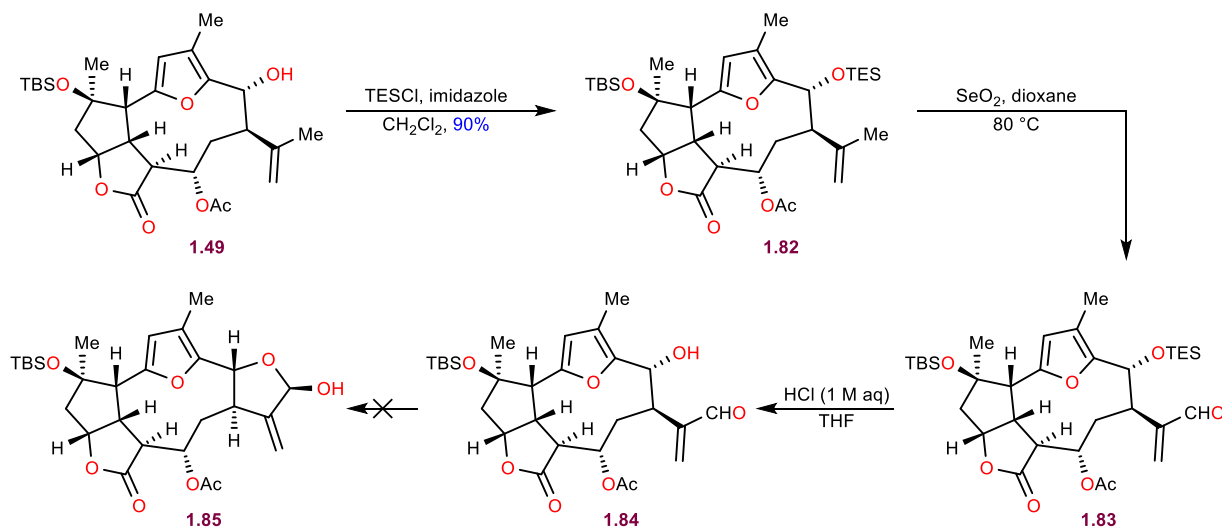
furan π -system and is significantly shifted upfield (0.43 ppm) compared to the proton that is pointing outside the macrocycle (1.59 ppm).^{61,62}



Scheme 1.11: a. Synthesis of the macrocycle with the correct stereochemistry; b. Key NOE correlations (left), distinct chemical shifts of diastereotopic protons at C14 (right)

With macrocycle **1.49** at hand, obtained on 100 mg scale, our next goal was the formation of the hemiacetal in the eastern portion of the natural product (Scheme 1.12). For this purpose, the secondary alcohol in **1.49** had to be protected with a TES group (90%). The obtained product **1.82** was reacted with SeO_2 at 80 °C.⁶³ To our delight, allylic oxidation provided the desired aldehyde **1.83**. However, this aldehyde turned out to be quite unstable towards purification by column chromatography on either normal or reverse phase silica gel nor basic or neutral alumina. Therefore, we decided to take this intermediate forward crude and treat it with 1 M aqueous HCl to remove the TES group and promote hemiacetal formation. Even though TES removal was efficient, NMR analysis has revealed that the aldehyde functionality was still present in **1.84**,

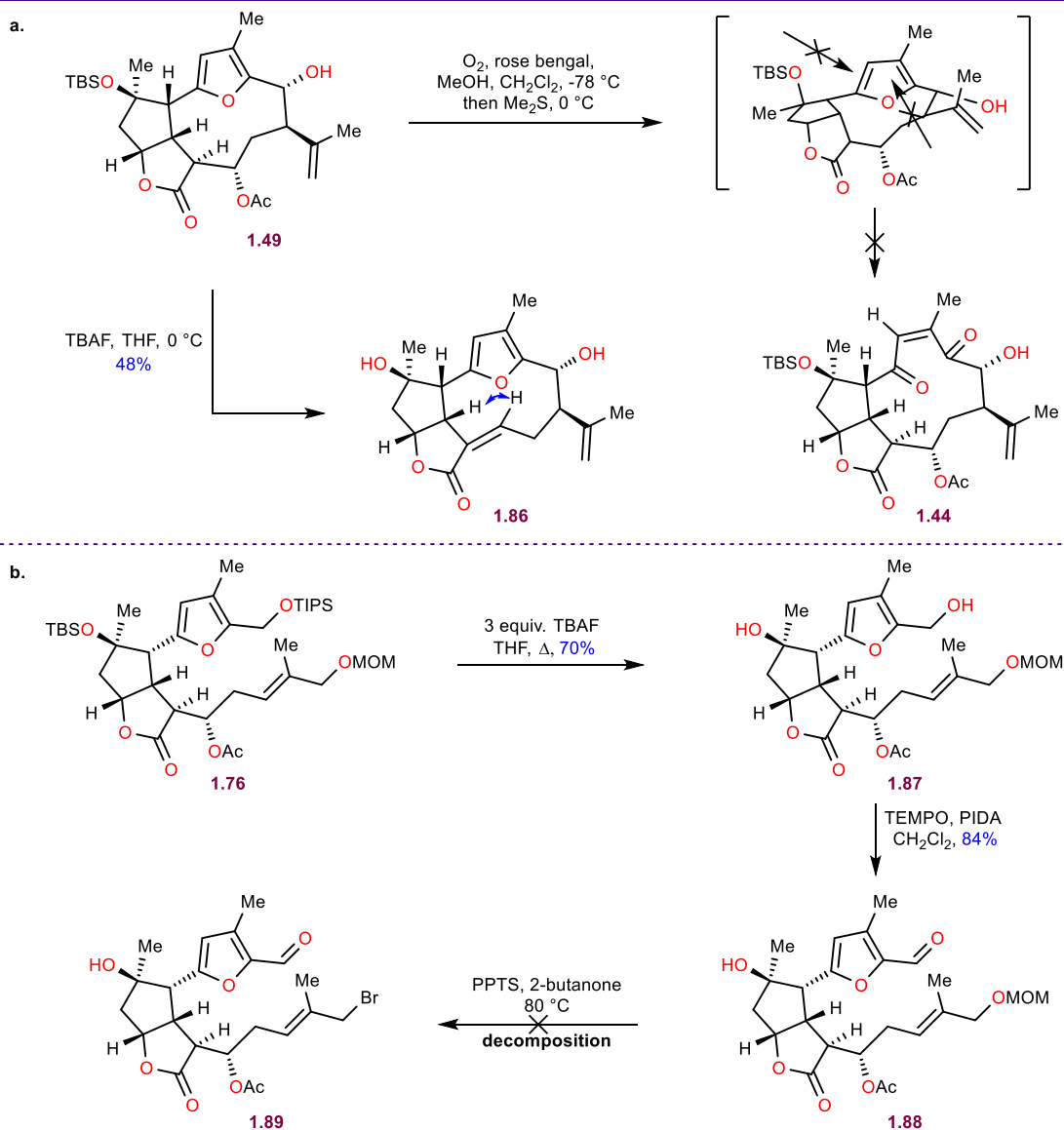
indicating that formation of hemiacetal **1.85** is prohibited at this stage. This is likely due to the significant increase of strain within the macrocycle that would result from the formation of an *anti*-fused five-membered ring. Henceforward, we decided to leave the synthesis of this hemiacetal for the very end of our synthetic sequence and instead focus on the key Norrish-Yang photocyclization step.



Scheme 1.12: Attempted synthesis of the *anti*-[5.10] ring fusion

To attempt the transannular cyclization, we had to reveal the reactive enedione functionality. However, initial attempts at obtaining enedione **1.44** by oxidizing furan **1.49** with singlet oxygen weren't fruitful, presumably because both faces of the furan were sterically blocked, one by the macrocycle and the other one by the TBS group (Scheme 1.13a). Therefore, we decided to deprotect the bulky TBS group first, reasoning that removal of this group will expose one face of the furan for attack by singlet oxygen. Unexpectedly, this step turned out to be quite challenging. Basic fluoride sources like TBAF led to competitive elimination of the acetate group (**1.49**→**1.86**). On the other hand acidic fluoride sources like HF didn't give any conversion, until the reaction mixture was heated up, in which case decomposition of the electron-rich furan occurred. Interestingly, acetate elimination with TBAF wasn't observed on the acyclic precursor **1.76** (Scheme 1.13b). When this substrate was heated in THF with 3 equiv. of TBAF, clean deprotection of both TBS and TIPS groups resulted in the formation of diol **1.87** in 70% yield. Therefore, we switched our focus to elaborating this substrate into the macrocycle. Oxidation of furfuryl alcohol was uneventful, affording aldehyde **1.88** in 84% yield. In spite of this initial success, an insurmountable hurdle was reached at the MOM deprotection step. Heating compound

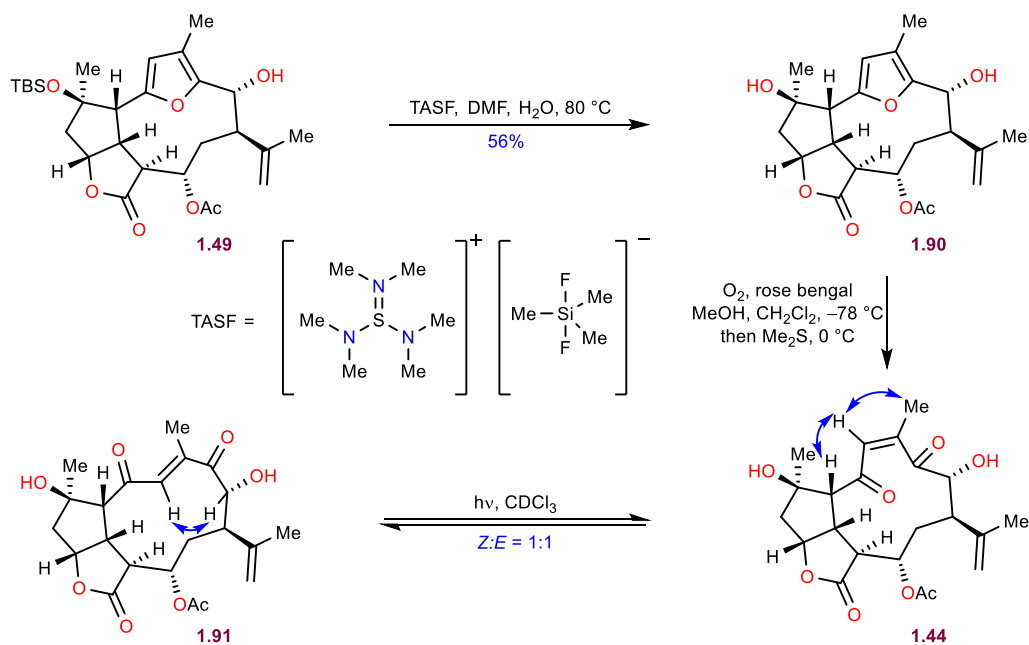
1.88 in the presence of PPTS resulted in complete decomposition, likely due to ionization of the free tertiary alcohol.



Scheme 1.13: a. Unsuccessful attempts at forming the macrocyclic enedione; b. TBS deprotection on the acyclic system

At this moment, we decided to reinvestigate the TBS deprotection step on macrocycle **1.49** (Scheme 1.14). After extensive experimentation, we have eventually discovered that tris(dimethylamino)sulfonium difluorotrimethylsilicate (TASF) is mild enough to provide us with the desired product **1.90**, albeit with varying degrees of elimination. After scrupulous investigation of this transformation, it was realized that the content of water in the reaction mixture had a significant role in reproducibility.⁶⁴ If the reaction is run under strictly anhydrous conditions, the dominant pathway is elimination. On the other hand, if too much water is added, no conversion

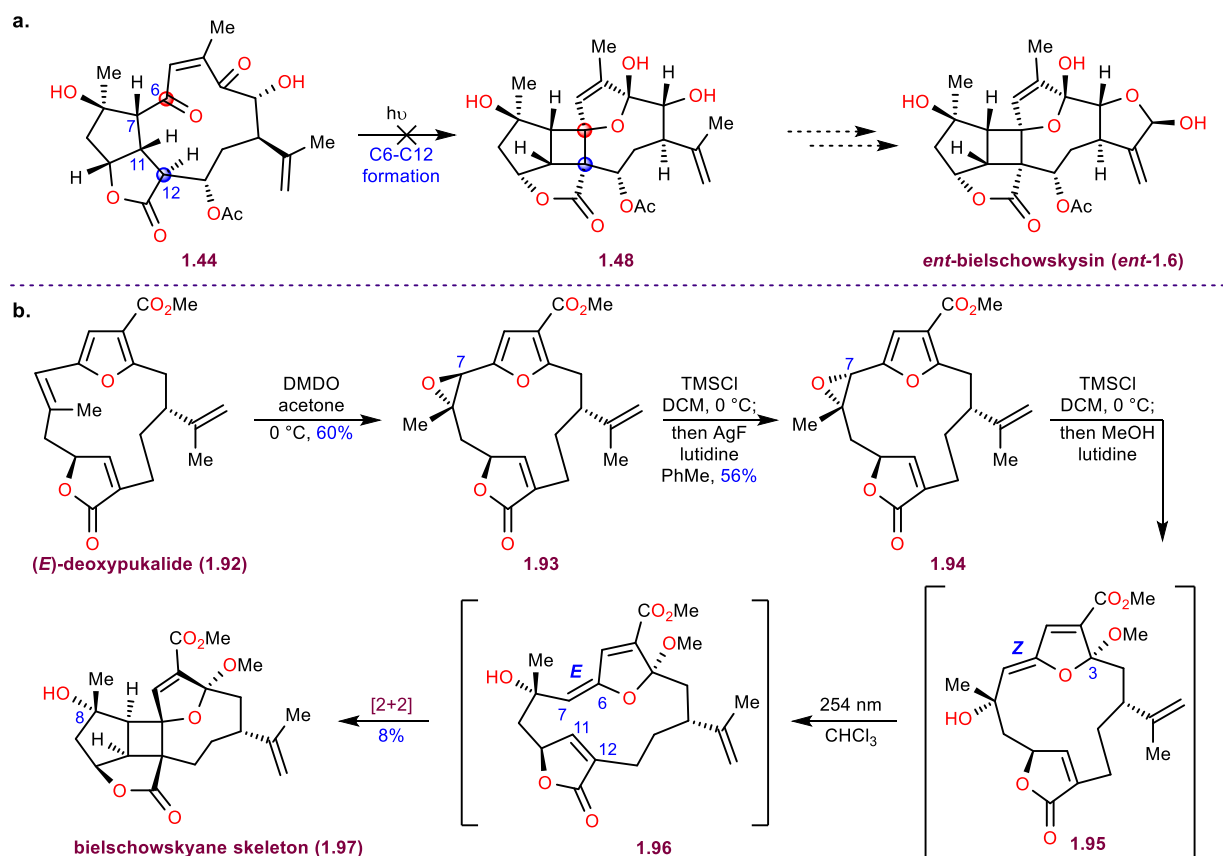
occurs. The optimal amount of water in our system was determined to be 200 equiv. and the reaction temperature of 80 °C. In practice, strictly anhydrous DMF was used as the solvent, and was subsequently dosed with 200 equiv. of water. The optimized conditions provided us with the desired product **1.90** in 56% yield with a small amount of elimination product which was separated by column chromatography. Singlet oxygen oxidation of furan **1.90** proceeded rapidly when rose bengal was used as the photosensitizer, confirming our hypothesis that the TBS group was previously preventing the oxidation by steric effects.^{65,66} This step produced the unstable enedione **1.44** which was immediately subjected to the next step after removing rose bengal by a short silica plug. While irradiation of this intermediate with a 254 nm lamp led to complete decomposition, a 365 nm lamp as well as reptile lamp, led to the establishment of a photostationary state of enedione **1.44** and compound **1.91** with 1:1 ratio after 1 hour of irradiation. Scrupulous NOE analysis of this mixture has revealed that double bond isomerization occurred (*Z*→*E*). Prolonged irradiation resulted in decomposition of both enediones, while the desired Norrish-Yang cyclization product wasn't observed in the reaction mixture.



Scheme 1.14: Synthesis and photochemistry of the macrocyclic enedione (key NOE correlations have been marked by blue arrows)

1.5 Conclusion

We have learned valuable lessons from our study concerning the future synthesis of bielschowskysin (**1.6**). Our mechanistic paradigm was based on the stepwise formation of the two C–C bonds of the highly strained cyclobutane. Whereas the C7–C11 was preformed (originates from enone **1.54**), the C6–C12 bond was supposed to be formed in a transannular fashion via the Norrish-Yang photocyclization (Scheme 1.15a). Since this step wasn't successful in forming **1.48**, we have concluded that the preformed C7–C11 bond imposes significant conformational constraints within the macrocycle, thereby prohibiting the transannular ring closure via formation of the C6–C12 bond. Therefore, the way of going forward regarding the synthesis of bielschowskysin (**1.6**), is through the bioinspired [2+2] transannular cycloaddition where both bonds of the cyclobutane (C7–C11 and C6–C12) are formed in a concerted fashion from a more flexible macrocyclic precursor. After the conclusion of our study, Roche's group has reported another advancement in their bioinspired strategy in 2021.⁴⁰ In this study, the complete bielschowskyane carbon framework **1.97** with the correct stereochemistry was synthesized for the



first time (Scheme 1.16b). Their semi-synthetic approach starts with epoxidation of (*E*)-deoxypukalide **1.92**. The stereochemistry at C7 of epoxide **1.93** had to be inverted via epoxide opening with TMSCl and subsequent epoxide reformation, which is facilitated by treating the chlorohydrine intermediate with AgF. The obtained compound **1.94** that now has the desired stereochemistry at C7 was then subjected to another epoxide opening with TMSCl, followed by trapping with MeOH to arrive at enol acetal **1.95**, where point(C7)-to-plane-to-point(C3) chirality transfer sets up the correct stereochemistry at C3. Irradiation of this intermediate resulted in isomerization of the enol acetal (*Z*→*E*) producing **1.96**. This transformation was enabled by the presence of the methyl ester group on the furan and is crucial for the success of the following [2+2] cycloaddition (as was previously explained in Scheme 1.3). This impressive cascade allowed for the formation of the bielschowskyane skeleton **1.97** in 8% yield.

Since Roche's study was semi-synthetic (performed on a model system), several challenges remain to be solved before the future completion of the total synthesis of Bielschowskysin **1.6** (Figure 1.3). A substrate with higher oxidation states at positions C2 (alcohol), C13 (acetate), and C16 (aldehyde) would have to be prepared *de novo* and tested in the epoxide-opening/[2+2] cascade developed by the Roche lab. Moreover, it is currently unclear at which stage the strained *anti*-fused five-membered hemiacetal in the eastern portion molecule should be synthesized, whether before or after the formation of the [5.4.9]-framework. Additionally, the C18 methyl ester that promotes the cycloaddition must be reduced to a methyl group. Finally, the methyl acetal at C3 has to be converted to a hemiacetal. It is questionable whether its hydrolysis via an oxocarbenium ion is feasible at this stage, while on the other hand it is known from previous studies that the substrate for the [2+2] reaction containing a hemiacetal functionality rapidly tautomerizes to the enedione (Scheme 1.2). Therefore, a different acetal might have to be used instead, that could be converted to a hemiacetal, after the cycloaddition step, under mild non-hydrolytic conditions.

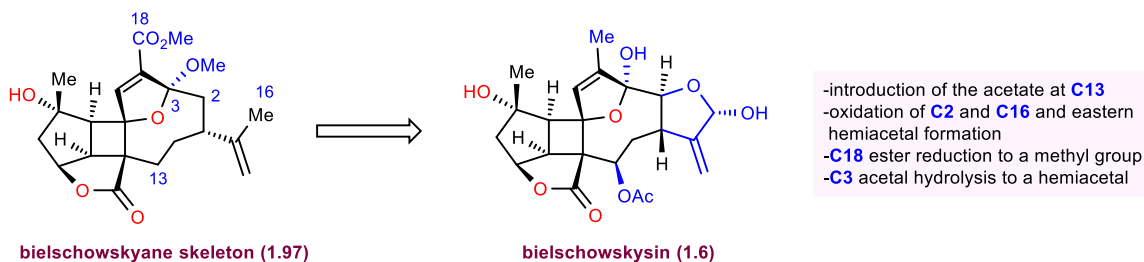
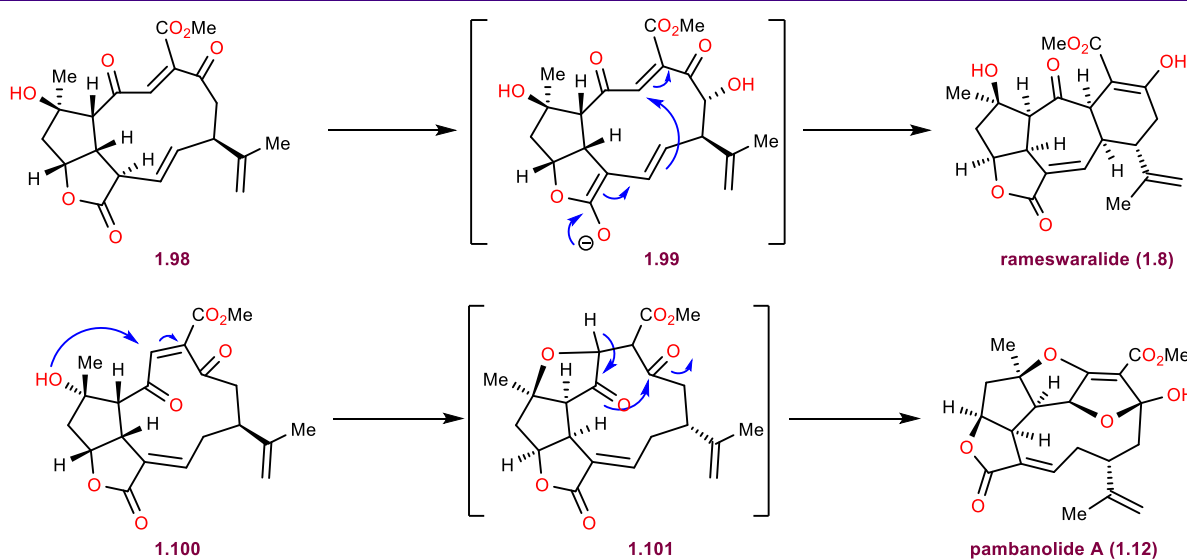


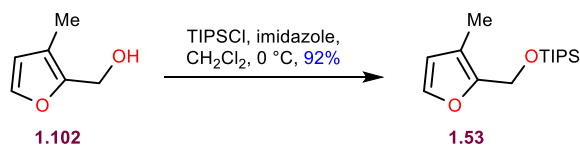
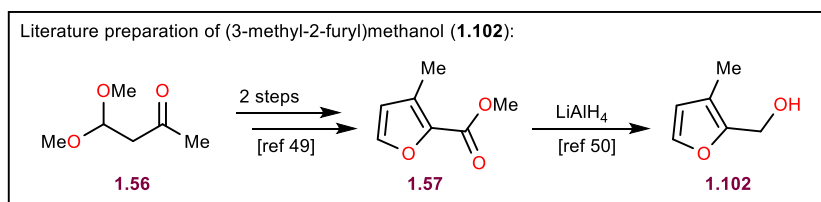
Figure 1.3: Remaining challenges in the synthesis of bielschowskysin

Even though we weren't able to form the final C–C bond of the core structure of bielschowskysin, related macrocyclic enediones have been proposed by Pattenden as intermediates in biosynthetic pathways towards other members of the furanocembranoid family, such as rameswaralide (**1.8**) and pambanolide A (**1.12**) (Scheme 1.16).⁵ In this study, we have shown that these compounds are indeed viable intermediates and can be obtained efficiently via oxidation/photoisomerization of macrocyclic furans. We hope that our investigation will inspire future endeavors towards the synthesis of these natural products as well as other furanocembranoids and norcembranoids via enediones **1.98** and **1.100** or related intermediates derived by intercepting furan-embedded macrocycles related to **1.49**.¹⁵



Scheme 1.16: Macrocyclic enediones are proposed as intermediates in the biosynthetic pathways of rameswaralide and pambanolide A

1.6 Experimental Section



TIPS-protected furan **1.53**:

(3-Methyl-2-furyl)methanol (**1.102**)^{49,50} (42.3 g, 377 mmol, 1.0 equiv.) was dissolved in CH₂Cl₂ (380 mL, 1.0 M). The solution was cooled to 0 °C and imidazole (56.4 g, 830 mmol, 2.2 equiv.) was added in one portion. After 5 minutes, TIPSCl (88.8 mL, 415 mmol, 1.1 equiv.) was added slowly at the same temperature. The mixture was left to warm to room temperature and stir for 6 hours. The reaction was quenched with NH₄Cl (sat. aq. 400 mL). The organic phase was separated, and the aqueous layer was extracted with CH₂Cl₂ (2 × 200 mL). The combined organic extracts were dried over MgSO₄, filtered, and concentrated. The crude was passed through a silica pad (SiO₂, hexanes : EtOAc = 25:1) to provide the desired product **21** as a colorless liquid (93.5 g, 348 mmol, 92%).

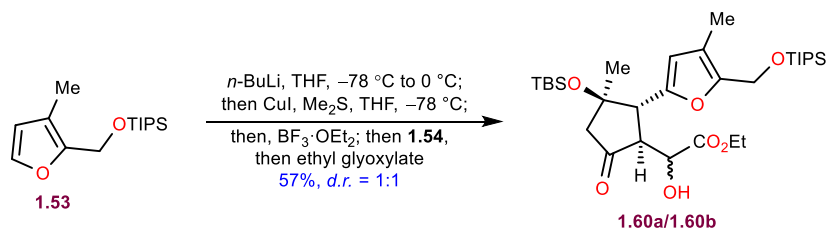
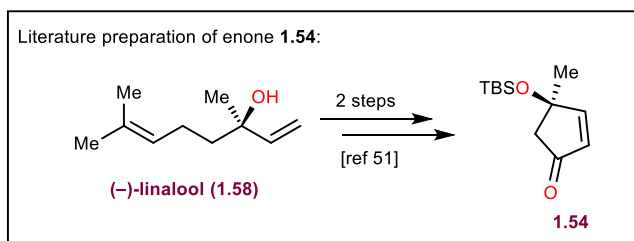
R_f = 0.4 (SiO₂, hexanes : EtOAc = 25:1)

¹H NMR (500 MHz, CDCl₃) δ 7.28 (d, *J* = 1.8 Hz, 1H), 6.18 (d, *J* = 1.7 Hz, 1H), 4.66 (s, 2H), 2.04 (s, 3H), 1.18–1.10 (m, 3H), 1.09–1.06 (m, 18H).

¹³C{¹H} NMR (126 MHz, CDCl₃) δ 149.7, 141.1, 116.8, 113.0, 56.4, 18.1, 12.2, 10.0.

HRMS: (ES⁺, *m/z*) [M+Na]⁺ calcd. for C₁₅H₂₈O₂NaSi, 291.1756; found 291.1758.

IR: (ATR, neat, cm⁻¹): 2942 (m), 2866 (s), 1463 (w), 1159 (w), 1081 (s), 1061 (s).



Aldol product **1.60a/1.60b**:

To a cooled (−78 °C) solution of furan **1.53** (22.4 g, 83.5 mmol, 2.1 equiv.) in THF (170 mL, 0.50 M) was added *n*-BuLi (55 mL, 87.5 mmol, 1.60 M in hexanes, 2.2 equiv.). The flask was then

transferred to an ice bath and left at 0 °C for 30 minutes. Then, the obtained yellow solution was cooled back to -78 °C. In a separate flask, Me₂S (11.7 mL, 159 mmol, 4.0 equiv.) was added to a suspension of CuI (7.57 g, 39.8 mmol, 1.0 equiv.) in THF (99 mL, 0.4 M) and the mixture was stirred until a clear solution formed. This solution was cannulated into the solution of the furyl-lithiate (no change in appearance). The resulting solution was stirred for 15 minutes at -78 °C. BF₃•OEt₂ (14.7 mL, 119 mmol, 3.0 equiv.) was added to the cuprate. After 15 min at -78 °C, the solution became red. Then, a solution of enone **1.54**⁵¹ (9.00 g, 39.8 mmol, 1.0 equiv.) in THF (40 mL, 1.0 M) was added dropwise to the former solution via a cannula. The resulting suspension was stirred for 1 hour at -78 °C followed by the dropwise addition of freshly distilled ethyl glyoxylate⁶⁷ (19.7 mL, 199 mmol, 5.0 equiv.). The resulting mixture was stirred for 30 min. The reaction was subsequently quenched by the addition of a mixture of NH₄Cl (sat. aq. 320 mL) and NH₃ (40 mL, 28-30% aqueous). After warming up to room temperature and stirring for 20 minutes, the mixture was extracted with EtOAc (3×300 mL). The combined organic layers were washed with brine (300 mL), dried over MgSO₄, filtered and concentrated. The obtained residue was purified by flash column chromatography (SiO₂, hexanes : EtOAc = 10:1 then 7:1) to yield the ketoester **4** as a mixture of diastereomers **1.60a/1.60b** (13.2 g, 22.6 mmol, 57%, d.r. = 1:1).

The diastereomers were separated for characterization:

1.60a:

$[\alpha]_D^{23} = -43.7^\circ$ (c = 13.9 mg/mL, CHCl₃)

$R_f = 0.4$ (SiO₂, hexanes : EtOAc = 5:1)

¹H NMR (500 MHz, CDCl₃) δ 6.07 (s, 1H), 4.64 (s, 2H), 4.35 (dq, *J* = 11.0, 7.3 Hz, 1H), 4.29 (dq, *J* = 10.7, 7.3 Hz, 1H), 4.10 (dd, *J* = 4.1, 2.8 Hz, 1H), 3.68 (d, *J* = 12.6 Hz, 1H), 3.23 (dd, *J* = 12.7, 2.8 Hz, 1H), 3.13 (dd, *J* = 4.1, 1.4 Hz, 1H), 2.51 (d, *J* = 2.7 Hz, 2H), 2.02 (s, 3H), 1.32 (t, *J* = 7.1 Hz, 3H), 1.15 (s, 3H), 1.14 – 1.04 (m, 21H), 0.88 (s, 9H), 0.06 (s, 3H), 0.01 (s, 3H).

¹³C{¹H} NMR (126 MHz, CDCl₃) δ 212.5, 173.8, 149.7, 149.1, 117.8, 112.5, 77.7, 68.0, 62.4, 56.4, 55.5, 54.6, 50.5, 25.8, 25.0, 18.10, 18.07, 17.8, 14.3, 12.2, 10.1, -2.3, -2.4.

HRMS: (ES⁺, *m/z*) [M+Na]⁺ calcd. for C₃₁H₅₆O₇NaSi₂, 619.3462; found 619.3439.

IR (ATR, neat, cm⁻¹): 3506 (br), 2929 (m), 2865 (m), 1752 (s), 1565 (w), 1256 (w), 1093 (s), 1063 (s), 1014 (s).

1.60b:

$[\alpha]_D^{23} = -51.4^\circ$ (c = 15.5 mg/mL, CHCl₃)

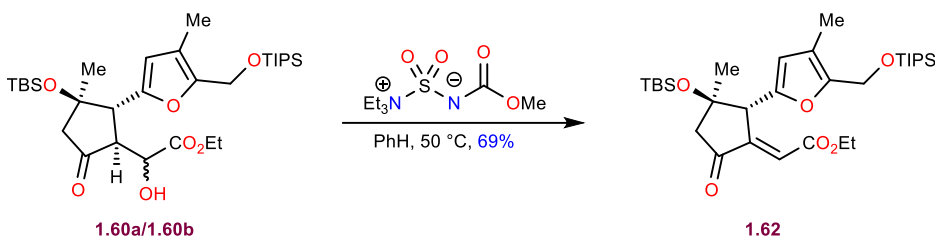
$R_f = 0.4$ (SiO₂, hexanes : EtOAc = 5:1)

¹H NMR (500 MHz, CDCl₃) δ 5.92 (s, 1H), 4.67 (dd, $J = 5.0, 2.6$ Hz, 1H), 4.59 (d, 12.8 Hz, 1H), 4.57 (d, $J = 12.8$ Hz, 1H), 4.05 – 3.97 (m, 1H), 3.72 (dq, $J = 10.6, 7.1$ Hz, 1H), 3.55 (d, $J = 11.4$ Hz, 1H), 3.13 (d, $J = 5.0$ Hz, 1H), 3.08 (dd, $J = 11.4, 2.6$ Hz, 1H), 2.55 (s, 2H), 1.97 (s, 3H), 1.14 (s, 3H), 1.13 – 1.04 (m, 24H), 0.85 (s, 9H), 0.04 (s, 3H), –0.02 (s, 3H).

¹³C{¹H} NMR (126 MHz, CDCl₃) δ 212.7, 173.4, 149.8, 149.0, 117.4, 112.6, 78.1, 68.4, 62.2, 56.3, 55.5, 54.3, 47.9, 25.8, 25.5, 18.09, 18.09, 18.05, 14.0, 12.2, 10.0, –2.3, –2.4.

HRMS: (ES⁺, m/z) [M+Na]⁺ calcd. for C₃₁H₅₆O₇NaSi₂, 619.3462; found 619.3447.

IR (ATR, neat, cm⁻¹): 3508 (br), 2929 (m), 2866 (m), 1751 (s), 1569 (w), 1258 (w), 1090 (s), 1061 (s), 1014 (s).



Enone **1.62**:

The diastereomeric mixture of ketoesters **1.60a/1.60b** (13.2 g, 22.1 mmol, 1.0 equiv.) was dissolved in benzene (220 mL, 0.10 M) in a flask equipped with a reflux condenser. Burgess reagent⁶⁸ (9.48 g, 39.8 mmol, 1.8 equiv.) was added to the obtained solution. The mixture was heated to 50 °C. After 9 hours, the solution was allowed to cool to room temperature and NH₄Cl (sat. aq. 150 mL) was added. The layers were separated and the aqueous layer was extracted with benzene (2 × 100 mL). The organic layers were combined, dried over MgSO₄ and concentrated. The crude product was purified by flash column chromatography (SiO₂, hexanes : EtOAc = 15:1) to give the pure enone **1.62** (8.80 g, 15.2 mmol, 69%) as an orange oil.

$[\alpha]_D^{23} = 43.2^\circ$ ($c = 11.8$ mg/mL, CHCl₃)

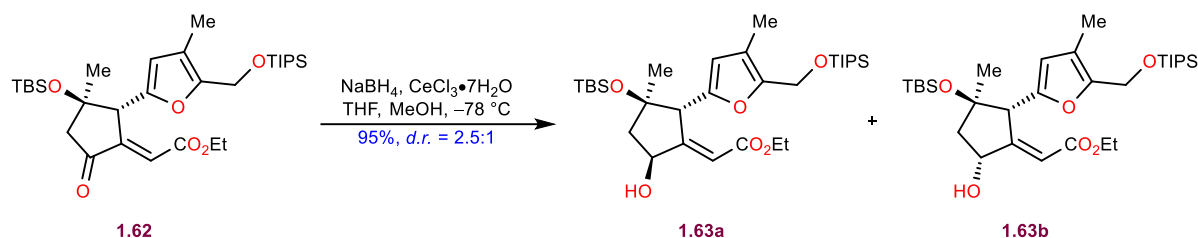
$R_f = 0.4$ (SiO₂, hexanes : EtOAc = 10:1)

¹H NMR (500 MHz, CDCl₃) δ 6.65 (d, $J = 1.8$ Hz, 1H), 5.90 (s, 1H), 4.70 (t, $J = 2.1$ Hz, 1H), 4.55 (m, 2H), 4.22 – 4.11 (m, 2H), 2.76 (d, $J = 17.4$ Hz, 1H), 2.47 (dd, $J = 17.4, 2.4$ Hz, 1H), 1.96 (s, 3H), 1.28 (s, 3H), 1.25 (d, $J = 7.1$ Hz, 2H), 1.03 (d, $J = 6.2$ Hz, 22H), 0.76 (s, 9H), 0.10 (s, 3H), 0.09 (s, 3H).

$^{13}\text{C}\{^1\text{H}\}$ NMR (126 MHz, CDCl_3) δ 205.1, 165.6, 152.1, 151.2, 149.1, 121.8, 117.5, 111.0, 79.7, 60.9, 56.2, 53.5, 52.2, 25.6, 24.3, 18.07, 18.07, 14.3, 12.2, 10.0, -2.4, -2.6.

HRMS: (ES+, m/z) [$\text{M}+\text{Na}$] $^+$ calcd. for $\text{C}_{31}\text{H}_{54}\text{O}_6\text{NaSi}_2$, 601.3357; found 601.3362.

IR (ATR, neat, cm^{-1}): 2930 (m), 2865 (m), 1741 (m), 1719 (s), 1660 (w), 1562 (w), 1091 (s), 1014 (s).



Allylic alcohols **1.63a/1.63b**:

Enone **1.62** (8.80 g, 15.2 mmol, 1.0 equiv.), was dissolved in THF (300 mL, 0.050 M). The obtained solution was cooled to $-78\text{ }^\circ\text{C}$. To this solution was added $\text{CeCl}_3 \cdot 7\text{H}_2\text{O}$ (11.3 g, 30.4 mmol, 2 equiv. dissolved in 76 mL of MeOH, 0.40 M). After stirring for 5 minutes at the same temperature, NaBH_4 (863 mg, 22.8 mmol, 1.5 equiv.) was added. The reaction was allowed to stir for 15 min at $-78\text{ }^\circ\text{C}$. Then, the reaction was quenched by the addition of sat. NH_4Cl (200 mL sat. aq) and diluted with ethyl acetate (200 mL). This mixture was allowed to stir until the temperature has reached room temperature. The obtained mixture was filtered through celite and transferred to a separation funnel. The layers were separated and the aqueous layer was extracted with ethyl acetate ($3 \times 200\text{ mL}$). The combined organic layers were washed with brine (300 mL), dried over MgSO_4 , filtered and concentrated under reduced pressure. The residue was purified by flash column chromatography (SiO_2 , hexanes : EtOAc = 8:1 - major diastereomer, then 5:1 - minor diastereomer) to yield the diastereomeric products in 95% combined yield (over two steps) and $d.r. = 2.5:1$. The major diastereomer **1.63a** (5.98 g, 10.3 mmol, 68%) was used for the next step, while the minor diastereomer **1.63b** (2.40 g, 4.13 mmol, 27%) was reoxidized to the starting enone with DMP.

1.63a:

$[\alpha]_{\text{D}}^{22} = 47.2^\circ$ ($c = 19.1\text{ mg/mL}$, CHCl_3)

$R_f = 0.3$ (SiO_2 , hexanes : EtOAc = 8:1)

^1H NMR (500 MHz, CDCl_3) δ 6.26 (t, $J = 1.6\text{ Hz}$, 1H), 5.80 (s, 1H), 4.72 (q, $J = 1.9\text{ Hz}$, 1H), 4.66 (ddd, $J = 11.6, 7.6, 1.6\text{ Hz}$, 1H), 4.56 (s, 2H), 4.09 (dddd, $J = 18.0, 10.8, 7.1, 3.7\text{ Hz}$, 2H),

Macrocycle **1.78**:

CrCl_2 (57.6 mg, 15 equiv.) was dissolved in DMF (15.6 mL, 0.0020 M, relative to the substrate). The substrate **1.77** (20.0 mg) was dissolved in DMF (1.56 mL) and the obtained solution was added to the former solution with a syringe pump over 5 hours. The reaction was left to stir overnight. Water (15 mL) was added and the mixture was extracted with EtOAc (3x15 mL). The combined organic layers were washed with water (3x15 mL) and brine (15 mL), dried over Mg_2SO_4 , filtered and concentrated. The obtained residue was purified by flash column chromatography (SiO_2 , hexanes : EtOAc = 3:1) to provide 10 mg of the macrocyclic product contaminated with oligomers/stereoisomers.

For the calculations in the next step, it was assumed that the material is 100% pure:

This residue obtained from the previous step (10.0 mg) was dissolved in CH_2Cl_2 (0.18 mL, 0.10 M) and the obtained solution was cooled to 0 °C. 2,6-lutidine (2.5 μL , 1.2 equiv.) was added, followed by the addition of TBSOTf (5.7 μL , 1.4 equiv.). After stirring for 15 min. the reaction was quenched with bicarbonate (sat. aq. 0.20 mL.). The layers were separated, and the aqueous layer was extracted with CH_2Cl_2 (2x0.20 mL). The combined organic layers were dried over MgSO_4 , filtered and concentrated. The obtained crude was purified by flash column chromatography (SiO_2 , hexanes : EtOAc = 10:1) to provide 7 mg of macrocycle **1.78** (33% over two steps) as a yellow oil.

^1H NMR (500 MHz, CDCl_3) δ 6.07 (s, 1H), 5.86 (ddt, $J = 16.3, 10.5, 5.7$ Hz, 1H), 5.29 (dq, $J = 19.96$ Hz, 1.55 Hz, 1H), 5.21 (dd, $J = 10.4, 1.4$ Hz, 1H), 4.97 (q, $J = 7.8$ Hz, 1H), 4.82 (t, $J = 1.6$ Hz, 1H), 4.78 (d, $J = 1.7$ Hz, 1H), 4.75 (d, $J = 1.7$ Hz, 1H), 4.51 (dt, $J = 5.7, 1.4$ Hz, 2H), 3.86 (d, $J = 12.4$ Hz, 1H), 3.45 (d, $J = 7.6$ Hz, 1H), 3.25 (t, $J = 3.6$ Hz, 1H), 3.10 (dt, $J = 12.4, 7.7$ Hz, 1H), 2.78 (ddd, $J = 16.0, 10.4, 3.4$ Hz, 1H), 2.49 (dd, $J = 14.7, 8.0$ Hz, 1H), 2.35 (d, $J = 10.3$ Hz, 1H), 2.04-1.97 (m, 5H), 1.79 (s, 3H), 1.42 (s, 3H), 0.86 (s, 9H), 0.83 (s, 9H), 0.09 (d, $J = 2.4$ Hz, 6H), 0.00 (s, 3H), -0.14 (s, 3H).

$^{13}\text{C}\{^1\text{H}\}$ NMR (126 MHz, CDCl_3) δ 173.8, 155.3, 151.9, 150.2, 147.5, 131.6, 118.9, 114.9, 114.7, 112.4, 82.9, 79.3, 78.4, 68.6, 66.8, 56.3, 53.6, 51.9, 51.3, 49.0, 36.1, 29.0, 25.9, 25.8, 22.7, 18.3, 18.0, 9.5, -2.1, -2.2, -5.0, -5.2.

$^{13}\text{C}\{^1\text{H}\}$ NMR (126 MHz, CDCl_3) δ 178.7, 150.5, 150.0, 136.0, 123.0, 117.4, 113.6, 95.9, 85.8, 84.4, 73.6, 72.5, 56.3, 55.5, 55.1, 48.6, 46.8, 45.77, 33.0, 25.8, 24.2, 18.1, 18.1, 14.4, 12.2, 10.0, -2.2, -2.3.

HRMS: (ES+, m/z) $[\text{M}+\text{Na}]^+$ calcd. for $\text{C}_{37}\text{H}_{66}\text{O}_8\text{NaSi}_2$, 717.4194; found 717.4227.

IR: (ATR, neat, cm^{-1}): 3460 (br), 2945 (s), 2865 (m), 1769 (m), 1463 (w), 1052 (s).

1.74b:

$[\alpha]_{\text{D}}^{23} = 33.8^\circ$ ($c = 16.6$ mg/mL, CHCl_3)

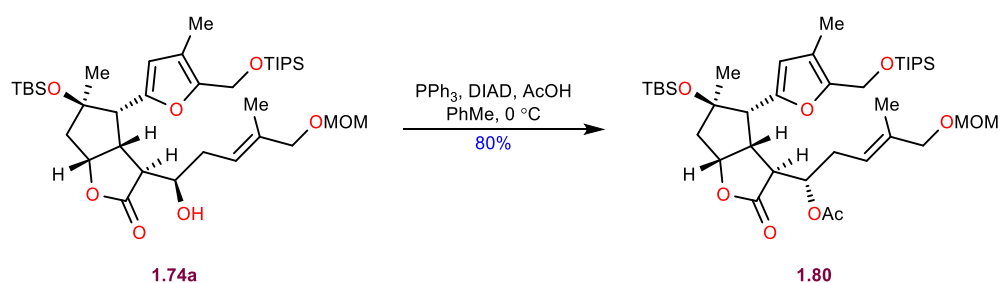
Rf = 0.3 (SiO_2 , hexanes : EtOAc = 3:1)

^1H NMR (500 MHz, CDCl_3) δ 5.89 (s, 1H), 5.41 – 5.35 (m, 1H), 5.08 (ddd, $J = 8.9, 7.3, 5.9$ Hz, 1H), 4.60 (d, $J = 1.0$ Hz, 2H), 4.56 (d, $J = 12.9$ Hz, 1H), 4.52 (d, $J = 12.8$ Hz, 1H), 4.10 – 4.05 (m, 1H), 3.93 (d, $J = 11.8$ Hz, 1H), 3.89 (d, $J = 11.8$ Hz, 1H), 3.52 (td, $J = 8.8, 3.4$ Hz, 1H), 3.36 (s, 3H), 3.19 (dd, $J = 9.1, 1.6$ Hz, 1H), 2.34 (dd, $J = 7.4, 1.8$ Hz, 1H), 2.30 – 2.22 (m, 2H), 2.15 (t, $J = 3.2$ Hz, 1H), 2.11 – 2.04 (m, 2H), 1.96 (s, 3H), 1.67 (d, $J = 1.3$ Hz, 3H), 1.16 (s, 3H), 1.14 – 1.03 (m, 21H), 0.87 (s, 9H), 0.12 (d, $J = 0.9$ Hz, 6H).

$^{13}\text{C}\{^1\text{H}\}$ NMR (126 MHz, CDCl_3) δ 179.6, 150.7, 149.9, 136.3, 122.6, 117.4, 113.4, 95.9, 86.0, 84.9, 73.6, 71.2, 56.3, 55.5, 55.2, 49.6, 46.8, 42.3, 33.8, 25.8, 24.2, 18.1, 18.1, 14.4, 12.2, 9.9, -2.2, -2.3.

HRMS: (ES+, m/z) $[\text{M}+\text{Na}]^+$ calcd. for $\text{C}_{37}\text{H}_{66}\text{O}_8\text{NaSi}_2$, 717.4194; found 717.4216.

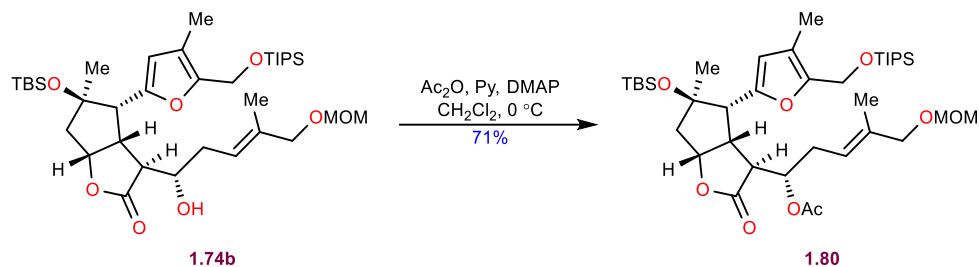
IR: (ATR, neat, cm^{-1}): 3450 (br), 2930 (s), 2865 (m), 1769 (m), 1463 (w), 1051 (s).



Acetate 1.80:

The major aldol product **1.74a** (1.11 g, 1.60 mmol, 1.0 equiv.), was dissolved in toluene (16 mL, 0.10 M). The solution was cooled to 0°C , followed by the addition of PPh_3 (838 mg, 3.19 mmol, 2.0 equiv.) and AcOH (glacial, 0.274 mL, 4.79 mmol, 3.0 equiv.). To the obtained mixture, DIAD (0.621 mL, 3.19 mmol, 2.0 equiv.) was added dropwise. The reaction was left to warm to room

temperature and stir for 3 hours. The solvent was removed in vacuo and the residue was purified by flash column chromatography (SiO₂, hexanes : EtOAc = 6:1) to give the acetate **1.80** (0.94 g, 1.60 mmol, 80%) as a clear oil.



The minor aldol product **1.74b** (521 mg, 0.750 mmol, 1.0 equiv.) was dissolved in CH₂Cl₂ (7.5 mL, 0.10 M). The solution was cooled to 0 °C, and pyridine (97 μL, 1.20 mmol, 1.6 equiv.) was added, followed by DMAP (9.2 mg, 75 μmol, 0.10 equiv.). To the obtained mixture, Ac₂O (99 μL, 1.05 mmol, 1.4 equiv.) was added dropwise at the same temperature. The reaction was left to warm up to room temperature and stir overnight. Then the reaction was quenched with NaHCO₃ (sat. aq. 5 mL). The layers were separated and the aqueous layer was extracted with CH₂Cl₂ (2×7 mL). The combined organic layers were dried over MgSO₄, filtered and concentrated. The obtained residue was purified by flash column chromatography (SiO₂, hexanes : EtOAc = 5:1) to give acetate **1.80** (392 mg, 532 μmol, 71%) as a clear oil.

$[\alpha]_D^{23} = 34.2^\circ$ (c = 12.6 mg/mL, CHCl₃)

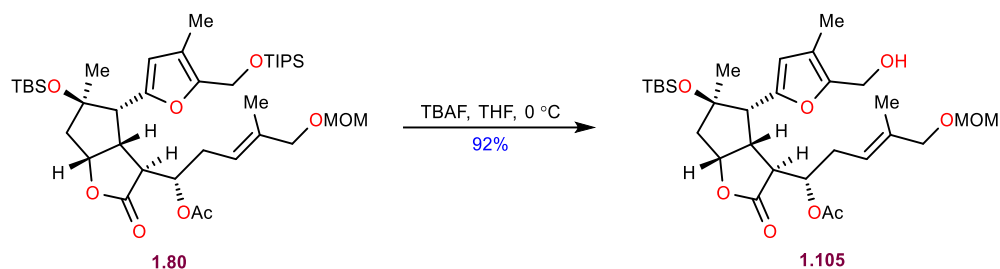
$R_f = 0.2$ (SiO₂, hexanes : EtOAc = 5:1)

¹H NMR (500 MHz, CDCl₃) δ 5.90 (s, 1H), 5.26 – 5.21 (m, 1H), 5.16 (ddd, *J* = 7.7, 6.3, 3.2 Hz, 1H), 5.05 (td, *J* = 7.7, 5.7 Hz, 1H), 4.55 (m, 3H), 4.50 (d, *J* = 12.9 Hz, 1H), 3.85 (s, 2H), 3.51 – 3.46 (m, 1H), 3.35 (s, 3H), 3.18 (d, *J* = 1.7 Hz, 1H), 2.55 – 2.48 (m, 1H), 2.35 (dd, *J* = 7.4, 1.9 Hz, 1H), 2.30 – 2.20 (m, 3H), 1.99 (s, 3H), 1.95 (s, 3H), 1.66 (d, *J* = 1.4 Hz, 3H), 1.15 (s, 3H), 1.05 (dd, *J* = 6.7, 3.7 Hz, 21H), 0.88 (s, 9H), 0.13 (s, 3H), 0.13 (s, 3H).

¹³C{¹H} NMR (126 MHz, CDCl₃) δ 177.9, 169.7, 150.2, 150.1, 135.9, 120.9, 117.3, 113.6, 95.6, 86.0, 84.7, 73.5, 72.8, 56.3, 55.4, 55.2, 47.0, 46.63, 43.0, 30.9, 25.7, 24.1, 21.0, 18.1, 18.1, 14.3, 12.1, 9.9, -2.2, -2.4.

HRMS: (ES⁺, *m/z*) [M+Na]⁺ calcd. for C₃₉H₆₈O₉NaSi₂, 759.4300; found 759.4288.

IR (ATR, neat, cm⁻¹): 2930 (m), 2865 (m), 1774 (s), 1749 (s), 1569 (w), 1232 (s), 1052 (s), 999 (s).



Alcohol **1.105**:

Acetate **1.80** (1.31 g, 1.88 mmol, 1.0 equiv.) was dissolved in THF (38 mL, 0.050 M) and the resulting solution was cooled to 0 °C. TBAF (2.1 mL, 2.07 mmol, 1.1 equiv., 1.0 M in THF) was added dropwise and the reaction was left to stir for 2 hours at 0 °C at which point it was diluted with EtOAc (30 mL) and quenched with NH₄Cl (aq. sat. 30 mL). The layers were separated and the aqueous layer was extracted with EtOAc (2×30 mL). The organic layers were combined, washed with brine (50 mL), dried over MgSO₄, filtered and concentrated to yield the crude product which was purified by flash column chromatography (SiO₂, hexanes : EtOAc = 3:2) to give alcohol **1.105** as a clear oil (1.01 g, 1.74 mmol, 92%).

$[\alpha]_D^{23} = 10.2^\circ$ ($c = 13.2$ mg/mL, CHCl₃)

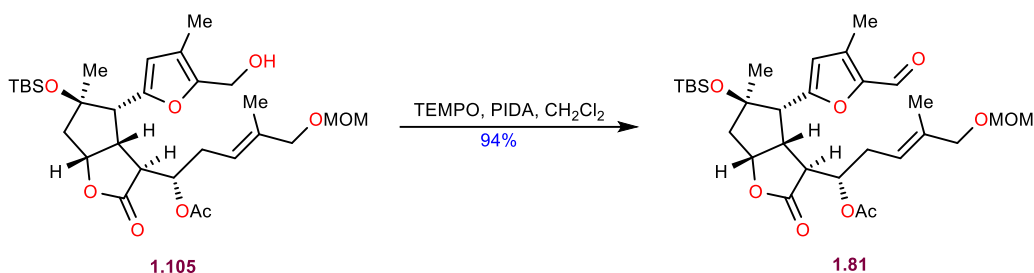
R_f = 0.3 (SiO₂, hexanes : EtOAc = 3:2)

¹H NMR (500 MHz, CDCl₃) δ 5.95 (s, 1H), 5.25 (ddd, $J = 8.2, 4.7, 1.4$ Hz, 1H), 5.16 (ddd, $J = 7.4, 6.3, 3.5$ Hz, 1H), 5.11 (td, $J = 7.8, 5.4$ Hz, 1H), 4.56 (d, $J = 0.9$ Hz, 2H), 4.44 (dd, $J = 13.7, 4.1$ Hz, 1H), 4.37 (dd, $J = 13.6, 8.7$ Hz, 1H), 3.87 (s, 2H), 3.49 (td, $J = 8.5, 2.3$ Hz, 1H), 3.36 (d, $J = 1.2$ Hz, 3H), 3.17 (dd, $J = 8.8, 1.8$ Hz, 1H), 2.52 (dt, $J = 13.8, 6.7$ Hz, 1H), 2.42 (ddd, $J = 14.2, 7.5, 1.8$ Hz, 1H), 2.37 – 2.32 (m, 1H), 2.27 (dd, $J = 14.7, 7.5$ Hz, 1H), 2.22 (dd, $J = 14.1, 5.3$ Hz, 1H), 2.16 (dd, $J = 3.6, 2.3$ Hz, 1H), 2.01 (d, $J = 1.2$ Hz, 3H), 1.97 (d, $J = 1.2$ Hz, 3H), 1.66 (d, $J = 1.5$ Hz, 3H), 1.16 (s, 3H), 0.88 (s, 9H), 0.14 (s, 3H), 0.13 (s, 3H).

¹³C{¹H} NMR (126 MHz, CDCl₃) δ 179.0, 169.7, 150.8, 150.2, 136.0, 120.7, 118.0, 113.8, 95.6, 85.6, 85.2, 73.2, 72.7, 55.4, 55.3, 55.0, 47.6, 46.8, 43.5, 30.8, 25.7, 24.3, 21.1, 18.1, 14.3, 9.8, –2.2, –2.4.

HRMS: (ES⁺, m/z) [M+Na]⁺ calcd. for C₃₀H₄₈O₉NaSi, 603.2965; found 603.2964.

IR (ATR, neat, cm⁻¹): 3477 (br), 2952 (m), 2930 (m), 1771 (s), 1747 (s), 1568 (w), 1232 (s), 1032 (s), 998 (s).



Aldehyde **1.81**:

To a solution of alcohol **1.105** (780 mg, 1.34 mmol, 1.0 equiv.) in CH_2Cl_2 (13 mL, 0.10 M) were added TEMPO (42 mg, 0.269 mmol, 0.20 equiv.) and PIDA (519 mg, 1.61 mmol, 1.2 equiv.) at room temperature. After 1 hour, the reaction was quenched with $\text{Na}_2\text{S}_2\text{O}_3$ (sat. aq. 10 mL). The layers were separated and the aqueous layer was extracted with CH_2Cl_2 (2×10 mL). The combined organic layers were dried over MgSO_4 , filtered and concentrated to give the crude product. Purification was done by flash column chromatography (SiO_2 , hexanes : EtOAc = 2:1) to provide pure aldehyde **1.81** (732 mg, 1.26 mmol, 94%) as an orange oil.

$[\alpha]_{\text{D}}^{23} = 44.1^\circ$ ($c = 19.4$ mg/mL, CHCl_3)

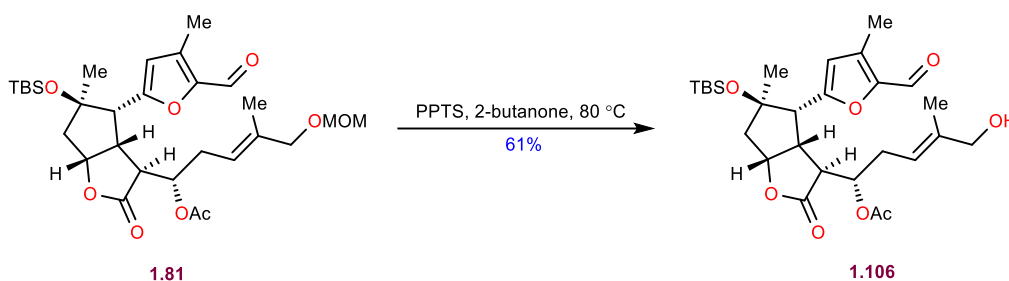
Rf = 0.3 (SiO_2 , hexanes : EtOAc = 2:1)

^1H NMR (500 MHz, CDCl_3) δ 9.65 (s, 1H), 6.15 (s, 1H), 5.24 (ddt, $J = 8.2, 6.9, 1.4$ Hz, 1H), 5.18 (ddd, $J = 7.7, 6.3, 3.4$ Hz, 1H), 5.09 (td, $J = 7.7, 5.5$ Hz, 1H), 4.56 (s, 2H), 3.85 (s, 2H), 3.57 (td, $J = 8.6, 2.9$ Hz, 1H), 3.34 (s, 4H), 2.54 (dt, $J = 13.7, 6.6$ Hz, 1H), 2.46 (ddd, $J = 14.3, 7.4, 1.8$ Hz, 1H), 2.32 (s, 3H), 2.29 – 2.19 (m, 3H), 2.01 (s, 3H), 1.66 (d, $J = 1.4$ Hz, 3H), 1.18 (s, 3H), 0.89 (s, 9H), 0.15 (s, 3H), 0.14 (s, 3H).

$^{13}\text{C}\{^1\text{H}\}$ NMR (126 MHz, CDCl_3) δ 178.2, 177.3, 169.6, 157.4, 148.9, 136.2, 133.6, 120.3, 115.7, 95.6, 85.8, 84.4, 73.3, 72.6, 55.6, 55.4, 46.9, 46.7, 43.1, 30.8, 25.6, 24.1, 21.0, 18.0, 14.3, 10.6, -2.2, -2.5.

HRMS: (ES⁺, m/z) $[\text{M}+\text{Na}]^+$ calcd. for $\text{C}_{30}\text{H}_{46}\text{O}_9\text{NaSi}$, 601.2809; found 601.2791.

IR (ATR, neat, cm^{-1}): 2952 (m), 2930 (m), 2857 (w), 1774 (s), 1746 (m), 1679 (s), 1598 (w), 1231 (s), 1033 (s), 997 (s).



Alcohol **1.106**:

To a solution of aldehyde **1.81** (687 mg, 1.19 mmol, 1.0 equiv.) in 2-butanone (12 mL, 0.10 M) in a pressure tube was added PPTS (1.79 g, 7.12 mmol, 6.0 equiv.). The mixture was heated to 80 °C and left to stir overnight. The solution was cooled to room temperature and concentrated. The residue was dissolved in CH₂Cl₂ (30 mL) and washed with brine (2×20 mL). The organic layer was dried over MgSO₄, filtered and concentrated. The obtained crude product was purified by flash column chromatography (SiO₂, hexanes : EtOAc = 1:1) to give alcohol **1.106** (389 mg, 0.727 mmol, 61%) as a yellow foam.

$[\alpha]_D^{23} = 91.9^\circ$ (c = 10.0 mg/mL, CHCl₃)

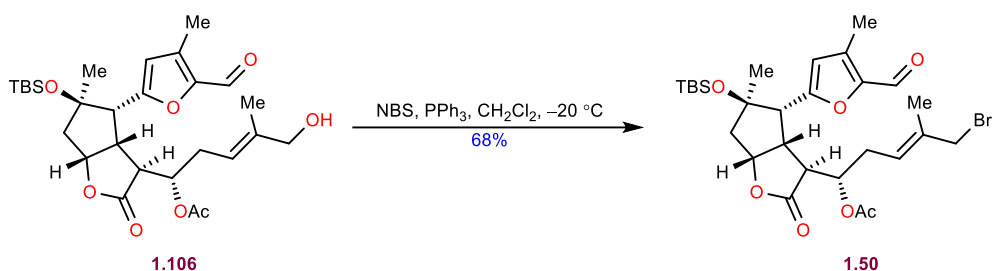
$R_f = 0.3$ (SiO₂, hexanes : EtOAc = 1:1)

¹H NMR (500 MHz, CDCl₃) δ 9.63 (s, 1H), 6.15 (s, 1H), 5.22 (t, J = 7.8 Hz, 1H), 5.20 – 5.14 (m, 1H), 5.09 (td, J = 7.8, 5.4 Hz, 1H), 3.95 (s, 2H), 3.59 (td, J = 8.6, 2.8 Hz, 1H), 3.36 (dd, J = 8.9, 1.7 Hz, 1H), 2.56 (dt, J = 13.8, 6.6 Hz, 1H), 2.48 (ddd, J = 14.4, 7.4, 1.8 Hz, 1H), 2.32 (s, 3H), 2.28 – 2.19 (m, 3H), 2.01 (s, 3H), 1.67 (s, 3H), 1.22 (s, 3H), 0.89 (s, 9H), 0.15 (s, 3H), 0.15 (s, 3H).

¹³C{¹H} NMR (126 MHz, CDCl₃) δ 177.8, 177.5, 169.7, 157.8, 148.7, 139.4, 118.0, 115.4, 85.7, 84.5, 73.5, 68.1, 55.6, 46.8, 46.8, 43.3, 30.7, 25.7, 25.7, 24.1, 21.1, 18.1, 14.0, 10.6, -2.2, -2.4.

HRMS: (ES⁺, *m/z*) [M+Na]⁺ calcd. for C₂₈H₄₂O₈NaSi, 557.2547; found 557.2552.

IR (ATR, neat, cm⁻¹): 3484 (br), 2953 (m), 2929 (m), 2856 (w), 1772 (s), 1748 (m), 1678 (m), 1598 (w), 1233 (s), 997 (s).



Bromide **1.50**:

To a solution of alcohol **1.106** (338 mg 0.632 mmol, 1.0 equiv.) in CH_2Cl_2 (13 mL, 0.050 M) at $-20\text{ }^\circ\text{C}$ was added PPh_3 (249 mg, 0.948 mmol, 1.5 equiv.) followed by NBS (169 mg, 0.948 mmol, 1.5 equiv.). After stirring for 30 minutes at the same temperature, water was added (10 mL) and the layers were separated. The aqueous layer was extracted with CH_2Cl_2 (2×10 mL), The organic layers were combined, dried over MgSO_4 , filtered and concentrated. The obtained crude material was purified by flash column chromatography (SiO_2 , hexanes : EtOAc = 3:1) to give bromide **1.50** (256 mg, 0.428 mmol, 68%) as a yellow foam.

$[\alpha]_{\text{D}}^{23} = 44.9^\circ$ ($c = 10.4$ mg/mL, CHCl_3)

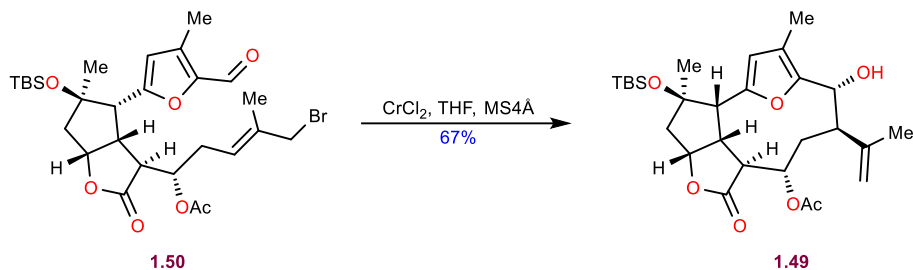
$R_f = 0.5$ (SiO_2 , hexanes : EtOAc = 2:1)

$^1\text{H NMR}$ (500 MHz, CDCl_3) δ 9.65 (d, $J = 1.0$ Hz, 1H), 6.18 (s, 1H), 5.40 (t, $J = 7.5$ Hz, 1H), 5.18 (td, $J = 6.9, 3.7$ Hz, 1H), 5.10 (td, $J = 7.7, 5.3$ Hz, 1H), 3.87 (s, 2H), 3.55 (td, $J = 8.5, 2.8$ Hz, 1H), 3.35 (d, $J = 8.6$ Hz, 1H), 2.55 – 2.43 (m, 2H), 2.33 (s, 3H), 2.30 – 2.20 (m, 3H), 2.02 (d, $J = 0.9$ Hz, 3H), 1.76 (s, 3H), 1.61 (br, 1H), 1.18 (s, 3H), 0.89 (d, $J = 0.9$ Hz, 9H), 0.15 (s, 3H), 0.14 (s, 3H).

$^{13}\text{C}\{^1\text{H}\}$ NMR (126 MHz, CDCl_3) δ 178.2, 177.1, 169.6, 157.2, 148.9, 136.2, 123.8, 115.9, 85.8, 84.4, 72.8, 55.6, 47.0, 46.7, 43.2, 40.3, 31.6, 25.7, 25.7, 24.2, 21.0, 18.1, 15.1, 10.7, -2.2 , -2.4 .

HRMS: (ES+, m/z) $[\text{M}+\text{H}]^+$ calcd. for $\text{C}_{28}\text{H}_{42}\text{O}_7\text{Si}^{79}\text{Br}$, 597.1883; found 597.1885.

IR (ATR, neat, cm^{-1}): 2953 (m), 2929 (m), 2856 (m), 1773 (s), 1748 (m), 1679 (s), 1627 (w), 1598 (w), 1225 (s), 997 (s).



Macrocycle **1.49**:

THF (90 mL, 2.2 mM in respect to the substrate) was added to a flask containing CrCl_2 (494 mg, 4.02 mmol, 20 equiv.) and powdered MS4Å (2.0 g). In a separate flask, bromide **1.50** (120 mg, 0.201 mmol, 1.0 equiv.) was dissolved in THF (9 mL) and the obtained solution was taken into a glass syringe and added dropwise to the former solution with a syringe pump over 10 hours. After stirring for 6 more hours, the mixture was filtered through celite and quenched with H_2O (30 mL). The obtained solution was concentrated until most of the THF has evaporated. The residue was transferred to a separation funnel and extracted with EtOAc (3×20 mL). The combined organic layers were washed with brine (30 mL), dried over MgSO_4 , filtered and concentrated. The obtained residue was purified by flash column chromatography (SiO_2 , hexanes : EtOAc = 2:1) to give macrocycle **1.49** (71 mg, 0.137 mmol, 68%) as a pale foam.

$[\alpha]_D^{23} = 2.2^\circ$ ($c = 12.7 \text{ mg/mL}$, CHCl_3)

$R_f = 0.4$ (SiO_2 , hexanes : EtOAc = 2:1)

$^1\text{H NMR}$ (500 MHz, CDCl_3) δ 6.02 (s, 1H), 5.26 (ddd, $J = 12.2, 3.3, 1.4 \text{ Hz}$, 1H), 5.10 (d, $J = 1.7 \text{ Hz}$, 1H), 5.08 (t, $J = 1.6 \text{ Hz}$, 1H), 4.99 (ddd, $J = 8.9, 6.2, 3.7 \text{ Hz}$, 1H), 4.52 (dd, $J = 10.0, 2.5 \text{ Hz}$, 1H), 3.70 (dd, $J = 7.5, 1.5 \text{ Hz}$, 1H), 3.41 (d, $J = 8.3 \text{ Hz}$, 1H), 3.29 (q, $J = 8.3 \text{ Hz}$, 1H), 2.55 (dd, $J = 9.5, 6.2 \text{ Hz}$, 1H), 2.25 – 2.19 (m, 2H), 2.10 (br, 1H), 2.06 (s, 3H), 1.92 (s, 3H), 1.82 (s, 3H), 1.59 (ddd, $J = 13.6, 7.0, 3.4 \text{ Hz}$, 1H), 1.42 (s, 3H), 0.86 (s, 9H), 0.43 (ddd, $J = 13.6, 12.1, 1.4 \text{ Hz}$, 1H), 0.08 (s, 3H), 0.05 (s, 3H).

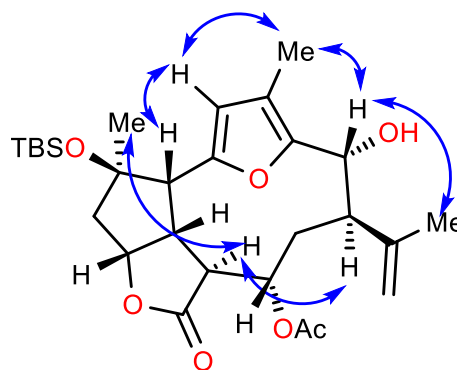
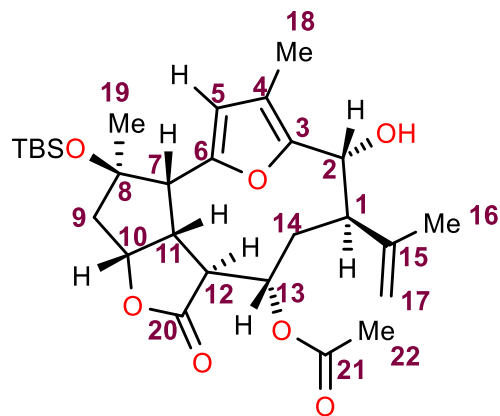
$^{13}\text{C}\{^1\text{H}\} \text{NMR}$ (126 MHz, CDCl_3) δ 177.9, 169.2, 151.8, 149.8, 143.9, 122.4, 116.7, 113.6, 80.3, 80.0, 73.9, 65.8, 54.2, 51.9, 48.7, 45.7, 42.3, 31.5, 27.2, 25.8, 21.1, 18.5, 18.0, 9.9, -2.1, -2.3.

HRMS: (ES^+ , m/z) $[\text{M}+\text{H}]^+$ calcd. for $\text{C}_{28}\text{H}_{43}\text{O}_7\text{Si}$, 519.2778; found 519.2789.

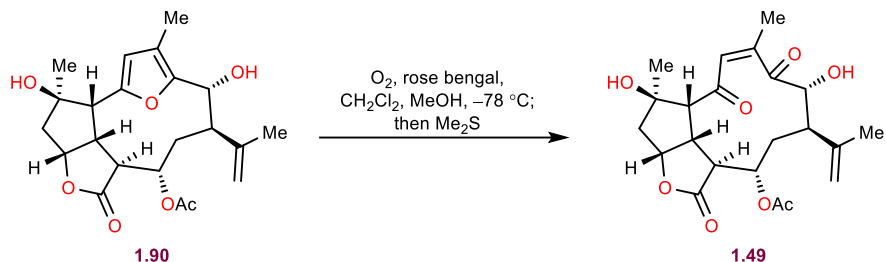
IR (ATR, neat, cm^{-1}): 3464 (br), 2954 (m), 2929 (m), 2856 (w), 1770 (s), 1647 (w), 1563 (w), 1218 (s), 1027 (s).

Full assignment and selected NOE correlations:

position	δ_{H} (ppm)	δ_{C} (ppm)
1	2.55	51.9
2	4.52	65.8
3	/	149.8
4	/	122.4
5	6.02	113.6
6	/	151.8
7	3.41	54.2
8	/	80.3
9	2.25–2.19	48.7
10	4.99	80.0
11	3.29	42.3
12	3.71	45.7
13	5.26	73.9
14	1.59/0.43	31.5
15	/	143.9
16	1.82	18.5
17	5.08/5.11	116.7
18	2.06	9.9
19	1.42	27.2
20	/	177.9
21	/	169.2
22	1.92	21.1
OH	2.10	/
TBS	0.86/0.08/0.05	25.8/18.0/–2.1/–2.3

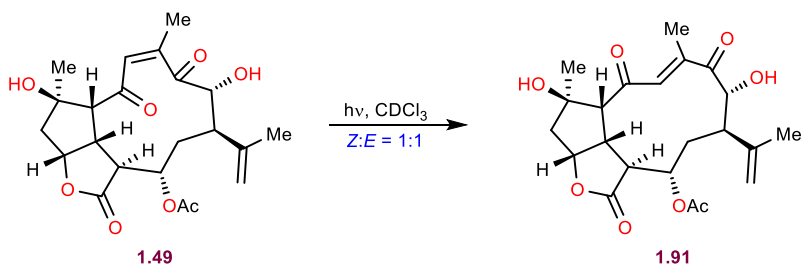


Key NOE correlations are marked



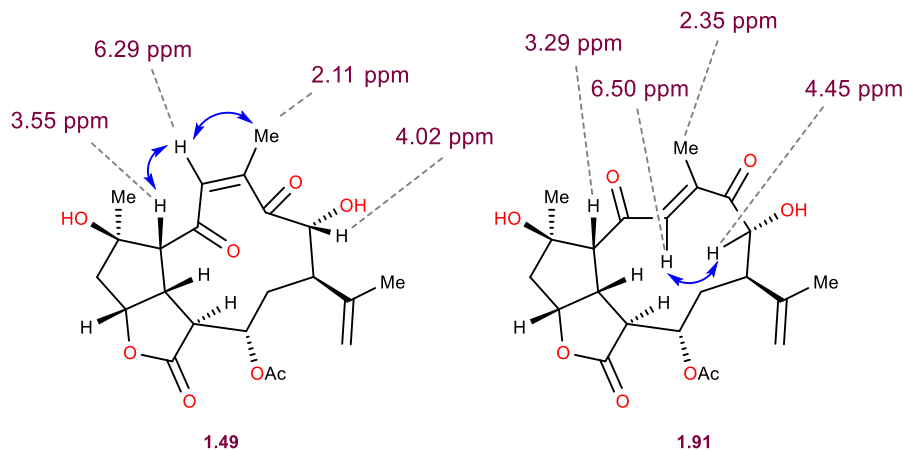
Enedione **1.49**:

Diol **1.90** (1.0 mg, 2.5 μmol , 1.0 equiv.) was dissolved in a mixture of CH_2Cl_2 (0.20 mL) and MeOH (0.10 mL). A single crystal of rose bengal was added. The mixture was cooled to $-78\text{ }^\circ\text{C}$. Oxygen was bubbled through the reaction mixture with a balloon while being irradiated with a visible light lamp (19.5 W) for 20 minutes. The lamp was turned off, and Me_2S (0.050 mL) was added at $-78\text{ }^\circ\text{C}$. The dry ice bath was switched to a regular ice bath. After stirring for 1 hour at $0\text{ }^\circ\text{C}$, the solvent was removed in vacuo. The obtained residue was rapidly filtered through a silica plug (CH_2Cl_2 : MeOH=95:5) to remove rose bengal. The unstable enedione **1.49** was used for the next step immediately.



Enedione **1.91**:

Enedione **1.49** obtained in the previous step was dissolved in $CDCl_3$ (0.30 mL) in an NMR tube. The tube was irradiated with a reptile lamp (100 W). The reaction progress was monitored by ^1H NMR. After 20 minutes, the ratio of the enediones was $Z(\mathbf{1.49}) : E(\mathbf{1.91}) = 1.4:1$. At this point, NMR spectra were taken for characterization. If the reaction mixture is being irradiated for 1 hour, a photostationary state is achieved with the ratio $Z : E = 1:1$, but with noticeable decomposition. Key NOE correlations that were indicative of the isomerization are shown below:



X-Ray Data for bicyclic lactone 1.66

Warning: raw dataset was not collected with high average redundancy and lacks absorption correction. Therefore, the data presented is for the purposes of qualitative assessment of unit cell contents, such as atom types, connectivity, and relative stereochemistry.

Single crystal for the experiment were obtained by vapor diffusion of pentane into a solution of **1.66** in EtOAc. A suitable specimen was mounted on Cryo-Loop using Paratone-N oil. Data were acquired and integrated with APEX3 software with on a Bruker D8 Venture diffractometer equipped with Photon II detector. The crystal was kept at 100 K during data collection. No absorption correction was performed. Using OLEX2,⁶⁹ the structure was solved with the XT⁷⁰ structure solution program using Intrinsic Phasing and and refined with the XL⁷¹ refinement package using full-matrix least squares minimization against F2.

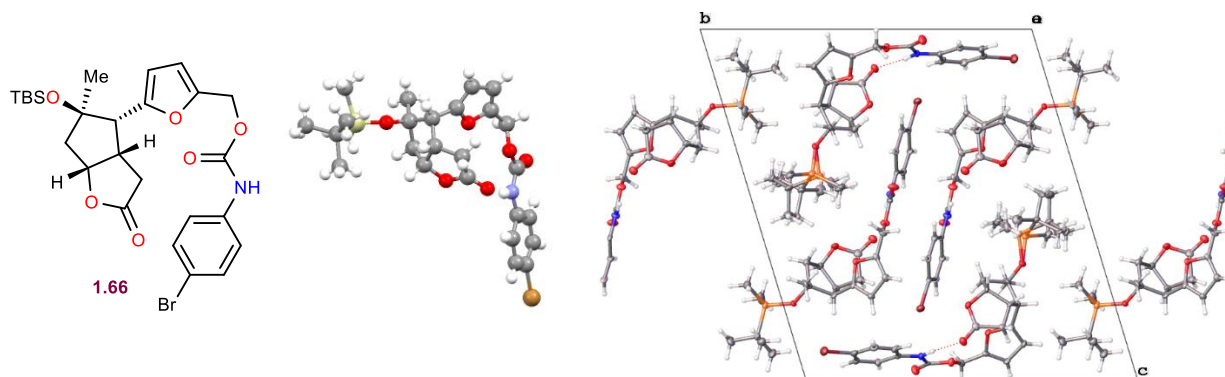


Table 1 Crystal data and structure refinement for dd25v_0m.

Identification code	dd25v_0m
Empirical formula	C ₂₆ H ₃₄ BrNO ₆ Si

Formula weight	564.54
Temperature/K	101.13
Crystal system	triclinic
Space group	<i>P</i> $\bar{1}$
<i>a</i> /Å	7.1706(2)
<i>b</i> /Å	19.1013(6)
<i>c</i> /Å	20.8410(6)
α /°	105.880(2)
β /°	93.771(2)
γ /°	99.829(2)
Volume/Å ³	2686.18(14)
<i>Z</i>	4
ρ_{calc} /cm ³	1.396
μ /mm ⁻¹	1.615
<i>F</i> (000)	1176.0
Crystal size/mm ³	n / a
Radiation	MoK α (λ = 0.71073)
2 Θ range for data collection/°	4.39 to 50.976
Index ranges	-8 \leq <i>h</i> \leq 8, -23 \leq <i>k</i> \leq 22, -24 \leq <i>l</i> \leq 25
Reflections collected	29153
Independent reflections	9703 [<i>R</i> _{int} = 0.5372, <i>R</i> _{sigma} = 0.4909]
Data/restraints/parameters	9703/734/706
Goodness-of-fit on <i>F</i> ²	0.652
Final <i>R</i> indexes [<i>I</i> \geq 2 σ (<i>I</i>)]	<i>R</i> ₁ = 0.0573, <i>wR</i> ₂ = 0.0965
Final <i>R</i> indexes [all data]	<i>R</i> ₁ = 0.1524, <i>wR</i> ₂ = 0.1161
Largest diff. peak/hole / e Å ⁻³	0.37/-0.74

51. Brill, Z. G.; Grover, H. K.; Maimone, T.J. *Science* **2016**, *352*, 1078–1082.
52. Yamamoto, Y.; Yamamoto, S.; Yatagai, H.; Ishihara, Y.; Maruyama, K. *J. Org. Chem.* **1982**, *47*, 119–126.
53. Burgess, E. M.; Penton Jr. H. R.; Taylor, E. A. *J. Org. Chem.* **1973**, *38*, 26–31.
54. Shimomaki, K.; Kusama, H.; Iwasawa, N. *Chem. Eur. J.* **2016**, *22*, 9953–9957.
55. Kuethe, J. T.; Wong, A.; Wu, J.; Davies, I. W.; Dormer P. G.; Welch, C. J.; Hillier, M. C.; Hughes, D. L.; Reider P. J. *J. Org. Chem.* **2002**, *67*, 5993–6000.
56. Suemune, H.; Maruoka, H.; Saeki, S.; Sakai, K. *Chem. Pharm. Bull.* **1986**, *34*, 4629–4634.
57. Saitman, A.; Theodorakis, E. A. *Org. Lett.* **2013**, *15*, 2410–2413.
58. Baldwin, J. E.; Bulger, P. G.; Marquez, R. *Tetrahedron* **2002**, *58*, 5441–5452.
59. Adinolfi, M.; Barone, G.; Guariniello, L.; Iadonisi, A. *Tetrahedron Letters* **2000**, *41*, 9305–9309.
60. Monti, H.; Léandri, G.; Klos-Ringuet M.; Corriol, C. *Synthetic Communications* **1983**, *13*, 1021–1026.
61. Tsuge, A.; Otsuka, M.; Moriguchi, T.; Sakata, K. *Org. Biomol. Chem.* **2005**, *3*, 3590–3593.
62. Haynes, S. W.; Sydor, P. K.; Corre C.; Song, L.; Challis, G. L. *J. Am. Chem. Soc.* **2011**, *113*, 1793–1798.
63. Kimbrough, T. J. (2011) *Synthesis of Coralloidolide B, Coralloidolide C, Photochemical Synthesis of Intricarene and Progress Towards the Synthesis of Bielschowskysin* (Doctoral dissertation, UC Berkeley).
64. Scheidt, K. A.; Bannister, T.D.; Tasaka, A.; Wendt, M. D.; Savall, B. M.; Fegley, G. J.; Roush, W. R. *J. Am. Chem. Soc.* **2002**, *124*, 6981–6990.
65. Marhsall, J. A.; Bartley, G. A.; Wallace E. M. *J. Org. Chem.* **1996**, *61*, 5729–5735.
66. Li, Y.; Pattenden, G. *Tetrahedron Letters* **2011**, *52*, 3315–3319.
67. Ethyl glyoxylate was bought from Oakwood as a 50% solution in toluene. Distillation was done according to: Terada, M.; Soga, K.; Momiyama, N. *Angew. Chem. Int. Ed.* **2008**, *47*, 4122–4125. The amount of P₂O₅ used varied for different bottles of commercial ethyl glyoxylate. Most commonly, the drying agent was added until a clear light-green non-viscous liquid started distilling (monomeric ethyl glyoxylate). Note that too much P₂O₅ leads to irreversible polymerization.

68. Burgess reagent was prepared according to: Burgess, E. M.; Penton, H. R. Jr.; Taylor, E. A.; Williams, W. M. *Org. Synth.* **1977**, *56*, 40.
69. Dolomanov, O. V.; Bourhis, L. J.; Gildea, R. J.; Howard, J. A. K.; Puschmann, H. *J Appl. Cryst.* **2009**, *42*, 339–341.
70. Sheldrick, G. M. *Acta Cryst.* **2015**, *A71*, 3–8.
71. Sheldrick, G. M. *Acta Cryst.* **2008**, *A64*, 112–122.

1.7 Acknowledgements and Contributions

A. Shved is acknowledged for obtaining X-ray crystallography data. D. L. Olson and L. Zhu are acknowledged for NMR spectroscopic assistance. F. Sun is acknowledged for assistance with mass spectrometry. Y. Zhou, M. M. Kincanon and D. B. Ryffel performed scale-ups of early synthetic intermediates. P. Kravljanc has explored an alternative macrocyclization strategy that wasn't mentioned here. Synthesis planning and forward synthesis including initial scale-ups, optimizations, frontline exploration and data analysis were performed by M. Nesic.

CHAPTER 2: TOTAL SYNTHESIS OF DAROBACTIN A[†]

2.1 Introduction

Ribosomally synthesized and post-translationally modified peptides (RiPPs) represent a diverse family of natural product, of which many members exhibit impressive bioactivities.^{1,2,3} The biosynthesis of these molecules is based on the assembly of a precursor peptide in the ribosome that is afterwards involved in various post-translational modifications often catalyzed by radical SAM (rSAM) and P450 enzymes. Commonly, these post-translational modifications result in macrocyclizations via cross-linking of amino acid side chains. Representative examples of such macrocyclic peptides are shown in Figure 2.1.

In recent years, antibiotic resistance has emerged as one of the biggest threats facing humanity, with many new strains of bacteria (particularly gram-negative bacteria) becoming resistant to common therapies.^{4,5} This is caused by the misuse of available antibiotics and is aggravated with the stagnation in the development of new treatments.^{6,7}

In 2019, the Lewis group has disclosed a novel ribosomally synthesized and post-translationally modified bismacrocyclic heptapeptide named darobactin A (**2.1** Figure 2.1). The natural product was isolated from *Photorhabdus khanii*, a gut bacteria symbiont of entomopathogenic nematodes (isolation yield 3 mg/L).⁸ Its structure is decorated with very interesting connectivity patterns (**2.1**, Figure 2.2a). The unique ether linkage between the two tryptophans is activated at the β -position of the eastern tryptophan and is likely to be somewhat unstable due to the presence of the electron-rich indole ring in its vicinity. The tryptophan-lysine connectivity was previously discovered in streptide (**2.3**, Figure 2.1), but has the opposite stereochemistry when compared to darobactin.⁹ Lastly, there are two highly strained macrocycles – a 15-membered ring in the western part and a 14-membered ring in the eastern portion of the molecule. Both of these have the potential of exhibiting atropisomerism.

Darobactin A has displayed remarkable antibacterial activity, targeting selectively gram-negative bacteria strains while simultaneously demonstrating no activity against commensal

[†]Portions of the herein described work have been previously published: Nesic, M.; Ryffel, D. B.; Maturano J.; Shevlin, M.; Pollack, S. R.; Gauthier, D. R.; Trigo-Mourino, P.; Zhang, L.-K.; Schultz, D.; McCabe Dunn, J.; Campeau, L.-C.; Patel, N. R.; Petrone, D. A.; Sarlah, D. *J. Am. Chem. Soc.* **2022**, *144*, 14026–14030

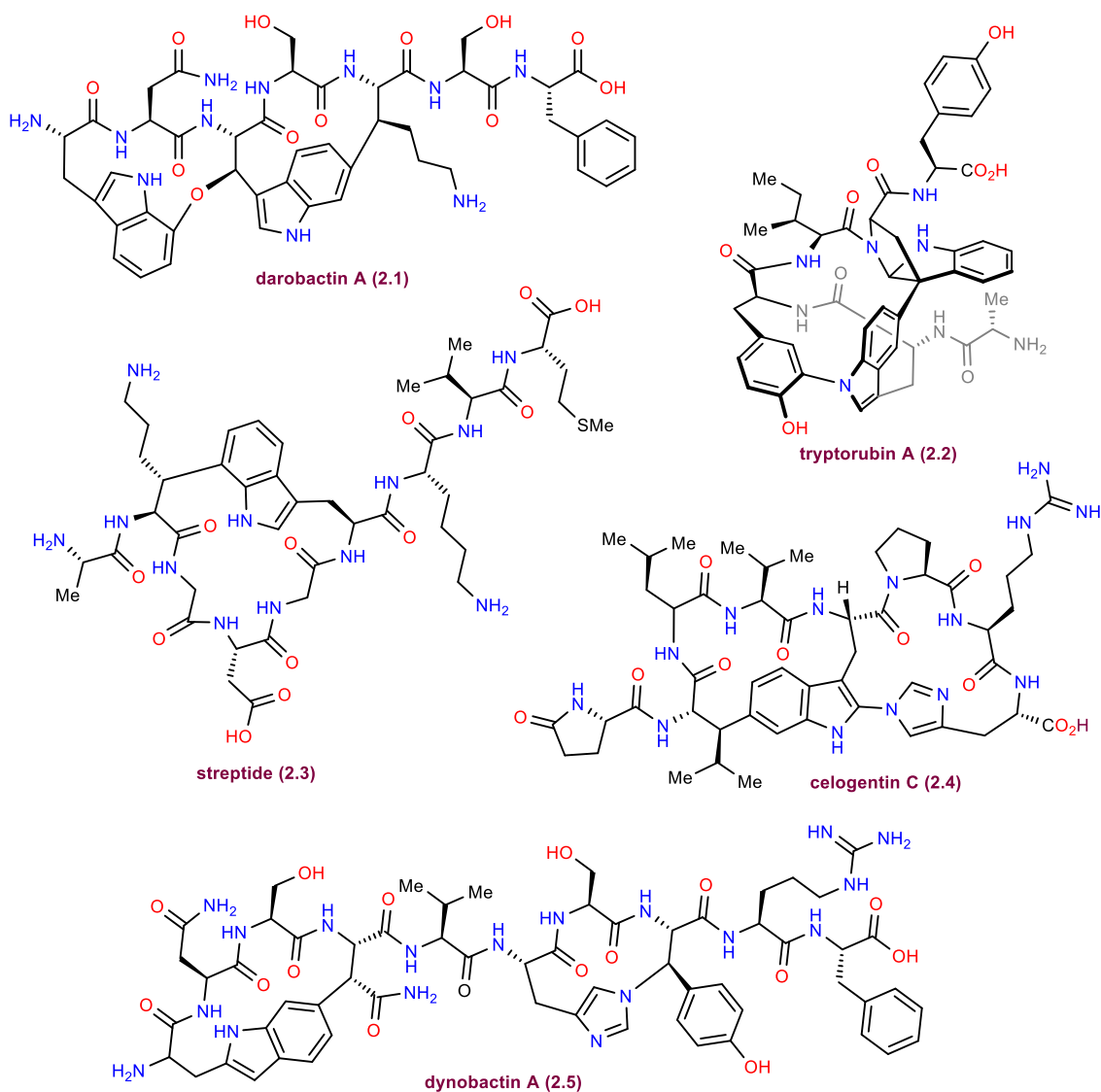


Figure 2.1: Selected examples of RiPPs

strains of gram-positive gut bacteria. The impressive selectivity is achieved through a completely novel mechanism of action. This antibiotic binds to the BamA subunit of the β -barrel assembly machinery (Bam) protein complex, which is unique to gram-negative bacteria and is located on their outer membrane (Figure 2.2b).^{10,11} The Bam complex is responsible for the folding and insertion of outer membrane proteins. Notably, both macrocycles of darobactin A have significant influence on its bioactivity. More specifically, they are holding the peptide backbone in a β -sheet conformation, in result reducing the entropic cost of binding to the β 1 strand of BamA (Figure 2.2c). It is postulated that upon binding of darobactin A to BamA, the Bam complex is stabilized in its inactive conformation, being unable to perform its normal function. Therefore, new outer

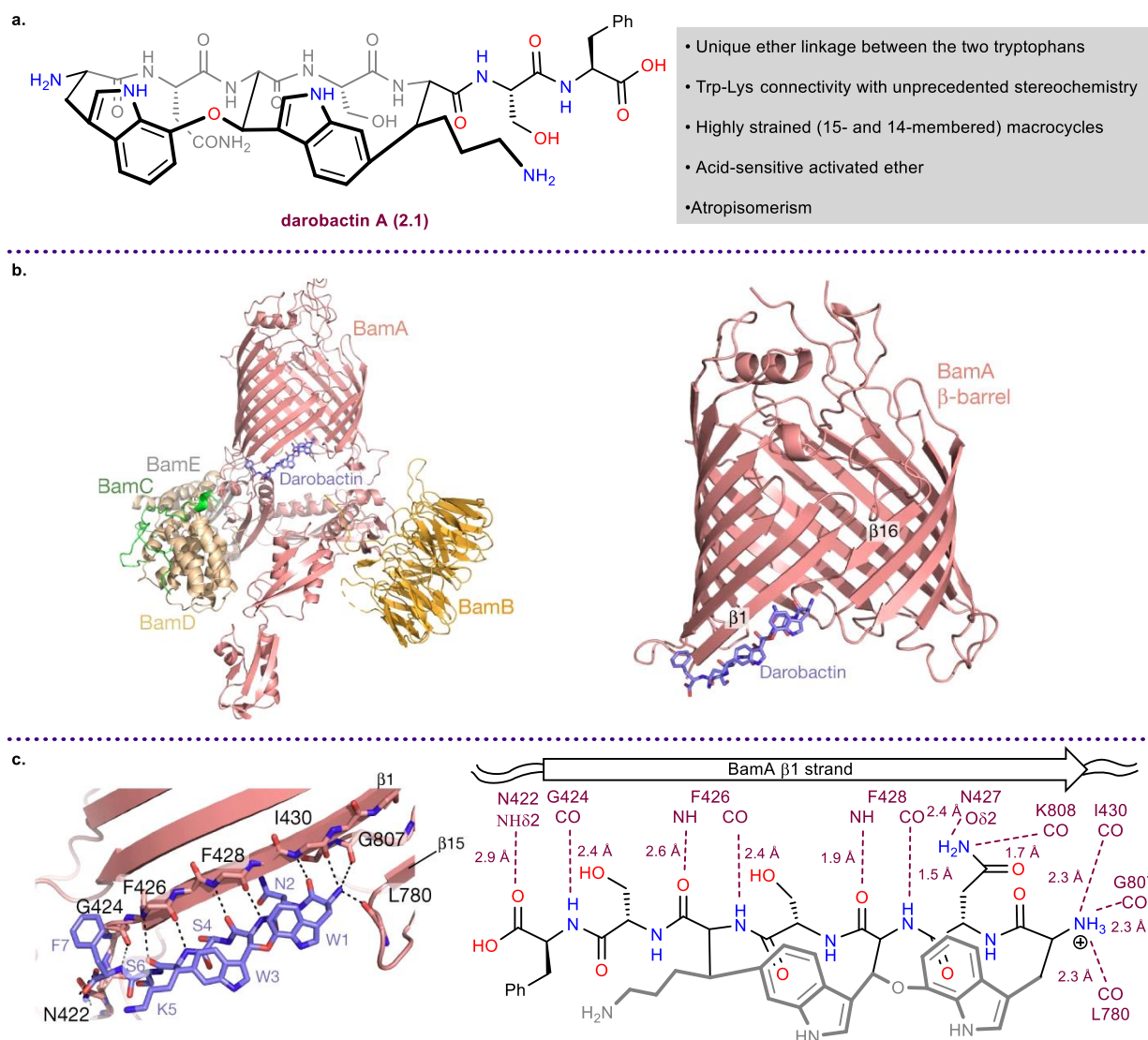
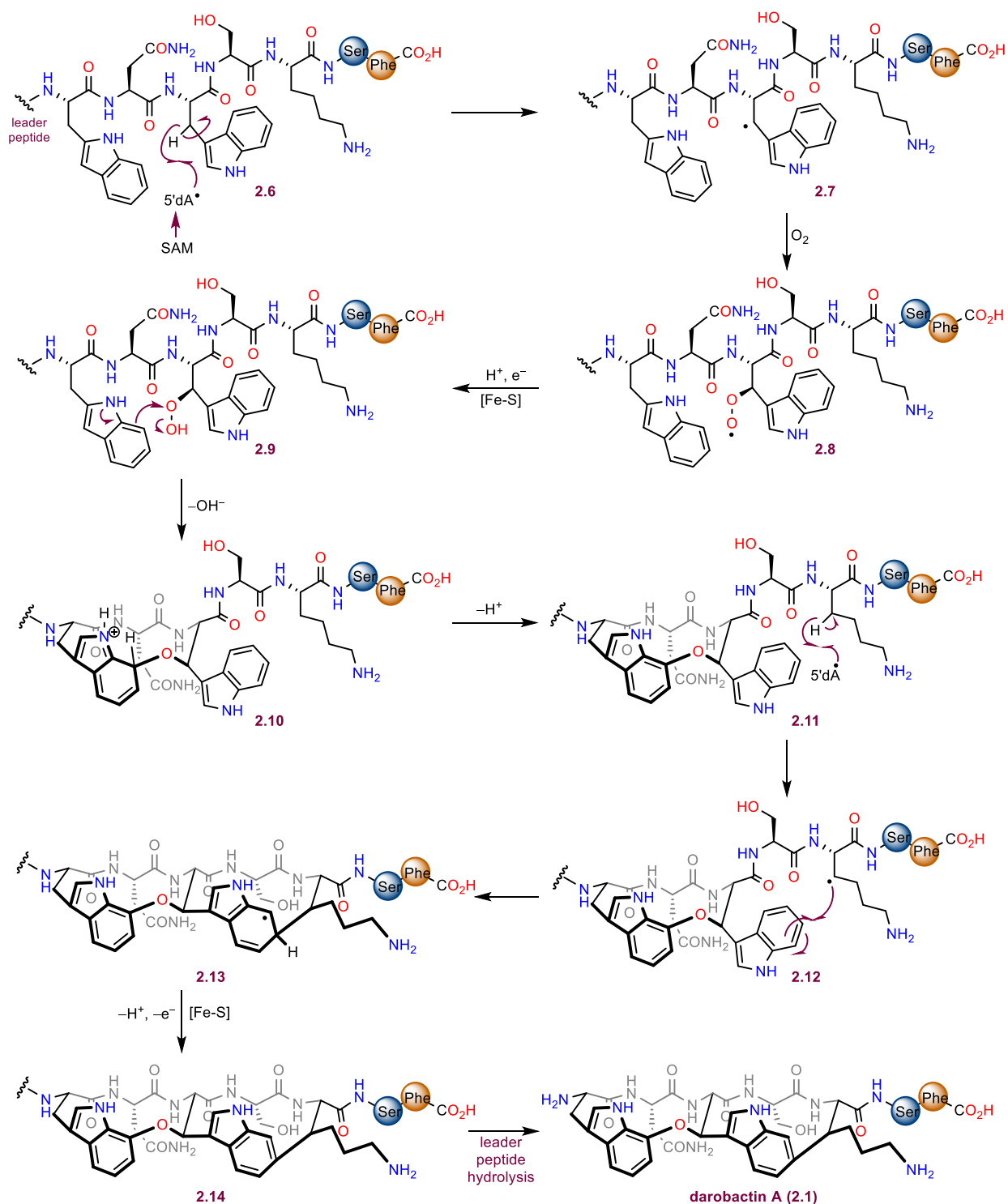


Figure 2.2: a. Perspective view of darobactin A and structural features; b. Darobactin A inside Bam (left) and bonded to BamA (right); c. detailed view of the binding with the β 1-strand of BamA

membrane proteins can't be folded properly, which disrupts the working of the outer membrane and subsequently results in the death of the pathogen. By binding to an outer membrane receptor, darobactin doesn't have to pass through the cell membrane of gram-negative bacteria, bypassing the biggest challenge that an antibiotic targeting these pathogens has to overcome.

Since darobactin A is a RiPP, its biosynthesis starts with the assembly of the linear heptapeptide by the ribosome. Then, a single enzyme called DarE is responsible for crosslinking the side chains of the two tryptophans and lysine, resulting in the formation of both macrocycles.¹²⁻¹⁴ DarE is a rSAM enzyme and works in the manner depicted in Scheme 2.1.¹⁵ (S)-adenosyl

methionine (SAM) is first converted to 5'-deoxyadenosyl radical (5'dA). This reactive species abstracts the β -hydrogen of the central tryptophan in **2.6** producing radical **2.7** that is trapped by



Scheme 2.1: Current biosynthetic proposal for darobactin A

oxygen affording peroxy radical **2.8**. Subsequent electron transfer with an iron-sulfur cluster [Fe-S] and protonation result in the formation of hydroperoxyde **2.9**.¹⁴ This sequence makes DarE a rare example of a rSAM oxygenase. One possibility for the formation of the western macrocycle is through electrophilic aromatic substitution at the C7 position of the western indole where the previously formed hydroperoxide is acting as the electrophile (**2.9**→**2.10**). Upon rearomatization of the indole, the western macrocycle **2.11** is established. The formation of the eastern macrocycle occurs only after the formation of the western one.¹³ Thereafter, another 5'-deoxyadenosyl radical abstracts the β -hydrogen of lysine and the obtained β -radical **2.12** adds to the C6 position of the eastern indole (**2.12**→**2.13**).¹² Electron transfer with [Fe-S] cluster and proton loss result in rearomatization of the indole **2.14**. At last, hydrolytic removal of the leader peptide reveals darobactin A (**2.1**).

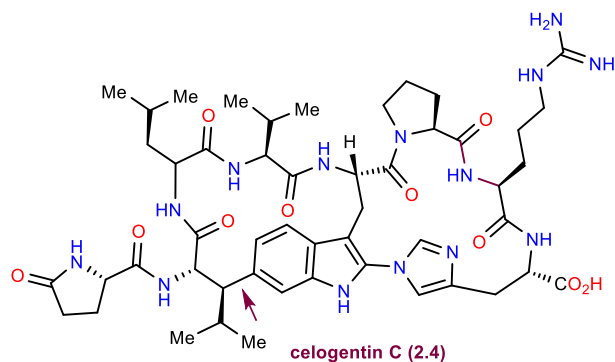
The interesting structural features and impressive bioactivity of this natural product sparked our interest in synthesizing it. In addition, a total synthesis would provide an entry into darobactin analogs that are inaccessible through genome mining and silent gene expression.¹⁶⁻¹⁸

2.2 Previous total syntheses of RiPPs

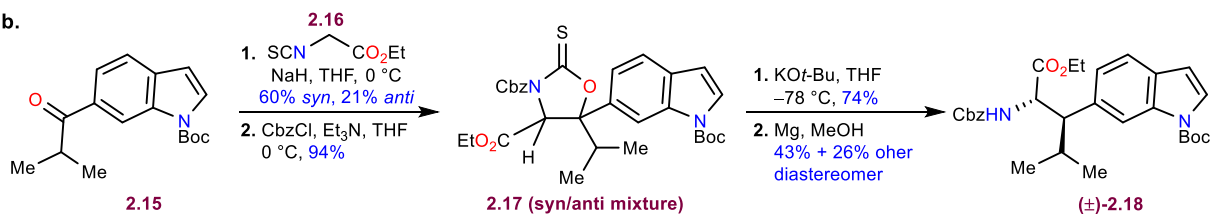
RiPPs have inspired synthetic chemists to develop clever ways of forging the non-canonical connectivity patterns present between the amino acid side-chains.¹⁹⁻²¹ Several elegant syntheses will be presented below to showcase the different approaches towards the formation of these linkages and the ensuing macrocycles.

Celogentin C (**2.4**) was isolated in 2001 and contains a bismacrocylic framework, where the western macrocycle is cross-linked at the C6 position of tryptophan and β -position of lysine (Scheme 2.2a).²² Several research groups have published vastly different approaches for the formation of this connectivity. In 2006, Moody's group has reported their synthetic study towards celogentin C (**2.4**).²³ Starting with indole **2.15**, an aldol addition was performed with the lithium enolate of ester **2.16** where the resulting alkoxyde attacks the isothiocyanate to form an oxazolidinethione ring (Scheme 2.2b). The free amine is subsequently protected with a Cbz group affording **2.17** as a syn/anti mixture. Elimination with KO*t*-Bu formed an α,β -unsaturated ester that was reduced with Mg in MeOH producing **2.18** as a mixture of diastereomers where the major

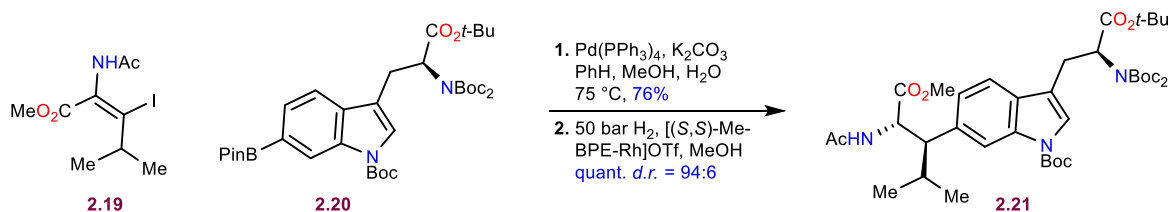
a.



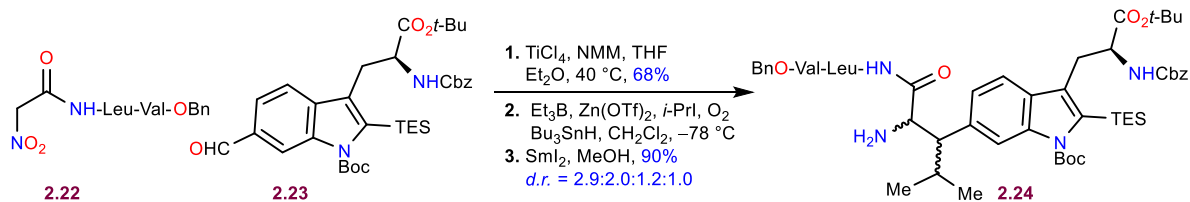
b.



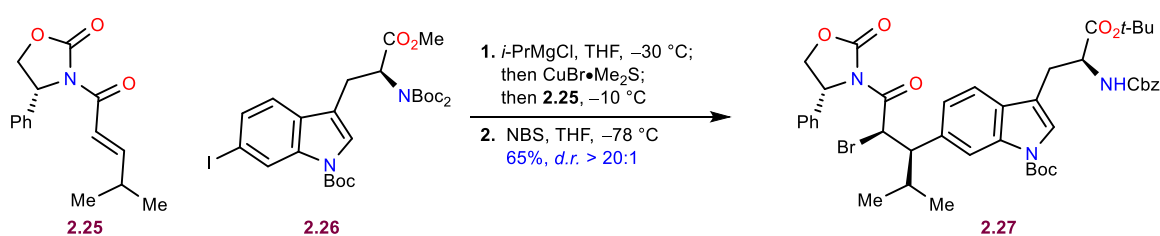
c.



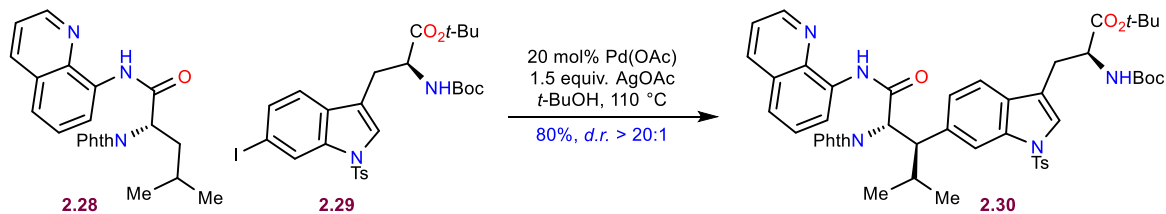
d.



e.



f.

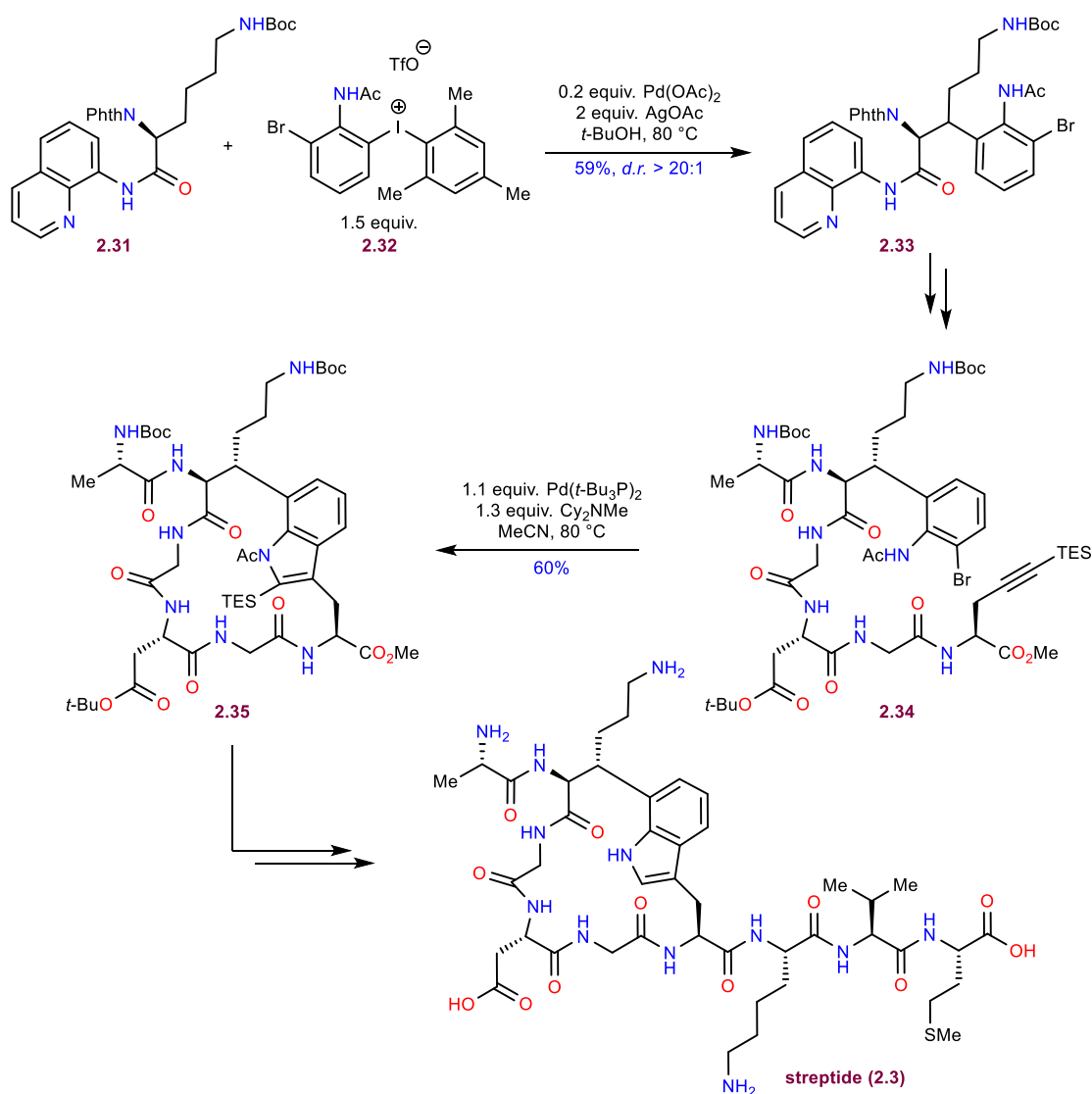


Scheme 2.2: a. Structure of celogentin C with the Trp-Leu C–C linkage emphasized; Different strategies for connecting Trp and Leu by b. aldol chemistry; c. asymmetric hydrogenation; d. radical conjugate addition; e. conjugate addition with a chiral auxiliary and f. C–H activation chemistry

one was taken further after chromatographic separation (43% yield). Since this compound was still a racemate, separation of the enantiomers was done at a later stage and the study concluded with the formation of the western marocycle. In 2008, Campagne's lab has disclosed their attempt at the synthesis of the tryptophan-leucine residue via asymmetric hydrogenation (Scheme 2.2c).²⁴ Iodoenamide **2.19** was unified with boronate **2.20** via Suzuki coupling and the resulting olefin was hydrogenated with a chiral rhodium catalyst affording **2.21**. In contrast to Moody's route, the asymmetric hydrogenation was highly stereoselective. However, it required the enamide nitrogen to be protected as an acetamide, which was difficult to deprotect. If a Cbz group is used instead, the stereoselectivity is greatly diminished. The first total synthesis of celogentin C (**2.4**) was published by Castle in 2009 (Scheme 2.2d).^{25,26} His approach at connecting leucine with tryptophan relied on a Knoevenagel condensation between **2.22** and **2.23**. The isopropyl group is added to the obtained nitroolefin via radical conjugate addition resulting in four diastereomers of **2.24** after reduction of the nitro group with SmI₂. In a similar vein to Moody's approach, the low stereoselectivity required the separation of four stereoisomers, thereby significantly reducing material throughput. While two of them could be separated at this stage, the remaining two could only be separated after further derivatization. In 2010, Jia and coworkers have reported their synthesis of celogentin C where the tryptophan-lysine linkage is formed in a stereoselective manner (Scheme 2.2e).²⁷ Their approach was centered on the conjugate addition of the organocuprate species derived from iodotryptophan **2.26**, where the stereoselectivity was enforced through the presence of Evans' auxiliary on the Michael acceptor **2.25**. The resulting enolate was trapped with NBS, to afford bromide **2.27** as a single diastereomer that was elaborated into the natural product in 13 steps. In the same year, Chen's group has published another total synthesis of celogentin C with a highly elegant solution to the stereoselectivity issue.²⁸ They made use of C-H activation chemistry to connect leucine derivative **2.28** and iodotryptophan **2.29**, producing **2.30** in excellent yield (80%) as a single diastereomer. The only inconvenience with this strategy is the necessary presence of the 8-aminoquinoline directing group and protection of the α -nitrogen of leucine with a phthaloyl group. Manipulations required to introduce these groups and then to remove them after the C-H activation, lowered the step economy of the synthesis. In all of these approaches, the macrocycles were formed through macrolactamization.

Streptide (**2.3**) is a macrocyclic RiPP isolated in 2015 by Seyedsayamdost. This natural product has the β -position of lysine and the the C7 position of tryptophan cross-linked to form the

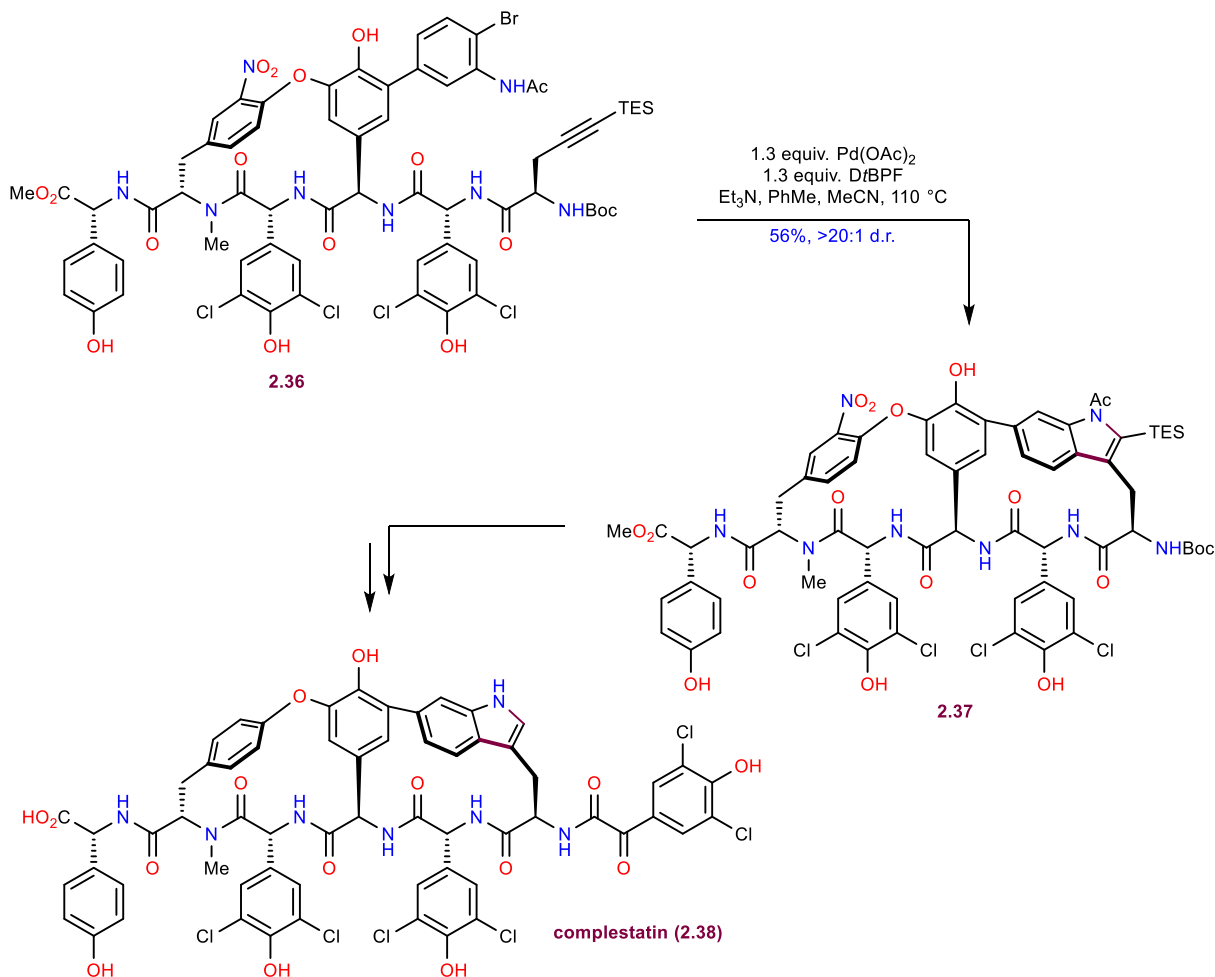
20-membered ring.⁹ The molecule has succumbed to total synthesis in 2019, by the work of Boger and co-workers (Scheme 2.3).²⁹ Inspired by Chen's application of C–H activation in the synthesis of celogentin C, they have decided to employ a similar approach to the formation of the tryptophan-lysine linkage. However, instead of employing a tryptophan derivative as the electrophile, a bromoacetanilide precursor has been chosen that could be later elaborated into the indole ring. A hypervalent iodine derivative **2.32** turned out to be most efficient one in this challenging step and allowed for the highly successful C–H insertion with lysine derivative **2.31**. The product **2.33** was obtained as a single diastereomer in 59% yield. If an aryl iodide is used instead of the iodonium salt, the yield would drop to 27%. Intermediate **2.33** was elaborated in a few steps into compound



Scheme 2.3: Total synthesis of streptide

2.34. Macrocyclization was then performed via Larock indole synthesis to produce **2.35** in 60% yield. From here, streptide (**2.3**) could be obtained in several uneventful steps.

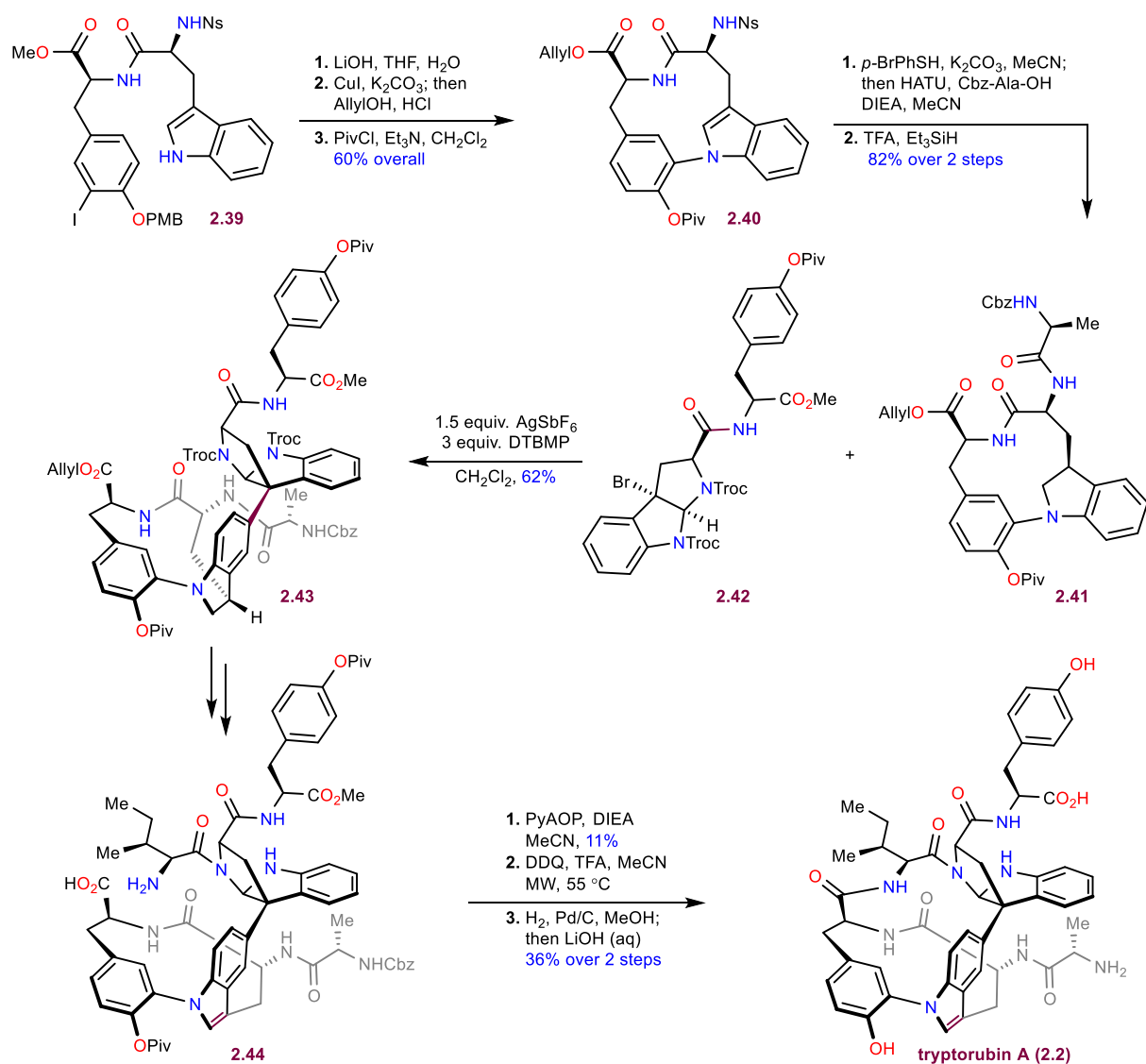
The impressive macrocyclization via Larock indole synthesis has been previously utilized by the Boger lab in their total synthesis of the nonribosomal peptide (NRP) complestatin (**2.38**, Scheme 2.4).³⁰⁻³² Advanced intermediate **2.36** was treated with 1.3 equiv. of Pd(OAc)₂ in the presence of 1,1'-Bis(di-*tert*-butylphosphino)ferrocene (DtBPF) ligand and triethylamine at 110 °C to furnish the bismacrocycle **2.37** in 56% yield as a single diastereomer/atropisomer. Complestatin (**2.38**) could be obtained in a couple of steps from this intermediate.



Scheme 2.4: Total synthesis of complestatin

Tryptorubin (**2.2**) is a bismacroyclic ribosomally synthesized and post-translationally modified hexapeptide stapled through a C–C connectivity between the two tryptophans, as well as an N–C linkage between one of the tryptophans and tyrosine (Scheme 2.5).³³ In 2020, Baran and co-workers have published the synthesis of this intriguing natural product.³⁴ The N–C linkage

between tryptophan and tyrosine was created through an Ullmann C–N coupling in the following manner: methyl ester **2.39** was hydrolyzed to the carboxylic acid, and this compound was subjected to the Ullmann coupling with CuI. Upon re-protection of the carboxylic acid as an allyl ester, product **2.40** was isolated in 60% overall yield. Subsequently, the Ns group was removed and the obtained free amine was coupled to Cbz-Ala-OH. The indole ring was then reduced to indoline **2.41** via ionic reduction with TFA and Et₃SiH. The reduction of the indole ring was crucial for the atroposelectivity of the second macrocyclization reaction. If the indole is not reduced, the second macrocycle could be obtained only as the undesired atropisomer. The C–C crosslink was formed next. Upon treatment of bromide **2.42** with AgSbF₆, ionization occurs and the formed carbocation

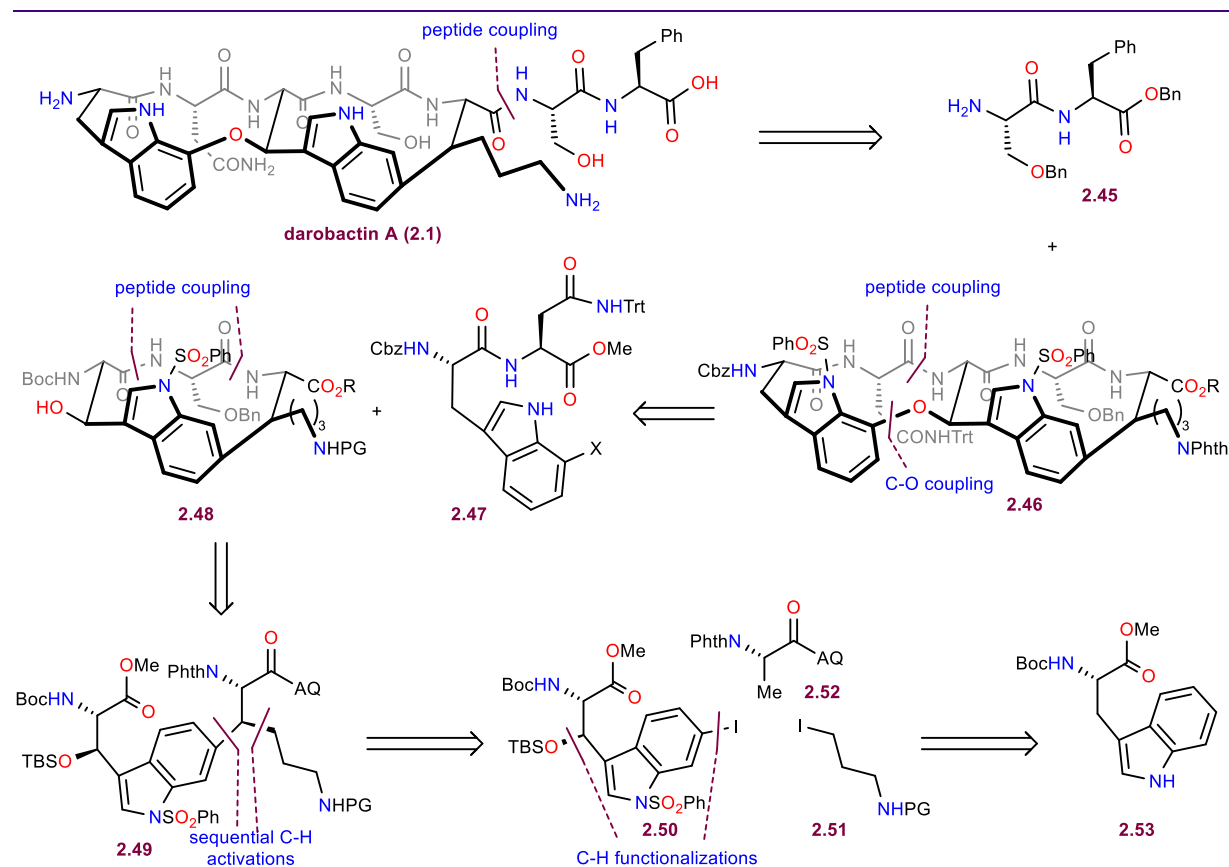


Scheme 2.5: Total synthesis of tryptorubin A

is trapped by the electron-rich indoline ring of **2.41**. The coupled product **2.43** was obtained in 62% yield. In several steps, this intermediate was elaborated into precursor **2.44** for the 2nd macrocyclization step. Macrolactamization with PyAOP was employed for this purpose (11% yield). Following that, the indoline was reoxidized back to the indole with DDQ and upon global deprotection, tryptorubin A (**2.2**) was obtained in 36% yield over 2 steps.

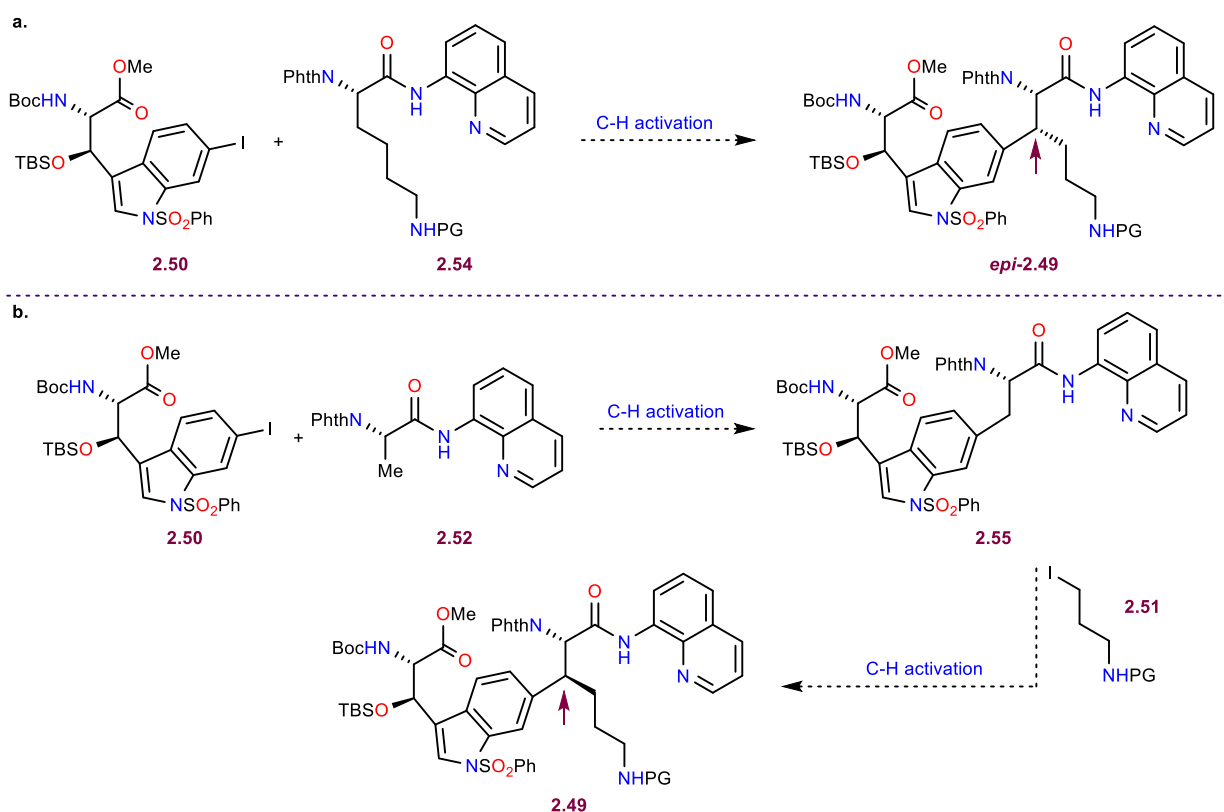
2.3 Initial retrosynthetic analysis

In the previously described syntheses of RiPPs, many innovative approaches have been described for the synthesis of different cross-links between amino acids. Darobactin A (**2.1**) contains two such linkages, the C–C bond between the eastern tryptophan and lysine and an ether link between the two tryptophans. Our initial retrosynthetic analysis for this molecule is depicted in Scheme 2.6. The serine–phenylalanine dipeptide **2.45** could be excised from darobactin A (**2.1**) via a peptide coupling revealing bismacrocycle **2.46**. Next, we envisioned the disconnection of the western macrocycle through peptide coupling between the eastern tryptophan and asparagine, as



Scheme 2.6: Retrosynthetic analysis of darobactin A (AQ = 8-aminoquinoline, PG = protecting group)

well as formation of the challenging alkyl-aryl ether between the tryptophans. Since this connectivity pattern has no precedent, we would have to gauge numerous C–O coupling methods for their efficiency in making the cross-link between **2.48** and **2.47**. The eastern macrocycle would be assembled via successive peptide coupling between serine and intermediate **2.49**. This fragment, contains the testing C(sp²)–C(sp³) bond. This linkage has precedent in streptide (**2.3**, Scheme 2.3) albeit with the opposite configuration at the β-carbon of lysine and is similar to the leucine–tryptophan linkage in celogentin C (**2.4** Scheme 2.2). As explained previously, several methods that were utilized for the formation of such a bond in celogentin C (**2.4**) proceeded with poor stereoselectivity and the most elegant solution was the C–H activation by Chen et al. A modification of this method was later employed by Boger in the synthesis of streptide (**2.3**). We reasoned that we could utilize the same methodology to disconnect the C(sp²)–C(sp³) in darobactin A (**2.1**). However, a direct C–H activation between a lysine derivative such as **2.54** with iodotryptophan **2.50** would lead to the formation of *epi*-**2.49** as it is known that these reactions proceed through an *anti*-palladacycle intermediates (Scheme 2.7a).³⁵ To obtain the correct diastereomer, we would have to perform two successive C–H activations (Scheme 2.7b). Starting

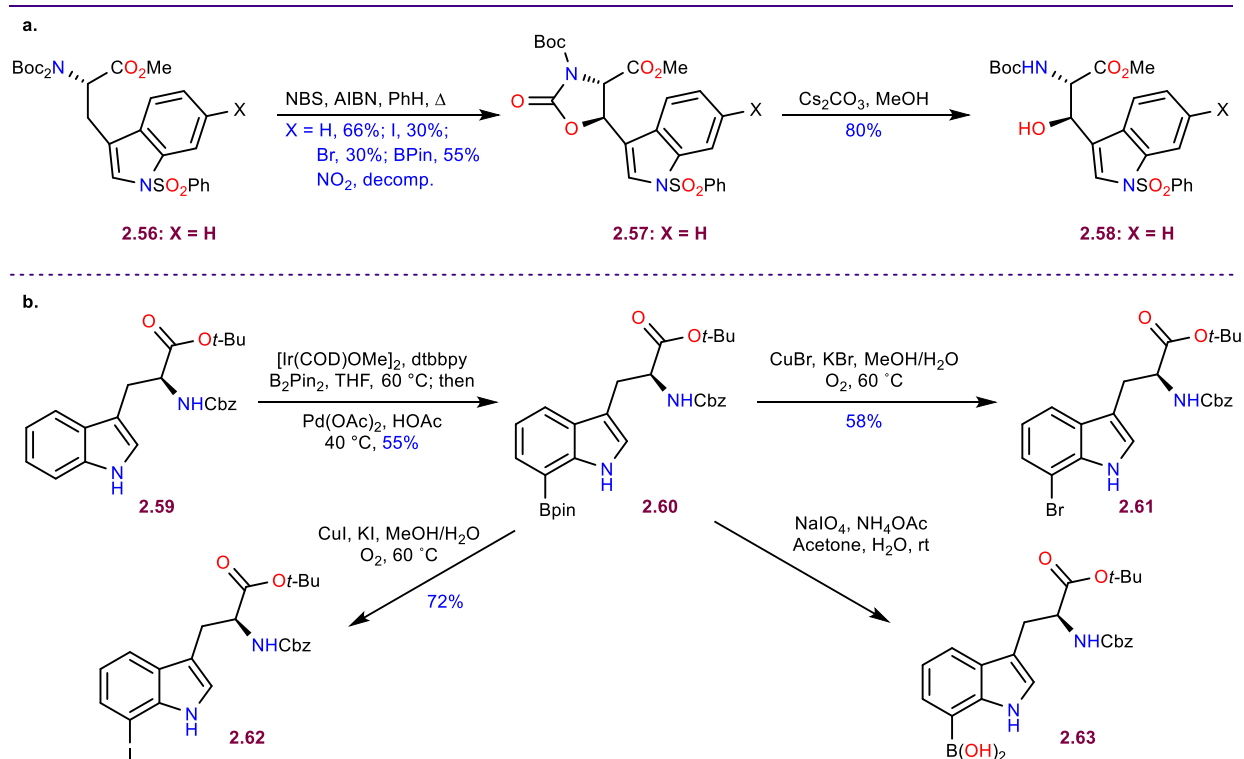


Scheme 2.7: a. Coupling of Lys with Trp via direct C–H activation would give the wrong stereochemistry; b. Sequential C–H activation on alanine derivative would provide the desired diastereomer

from alanine derivative **2.52**, the first C–H activations/coupling would be done with iodotryptophan **2.50** to furnish **2.55**. The second C–H activation would be performed subsequently on this intermediate with iodoamine **2.51** to afford **2.49**, now with the proper stereochemistry at the β -position of lysine. This strategy allows us to disconnect **2.49** into iodotryptophan **2.50**, protected iodoamine **2.51** and alanine derivative **2.52** (Scheme 2.6). Iodotryptophan **2.49** could be obtained through C–H functionalization at the β and C6 positions of commercially available tryptophan **2.53**.

2.4 Synthetic studies

We started our synthetic endeavor with the exploration of different ways for the formation of the alkyl-aryl ether moiety between the tryptophans. Initially we decided to focus on stereoretentive C–O coupling methods where the stereochemistry at the β -carbon of tryptophan is going to be preserved in the coupling product. For this purpose, we had to install a hydroxyl group at this position (Scheme 2.8a). This was achieved through known methodology, developed by Crich, that is based on radical bromination at this activated position, followed by the formation of a cyclic carbamate via displacement of the bromide with the Boc group in the same pot.³⁶ After

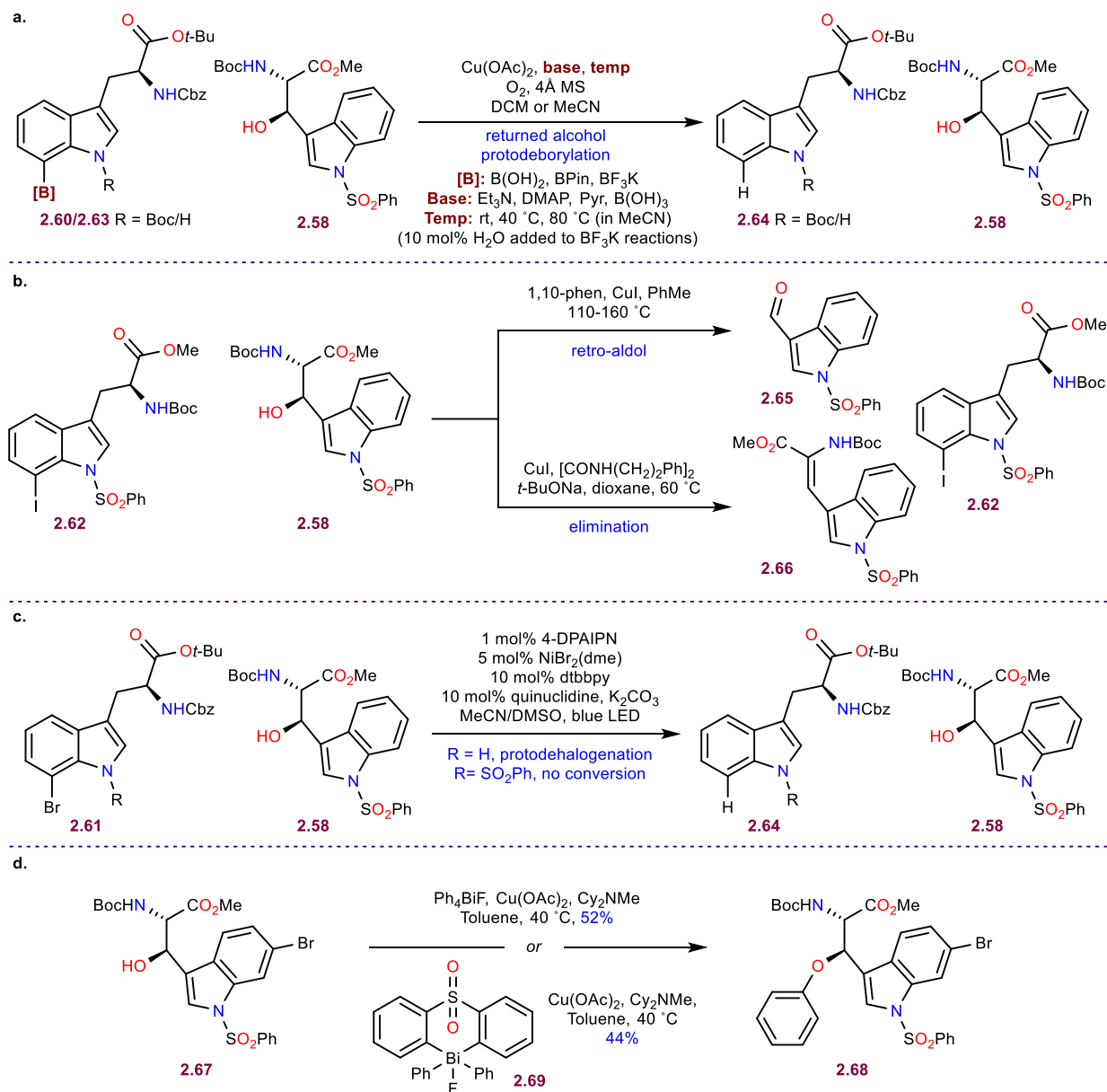


Scheme 2.8: a. Introduction of the β -OH group on tryptophan; b. Syntheses of different tryptophan-derived coupling partners

evaluating substrates with different functionalities at C6, it was evident that this step is most efficient on the unfunctionalized tryptophan **2.56**. The corresponding carbamate **2.57** was obtained in 66% yield and methanolysis afforded the free alcohol **2.58** in 80% yield. At this time, we decided to utilize **2.58** that is lacking functionality at the C6 position, as a model system for the exploration of different C–O couplings. For the same purpose, we have prepared a variety of differently C-7 functionalized tryptophan coupling partners (Scheme 2.8b). Starting with **2.59**, a bisborylation was performed in positions C2 and C7, where the more labile C2-boronate is subjected to protodeborylation with Pd(OAc)₂ and HOAc affording boronate **2.60**.³⁷ This highly versatile intermediate could then be elaborated into iodotryptophan **2.61**, bromotryptophan **2.62** and boronic acid **2.63** that would be used for various couplings.

The stage was set for the exploration of the ether formation between the two tryptophans. However, forging the C–O bond turned out to be remarkably challenging. At first, we attempted Chan-Lam coupling of alcohol **2.58** with a variety of C7-boron derivatives of tryptophan such as **2.60** and **2.63** (Scheme 2.9a).^{33,39} In no case we could observe the formation of the desired product, being able to isolate recovered starting material **2.58** and the protodeborylation product **2.64**. We turned our attention to the exploration of Ullmann coupling between iodotryptophan **2.62** and alcohol **2.58**, but to our dismay, we could only isolate retro-aldol **2.65** or elimination **2.66** products (Scheme 2.9b).⁴⁰⁻⁴² A photoredox C–O coupling that utilized bromotryptophan **2.61** didn't work either, resulting in protodebromination **2.64**.^{43,44} The first successful etherification was done by the Barton-Mukaiyama reaction (Scheme 2.9d).^{45,46} C6-Bromo-β-hydroxy tryptophan **2.67** was reacted with tetraphenylbismuth(V)-fluoride to afford phenyl ether **2.68** in 52% yield. Since this reagent transfers only one out of the four aryl groups present, we decided to employ bismuthane **2.69** as the phenyl donor.⁴⁷ To our delight, the coupling worked again, giving **2.68** in 44% yield. With this encouraging result, we attempted preparing the analogous pentavalent bismuth species with tryptophan attached to it. However, the electron-rich indole made the bismuth reagents highly unstable, preventing us from isolating and henceforth utilizing them in the Barton-Mukaiyama etherification.

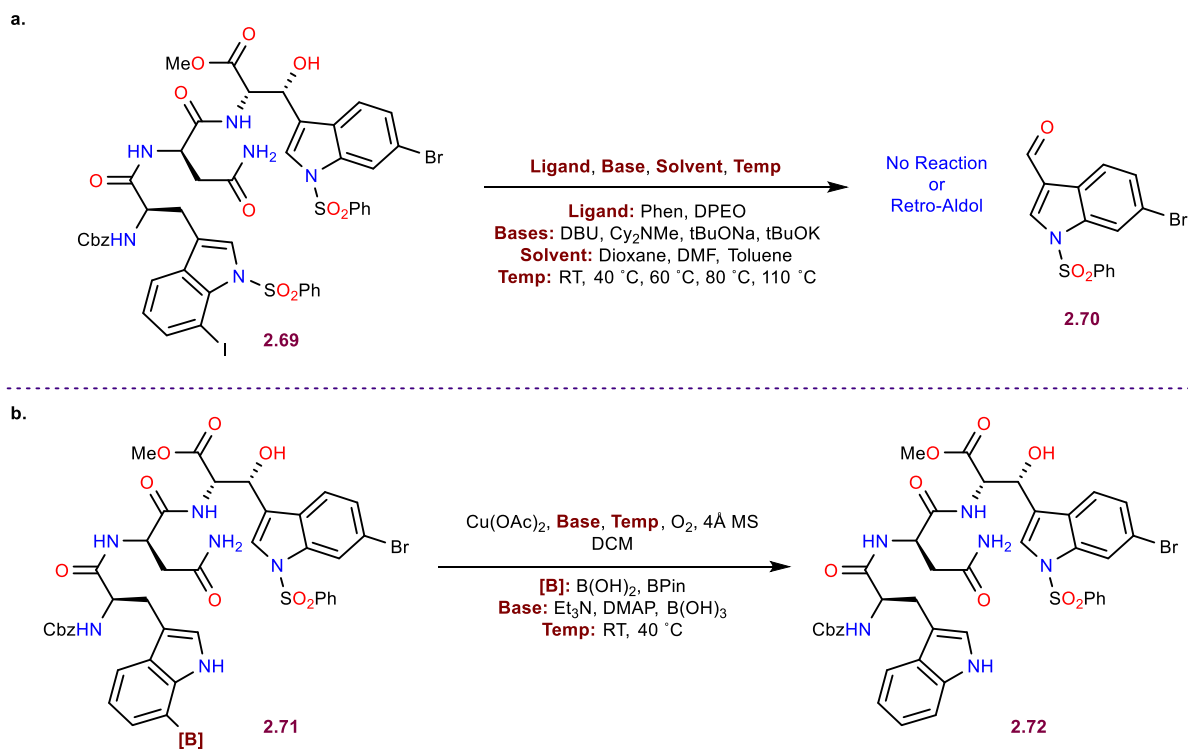
Ullmann coupling and Chan-Lam coupling were attempted as in an intramolecular fashion, to serve as the macrocycle-forming step. In a similar vein as the intermolecular variation, Ullmann coupling on macrocyclic precursor **2.69** resulted in retro-aldol giving aldehyde **2.70** (Scheme



Scheme 2.9: Different methods were attempted for the formation of the ether linkage: **a.** Chan-Lam coupling; **b.** Ullmann coupling; **c.** photoredox coupling; **d.** Barton-Mukaiyama etherification

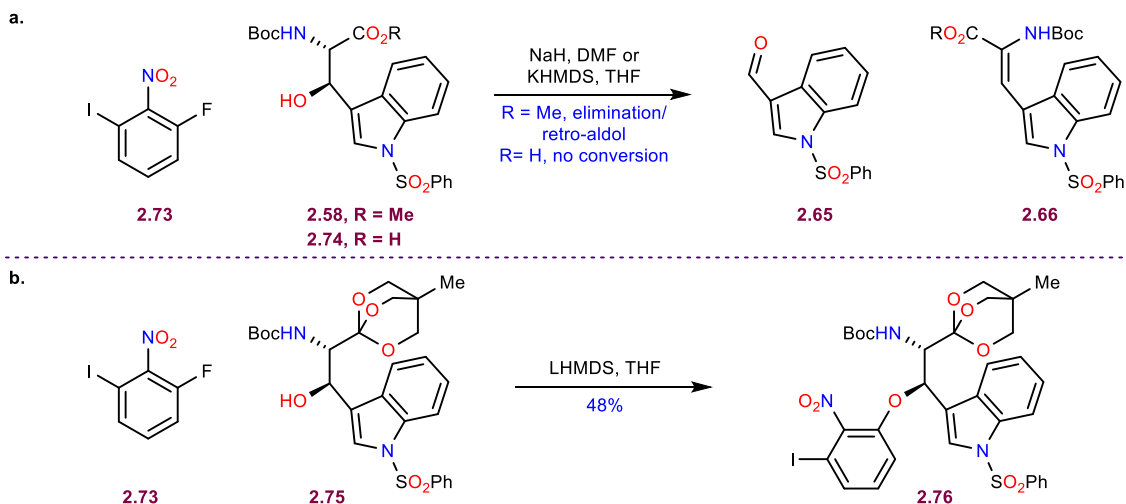
2.10a). The intramolecular Chan-Lam coupling wasn't productive on either the boronate or boronic acid of **2.71**, leading only to the protodeborylation product **2.72** (Scheme 2.10b).

Since transition metal catalyzed/mediated transformations on the free alcohol of the eastern tryptophan with different CO₂ coupling partners weren't fruitful, we resorted to kinetic deprotonation of the alcohol to convert it quantitatively to the corresponding highly nucleophilic alkoxide that would be engaged in an S_NAr reaction with a suitable electrophile. Nitroarene **2.73** was chosen as the substrate, as it could be later elaborated into tryptophan via Larock indole synthesis (Scheme



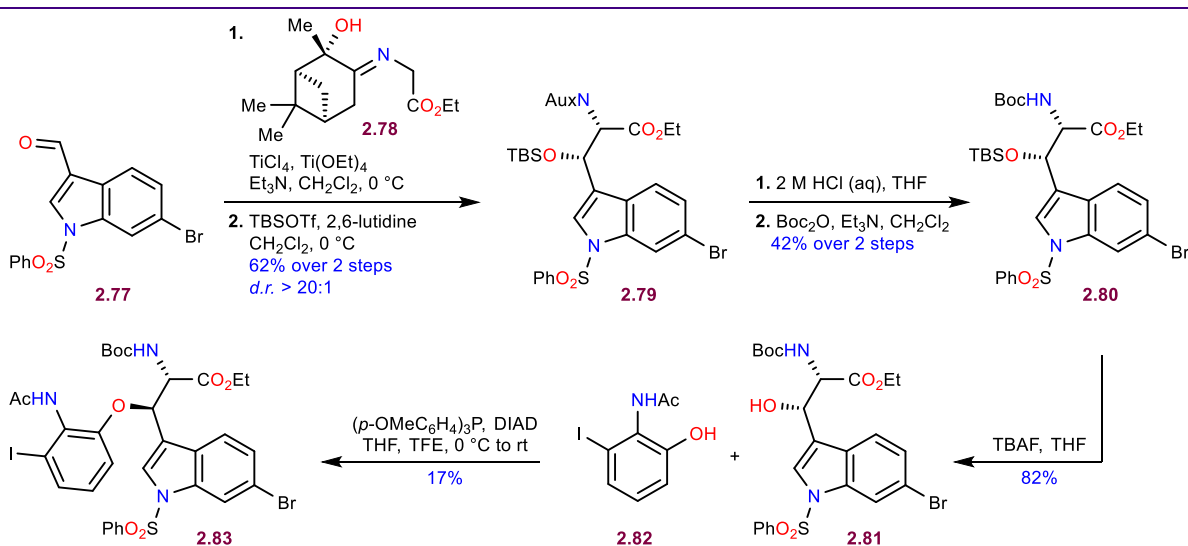
Scheme 2.10: C–O coupling as the macrocyclization step: a. Ullmann coupling; b. Chan-Lam coupling

2.11a). Upon attempted deprotonation of **2.58** which contains a methyl ester functionality, with NaH or KHMDS in the presence of nitroarene **2.73**, we could only observe retro-aldol fragmentation to **2.65** and elimination to **2.66**. The elimination is likely occurring on the desired S_NAr product due to its instability under basic conditions. To obviate this challenge, we decided to employ carboxylic acid **2.74** as the substrate for S_NAr. With excess of base, deprotonation of the carboxylic acid is expected to occur first, followed by deprotonation of the alkoxyde. If the



Scheme 2.11: S_NAr with: a. ester/carboxylic acid; b. orthoester

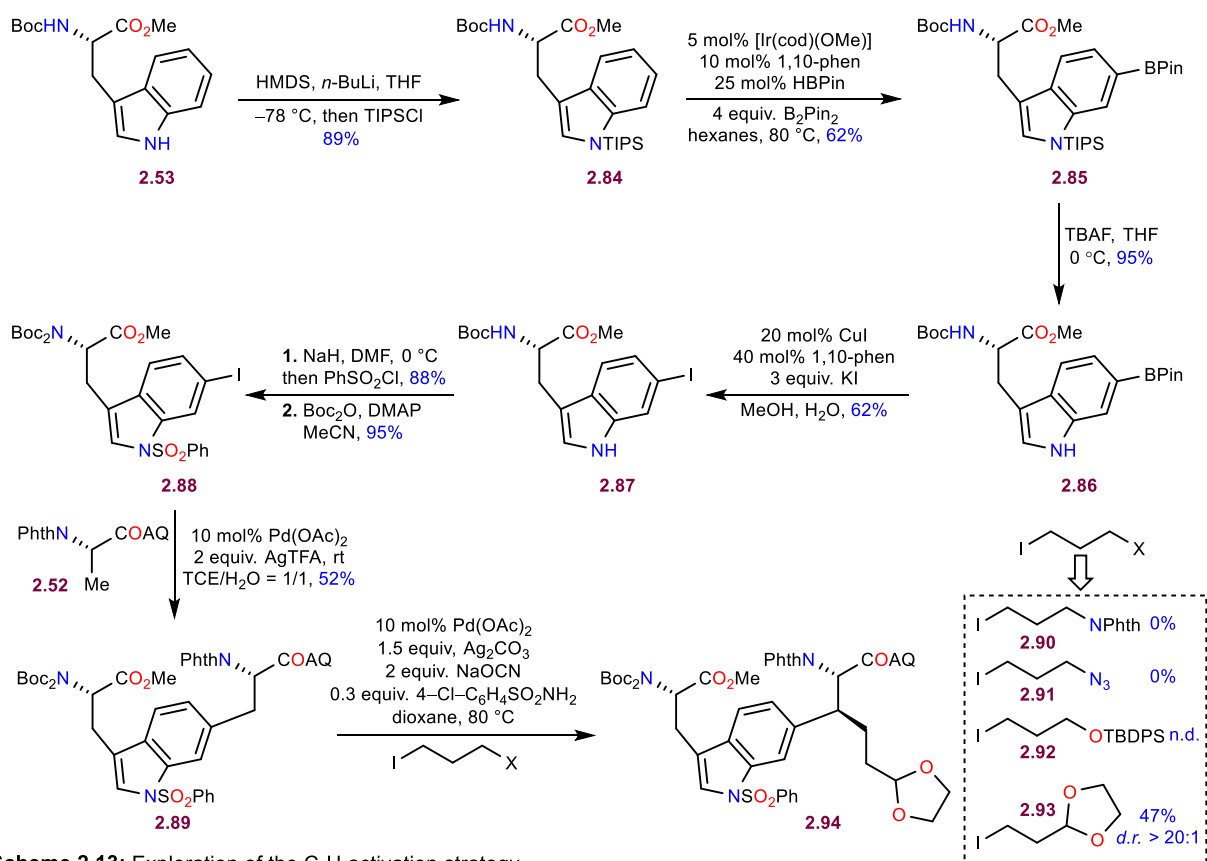
S_NAr product forms, it won't eliminate as readily as the ester, due to the presence of the carboxylate ion. In practice, we could only recover the starting materials of the reaction, **2.73** and **2.74**. At this point, we realized that the only way of achieving a successful S_NAr reaction would be by removing the electron-withdrawing carbonyl functionality in the tryptophan, either by protecting it as an orthoester or reducing it to the corresponding alcohol (Scheme 2.11b). We opted to use orthoester **2.75**, which indeed reacted with **2.73** when LHMDS was employed as the base, to finally afford the desired S_NAr product **2.76** in 48% yield. Even though this was the only instance of forming the alkyl-aryl ether through a stereoretentive transformation, thereby obtaining a product that we could potentially elaborate into the western macrocycle, the synthetic sequence required for making the orthoester was quite lengthy and harsh deprotection conditions were required to remove this protecting group. This rendered the stereoretentive C–O bond forming approach worth abandoning. Therefore, we turned our attention to forming the aryl-alkyl ether linkage via stereoinvertive C–O bond formation by utilizing the venerable Mitsunobu reaction.⁴⁸ However, performing the Mitsunobu reaction, required the synthesis of the diastereomer of the eastern tryptophan with the opposite configuration at the β -carbon when compared to **2.58** (which we synthesized previously by using Crich's radical bromination/carbamate formation methodology, Scheme 2.8a). A new synthetic sequence was developed for the synthesis of the epimer **2.80** via a highly diastereoselective aldol addition (Scheme 2.12). The aldol addition, developed by Cavallo, was performed on indole-carbaldehyde **2.77** with glycine derivative **2.78** that contains an α -pinene derived chiral auxiliary. The reaction is mediated by $TiCl(OEt)_3$ which is prepared in situ by



Scheme 2.12: Synthesis of epimer at the β -position of tryptophan

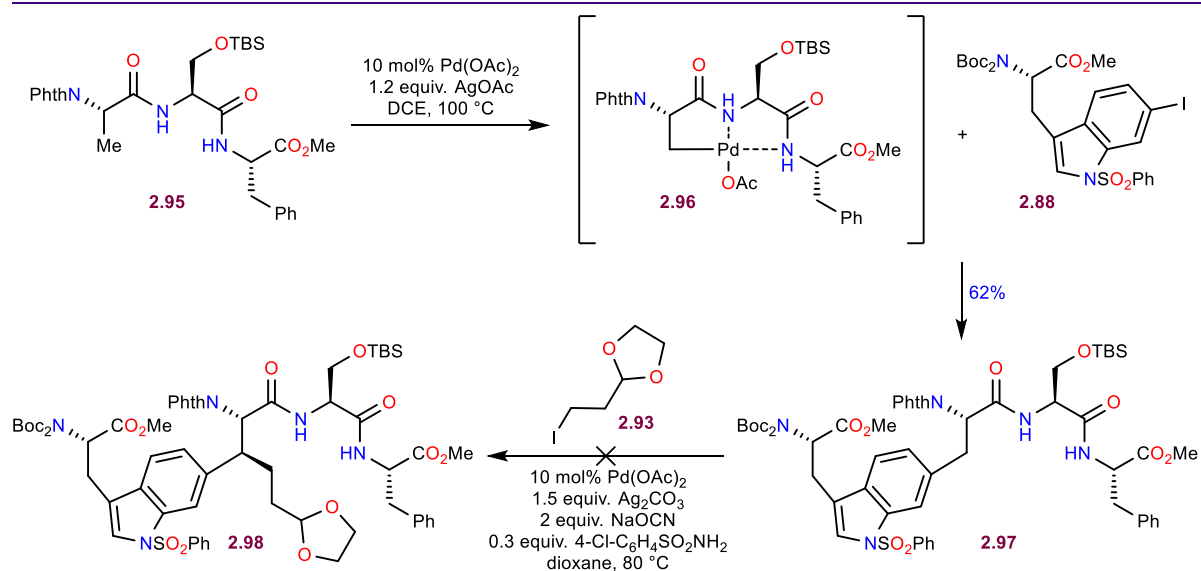
mixing TiCl_4 and $\text{Ti}(\text{OEt})_4$.⁴⁹⁻⁵¹ The aldol addition proceeded with excellent stereoselectivity to provide the unstable aldol product, which was immediately protected with TBSOTf, to prevent retro-aldol reaction, giving **2.79** in 62% over two steps. The labile imine auxiliary was then removed with aqueous HCl, and the obtained ammonium chloride was protected with a Boc group furnishing **2.80**. The TBS group was removed with TBAF to produce the free alcohol **2.81** that was primed for the ensuing Mitsunobu reaction with phenol **2.82**. The reaction proceeded in only 17% yield (under optimized conditions) to afford the alkyl-aryl ether **2.83** and was plagued by elimination and carbamate formation (resulting from Boc group attack on the activated alcohol).⁵² Moreover, separation of the desired product from the phosphine oxide byproduct was very challenging. This, combined with the low yield, deemed the stereoinvertive C–O bond formation strategy unscalable.

Simultaneously with the exploration of the various C–O couplings, we have worked on the formation of the C–C bond between lysine and tryptophan in the eastern portion of the natural product. Accomplishing this task wasn't trivial either. We started by exploring the sequential C–H



Scheme 2.13: Exploration of the C–H activation strategy

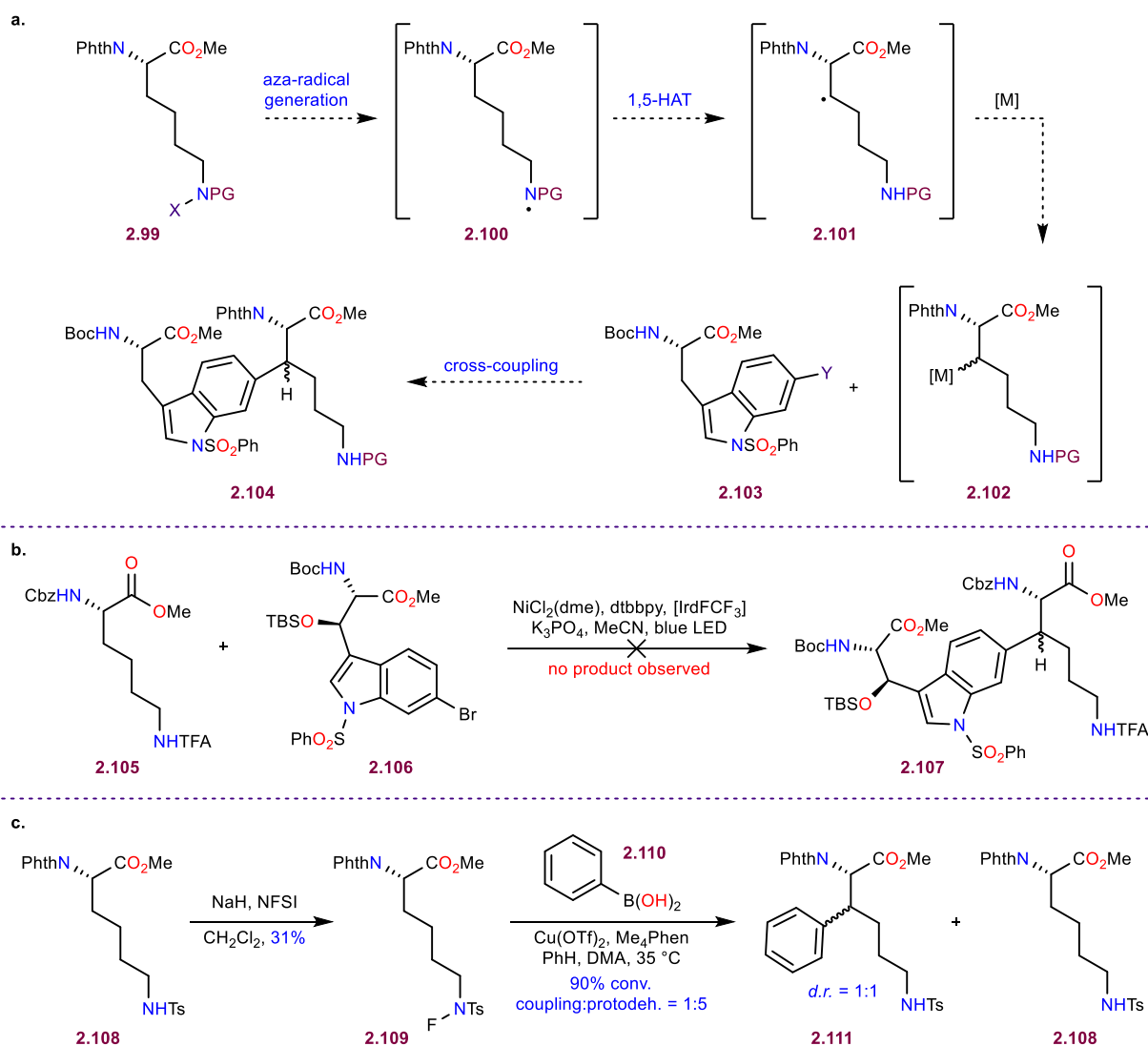
activation strategy which required the development a scalable synthesis of a iodotryptophan **2.88** (Scheme 2.13). Starting from Boc-Trp-OMe **2.53**, we decided to introduce the iodide in C6 position of the indole ring via Baran's modification of Hartwig's C-H borylation (Scheme 2.15).^{53,54} For this purpose, Boc-Trp-OMe **2.53** was silylated at the indole nitrogen with TIPSCl, to afford intermediate **2.84** in 89% yield, where the C2 and C7 positions are sterically blocked by the TIPS group and won't interfere with the ensuing borylation step. This substrate was then subjected to iridium catalyzed C-H borylation with B₂Pin₂ to produce borylated product **2.85** in 62% yield. Next, the TIPS group was deprotected with TBAF (95%) and the obtained product **2.86** was reacted with KI in the presence of a copper catalyst to convert the Bpin group to the iodide **2.87** (62%).⁵⁵ The iodide **2.87** was protected at the indole nitrogen with PhSO₂Cl (88%) which was followed by protection of the carbamate nitrogen with another Boc group resulting in the formation of the C-H activation substrate **2.88** (95%). The fully protected tryptophan **2.88** was then reacted with alanine **2.52** that contains an 8-aminoquinoline auxiliary (depicted as AQ in the Scheme 2.13), in the presence of Pd(OAc)₂ and AgTFA to effect the C-H activation and provide the desired product **2.89** in 52% yield.^{56,57} The more challenging, 2nd C-H activation that involves a C(sp³)-I electrophile, was evaluated with different substrates under conditions developed by Shi.⁵⁷ While phthaloyl-protected 3-iodopropylamine **2.90** failed to give the desired product, TBDPS protected alcohol **2.92** showed about 50% conversion after 2 days. Ultimately the dioxolane **2.93** reacted productively within 12 hours to provide the desired product **2.94** in 47% yield as a single diastereomer, whose stereochemistry assignment was based on literature precedent. Even though the concept was proven, multiple steps will be required to deal with all the protecting groups that were necessary for the success of the C-H activation: phthaloyl, 8-aminoquinoline and dioxolane. Therefore, a more streamlined approach would be highly desirable. To improve convergence, the 8-aminoquinoline group of alanine **2.52** could be replaced with the Ser-Phe dipeptide that would act as an isostere, chelating palladium and promoting C-H insertion in a similar manner to 8-aminoquinoline, as was shown by Yu (Scheme 2.14).⁵⁸ Tripeptide **2.95** was prepared and utilized in Yu's method. Palladacycle **2.96** successfully engaged in the desired transformation with iodotryptophan **2.88** producing **2.97** in 62% yield. Hence, the 1st C-H activation was more efficient on the substrate with the Ser-Phe dipeptide **2.96** (62%), than the 8-aminoquinoline protected alanine **2.52**. However, shortly after this encouraging result, the 2nd C-H



Scheme 2.14: Tripeptide templated C–H activation

activation/coupling between **2.97** and dioxolane **2.93** under the previously used conditions couldn't be achieved and didn't result in any conversion to the desired product **2.98**.

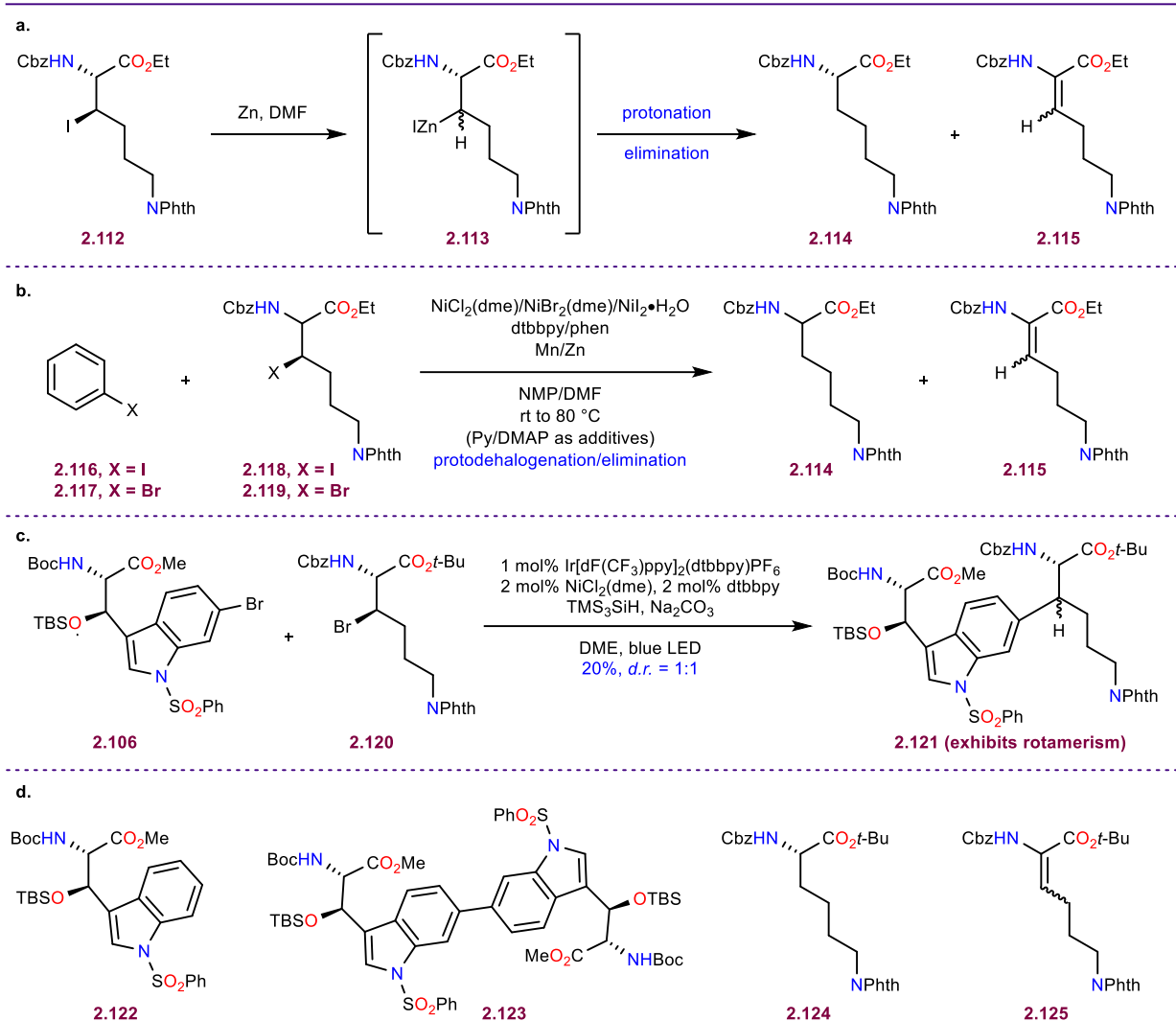
At this point, we were forced to explore alternative ways for cross-linking tryptophan with lysine and decided to pursue a biosynthetically inspired approach where formation of a radical in the β -position of lysine would be followed by cross-coupling with a suitable tryptophan derivative. While nature generates this radical via enzymatic catalysis (Scheme 2.1), achieving the same type of selectivity for hydrogen atom abstraction by purely chemical means would be extremely challenging. However, we realized that we could employ the ϵ -amino group of lysine in a 1,5-hydrogen atom transfer (HAT) reaction to do so (Scheme 2.15a). A suitable lysine-derived radical precursor **2.99** would be engaged in radical generation at the ϵ -amine forming **2.100**. Subsequent 1,5-HAT is expected to provide us with the desired β -radical **2.101** that upon recombination with a transitional metal would give **2.102**. A cross-coupling reaction of the organometallic species with a suitable tryptophan derivative **2.103** should afford the cross-linked product **2.104**. This intercepted Hofmann-Löffler-Freytag (HLF) reaction is expected to give a mixture of diastereomers at the β -position of lysine, however the α -amine protecting group as well as choice of the ester could potentially have some influence on this.⁵⁹ A method developed by the Rovis lab seemed to meet all the criteria for the desired transformation to occur (Scheme 2.15b).⁶⁰ Lysine derivative **2.105** (where the ϵ -amine is protected as a trifluoroacetamide) and bromotryptophan **2.106** were reacted under photoredox conditions, however no product **2.107** formation was



Scheme 2.15: a. Bioinspired approach for cross-linking tryptophan and lysine; b. Rovi's methodology; c. Nagib's methodology

observed. Our next attempt at an intercepted HLF reaction was based on Nagib's report, where fluorinated tosylamides are used as radical precursors (Scheme 2.15c).⁶¹ To this end, the tosylamide of lysine **2.108** was prepared. Fluorination with NFSI and NaH proceeded in 31% yield to furnish the fluorinated product **2.109**. Radical generation was done with copper catalysis and after 1,5-HAT, the organocuprate was coupled to phenylboronic acid **2.110** (which was used as a model system). With 90% conversion, the major products were the desired coupling product **2.111** and the protodehalogenation side product **2.108** with a ratio of 1:5. The coupling product was formed in a 1:1 diastereomeric ratio. Due to the low efficiency of this process, we decided to abandon the HLF approach that utilizes lysine that is unfunctionalized at the β -position, and instead

focus on cross coupling between lysine that is prefunctionalized at the β -position and C6-functionalized tryptophan.

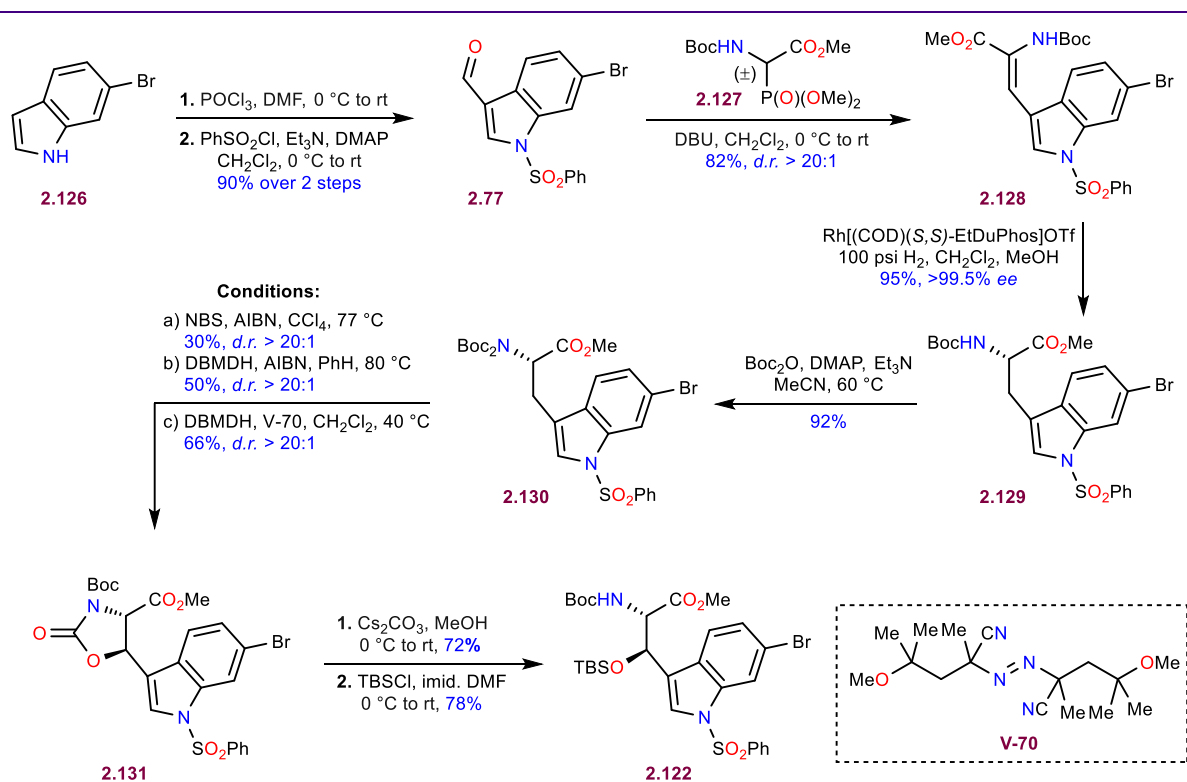


Scheme 2.16: a. Attempted Negishi cross-coupling; b. Weix cross-electrophile coupling; c. MacMillan photoredox coupling; d. Side products observed in the photoredox coupling

Negishi coupling was identified as a suitable method, based on the precedent application of this reaction in cross-coupling chemistry of iodothreonine with various aryl electrophiles.⁶² Iodolysine **2.112** was prepared and zinc insertion was attempted. The insertion was monitored by HPLC (upon quenching with DCl). From this analysis, it was apparent that the organozinc species **2.113** is highly unstable and rapidly undergoes elimination and protodemetalation to afford **2.114** and **2.115**, thereby preventing us from performing the Negishi coupling. Instead, we decided to investigate reductive cross-coupling, developed by Weix (Scheme 2.16b).⁶³ In this case a β -halolysine substrate – iodide **2.118** or bromide **2.119** is going to produce a β -radical in the presence

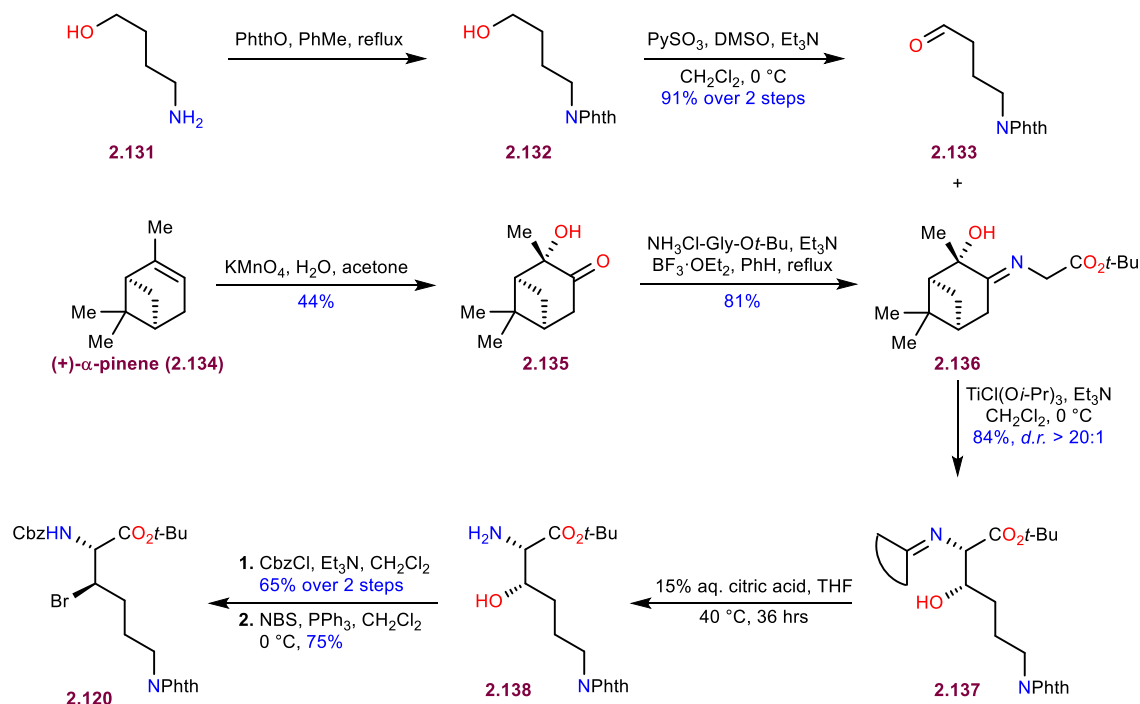
of manganese or zinc, which upon recombination with nickel should furnish an organometallic species that is bound to couple with a suitable aryl electrophile: iodo- or bromobenzene **2.113/2.114** that were used as model systems. The cross-electrophile coupling was attempted under various conditions, but to our dismay, only produced the protodehalogenation **2.114** and elimination **2.115** products. Next, we resorted to photoredox cross-electrophile coupling developed by the MacMillan lab (Scheme 2.16c).⁶⁴⁻⁶⁶ The transformation included an iridium photocatalyst, nickel catalyst and supersilane (TMS₃SiH) as the stoichiometric reductant. For the first time, we were able to forge the challenging C(sp²)-C(sp³) linkage by directly coupling bromotryptophan **2.106** and lysine.**2.120**. The tryptophan-lysine dipeptide was obtained in 20% yield, with a 1:1 diastomeric ratio at the β-carbon of lysine. The major side products identified in the crude reaction mixture were: protodebromination of tryptophan **2.122**, tryptophan homocoupling **2.123**, protodebromination **2.124** and elimination **2.125** of lysine. Extensive optimization efforts were required to improve the yield and potentially the diastereoselectivity of the reaction, but first we needed to develop scalable syntheses of the two substrates.

The synthesis of bromotryptophan **2.122** starts with Vilsmeier-Haack formylation at the most nucleophilic C3 position, which is followed by protection of the indole nitrogen with



Scheme 2.17: Synthesis of C6-bromotryptophan

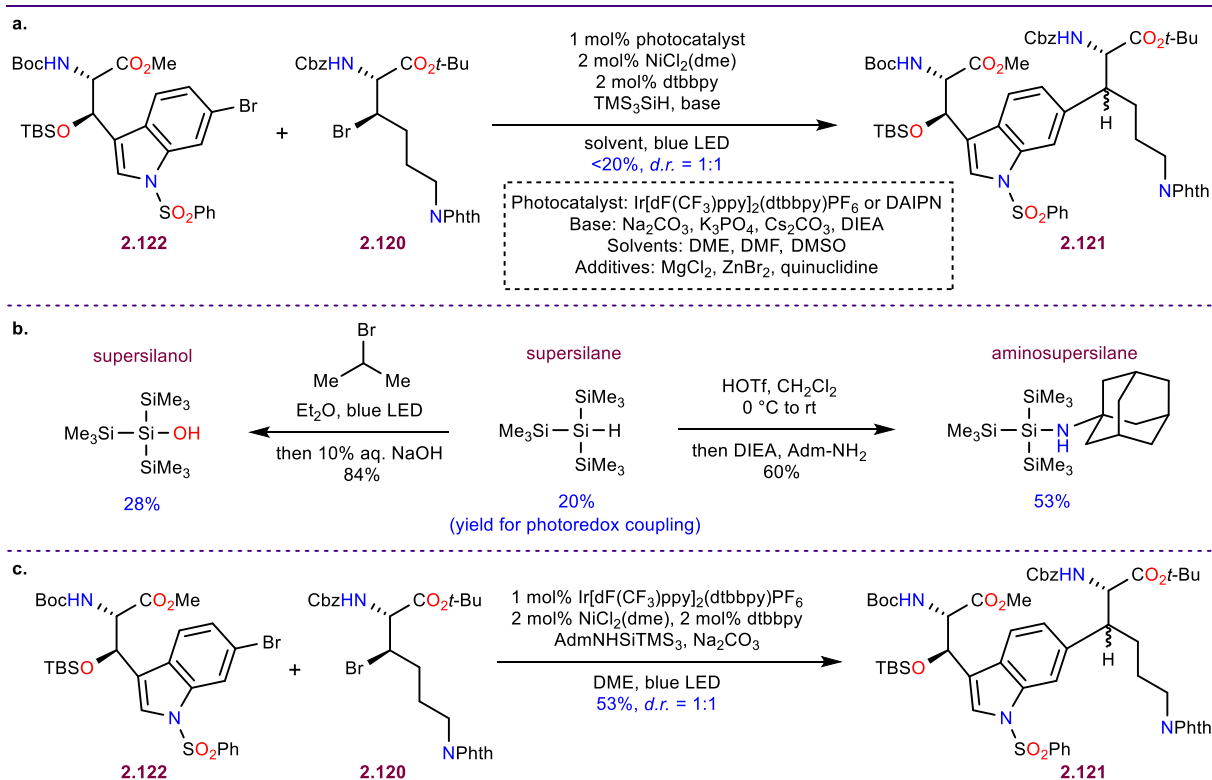
benzenesulfonyl chloride affording indole-carbaldehyde **2.77** in 90% yield (Scheme 2.17). The aldehyde is then subjected to a Horner-Wadsworth-Emmons reaction with phosphonate **2.127**. The unsaturated ester **2.128**, which was obtained as a single diastereomer, was subsequently hydrogenated with a chiral rhodium catalyst producing saturated ester **2.129** in quantitative yield and with exclusive enantioselectivity.⁶⁷ We planned to perform oxidation at the β -position by utilizing Crich carbamate formation that we have utilized previously.³⁶ For this purpose, another Boc group was attached to the α -amine. The obtained double Boc protected compound **2.130** was attempted in the radical bromination/carbamate formation method. However, under the initial conditions with NBS, AIBN as the radical initiator and in CCl_4 at reflux, the desired oxazolidinone **2.131** could only be obtained in 30% yield. The major side products were bromide elimination, instead of cyclization with Boc, as well as additional bromination/elimination tandem on the product **2.131**. After the 1st optimization round, we found improved reactivity when 1,3-dibromo-5,5-dimethylhydantoin (DBDMH) was used as the bromine source. Additionally, the solvent was changed to benzene and the reaction was performed at 80 °C, providing the product **2.131** in 50% yield. In the 2nd optimization round, various radical initiators were screened. The low-temperature initiator V-70 allowed us to run the reaction at a much lower temperature (reflux in CH_2Cl_2). The desired product was now obtained in 66% yield, as a single diastereomer. The oxazolidinone



Scheme 2.18: Synthesis of β -bromolysine

moiety was removed by methanolysis and the revealed alcohol was protected with a TBS group to furnish bromotryptophan **2.122** on multigram scale.

With a scalable route for the formation of the tryptophan coupling partner, we turned our attention to the development of a scalable bromolysine **2.120** synthesis (Scheme 2.18). A convenient way of synthesizing this fragment would be by exploiting the Cavallo-aldol addition, that we had applied previously for the synthesis of the bromotryptophan **2.81**, precursor for a Mitsunobu reaction (Scheme 2.12).⁴⁹⁻⁵¹ In this regard, we started the synthesis by protecting the amino group of 4-aminobutanol (**2.131**) with a phthaloyl protecting group. The obtained product **2.132** was oxidized under Parikh-Doering conditions to produce aldehyde **2.133**. The chiral component of the aldol addition **2.136** was prepared in 2 steps from (+)- α -pinene (**2.134**) according to a known sequence.⁶⁸ The aldol addition, mediated by titanium triisopropoxychloride affords the aldol product **2.137** as a single diastereomer in excellent yield (84%). The chiral imine auxiliary was removed under mildly acidic conditions to preserve the *t*-Bu ester. The revealed amine **2.138** was protected with a Cbz group and the free alcohol was converted to the secondary alkyl bromide **2.120** under Appel conditions. This synthetic sequence was highly scalable and allowed for the preparation of multigram quantities of bromolysine **2.120**.



Scheme 2.19: a. Optimization of the photoredox coupling; b. Evaluation of different reductants; c. Optimized conditions

With ample quantities of both coupling partners, optimization of the photoredox coupling commenced. High-throughput experimentation was applied to quickly screen a variety of conditions where different photocatalysts, bases, solvents and additives were examined (Scheme 2.19a). To our dismay, no coupling conditions could provide us with more than 20% yield of the coupling product **2.121**. Then, we decided to evaluate different reductants for this transformation (Scheme 2.19b). To this end, supersilane was converted to supersilanol, which when utilized in the photoredox coupling, resulted in an increase in yield to 28%.⁶⁹ Encouraged with this result, we decided to prepare another supersilane derivative, aminosupersilane which was more recently applied by the MacMillan lab for very challenging photoredox coupling of alkyl- and

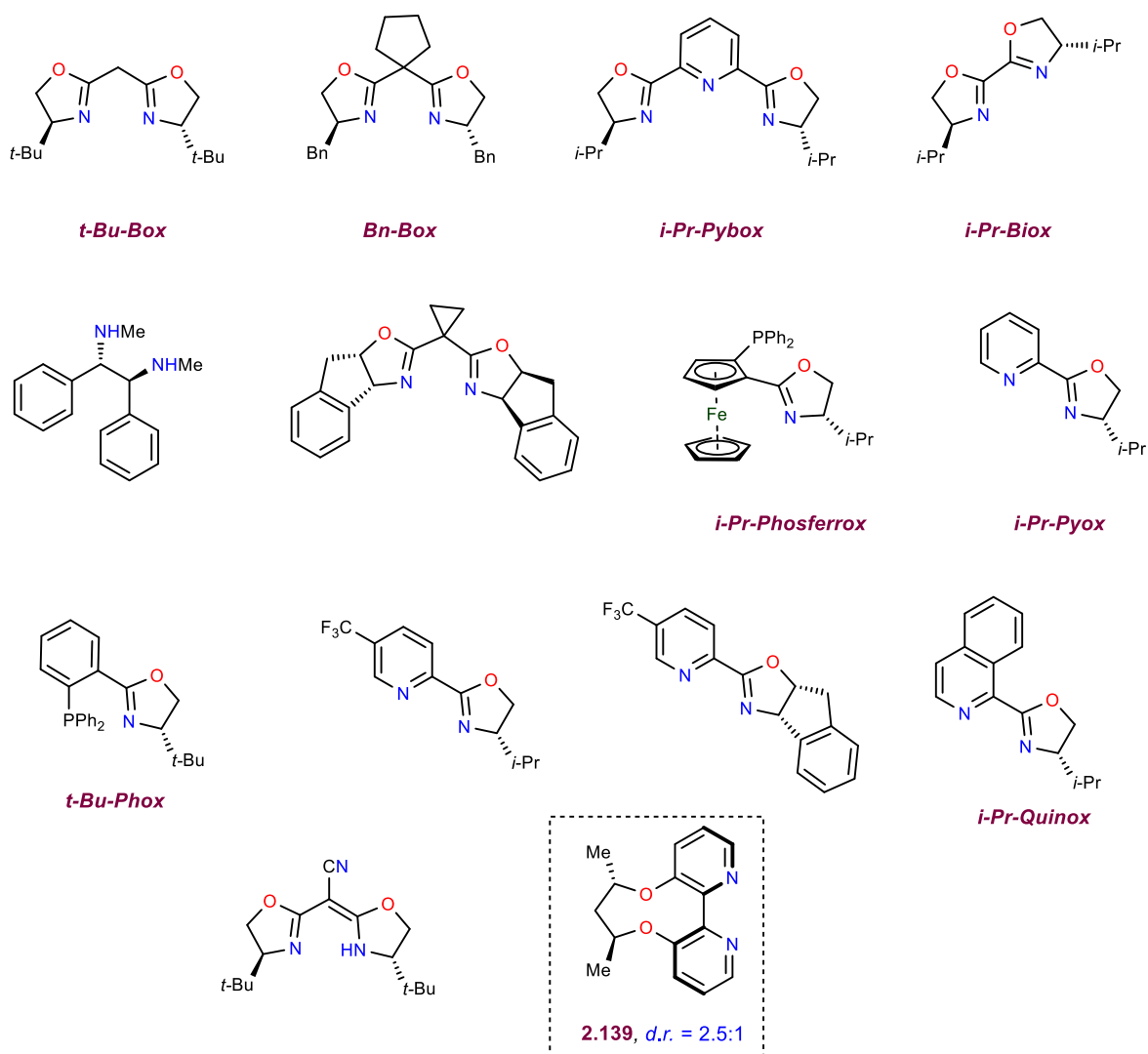
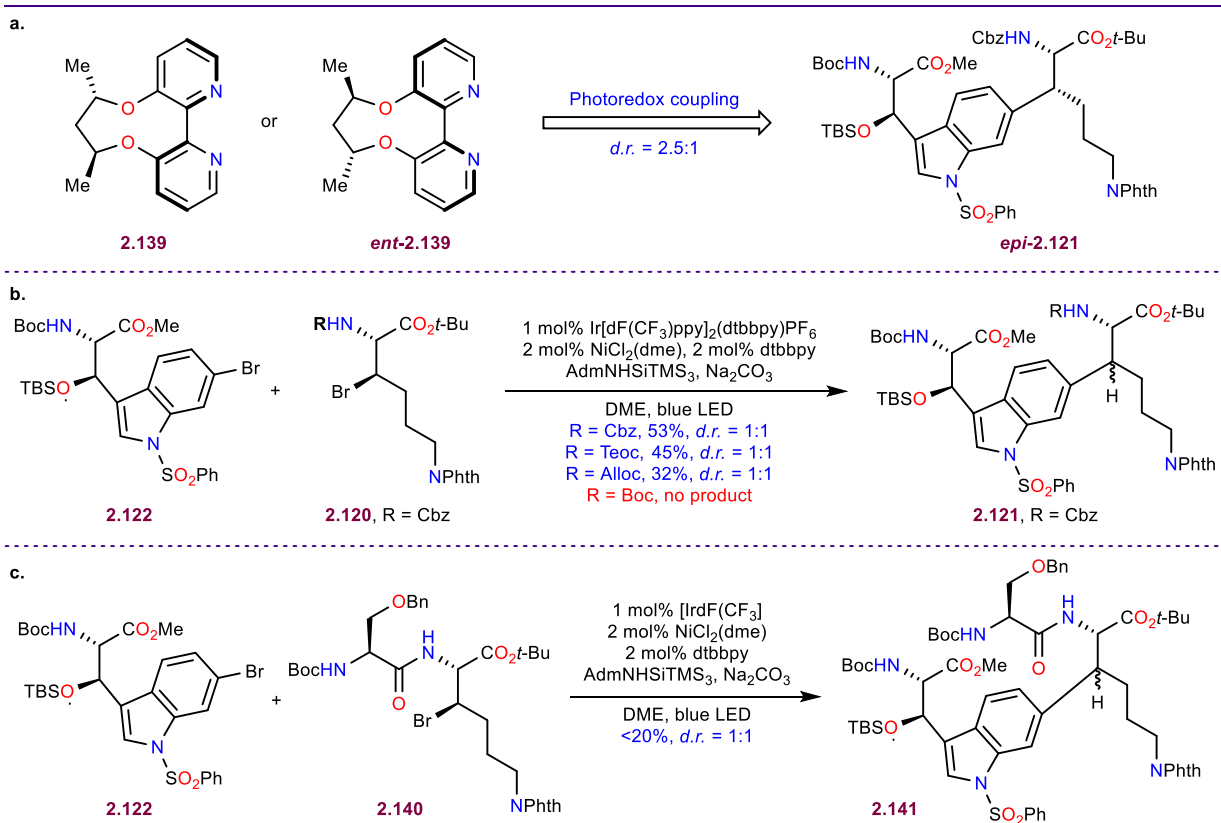


Figure 2.3: Chiral ligands screen

arylchlorides.⁶⁵ When aminosupersilane was used as the reductant for the photoredox coupling, the yield of the obtained product increased to satisfying 53% (Scheme 2.19c).

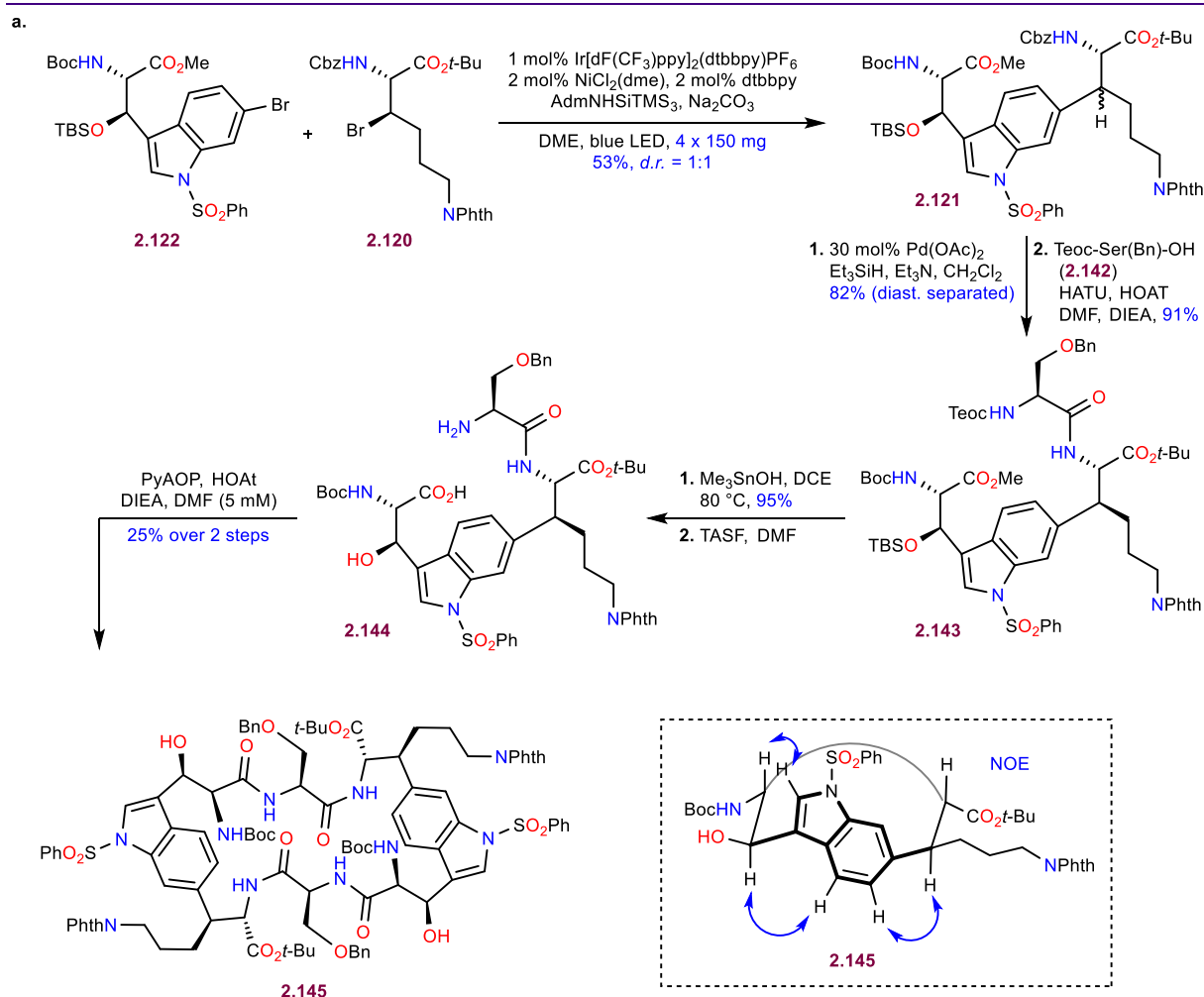
After optimizing the yield of the photoredox coupling, we turned our attention to improving the diastereoselectivity of this process. For this purpose, a variety of chiral ligands were prepared and screened (Figure 2.3). However, most of them resulted in either a similar reactivity pattern as the optimal achiral ligand dtbbpy (same *d.r.* and yield), or gave lower conversion to the product with a minimal change in the diastereoselectivity. Then, we decided to employ a chiral version of dtbbpy, the axially chiral ligand **2.139**.⁷⁰ To our delight, this ligand resulted in an increase in the diastereoselectivity to 2.5:1. We decided to prepare both enantiomers of this ligand and evaluate them separately in the photoredox coupling (Scheme 2.20a). Interestingly, both ligand favored the formation of the same product with the same diastereoselectivity. Later we found out that this was the undesired diastereomer *epi*-**2.121** of the coupling product. Since reagent control wasn't successful in improving the *d.r.* we switched to the analysis of substrate control. Different protecting groups at the α -amine of lysine were examined, to determine whether they will exhibit



Scheme 2.20: a. Enantiomeric axially chiral ligands give the same *d.r.*; b. Evaluation of different α -protecting groups on lysine; c. Photoredox coupling with Ser-Lys dipeptide

any influence on the diastereoselectivity (Scheme 2.20b). While Cbz provided us with the highest yield, Teoc and Alloc gave slightly lower yields, but the exact same *d.r.* When a Boc group is used, no conversion to the product **2.121** occurs, likely due to increased steric demands on the coupling provided by this bulky protecting group. We have also evaluated the efficiency of the serine-lysine dipeptide **2.140**. The diastereoselectivity was still the same, while the yield decreased significantly.

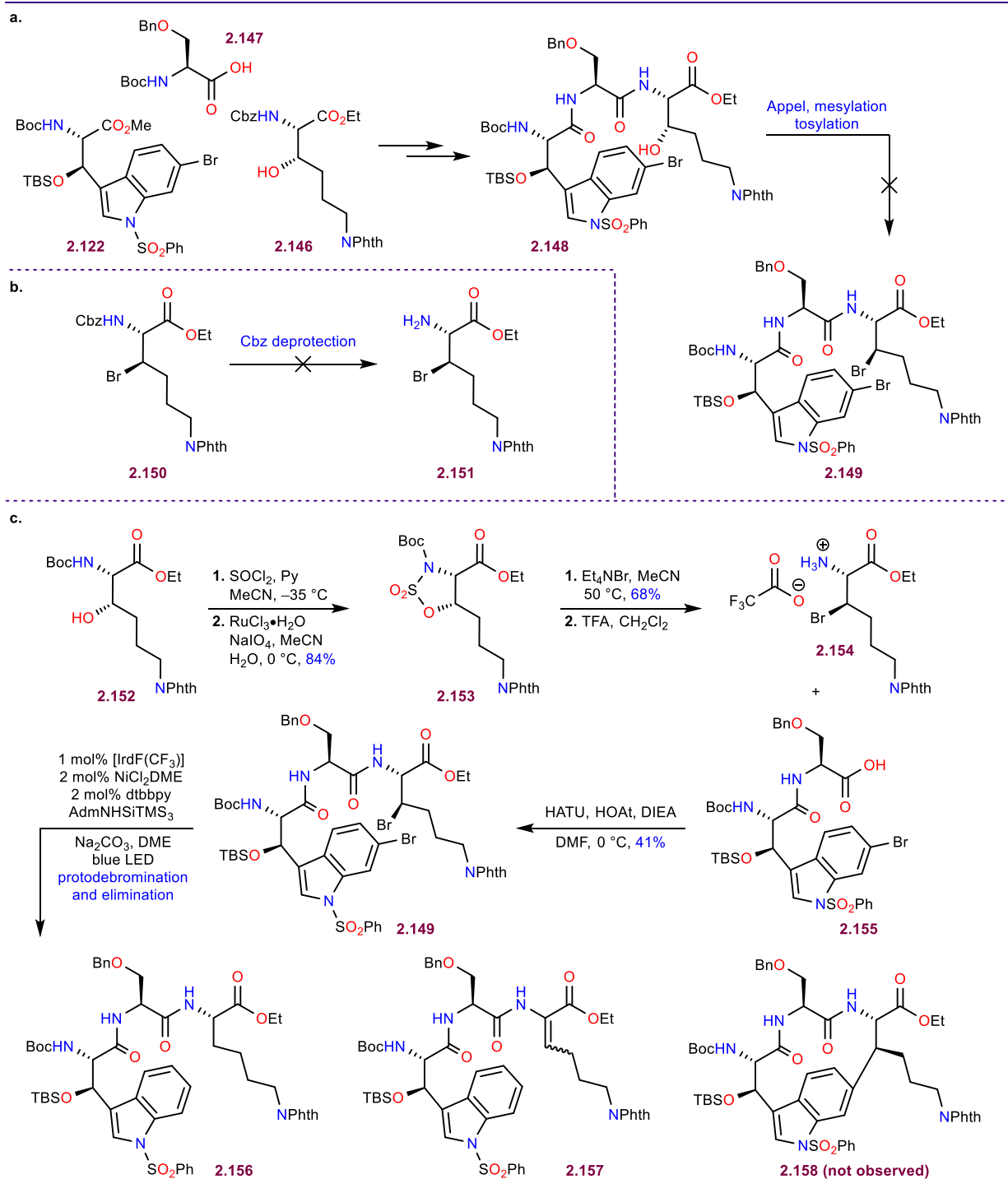
Simultaneously with our optimization efforts of the photoredox coupling, we were exploring frontline chemistry. These efforts eventually lead us to the macrolactamization step (Scheme 2.21). The first challenge towards the eastern macrocycle was performing the photoredox coupling on a decent scale to allow for good material throughput, keeping in mind that we obtain a diastereomeric mixture (1:1) where only one diastereomer is of use. However, this light initiated transformation had poor scalability. The larger the reaction vessel is, the more sluggish the reaction becomes, as light can't penetrate far inside the solution. Ultimately, we found that it is best to



Scheme 2.21: Attempted formation of the eastern macrocycle via macrolactamization

perform this transformation in four 8 mL vials (150 mg of **2.122** each) simultaneously, allowing us to obtain about 500–600 mg of the coupling product **2.121** as a diastereomeric mixture. Separation of the two diastereomers was very challenging and could only be achieved with chiral HPLC. Instead, we decided to attach serine first to see if we can perform the separation in a more streamlined/scalable manner. To this end, the mixture **2.121** was subjected to Cbz deprotection with *in situ* generated Pd(0) and Et₃SiH as the reductant/hydride source. To our delight, the resulting amine diastereomers were separable by normal phase column chromatography downstream. After the separation, we would take both amine diastereomers forward to determine their stereochemistry later (only the desired diastereomer is shown in Scheme 2.21). Subsequent coupling of the amine with serine **2.142** resulted in the formation tripeptide **2.143**. The methyl ester was hydrolyzed with Me₃SnOH and the Teoc protecting group was removed with TASF to furnish macrocyclic precursor **2.144**.⁷¹ Attempted macrolactamization with PyAOP and HOAt under high dilution in DMF (5 mM) resulted only in the formation of the macrocyclic dimer **2.145** (25% yield over two steps), likely due to the high strain that the macrocyclic monomer would contain. Nevertheless, we were able to confirm the stereochemistry at the β -position of lysine through NOE analysis.

We have encountered two immense challenges so far: we weren't able to improve the stereoselectivity of the photoredox coupling and we couldn't form the eastern macrocycle through macrolactamization. A potential solution to both of these challenges could be the employment of the photoredox coupling as the macrocyclization step. The eastern macrocycle is indeed formed in nature by forging this exact connectivity (Scheme 2.1). Our new, bionspired strategy would rely on having the labile β -bromide on lysine within a Trp-Ser-Lys tripeptide **2.149** (Scheme 2.22a). With this in mind, we combined three amino acid building blocks via peptide coupling: tryptophan **2.122**, serine **2.147** and β -hydroxylysine **2.146**. Attempted conversion of the alcohol **2.148** to the alkyl bromide **2.149** under a variety of conditions (Appel reaction, mesylation/tosylation) wasn't successful. Therefore, instead of pursuing a late-stage introduction of the bromide, we decided to have it installed early in the synthesis (Scheme 2.22b). However, the Cbz-protected β -hydroxylysine **2.150** couldn't be elaborated to the free amine **2.151**, as this compound is extremely labile. We decided to employ a Boc protecting group instead of Cbz, because after the introduction of the bromide, Boc removal can be done under mildly acidic conditions resulting in the formation of the ammonium salt that is expected to be much more stable. With this aim, we prepared **2.152**



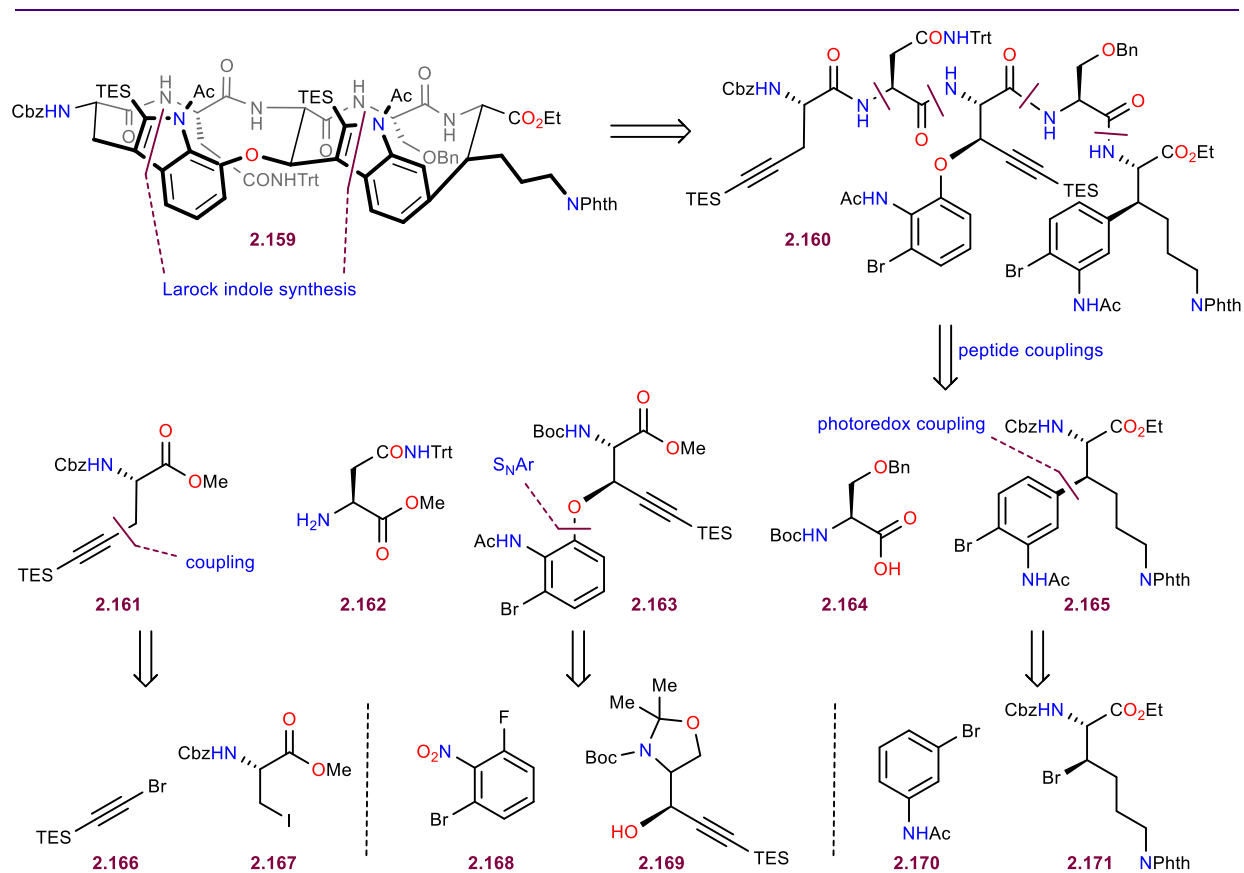
Scheme 2.22: a. Attempted late-stage bromide synthesis; b. Instability of the free aminobromide; c. Unsuccessful intramolecular photoredox coupling

with the Cavallo-aldol method. The ensuing bromide formation via Appel reaction was very sluggish on this system, probably due to sterics effected by the bulky Boc group. This prompted us to develop an alternative way of making it. After some trial and error, we found that **2.152** can be converted to the cyclic sulfamidate **2.153** in good yield, over 2 steps.⁷² This intermediate is

highly electrophilic at the β -carbon and a simple Finkelstein substitution with Et_4NBr produced the desired bromide in 68% yield. Subsequent removal of the Boc group with TFA revealed ammonium salt **2.154** which was a stable compound, as expected. In spite of the successful formation of the ammonium salt, the following peptide coupling would rely on the release of the reactive free amine that has an adjacent bromide. With this predicament, the peptide coupling of **2.154** with **2.155** proceeded in decent 41% yield, to still afford sufficient quantities of tripeptide **2.149**. The intramolecular photoredox coupling was performed with slow syringe addition (over 5-6 hours) of the substrate dissolved in DME into the solution of all reagents in DME while being irradiated with blue LEDs. This resulted in a complex mixture, where the major identified species were double protodebromination **2.156** and protodebromination with elimination **2.157**. The desired macrocycle **2.158** wasn't observed. In a similar vein to the attempted macrolactamization, the high strain associated with the eastern macrocycle prohibited its formation under these conditions. Therefore, our only option for its formation would be a transformation that can reliably form strained macrocycles via template effect or forms of a ring-expanded intermediate that can be subsequently ring-contracted.^{19,73} Moreover, we weren't able to develop satisfactory conditions for the formation of the ether linkage between the two tryptophans. All of this prompted us to completely change our approach and perform a revision of our retrosynthetic analysis.

2.5 Revised retrosynthetic analysis

Inspired by Boger's elegant syntheses of streptide (**2.3**, Scheme 2.3) and complestatin (**2.38**, Scheme 2.4), where the indole-containing macrocycles were formed through a Larock indole synthesis, we decided to apply a similar approach for disconnecting the two macrocycles of darobactin (Scheme 2.23).²⁹⁻³² The bismacrocyclic advanced intermediate **2.159** would be disassembled at both macrocycles through a double Larock indole synthesis revealing pentapeptide **2.160** which can be further disconnected into its constituting amino acids (**2.161-2.165**) via a series of peptide couplings. While asparagine **2.162** and serine **2.164** are commercially available, efficient synthetic routes towards the following non-canonical amino acids need to be developed: the western alkynyl amino acid **2.161**, the central alkynyl amino acid **2.163** containing the key aryl-alkyl ether linkage and the eastern fragment **2.165** that contains the $\text{C}(\text{sp}^2)\text{-C}(\text{sp}^3)$ cross-link. **2.161** could be formed through transition-metal coupling chemistry between bromo-TES-acetylene **2.166** and iodoserine **2.167**.⁷⁴ The aryl-alkyl ether in **2.165** could be synthesized through an $\text{S}_{\text{N}}\text{Ar}$



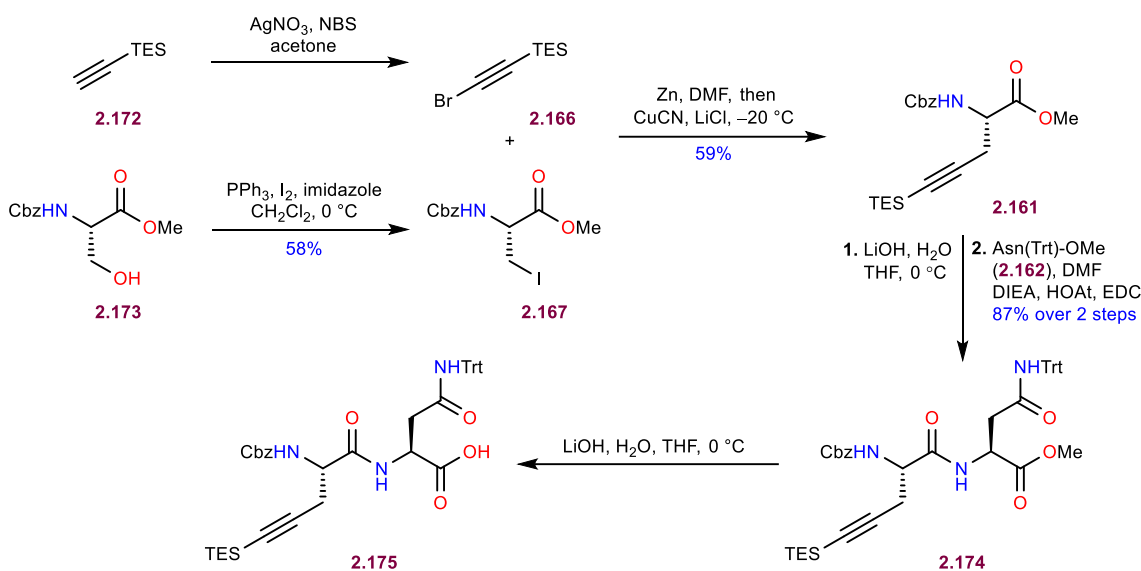
Scheme 2.23: Revised retrosynthetic analysis based on double Larock indole synthesis as the macrocyclization step

reaction of alcohol **2.169** and arene **2.168**. With lessons learned from our previous attempts at forging the C–O bond, we decided to use substrate **2.169** that has an alcohol oxidation state at the position where the methyl ester is supposed to be, to prevent elimination and retro-aldol side reactivity. Finally, **2.165** could be made by utilizing the optimized photoredox coupling conditions to connect 3-bromoacetanilide **2.170** and bromolysine **2.171**. After the coupling, a bromide has to be introduced within the arene at the position that is *para* to the newly formed linkage. The presented blueprint is highly convergent and should allow for a scalable synthesis of the Larock precursor, as well as provide us with enough flexibility to utilize modified fragments if proven necessary.

2.6 Forward Synthesis

The synthesis of the western fragment is depicted in Scheme 2.24. Bromination of TES-acetylene **2.172** afforded bromo-TES-acetylene **2.166**.^{74,75} On the other hand, serine derivative **2.173** was subjected to an Appel reaction⁷⁶ to furnish iodoserine **2.167** which subsequently

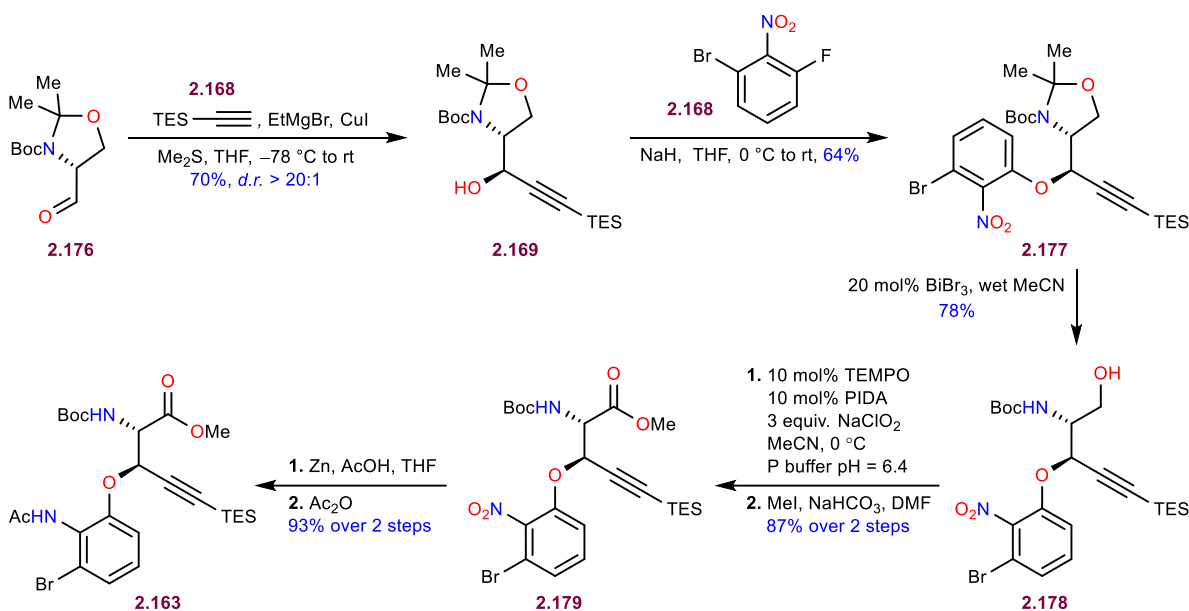
underwent zinc insertion. The obtained organozinc species was coupled to **2.166**, in a copper-mediated reaction, producing alkynyl amino acid **2.161**. Hydrolysis of the methyl ester was followed by peptide coupling with asparagine **2.162**. The resulting dipeptide **2.174** was subsequently hydrolyzed with LiOH to form the free carboxylic acid of western dipeptide fragment **2.175**.



Scheme 2.24: Synthesis of the western alkynyl amino acid

The synthesis of the central fragment starts with chelation controlled addition of TES-acetylene into commercially available (*D*)-Garner's aldehyde **2.176**.⁷⁷ The addition produced alcohol **2.169** as a single diastereomer. The ensuing S_NAr reaction was performed with NaH as the base and arene **2.168** as the electrophile to afford product **2.177** in 64% yield. The reaction was efficient, highly scalable and was a substantial improvement when compared to our previous attempts of forming the ether between two tryptophans. With the challenging C–O bond installed successfully, the acetonide protecting group had to be removed next. However, acetal hydrolysis under various acidic conditions led to simultaneous Boc deprotection. To preserve the Boc group, we had to employ very mild conditions for acetal removal. After several failed experiments we found that catalytic BiBr₃ in wet acetonitrile could afford the desired alcohol **2.178** in 78% yield.⁷⁸ The revealed primary alcohol was oxidized directly to the carboxylic acid with catalytic TEMPO, PIDA and superstoichiometric NaClO₂.^{79,80} The acid was converted to methyl ester **2.179** with MeI and NaHCO₃. Furthermore, the nitro group was reduced with zinc/acetic acid to afford the corresponding amine after workup. Lastly, we planned to protect the amine as an acetamide,

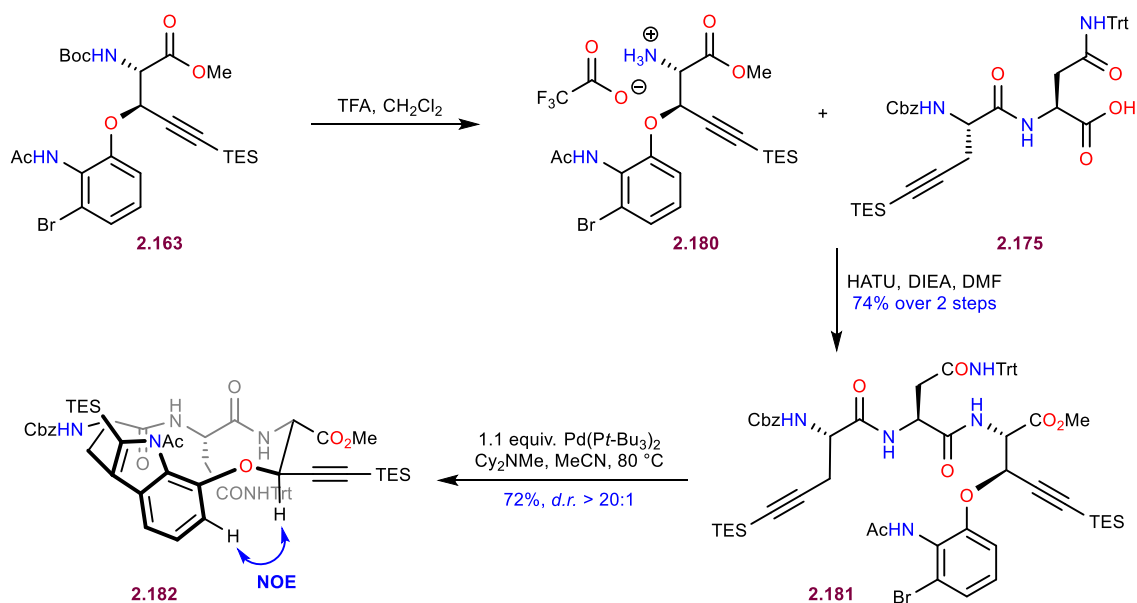
however the protection step wasn't as straightforward as expected it to be. Attempted protection with either AcCl or Ac₂O in the presence of a base or additive (such as DMAP) resulted in competitive double acetylation. The bisacetanilide couldn't be converted to the monoacetanilide under basic conditions, as the substrate was highly base-sensitive. Eventually we found that running the acetylation step in neat Ac₂O with no additives, results in the selective monoacetylation in 93% yield over 2 steps affording **2.163**.



Scheme 2.25: Synthesis of the central fragment

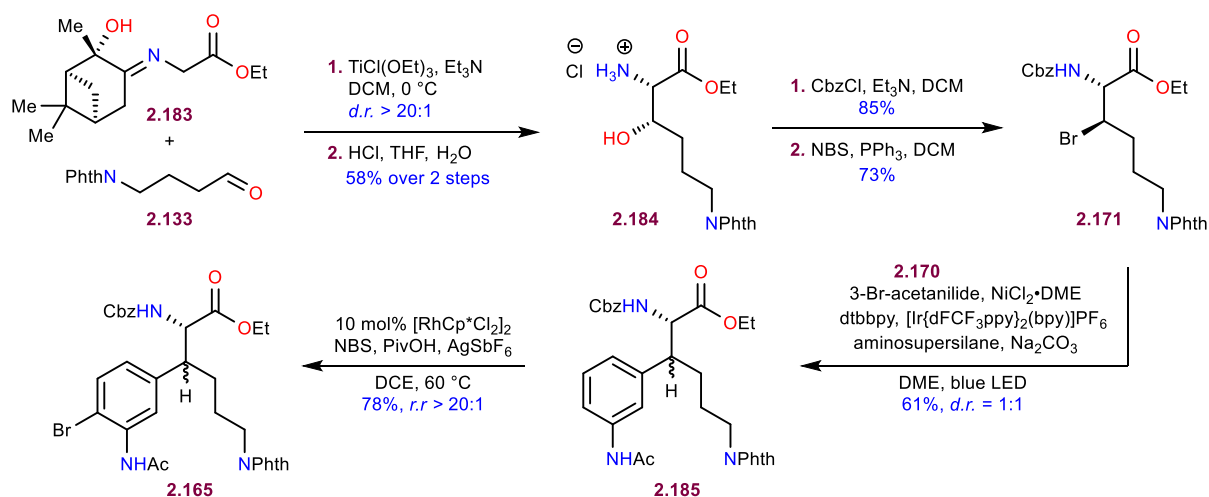
Before attempting the double Larock indole synthesis, we wanted to see whether we could form the two macrocycles separately by employing this methodology. With efficient and scalable routes towards the western **2.175** and central **2.163** fragments, the stage was set for the synthesis of the western macrocycle (Scheme 2.26). To this end, the Boc group of **2.163** was removed with TFA and the obtained ammonium salt was coupled to western fragment **2.175**. The resulting tripeptide **2.181** was primed for the macrocyclization step. To our delight, Larock indole synthesis with 1.1 equiv. of Pd(*t*-Bu₃P)₂ at 80 °C in MeCN under high dilution proceeded in 72% yield to afford western macrocycle **2.182** as the desired atropisomer exclusively (confirmed by NOE).⁸¹

With this highly encouraging result, our attention was brought to the synthesis of the eastern macrocycle by applying the same methodology. The key component needed for the assembly of the tripeptide linear precursor of the eastern macrocycle is fragment **2.165**. The synthesis of this fragment starts similarly as the synthesis of **2.120** (Scheme 2.18) that we used for the optimization of the photoredox coupling. However, now we needed an ethyl ester instead of *t*-



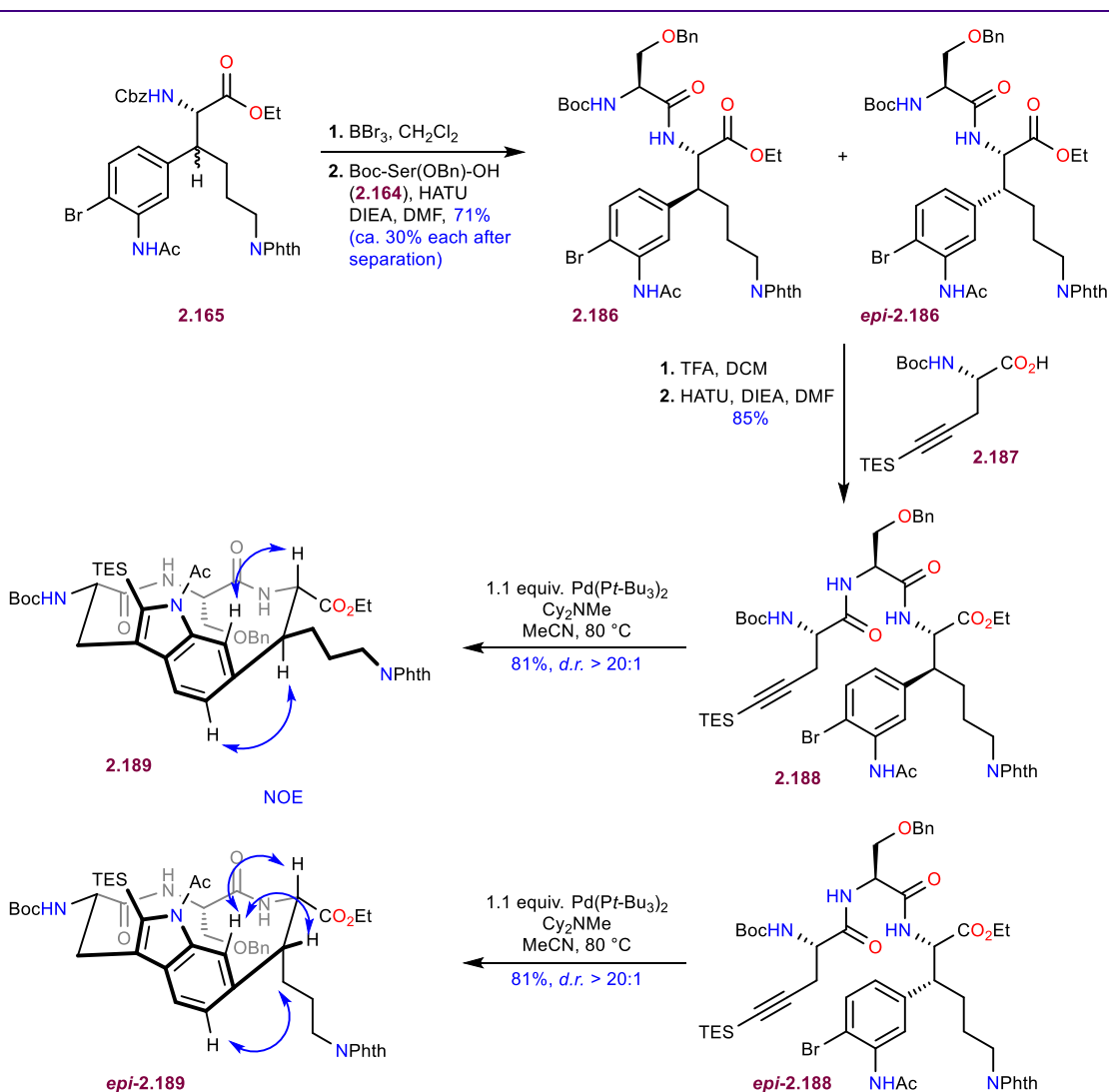
Scheme 2.26: Synthesis of the western macrocycle

butyl ester (Scheme 2.27). Cavallo-aldol addition between ethyl glycine derivative **2.183** and aldehyde **2.133** proceeded with exclusive diastereoselectivity.⁴⁹⁻⁵¹ The aldol product was prone to retro-aldol, hence we decided to remove the immine auxiliary immediately with aqueous HCl. The resulting ammonium chloride **2.184** was produced in 58% yield over 2 steps. Subsequent protection of the amine with Cbz-Cl was followed by an Appel reaction to convert the alcohol to alkyl bromide **2.171**. Then, we utilized the optimized photoredox coupling conditions to connect bromolysine **2.171** with 3-bromoacetanilide **2.170**.⁶⁴⁻⁶⁶ The challenging C–C bond was formed in 61% yield with *d.r.* = 1:1. The two diastereomers were inseparable at this stage, hence they were



Scheme 2.27: Synthesis of the eastern macrocycle

carried forward as a mixture and their stereochemistry was determined later (after macrocyclization). At this stage we had to install the bromide on the acetanilide **2.185** that will serve as a functional handle for the Larock indole synthesis later. This was achieved by applying acetanilide directed *ortho*-C–H bromination, developed by the Glorius lab.⁸² In the presence of NBS and a rhodium catalyst, the bromide **2.165** was obtained in 78% yield, as a single constitutional isomer. This route was short, but still suffered from poor scalability of the photoredox coupling and challenging separation of the two diastereomers. Nevertheless, we have obtained enough material to proceed with Larock macrocyclization studies (Scheme 2.28). We decided to pursue formation of the eastern macrocycle that would lack functionality at the β -position of the tryptophan, as it would allow us to get to the macrocycle quicker, so that we can

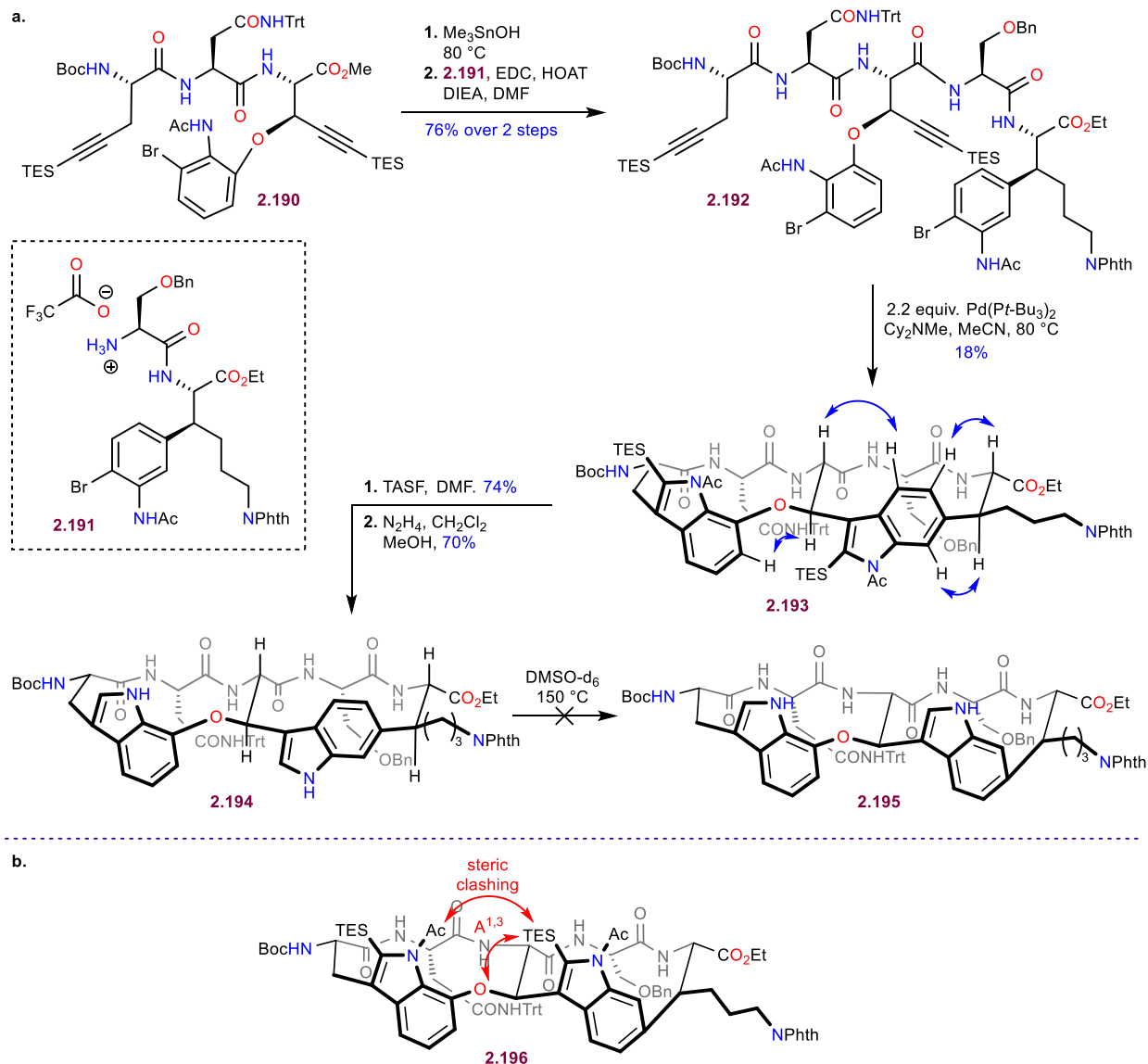


Scheme 2.28: Synthesis of the eastern macrocycle

confirm the stereochemistry of the two diastereomers obtained in the photoredox coupling (Scheme 2.28). With this in mind, bromide **2.165** was subjected to Cbz deprotection with BBR_3 and the obtained amine diastereomeric mixture was coupled to serine **2.164**.⁸³ The dipeptide was obtained in 71% over 2 steps. At this stage, the diastereomers could be separated by careful normal phase silica gel column chromatography. After this arduous separation, the two diastereomers **2.186** and *epi*-**2.186** were obtained in about 30% yield each and both were used further separately. Removal of the Boc group was followed by coupling with Boc protected alkynyl amino acid **2.187** which was prepared in the same manner as the Cbz-protected version in Scheme 2.24. The linear tripeptide macrocyclization precursors **2.188** and *epi*-**2.188** were produced in 85% yield each. Subsequent Larock indole synthesis with stoichiometric palladium at 80 °C afforded macrocycles **2.189** and *epi*-**2.189** in 85% yield, as single atropisomers. Through scrupulous NOE analysis, we were able to confirm that we have obtained the correct atropisomer of the macrocycle and we were also able to determine the stereochemistry at the β -position of the two lysine diastereomers that were obtained in the photoredox coupling.

The previously described macrocyclization studies were very promising and encouraged us to attempt the initially planned one-pot bismacrocyclization (Scheme 2.29a). For this purpose, the western tripeptide **2.190** was prepared (now with a Boc group instead of Cbz at the N-terminus) and subjected to peptide coupling with the central dipeptide **2.191** (made by Boc deprotection of the desired diastereomer **2.186** in Scheme 2.28). The obtained pentapeptide **2.192** was reacted with 2.2 equiv. of $\text{Pd}(\text{P}t\text{-Bu}_3)_2$ at 80 °C to participate in a double Larock indole synthesis, affording bismacrocycle **2.193** in 18% yield, which is still impressive for such a challenging step. However, upon detailed characterization by NOE analysis, it was determined that the eastern macrocycle formed as the undesired atropisomer. We reasoned that the desired atropisomer **2.196** cannot form since it would exhibit severe steric clashing between the western acetyl group and the eastern TES group, as well as $A^{1,3}$ strain between the TES group and the aryl ether (Scheme 2.29b). We decided to remove all protecting groups present on the two indoles of **2.193** and see if it is possible to convert the undesired atropisomer to the desired one via equilibration at high temperature. For this purpose, the two TES groups at the C-2 position of the indoles were removed efficiently with TASF, while the acetyl protecting groups present at the indole nitrogen were removed with hydrazine, to afford bismacrocycle **2.194**. Upon heating this compound in deuterated DMSO at

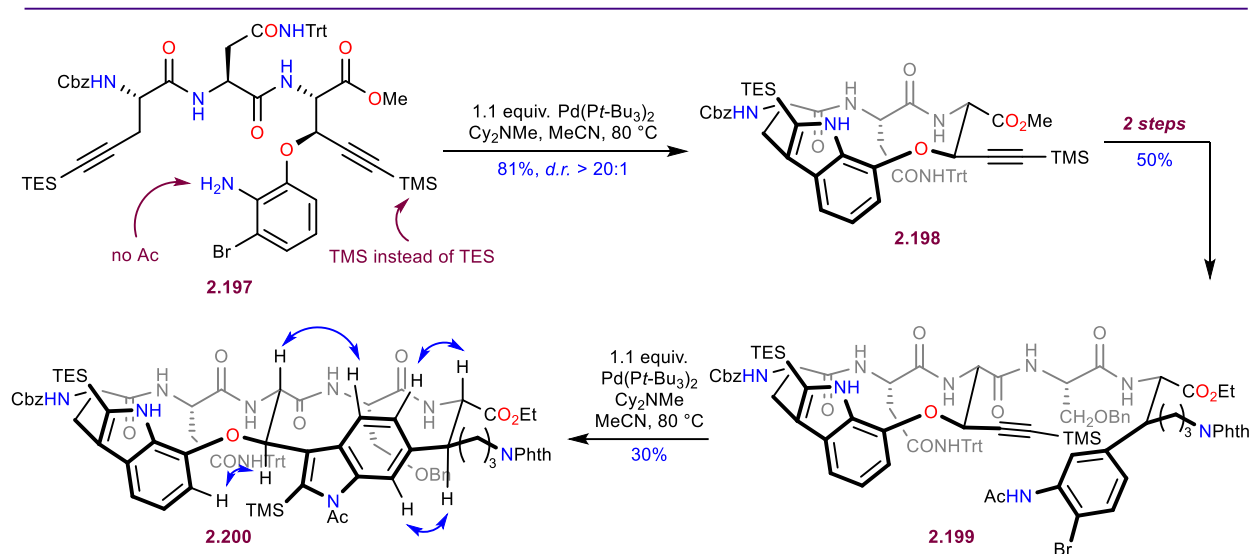
150 °C no equilibration was observed by NMR to produce atropisomer **2.195**, likely due to an extremely high kinetic barrier for indole rotation.



Scheme 2.29: a. Studies of bismacrocyclization via Larock indole synthesis; b. Severe steric clashing is expected in the desired atropisomer

Our next idea for solving the atropisomerism issue was to prepare a macrocyclization substrate that would lack an acetyl group on the western indole/arene and have a smaller TMS group instead of the TES group on the central alkynyl amino acid, to avoid the severe steric clashing explained in Scheme 2.29b. This idea developed into a west-to-east strategy where we would form the western macrocycle first and then the eastern macrocycle in a separate step (Scheme 2.30). To this end, linear precursor **2.197** that meets the previous criteria was prepared. The first Larock indole synthesis afforded the western macrocycle **2.198** in 81% yield as a single

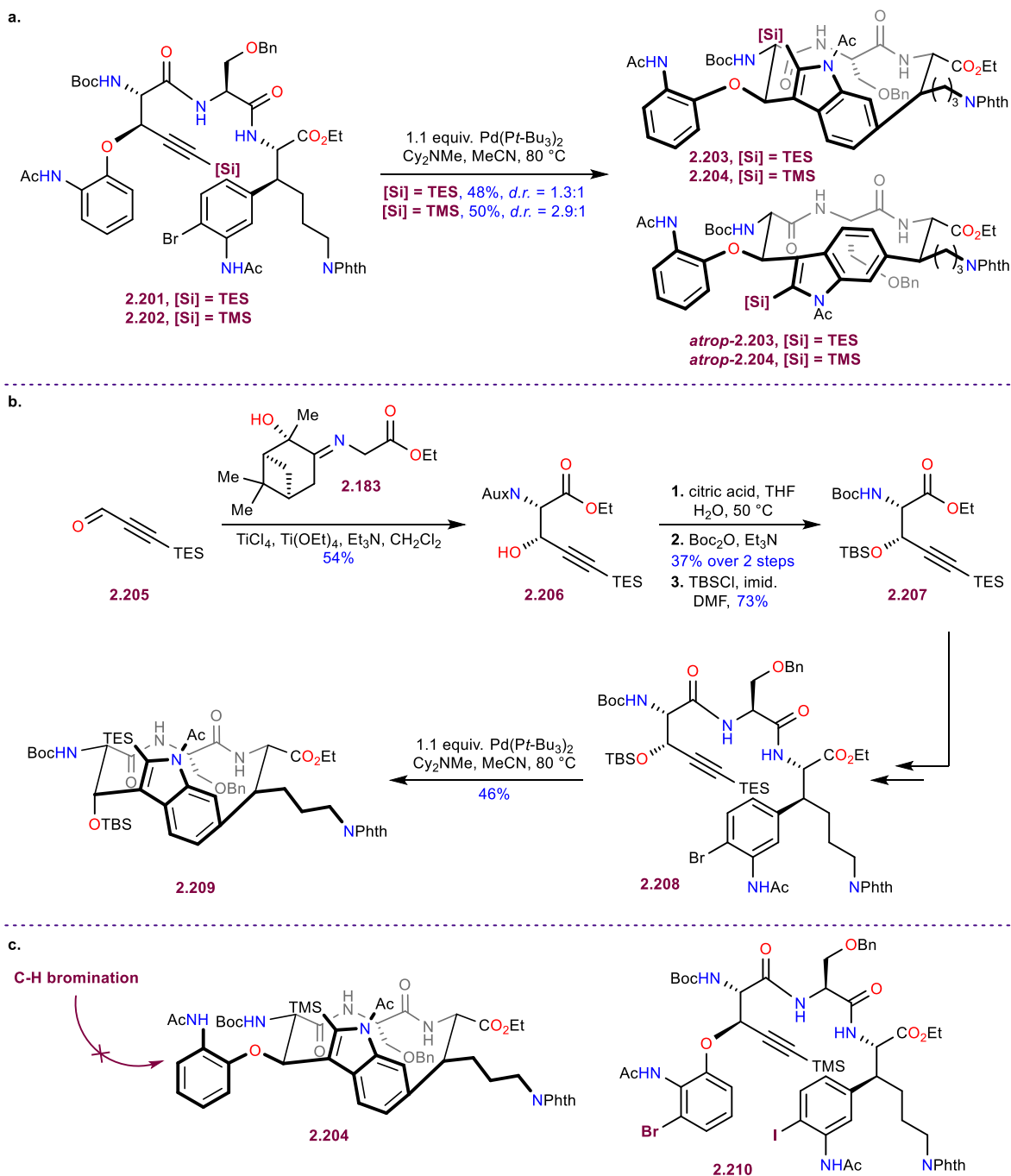
atropisomer. In two steps, this intermediate was elaborated into the precursor for the second macrocyclization **2.199**. The second annulation step produced the bismacrocycle **2.200** in 30% yield, with the eastern macrocycle again forming as the undesired atropisomer. At this point, we reasoned that if the western macrocycle is formed first, then the eastern macrocycle cannot form as the correct atropisomer, due to conformational constraints imposed by the western macrocycle and the silyl group in the central part of the molecule. We weren't able to elaborate **2.197** into a linear pentapeptide precursor for a double Larock macrocyclization because ester hydrolysis followed by peptide coupling resulted in the formation of a 7-membered lactam produced by the attack of the free aniline onto the activated carboxylic acid.



Scheme 2.30: West-to-east macrocyclization strategy

With the west-to-east strategy proving unproductive, we decided to change the directionality of the cyclization steps reasoning that if the eastern macrocycle is formed first and the western macrocycle is formed later, both of them could potentially form as the desired atropisomers. This was the basis of our east-to-west strategy depicted in Scheme 2.31. From our initial study for the formation of the eastern macrocycle, we were able to obtain the desired atropisomer exclusively (Scheme 2.28). However, in that model study there was no group on the propargylic position that would end up being the ether at the β -position of tryptophan. Now, we opted to prepare two different systems **2.201** and **2.202** (the difference between them being the silyl group attached to the alkyne) that would already contain the alkyl-aryl ether in the propargylic position, to see if the ether substituent will have any influence on the atroposelectivity (Scheme 2.31a). Both of these substrates would have an unfunctionalized western acetanilide, to prevent

interference with the palladium-catalyzed macrocyclization. When substrate **2.201**, that has a TES group on the alkyne, was subjected to Larock macrocyclization, the eastern macrocycle formed in 48% yield, as a mixture of atropisomers **2.203** and *atrop*-**2.203** with 1:1 ratio. On the other hand, when substrate **2.202**, that has a TMS group on the alkyne was treated under the exact same conditions, even though the eastern macrocycle was obtained in a similar yield (50%), the

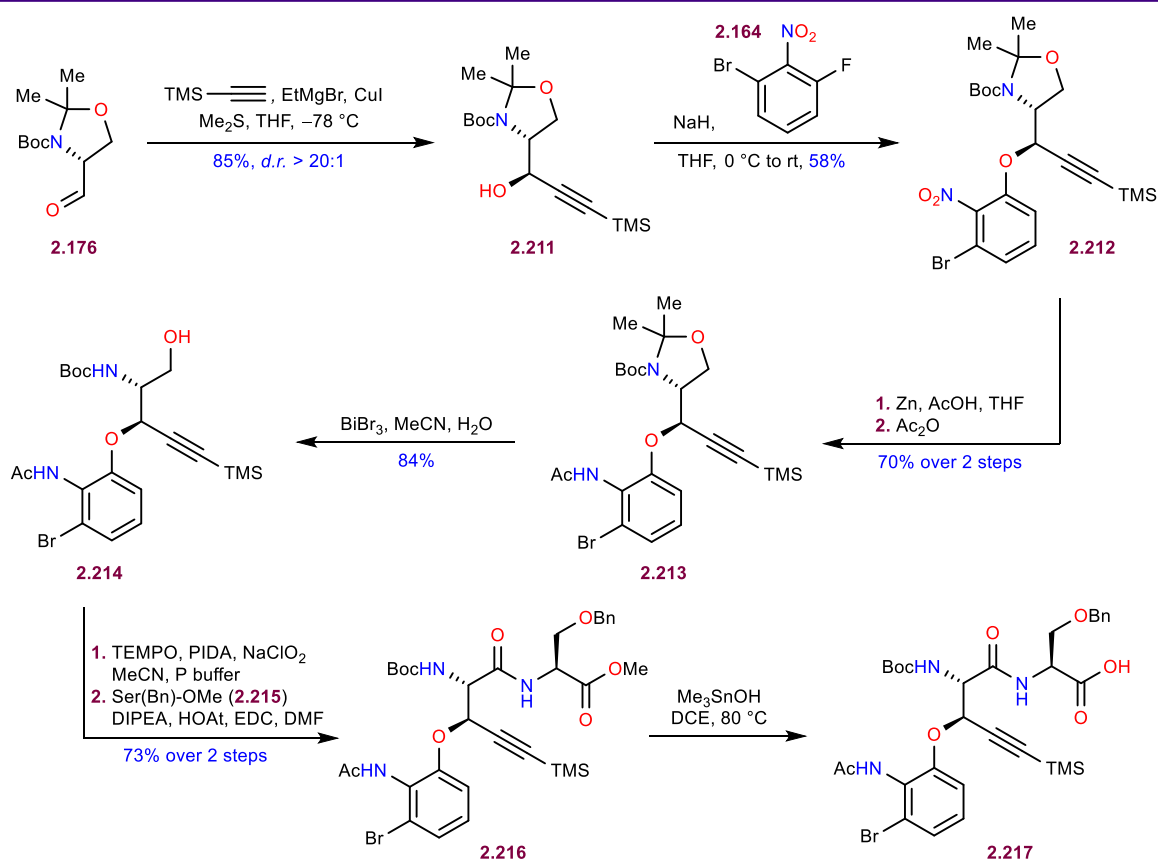


Scheme 2.31: a. Atroposelectivity in the formation of the eastern macrocycle with TES and TMS acetylenes; b. Synthesis of the epimeric TBS-ether and macrocyclization atroposelectivity; c. Plan for continuation of the east-to-west strategy

atropisomer ratio increased to 3:1 favoring the desired atropisomer **2.204** over *atrop*-**2.204**. This increase in atroposelectivity is likely due to decreased A^{1,3} strain between a smaller TMS group and the aryl ether when compared to the A^{1,3} strain between the bulkier TES group and the same ether. We also wanted to investigate the atroposelectivity on a system that would be epimeric at the β-position of the tryptophan (Scheme 2.31b). To prepare such a system, we utilized Cavallo-aldol on aldehyde **2.205** with glycine derivative **2.183**.^{49,50} The aldol product **2.206**, obtained in 54% yield, was subjected to auxiliary removal with aqueous citric acid. The revealed amine was protected with a Boc group, while the alcohol was protected as the TBS-ether **2.207**. In several steps, we have elaborated this substrate into tripeptide **2.208** that is epimeric at the propargylic position when compared to the previously employed cyclization substrates **2.201** and **2.202**. After treating this compound under Larock conditions, the macrocycle **2.209** formed in 46% yield as a single, desired atropisomer. The undesired atropisomer cannot form due to steric clashing that would exist between the TES and TBS groups. Even though the macrocyclization was more efficient on the epimer, subsequent TBS removal and Mitsunobu inversion would make this approach less convergent. Therefore, we decided to stick with the atroposelective Larock where substrate **2.202** with a TMS-alkyne is used. To continue with the synthesis, we had to install a functional handle on the western acetanilide of **2.204**. Expectedly, attempted acetanilide directed C–H bromination with either rhodium or palladium catalysts wasn't fruitful, due to the presence of numerous Lewis-basic sites in the molecule. Furthermore, we decided to design a substrate that would have both acetanilides prefunctionalized with functional handles that could be differentiated in the two Larock indole synthesis steps. More specifically, we want the functionality on the eastern arene to engage selectively in the first Larock indole synthesis, while the functionality on the western arene would remain intact and only engage in the second Larock later in the synthesis. This adequately timed cyclization sequence could be potentially achieved by utilizing substrate **2.210** that has an iodoacetanilide in the eastern portion and a bromoacetanilide in the western portion of the molecule, where palladium insertion into the C(sp²)–I bond is expected to occur faster and selectively in the presence of the C(sp²)–Br bond, allowing us to make the eastern macrocycle with the western bromoacetanilide intact.⁸⁴

To test this hypothesis, we had to prepare **2.210** on multigram scale by making some modifications to our formerly developed synthetic blueprint. Firstly, we streamlined the synthesis of our central fragment. Previously, this fragment was synthesized as the methyl ester **2.163** and

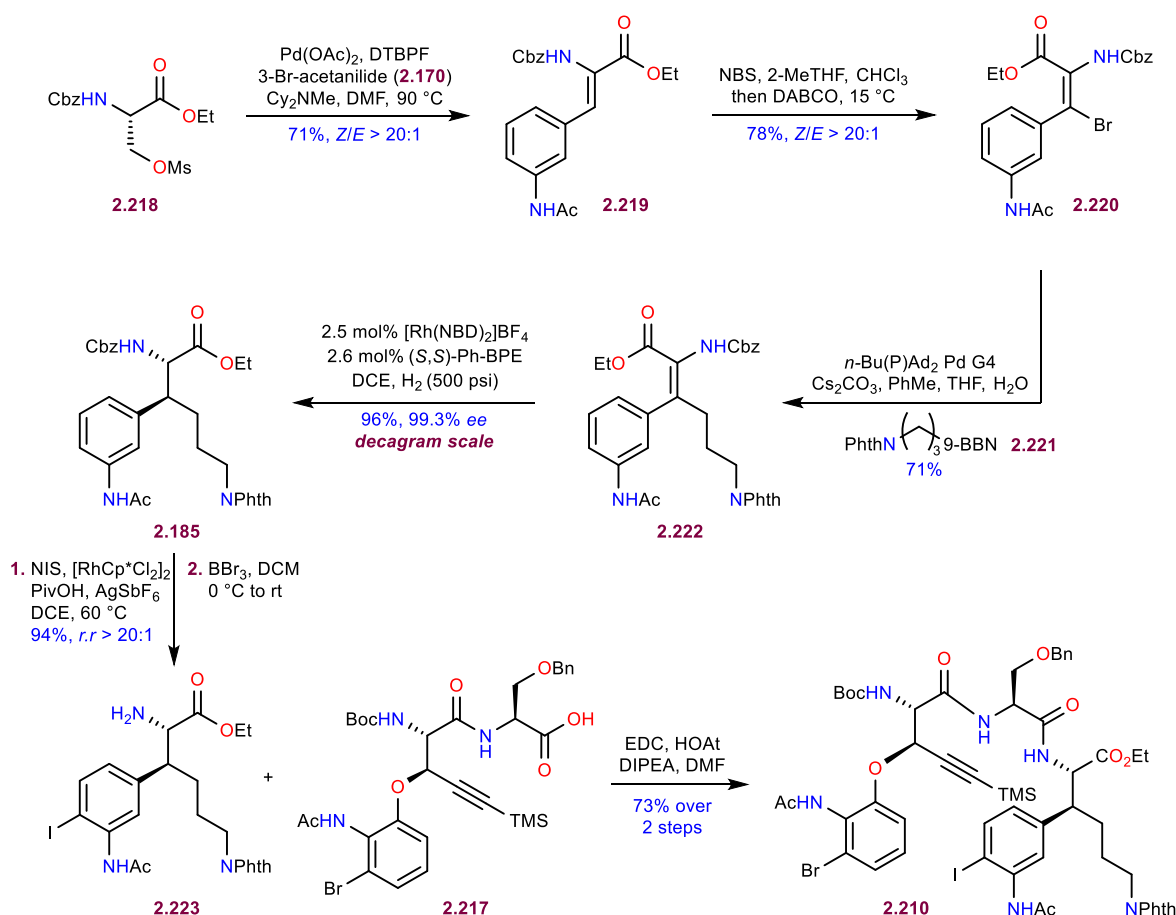
elaborated at the N-terminus by peptide coupling with the western dipeptide **2.175** (Schemes 2.25 and 2.26). Our new plan was to couple the central fragment at the C-terminus with serine, while keeping the N-terminus protected with a Boc group. This required us to change the order of steps, arriving at the modified sequence that is outlined in Scheme 2.32. Starting again with (*D*)-Garner's aldehyde **2.176**, chelation controlled addition of TMS-acetylene afforded alcohol **2.211** in 85% yield as a single diastereomer (Scheme 2.32).⁷⁷ The ensuing S_NAr reaction with arene **2.168** produced **2.212** in 58% yield. Now, the nitro group was converted to the acetanilide **2.213** first, and then the C-terminus carboxylic acid was revealed via acetonide deprotection (**2.213**→**2.214**) and alcohol oxidation. The resulting acid was coupled with serine **2.215**. Finally, the obtained dipeptide **2.216** was hydrolyzed with Me_3SnOH to afford acid **2.217**.⁷¹ Mild hydrolysis conditions had to be used, because stronger bases would eliminate the aryl ether and deprotect the TMS group.



Scheme 2.32: New route towards the central fragment

The synthesis of the β -aryl lysine fragment **2.185** had to be modified, as well. The major issues of our previous route were poor scalability of the photoredox coupling and challenging

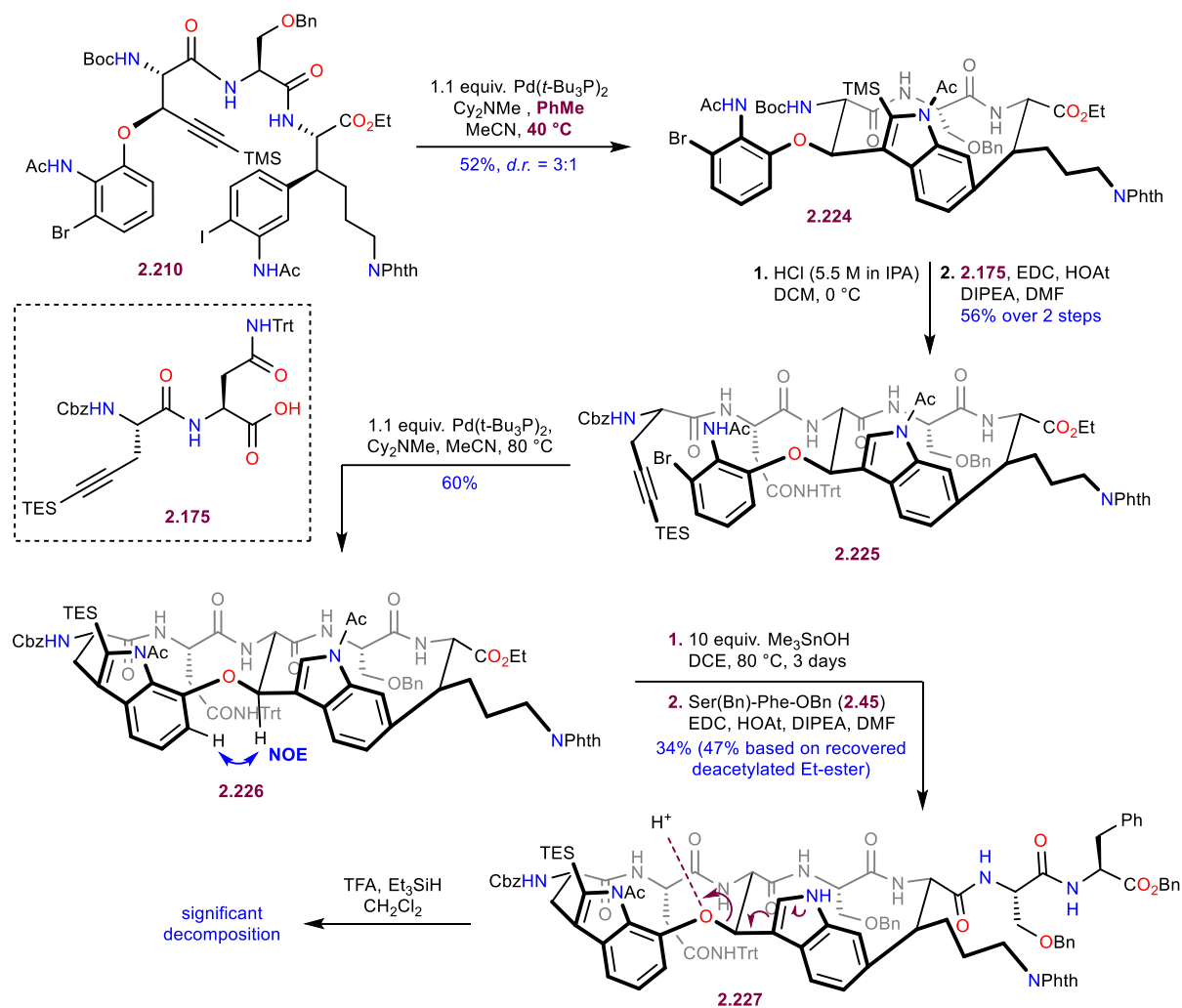
separation of the two diastereomer (Scheme 2.27). Moreover, now we needed to install an iodide on the acetanilide, instead of a bromide. In collaboration with *Merck & Co., Inc.* scientist, a new highly scalable route was developed that obviates all of the aforementioned challenges (Scheme 2.33). Starting with mesylated serine **2.218**, *in situ* elimination is followed by Heck coupling with **2.170** to afford enamide **2.219** in 71% yield (*Z/E* = 20:1).⁸⁵ Bromination at the β -position with NBS is accompanied with DABCO-mediated equilibration to afford β -bromoamide **2.220** as a single diastereomer.⁸⁶ Subsequent Suzuki coupling with borane **2.221** produced unsaturated ester **2.222** in 71% yield. A high-pressure asymmetric hydrogenation of this substrate under rhodium catalysis with (*S,S*)-Ph-BPE as the chiral ligand afforded the β -aryl lysine fragment **2.185** in quantitative yield with 99.3% *ee*.⁸⁷⁻⁹⁰ The previously utilized *ortho*-C–H halogenation was performed with NIS, instead of NBS and to our delight, produced iodoacetanilide in 94% yield as a single constitutional isomer.⁸² Deprotection of the Cbz group with BBr₃⁸³ afforded amine **2.223** that was subsequently coupled to **2.217** with EDC, to furnish the linear precursor **2.210** that was



Scheme 2.33: New route towards the eastern β -aryl lysine fragment and multigram synthesis of the tripeptide

primed for the halogen-selective Larock indole synthesis. Since the asymmetric hydrogenation could be performed on decagram scale (in contrast to the photoredox coupling that we could only run on 4 x 150 mg scale), we were able to obtain multigram quantities of **2.210** in a highly efficient process.

Now, the stage was set for the formation of the eastern macrocycle (Scheme 2.34). After some optimization, we figured out that by running Larock annulation at 40 °C, instead of the previously used 80 °C, we could achieve selective insertion of palladium into the C(sp²)-I bond of **2.210**, affording the eastern macrocycle **2.224** with a 3:1 atropisomeric ratio favoring the desired atropisomer, gratifyingly with the bromoacetanilide still intact. However, the yield for this transformation was variable. This was the result of poor solubility of the palladium catalyst and the amine base in acetonitrile at 40 °C. By adding toluene as a co-solvent, we were able to solve this issue and obtain the eastern macrocycle in a reproducible 52% yield.³⁰⁻³² With the main challenge in our synthesis, the atroposelective formation of the eastern macrocycle solved, we moved on towards the second Larock macrocyclization by elaborating **2.224** at the N-terminus. With HCl in isopropanol, the Boc and the indole C2-TMS group could be removed simultaneously. The obtained free amine was subjected to a peptide coupling with western dipeptide **2.175** (the synthesis of this fragment was depicted in Scheme 2.24). With that, we were able to form the precursor **2.225** for the 2nd Larock in 56% yield over 2 steps. To our delight, the Larock macrocyclization proceeded in 60% yield, giving us the bismacrocycle **2.226** with the western macrocycle existing as the desired atropisomer (confirmed by NOE analysis). All that was left at this stage was the attachment of the Ser-Phe dipeptide **2.45** in the far eastern portion (refer back to Scheme 2.6) and global deprotection. To this end, the ethyl ester **2.226** was subjected to hydrolysis with Me₃SnOH. However, the reaction was very sluggish and required large excess of the reagent, as well as prolonged reaction time. Moreover, deacetylation of the eastern indole was competitive with ester hydrolysis. A small amount of Cbz-protected side product was observed by HPLC, too. Although not completely obvious at this point, the accidental deacetylation significantly complicated the final deprotection step. First, the carboxylic acid with the unprotected eastern indole was coupled to the Ser-Phe dipeptide **2.45** to provide protected darobactin A **2.227** in 34% yield over 2 steps. This ultimate intermediate of the synthesis contained 8 protecting groups, of which several had to be removed under acidic conditions. We attempted the deprotection of the western indole TES group and Trt group (that is located on the asparagine residue) with TFA and

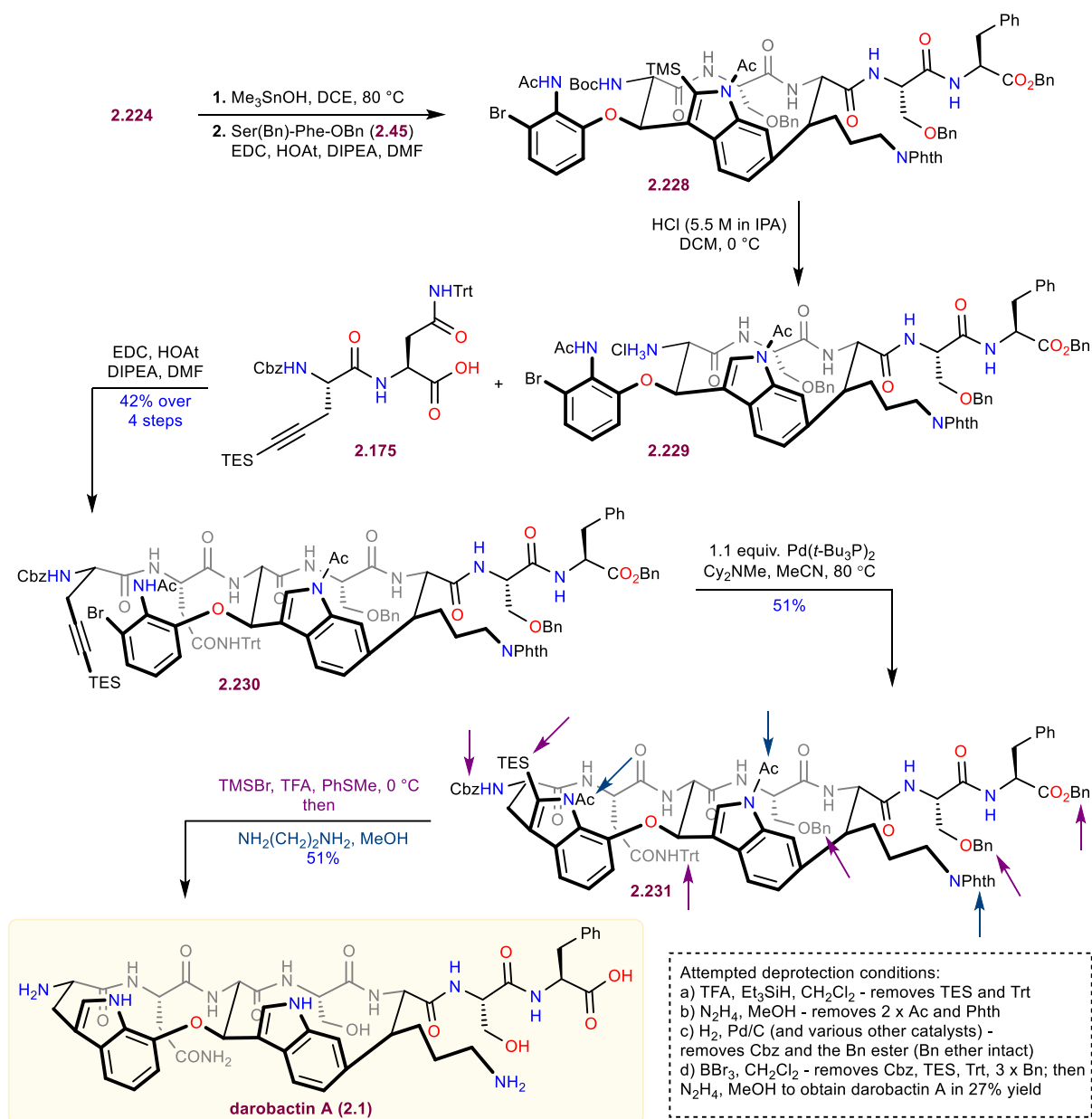


Scheme 2.34: Towards protected darobactin A

Et₃SiH as the cation scavenger. To our dismay, significant decomposition was observed. We speculated that protonation of the activated ether, located next to the electron-rich free eastern indole is causing the decomposition via facile C(sp³)–O bond cleavage. Being so close to the end of the synthesis, we had to find a way of solving this problem. The solution would be finding a way of preserving the acetyl group on the eastern indole until all acid-labile protecting groups are removed, and then reveal the free indole as the very last step of the synthesis. The way of achieving this was apparent, upon closer inspection of the ester hydrolysis step **2.226**→**2.227**. It was interesting that only the acetyl group of the eastern indole ring got removed, while the acetyl group on the western indole was intact. The major difference between the two indoles is that the western one still had a silyl group at the C2-position. Therefore, we reasoned that the TES group on the western indole is sterically blocking the acetyl group from being hydrolyzed by Me₃SnOH and all

that we needed to do to preserve the acetyl group on the eastern indole is to keep the TMS group still on the ring, and remove it only after ethyl ester hydrolysis. On the other hand, we knew that upon attempted Larock indole synthesis of the western indole, with TMS group present on the eastern indole, would result in severe steric clashing between TMS and the western acetyl group, likely prohibiting the macrocyclization from occurring.

With all this in mind, we realized that we could address these challenges by simply changing the order of steps in our endgame sequence (Scheme 2.35). Now starting with the eastern macrocycle **2.224**, elaboration of the system will occur at the C-terminus first and at the N-terminus later. Ethyl ester hydrolysis with Me_3SnOH proceeded with no deacetylation on this substrate, supporting our hypothesis that the TMS group is preventing its hydrolysis by sterics. However, the hydrolysis was somewhat irreproducible and from time to time would result in significant decomposition. Since the Larock indole synthesis step that is used to form **2.224** employs stoichiometric amounts of $\text{Pd}(t\text{-Bu}_3\text{P})_2$, we reasoned that small amounts of palladium are present in **2.224** even after purification by column chromatography. This adventitious palladium could be the reason for the observed decomposition in the subsequent hydrolysis step with Me_3SnOH . To make the sequence reproducible, we found that by stirring **2.224** with the palladium scavenger *N*-acetyl cysteine (aqueous), the majority of the transition metal impurities could be removed, while the minor part that remains, can be easily separated by column chromatography. By using palladium-free **2.224**, we could finally achieve reproducible results for the hydrolysis step. After the free carboxylic acid was revealed, peptide coupling with Ser-Phe furnished **2.228**. This compound exhibited poor solubility in most organic solvents, hence it was telescoped further without any purification. HCl in isopropanol was used again to remove Boc and TMS in the same step, affording **2.229** that was then coupled to the western dipeptide **2.175**. The resulting heptapeptide **2.226** was obtained in 42% over 4 steps. The second Larock annulation produced protected darobactin A **2.231** in 51% yield. The stage was now set for global deprotection. However, removing the 9 protecting groups wasn't a trivial task. Initially, we would remove TES and Trt with TFA. In this case, since the eastern indole is still protected with the acetyl group, no decomposition occurred corroborating our hypothesis about the activated ether decomposition pathway. Then, N_2H_4 could be used to remove the two acetyl groups, as well as the Phth group. The plan was to remove the Cbz and 3 Bn groups last with hydrogenolysis. To our dismay, even after our best efforts to optimize the hydrogenation step, we could only deprotect the terminal Cbz-



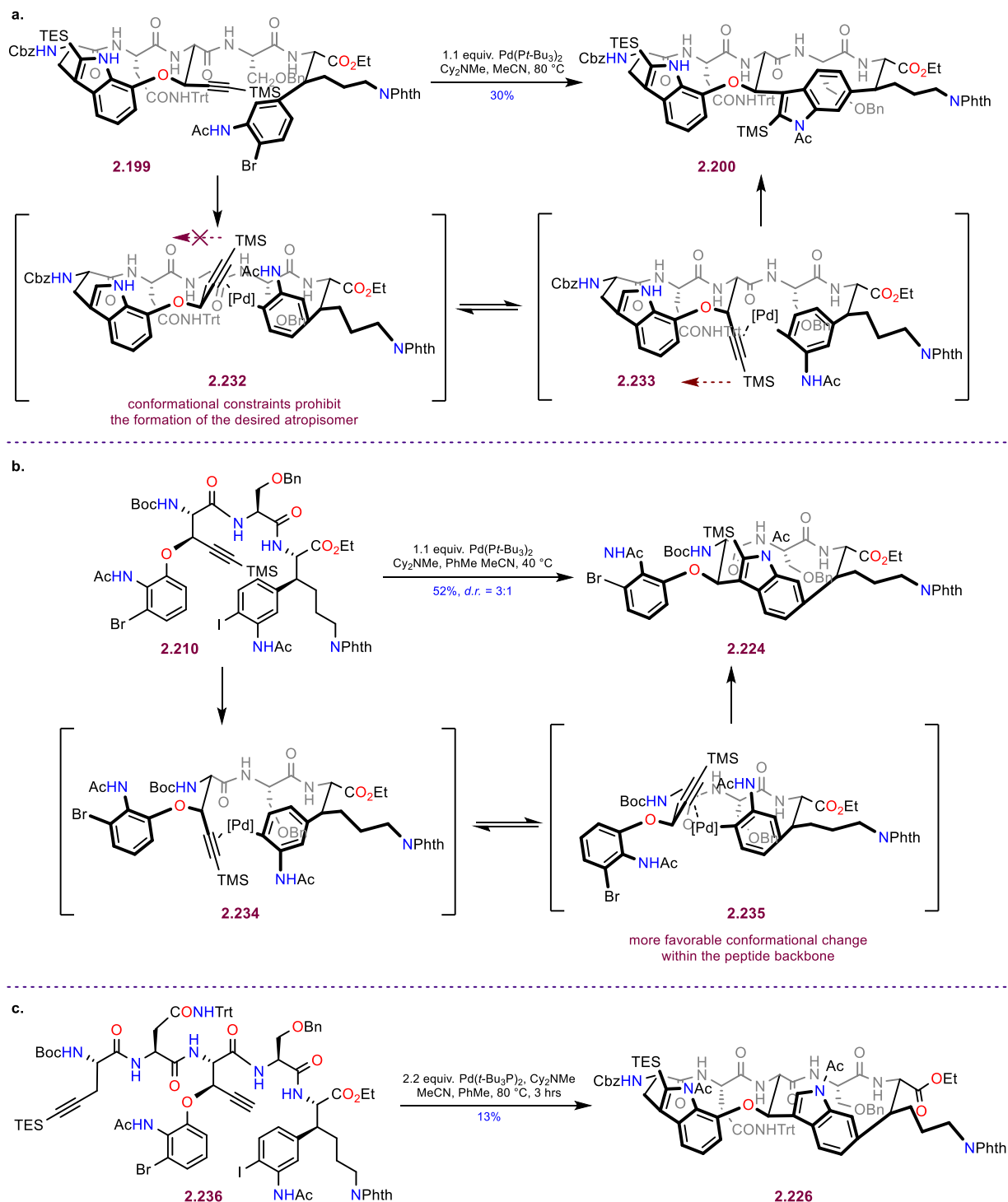
Scheme 2.35: Completion of the synthesis

carbamate and Bn-ester, while the serine Bn-ethers wouldn't participate in the hydrogenolysis. With higher catalyst loadings and hydrogen pressure, the commonly observed result would be complete decomposition. Therefore, we switched to the usage of Lewis acids for the removal of these groups. After several trials, we found that by treating **2.231** with BBr₃, the Cbz, TES, Trt and 3 Bn groups could be removed efficiently. Upon quenching the reaction mixture with aqueous NaHCO₃, hydrazine and MeOH were added. This resulted in the removal of the remaining 2 Ac groups and the Phth group to finally afford darobactin A (**2.1**). In spite of the successful

deprotection, purification of the natural product was extremely difficult due to the presence of borate esters from the BBr_3 step, as well as small amounts of darobactin A hydrazide that was inseparable from the target compound. This sequence was able to produce darobactin A (**2.1**) in circa 27% yield. Unsatisfied with the global deprotection conditions, we decided to search further. Eventually, we found that by employing Yajima's protocol that utilizes TMSBr , TFA and PhSMe , we could cleanly deprotect the Cbz, TES, Trt and 3 Bn groups.⁹¹ After concentration of the solution and trituration with toluene, a relatively clean intermediate could be obtained. We decided to perform the removal of the remaining three groups in the same pot. With this intent, we dissolved the ultimate intermediate in MeOH and treated it with ethylenediamine (instead of the more toxic hydrazine) to arrive at darobactin A (**2.1**) in a much better yield (51%) and with a more expedient purification. With that, we were able to perform the first total synthesis of darobactin A in 16 steps longest linear sequence, 1.5% overall yield and 5.5 mg of the natural product obtained in a single batch.⁹²

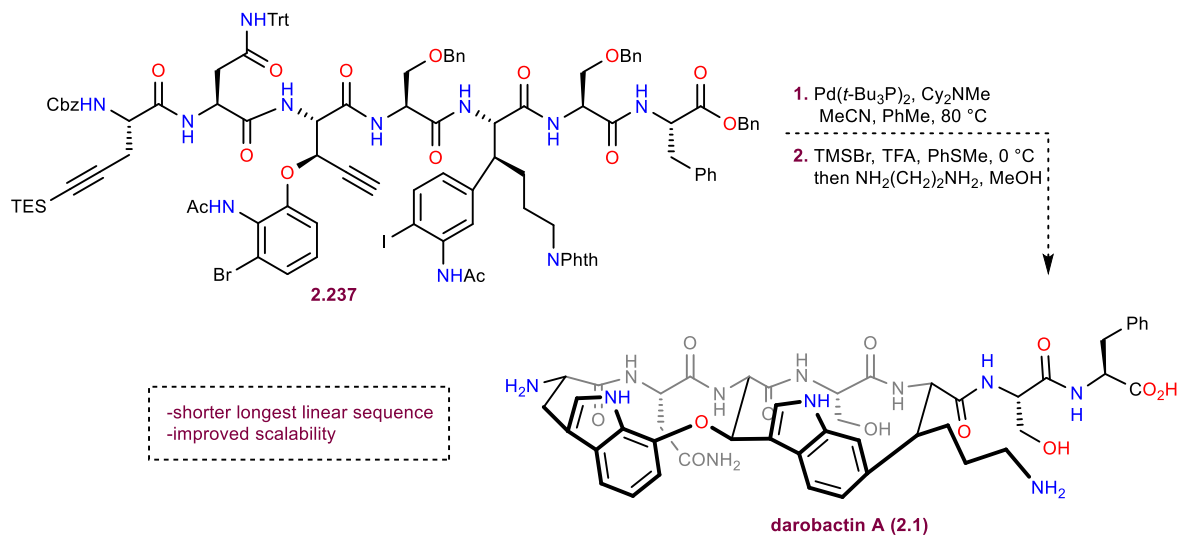
Even though the synthesis was complete, its scalability could still be improved. The two bottlenecks of our synthetic sequence are the sequential Larock indole synthesis steps to make the eastern and western macrocycle, respectively. These macrocyclizations involve the use of stoichiometric palladium and are done under high dilution, thereby severely decreasing the overall material throughput. A solution to this issue would be reinvestigation of the one-pot double Larock annulation and finding a way of obtaining the desired atropisomer with this transformation. This way, instead of having two bottlenecks in the synthesis, we would have only one. This would in turn result in better material throughput, henceforth enabling us to produce larger quantities of the natural product. An in depth analysis of the origin of atroposelectivity of the Larock macrocyclizations, that we had performed on different systems throughout our study could potentially provide us with a solution. With this in mind, we first analyzed the west-to-east strategy that provided the undesired atropisomer of the eastern macrocycle (Scheme 2.36a). Upon oxidative addition of palladium(0) into bromide **2.199**, the obtained organopalladium species can exist in two different productive conformation **2.232** and **2.233**. From these, migratory insertion into the alkyne would provide either the desired atropisomer of the eastern macrocycle (from conformer **2.233**) or the undesired one (from conformer **2.232**). Since only the undesired atropisomer **2.200** was observed in the reaction mixture, the transition state leading to the migratory insertion of **2.233** has to be lower in energy, as the reaction is under kinetic control. This indicates that the movement

of the TMS group towards the western macrocycle during migratory insertion of conformer **2.232** would result in a transition state with a much higher energy, prohibiting the formation of the desired atropisomer. However, when the directionality of the cyclization sequence is changed



Scheme 2.36: Analysis of atroposelectivity in the **a.** west-to-east and **b.** east-to-west cyclization strategies; **c.** Successful one pot double Larock macrocyclization

(east-to-west strategy), the eastern macrocycle forms as the desired atropisomer **2.224** (Scheme 2.36b). This means that the conformer **2.235** that leads to **2.224** has a more favorable conformational change during migratory insertion than the conformer **2.234** that would lead to the undesired atropisomer and this results in a 3:1 atropisomeric ratio. The selectivity is greatly diminished when the TMS group is replaced with a bulkier TES group (1:1 ratio, Scheme 2.31a). With all this in mind, we designed a linear pentapeptide bismacrocyclization precursor **2.236** that would have the following features (Scheme 2.36c): a TES group on the western alkyne (to govern the regioselectivity of the western Larock indole synthesis), no silyl group on the eastern alkyne (to improve atroposelectivity, anticipating that the regioselectivity of the eastern Larock indole synthesis will be controlled by the conformation of the peptide backbone), a bromide on the western acetanilide and an iodide on the eastern acetanilide (to properly time the cyclization sequence where the eastern macrocycle forms in advance of the western macrocycle). After subjecting this substrate to the one-pot bismacrocyclization, we were exhilarated to isolate the desired bismacrocycle in 13% yield with both macrocycles existing as the natural atropisomers. Knowing that **2.226** can't be elaborated into darobactin A (Scheme 2.34) due to deacetylation of the eastern indole upon attempted ethyl ester hydrolysis (since there is no silyl group to prevent the deacetylation), our plan for the 2nd generation synthesis of the natural product is to prepare the linear heptapeptide **2.237** and subject it to one-pot bismacrocyclization to arrive at darobactin A (**2.1**) after global deprotection (Scheme 2.37). The benefits of the new approach are improved convergence, which will result in a shorter longest linear sequence, as well as better scalability,



Scheme 2.37: Plan for the 2nd generation synthesis of darobactin A

now that the synthesis has only one bottleneck and it is located at the very end of the synthetic sequence.

2.7 Conclusion

Since the isolation of darobactin A in 2019,⁸ several research groups have utilized genome mining technology and silent gene expression to produce darobactin analogs (daropeptides), that would arise from the replacement of different amino acids in the peptide backbone.¹⁶⁻¹⁸ This has allowed for structure-activity relationship (SAR) studies that are summarized in Figure 2.4a. While exchanging the serine and lysine of the eastern macrocycle has moderate influence on the analog activity, changing the amino acids of the dipeptide side chain that is attached to the bismacrocycle (Ser-Phe) had the highest influence on bioactivity. After several permutations, Muller's group arrived at darobactin 22 (**2.238**), where the central serine is replaced with threonine, while the Ser-Phe side chain is replaced with Arg-Trp (Figure 2.4b).¹⁸ This analog has superior antibacterial

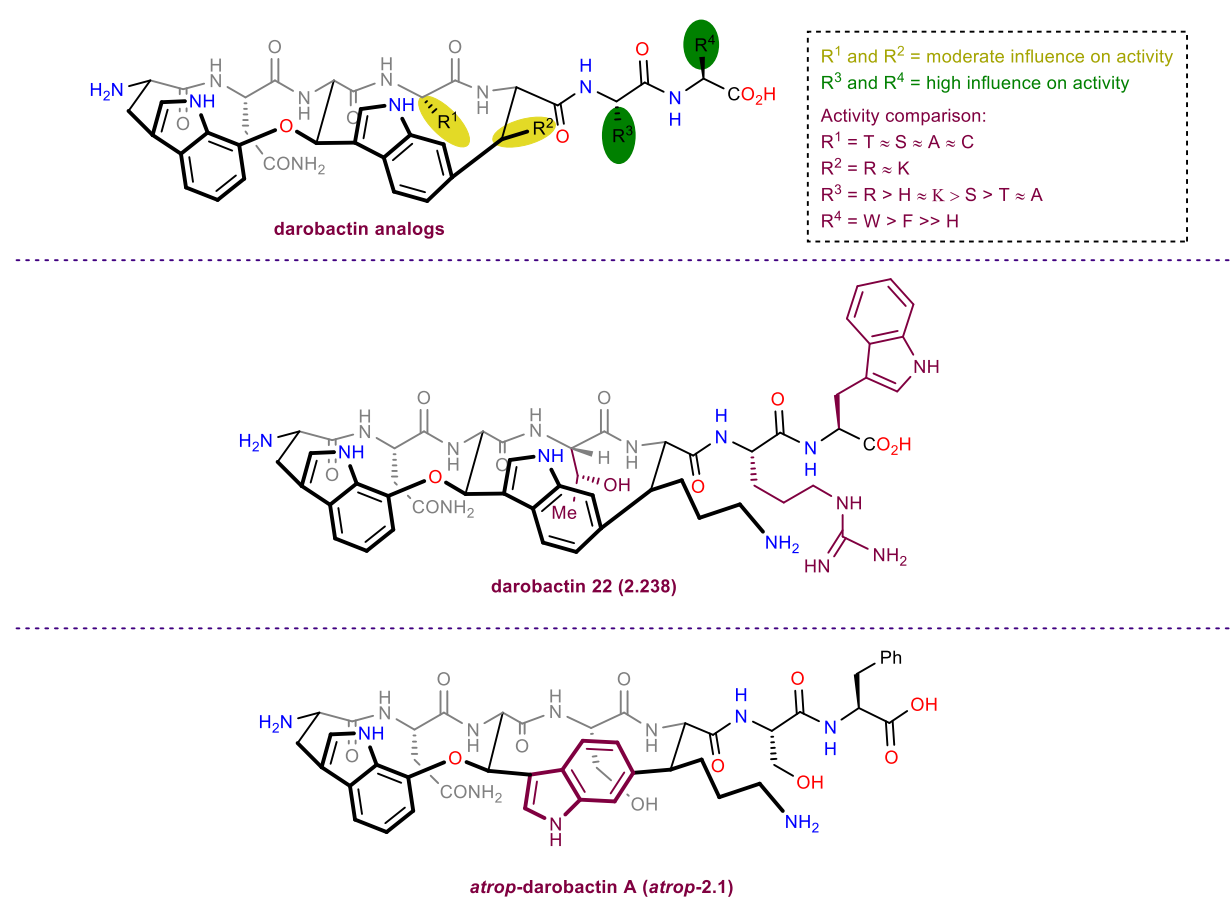
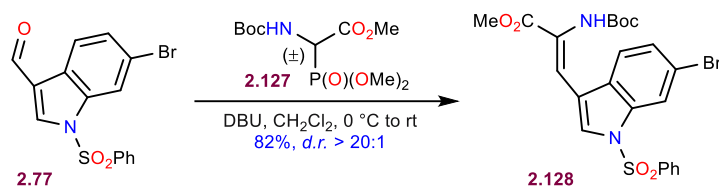


Figure 2.4: a. SAR studies on darobactin analogs; b. The structure of the most potent daropeptide, darobactin 22; c. The unnatural atropisomer of darobactin A

activity against most strains of gram-negative bacteria when compared to darobactin A (**2.1**). Powerful as it may be, gene expression still has to rely on the synthesis of analogs that would arise from incorporation of natural amino acids. Total synthesis on the other hand allows for the assembly of “unnatural” analogs where the natural amino acids can be replaced with a much larger variety of scaffolds. This would provide an entry into unexplored chemical space of daropeptides, resulting in analogs that could potentially have much more potent bioactivity and would also exhibit better pharmacokinetic properties. The synthetic blueprint that we have developed can meet this goal efficiently, due to its modularity and high convergence. Another analog of interest for future studies would be *atrop*-darobactin (*atrop*-**2.1**, Figure 2.4c) that we plan to obtain from **2.200** (Scheme 2.30) through coupling with Ser-Phe dipeptide and global deprotection. Its synthesis would allow us to investigate whether atropisomerism has an influence on the bioactivity through conformational changes within the eastern macrocycle. Finally, the knowledge that was accumulated throughout our investigation is expected to facilitate future studies in the synthesis of macrocyclic RiPPs such as the recently isolated dynobactin (**2.5**, Figure 2.1), which exhibits similar antibacterial activity and mechanism of action as darobactin A (**2.1**).⁹³

2.8 Experimental Section



Unsaturated ester **2.128**:

To a suspension of **2.77** (13.5 g, 37.1 mmol, 1 equiv.) and (±)-Boc- α -phosphonoglycine **2.127** (12.1 g, 40.8 mmol, 1.1 equiv.) in DCM (130 mL, 0.30 M) at 0 °C was added DBU (6.15 mL, 40.8 mmol, 1.1 equiv.), dropwise. The solution was allowed to warm to room temperature and stirred until complete by TLC (4 hours). The reaction mixture was transferred to a separatory funnel, diluted with DCM (100 mL) and washed with 1 M HCl (1 x 100 mL). The aqueous layer was extracted with DCM (2 x 100 mL). Organics were combined, dried over MgSO₄, filtered, and concentrated under reduced pressure. The resulting solid was recrystallized from ethanol to yield **2.218** as a white solid (15.5 g, 28.9 mmol, 72%).

$R_f = 0.3$ (SiO₂, hexanes : EtOAc = 3:1)

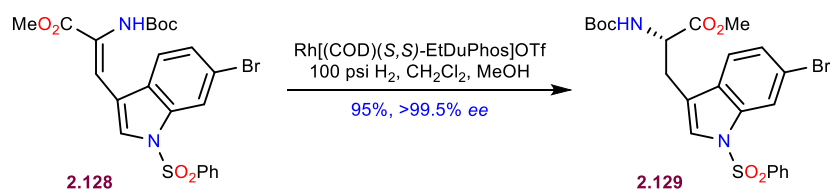
$t_{m.p.} = 178.7\text{--}181.8\text{ }^\circ\text{C}$

¹H NMR (500 MHz, CDCl₃) δ 8.13 (s, 1H), 7.89 (d, $J = 7.9$ Hz, 2H), 7.81 (s, 1H), 7.58 (t, $J = 7.5$ Hz, 1H), 7.53 (d, $J = 8.5$ Hz, 1H), 7.51 – 7.46 (m, 3H), 7.40 (d, $J = 8.5$, 1H), 6.36 (s, 1H), 3.87 (s, 3H), 1.46 (s, 9H).

¹³C{¹H} NMR (126 MHz, CDCl₃) δ 165.7, 152.5, 137.8, 135.1, 134.5, 129.7, 128.9, 128.2, 127.3, 127.0 (2x), 121.0, 120.5, 119.1, 116.8, 116.0, 81.6, 52.9, 28.3.

HRMS: (ES⁺, m/z) [M+Na]⁺ calcd. for C₂₃H₂₃N₂O₆NaS⁷⁹Br, 557.0358; found 557.0353.

IR (ATR, neat, cm⁻¹): 3318 (br), 2979 (w), 1710 (s), 1248 (s), 1175 (s), 1136 (s), 581 (s).



Bromotryptophan **2.219**:

Degassed DCM (150 mL) was added via syringe to a high-pressure hydrogenation vessel containing **2.218** (13.8 g, 25.7 mmol) under nitrogen. Then (+)-1,2-bis((2*S*,5*S*)-2,5-diethylphospholano)benzene(1,5-cyclooctadiene)rhodium(I) trifluoromethanesulfonate (170 mg, 0.257 mmol, 1 mol%) in degassed methanol (75 mL, total concentration = 0.1 M) was added and the reaction vessel was sealed tightly. The vessel was charged with hydrogen gas (80 psi) and discharged slowly (3 cycles). The vessel was charged with hydrogen gas (80 psi), and the inlet was closed tightly. After 36 hours, the vessel was slowly discharged and the crude reaction mixture was filtered through a silica gel pad. The pad was washed with DCM (3 x 75 mL), and the filtrate was concentrated under reduced pressure to yield **2.219** (13.8 g, 25.7 mmol, 99% yield, >99.5% ee). The crude material was carried forward without further purification. A small sample was columned (4:1 Hexanes/Ethyl Acetate) for characterization.

$[\alpha]_D^{22} = 19.9^\circ$ (c = 12.0 mg/mL, CHCl₃)

$R_f = 0.3$ (SiO₂, hexanes : EtOAc = 3:1)

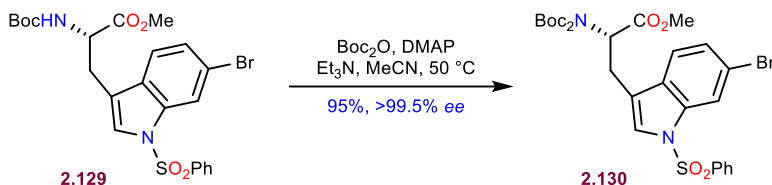
$t_{m.p.} = 62.0\text{--}65.5\text{ }^\circ\text{C}$

¹H NMR (500 MHz, CDCl₃) δ 8.15 (s, 1H), 7.84 (d, *J* = 7.8 Hz, 2H), 7.60 – 7.55 (m, 1H), 7.48 (t, *J* = 7.7 Hz, 2H), 7.37 – 7.30 (m, 3H), 5.04 (d, *J* = 7.8 Hz, 1H), 4.60 (q, *J* = 6.2 Hz, 1H), 3.62 (s, 3H), 3.21 (dd, *J* = 14.7, 5.7 Hz, 1H), 3.12 (dd, *J* = 14.9, 5.4 Hz, 1H), 1.44 (s, 9H).

¹³C{¹H} NMR (126 MHz, CDCl₃) δ

HRMS: (ES⁺, *m/z*) [M+Na]⁺ calcd. for C₂₃H₂₅N₂O₆NaS⁷⁹Br, 559.0514; found 559.0526.

IR (ATR, neat, cm⁻¹): 3396 (br), 2977 (w), 1743 (m), 1711 (m), 1367 (m), 1174 (s), 606 (m).



Tryptohan **2.130**:

2.219 (13.8 g, 25.6 mmol, 1.0 equiv.), was dissolved in acetonitrile (100 mL). To this was added Et₃N (10.7 mL, 76.8 mmol, 3.0 equiv.). In a separate vessel, 4-dimethylaminopyridine (6.26 g, 51.2 mmol, 2.0 equiv.) was dissolved in acetonitrile (100 mL). To this was added Boc₂O (17.6 mL, 76.8 mmol, 3.0 equiv.). This mixture was sonicated until homogenous and added slowly to the solution of **2.129**. The resultant mixture was heated to 50 °C under a reflux condenser until complete by TLC (5 hours). Celite was added to the reaction mixture and it was concentrated in vacuo. The crude product was purified by silica gel chromatography (6:1 Hexanes/Ethyl Acetate) to yield **2.130** as a yellow foam (15.1 g, 23.6 mmol, 92%).

[α]_D²² = -91.2° (c = 15.0 mg/mL, CHCl₃)

R_f = 0.4 (SiO₂, hexanes : EtOAc = 3:1)

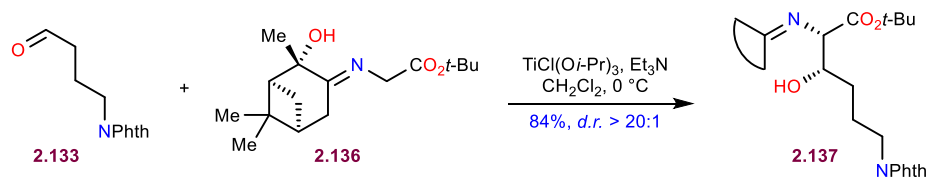
t_{m.p.} = 73.0–77.0 °C

¹H NMR (500 MHz, CDCl₃) δ 8.12 (s, 1H), 7.85 (d, *J* = 8.1 Hz, 2H), 7.58 – 7.53 (m, 1H), 7.47 (t, *J* = 7.7 Hz, 2H), 7.40 – 7.32 (m, 3H), 5.14 (dd, *J* = 9.9, 5.0 Hz, 1H), 3.75 (d, *J* = 1.0 Hz, 3H), 3.47 (dd, *J* = 15.1, 5.1 Hz, 1H), 3.32 (dd, *J* = 15.0, 10.0 Hz, 1H), 1.33 (d, *J* = 1.1 Hz, 18H).

¹³C{¹H} NMR (126 MHz, CDCl₃) δ 170.7, 152.0, 138.2, 135.8, 134.1, 129.8, 129.6, 126.9, 126.7, 125.2, 120.9, 118.7, 118.6, 116.7, 83.4, 58.0, 52.6, 27.9, 25.7.

HRMS: (ES⁺, *m/z*) [M+Na]⁺ calcd. for C₂₈H₃₃N₂O₈NaS⁷⁹Br, 659.1039; found 659.1016.

IR (ATR, neat, cm⁻¹): 2981 (w), 1830 (w), 1728 (s), 1368 (s), 1169 (s), 1142 (s), 754 (s).



Aldol **2.137**:

To a solution of $\text{Ti}(\text{O}i\text{-Pr})_4$ (8.0 mL, 26.5 mmol, 0.9 equiv) in DCM (75 mL) at 0 °C was added TiCl_4 (0.97 mL, 8.82 mmol, 0.3 equiv). The solution was stirred for 15 minutes at 0 °C before added to a solution of 2-((1*S*,2*S*,5*S*)-2-hydroxypinan-3-imino)glycinate **2.136** (9.10 g, 32.3 mmol, 1.1 equiv) in DCM (250 mL) at 0 °C. A fine powder of 4-phthalimidobutanal **2.133** (6.39 g, 29.4 mmol, 1.0 equiv) was added to the mixture at the same temperature. Triethylamine (8.20 mL, 58.8 mmol, 2.0 equiv) was subsequently added, and the reaction was stirred at 0 °C. After consumption of 4-phthalimidobutanal (about 3 hours, followed by TLC), brine (300 mL) was added and the obtained mixture was let to stir for 30 minutes while warmed up to room temperature. The resulting bilayer suspension was filtered through celite. The organic layer was separated, and the aqueous layer was extracted with dichloromethane (2 × 200 mL). The combined organic layers were dried over anhydrous magnesium sulfate, filtered and concentrated under reduced pressure. The obtained residue was purified by column chromatography (SiO_2 , hexanes/EtOAc = 1:2 + 5% NEt_3) to afford the aldol product **2.137** as a white foam (single diastereomer, 12.3 g, 24.7 mmol, 84%).

$[\alpha]_D^{22} = -39.9^\circ$ ($c = 17.5$ mg/mL, CHCl_3)

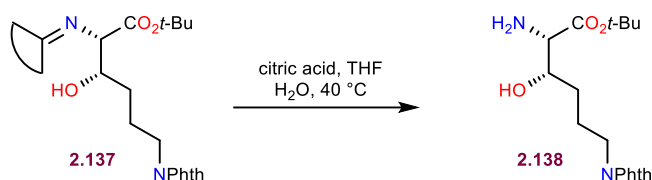
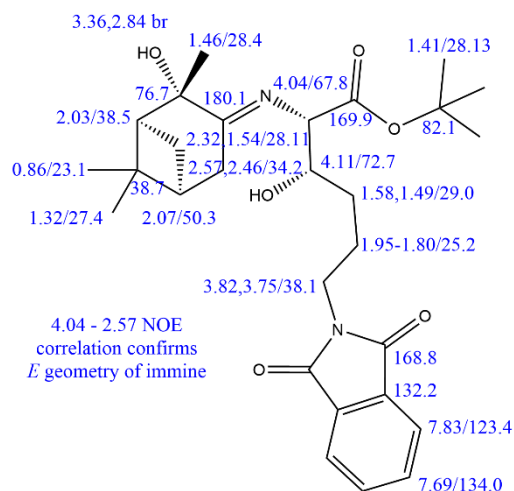
$R_f = 0.2$ (SiO_2 , hexanes : EtOAc = 1:2 + 5% Et_3N)

$^1\text{H NMR}$ (500 MHz, CDCl_3) δ 7.83 (dd, $J = 5.5, 3.0$ Hz, 2H), 7.69 (dd, $J = 5.5, 3.0$ Hz, 2H), 4.11 (q, $J = 5.8$ Hz, 1H), 4.04 (d, $J = 6.0$ Hz, 1H), 3.82 (dt, $J = 14.2, 7.2$ Hz, 1H), 3.75 (dt, $J = 13.5, 6.5$ Hz, 1H), 3.36 (br, 1H), 2.84 (br, 1H), 2.57 (d, $J = 18.0$ Hz, 1H), 2.46 ($J = 18.0$ Hz, 1H), 2.32 (ddt, $J = 8.5, 6.0, 3.0$ Hz, 1H), 2.07 (t, $J = 5.9$ Hz, 1H), 2.03 (d, $J = 5.8$ Hz, 1H), 1.95 – 1.80 (m, 2H), 1.62 – 1.53 (m, 2H), 1.52 – 1.44 (m, 4H), 1.41 (s, 9H), 1.32 (s, 3H), 0.86 (s, 3H).

$^{13}\text{C}\{^1\text{H}\}$ NMR (126 MHz, CDCl_3) δ 180.1, 169.6, 168.8, 134.0, 132.2, 123.4, 82.1, 76.7, 72.7, 67.8, 50.3, 38.7, 38.5, 38.1, 34.2, 29.0, 28.4, 28.13, 28.11, 27.4, 25.2, 23.1.

HRMS: (ES^+ , m/z) $[\text{M}+\text{H}]^+$ calcd. for $\text{C}_{28}\text{H}_{39}\text{N}_2\text{O}_6$, 499.2808; found 499.2794.

IR (ATR, neat, cm^{-1}): 3373 (br), 2976 (w), 2935 (w), 1771 (w), 1706 (s), 1396 (m), 1367 (m), 1154 (m), 720 (m).



Aminoalcohol **2.138**:

To a solution of **2.137** (10.8 g, 21.7 mmol, 1.0 equiv) in THF (167 mL) was added a 15% aqueous solution of citric acid (54.1 mL, 42.2 mmol, 1.95 equiv). The reaction mixture was stirred at 40 °C for 36 h. THF was removed by concentration in vacuo, and the remaining mixture was washed with ether (2 x 100 mL), neutralized with solid Na₂CO₃, and extracted with EtOAc (3 x 150 mL). The combined organic layers were dried over anhydrous magnesium sulfate, filtered, and concentrated under reduced pressure. The crude mixture was taken forward without additional purification.

For characterization, the crude product was purified by column chromatography (SiO₂, DCM:MeOH = 20:1) to give the pure product as a yellow oil (75% yield).

$[\alpha]_D^{23} = 0.6^\circ$ (c = 15.5 mg/mL, CHCl₃)

$R_f = 0.2$ (SiO₂, DCM : MeOH = 95:5)

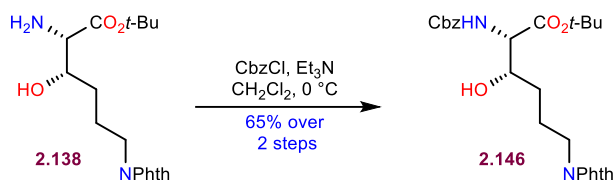
¹H NMR (500 MHz, CDCl₃) δ 7.83 (dd, *J* = 5.6, 3.1 Hz, 2H), 7.70 (dd, *J* = 5.5, 3.1 Hz, 2H), 3.80 (dt, *J* = 9.1, 4.1 Hz, 1H), 3.73 (d, *J* = 7.1 Hz, 1H), 3.72 (d, *J* = 7.1 Hz, 1H), 3.45 (d, *J* = 4.6 Hz,

1H), 2.20 (br, 3H), 1.93 (ddt, $J = 13.1, 9.2, 6.6$ Hz, 1H), 1.78 (ddt, $J = 16.4, 13.7, 7.2$ Hz, 1H), 1.47-1.34 (m, 11H).

$^{13}\text{C}\{^1\text{H}\}$ NMR (126 MHz, CDCl_3) δ 172.9, 168.6, 134.0, 132.3, 123.3, 82.1, 72.0, 59.0, 37.9, 29.5, 28.1, 25.4

HRMS: (ES+, m/z) $[\text{M}+\text{H}]^+$ calcd. for $\text{C}_{18}\text{H}_{25}\text{N}_2\text{O}_5$, 349.1763; found 349.1747.

IR (ATR, neat, cm^{-1}): 3373 (br), 2976 (w), 2935 (w), 1771 (w), 1706 (s), 1396 (m), 1367 (m), 1154 (m), 720 (m).



Hydroxylysine **2.146**:

To the crude mixture of **2.138** (7.54 g, 21.6 mmol, 1.0 equiv) dissolved in DCM (216 mL) at 0°C was added triethylamine (7.54 mL, 54.1 mmol, 2.5 equiv) and CbzCl (3.71 mL, 26.0 mmol, 1.2 equiv). Upon consumption (by TLC), the reaction mixture was quenched with 1 M HCl (100 mL). The organic layer was separated, and the aqueous layer was extracted with dichloromethane (2×100 mL). The combined organic layers were dried over anhydrous magnesium sulfate, filtered and concentrated under reduced pressure. The obtained residue was purified by column chromatography (SiO_2 , hexanes:EtOAc = 2:1 then 1:1) to afford **2.146** as a white foam (6.76 g, 14.0 mmol, 65%).

$[\alpha]_{\text{D}}^{23} = 13.7^\circ$ ($c = 16.0$ mg/mL, CHCl_3)

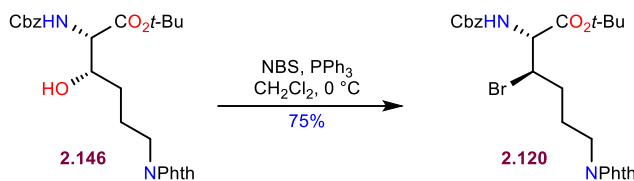
$R_f = 0.2$ (SiO_2 , hexanes : EtOAc = 2:1)

^1H NMR (500 MHz, CDCl_3) δ 7.82 (dd, $J = 5.4, 3.1$ Hz, 2H), 7.70 (dd, $J = 5.5, 3.1$ Hz, 2H), 7.39 – 7.29 (m, 5H), 5.69 (d, $J = 7.5$ Hz, 1H), 5.09 (d, $J = 2.7$ Hz, 2H), 4.31 (dd, $J = 7.7, 3.5$ Hz, 1H), 3.95 (dt, $J = 8.7, 3.9$ Hz, 1H), 3.73 (t, $J = 7.1$ Hz, 2H), 1.97 – 1.85 (m, 1H), 1.79 (dq, $J = 13.9, 6.6$ Hz, 1H), 1.44 (s, 11H).

$^{13}\text{C}\{^1\text{H}\}$ NMR (126 MHz, CDCl_3) δ 169.2, 168.6, 156.7, 136.2, 134.1, 132.2, 128.7, 128.4, 128.3, 123.4, 83.3, 73.0, 67.4, 59.3, 37.7, 30.3, 28.1, 25.4.

HRMS: (ES+, m/z) $[\text{M}+\text{Na}]^+$ calcd. for $\text{C}_{26}\text{H}_{30}\text{N}_2\text{O}_7\text{Na}$, 505.1951; found 505.1944.

IR (ATR, neat, cm^{-1}): 3424 (br), 2976 (w), 2937 (w), 1771 (w), 1704 (s), 1396 (m), 1367 (m), 1154 (m), 720 (m).



Bromolysine 2.120:

To a solution of triphenylphosphine (7.35 g, 28.0 mmol, 2 equiv) in DCM (70 mL) at 0 °C was added NBS portionwise (4.99 g, 28.0 mmol, 2 equiv). The solution was stirred for 15 min at 0 °C, followed by the dropwise addition of a solution of **2.146** (6.76 g, 14.0 mmol, 1.0 equiv) in DCM (70 mL). The mixture was left to warm up to room temperature and continued to stir for 36 hours. Upon completion, DCM was removed by reduced pressure and the crude mixture was purified by column chromatography (SiO₂, hexanes:EtOAc = 3:1 to 2:1) to afford **2.120** as a white foam (4.58 g, 8.40 mmol, 60%).

$[\alpha]_{\text{D}}^{23} = 20.4^\circ$ ($c = 15.5$ mg/mL, CHCl₃)

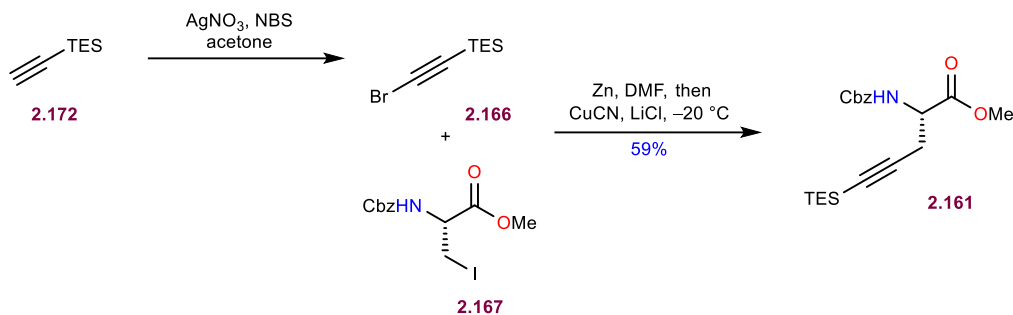
$R_f = 0.3$ (SiO₂, hexanes : EtOAc = 3:1)

¹H NMR (500 MHz, CDCl₃) δ 7.84 (dd, $J = 5.5, 3.1$ Hz, 2H), 7.71 (dd, $J = 5.5, 3.1$ Hz, 2H), 7.40 – 7.29 (m, 5H), 5.46 (d, $J = 9.5$ Hz, 1H), 5.08 (d, $J = 12.4$ Hz, 1H), 5.05 (d, $J = 12.2$ Hz, 1H), 4.59 (dd, $J = 9.5, 2.2$ Hz, 1H), 4.55 (t, $J = 5.5$ Hz, 1H), 3.72 (t, $J = 6.2$ Hz, 2H), 1.96 – 1.86 (m, 4H), 1.48 (s, 9H).

¹³C{¹H} NMR (126 MHz, CDCl₃) δ 168.4, 168.2, 156.6, 136.1, 134.1, 132.2, 128.7, 128.4, 128.3, 123.4, 83.4, 67.4, 58.5, 56.3, 37.0, 33.2, 28.1, 26.9.

HRMS: (ES⁺, m/z) $[M+Na]^+$ calcd. for C₂₆H₃₉N₂O₆⁷⁹BrNa, 567.1107; found 567.1093.

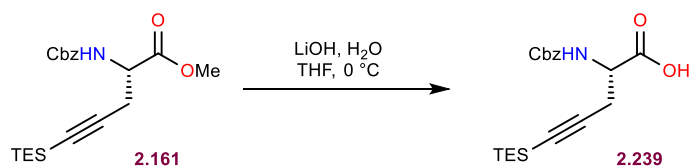
IR (ATR, neat, cm^{-1}): 3373 (br), 2976 (w), 2935 (w), 1771 (w), 1706 (s), 1396 (m), 1367 (m), 1154 (m), 720 (m).



Alkynyl amino acid **2.161**:

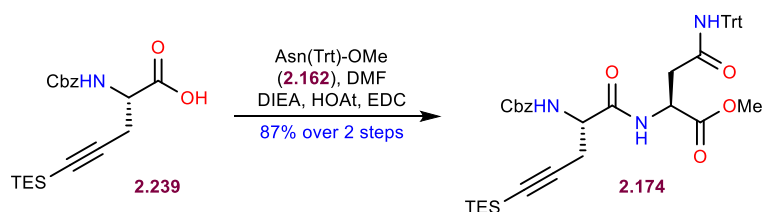
Triethyl(ethynyl)silane **2.172** (1.17 g, 8.33 mmol, 1.4 equiv.) was dissolved in acetone (28 mL, 0.3 M). Silver nitrate (141 mg, 833 μmol , 0.14 equiv.) and recrystallized NBS (1.59 g, 8.92 mmol, 1.5 equiv.) were added successively, each in a single portion. After 2 hours, the reaction mixture was quenched by its addition to ice water (20 mL), extracted with pentane (2×20 mL), washed with brine (20 mL), dried over MgSO_4 , filtered and concentrated. The crude material **2.166** was used directly in the coupling reaction.

To a flask containing the zinc dust (1.40 g, 21.4 mmol, 3.6 equiv.) was added DMF (6 mL), followed by 1,2-dibromoethane (103 μL , 1.19 mmol, 0.2 equiv.). The suspension was heated at $80\text{ }^\circ\text{C}$ for 30 minutes. After cooling to room temperature, distilled TMSCl (75.5 μL , 595 μmol , 0.1 equiv.) was added and the suspension was stirred an additional 30 minutes at room temperature. To this suspension was added Cbz-iodoserine methyl ester **2.167** (2.16 g, 5.95 mmol, 1.0 equiv.) in DMF (4 mL) over 2 minutes, which resulted in an exotherm. After returning to room temperature, stirring was ceased and the alkyl zinc reagent was transferred dropwise via cannula to a cooled ($-20\text{ }^\circ\text{C}$) solution of CuCN (479 mg, 5.35 mmol, 0.9 equiv.) and LiCl (454 mg, 10.7 mmol, 1.8 equiv.) in DMF (10 mL; 0.25 M total concentration relative to alkyl iodide). After a period of 15 minutes, neat 1-bromo-2-triethylsilylacetylene was added dropwise to the reaction mixture at the same temperature. The reaction mixture was then allowed to slowly warm to room temperature over a 3-hour period and stirring was continued at that temperature overnight. Then, the reaction was quenched by the addition of water (100 mL) and extracted with Et_2O (3×50 mL). The organic extracts were washed with brine (50 mL), dried over MgSO_4 , filtered and concentrated. The crude product was purified by flash column chromatography (SiO_2 , Hex/ EtOAc = 5:1) to yield alkyne **2.161** (1.32 g, 3.51 mmol, 59% based on iodoserine). Characterization data matched that of a previous report.⁹⁴



Acid **2.239**:

Alkyne **2.161** (1.60 g, 4.26 mmol, 1.0 equiv.) was dissolved in THF (21 mL) and water (10 mL) and cooled to 0 °C. A 1 M aqueous solution of LiOH (153 mg, 6.39 mmol, 6.39 mL, 1.5 equiv.) was added dropwise and the reaction was allowed to warm to room temperature. After 1 hour, the reaction was complete (by TLC analysis), and was quenched by the slow addition of 1 M aqueous HCl until the pH was around 4. The reaction mixture was extracted with EtOAc (3 x 70 mL), the organic layers were combined, washed with brine (50 mL), dried with MgSO₄, and concentrated. The crude acid **2.239** was used without further purification (assumed quantitative yield, 1.54 g, 4.26 mmol).



Methyl ester **2.174**:

Acid **2.239** (1.54 g, 4.26 mmol, 1.0 equiv.) and H-Asn(Trt)-OMe **2.162** (1.82 g, 4.69 mmol, 1.1 equiv.) were dissolved in DMF (45 mL) (0.1 M) and cooled to 0 °C. To this solution was added DIPEA (1.78 mL, 10.2 mmol, 2.4 equiv.), HOAt, (696 mg, 5.11 mmol, 1.2 equiv.), and EDC (980 mg, 5.11 mmol, 1.2 equiv.) in that order. The mixture was allowed to warm to room temperature and left to stir overnight. The reaction was quenched by addition of aqueous 1 M HCl (60 mL) and the mixture was transferred to a separatory funnel. The layers were separated and the aqueous layer was extracted with ethyl acetate (3 x 60 mL). The combined organic layers were washed with saturated aqueous NaHCO₃ (40 mL), water (40 mL), and brine (40 mL), followed by drying over MgSO₄, filtration and removal of the solvent *in vacuo*. The crude product was purified by flash column chromatography (SiO₂, Hex/EtOAc = 2:1 to 1:1) to yield the methyl ester **2.174** (2.72 g, 3.72 mmol, 87% yield over 2 steps) as a white solid.

$[\alpha]_{\text{D}}^{23} = 62.3^\circ$ (c = 4.0, CHCl₃)

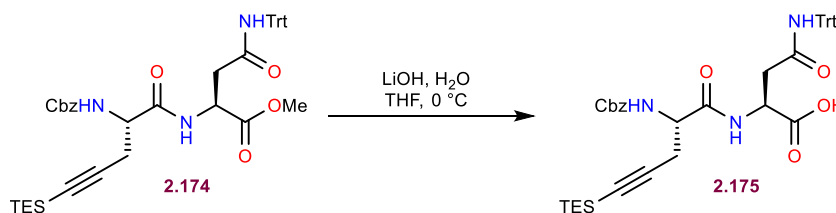
$R_f = 0.2$ (SiO₂, 2:1 hexanes : EtOAc)

¹H NMR (600 MHz, CDCl₃) δ 7.28 (tt, $J = 27.2, 5.9$ Hz, 14H), 7.16 (d, $J = 7.8$ Hz, 7H), 6.70 (s, 1H), 5.44 (d, $J = 7.8$ Hz, 1H), 5.08 (q, $J = 12.2$ Hz, 2H), 4.79 (dt, $J = 8.8, 4.4$ Hz, 1H), 4.29 (q, $J = 6.7$ Hz, 1H), 3.65 (s, 3H), 3.06 (dd, $J = 15.9, 4.2$ Hz, 1H), 2.76 (td, $J = 16.8, 5.0$ Hz, 2H), 2.65 (dd, $J = 17.2, 7.0$ Hz, 1H), 0.94 (t, $J = 7.9$ Hz, 9H), 0.54 (q, $J = 7.9$ Hz, 6H).

¹³C{¹H} NMR (151 MHz, CDCl₃) δ 171.04, 169.87, 169.30, 155.93, 144.38, 136.28, 128.75, 128.62, 128.24, 128.17, 127.33, 102.05, 85.84, 71.06, 67.24, 53.54, 52.86, 49.24, 38.32, 24.26, 7.57, 4.43.

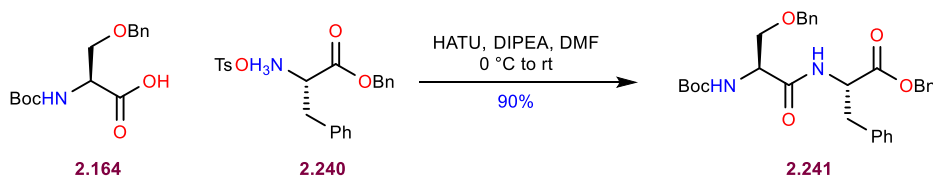
HRMS: (ES+) m/z : [M+H]⁺ calcd. for C₅₅H₆₄N₆O₁₂Si⁷⁹Br, 1107.3535; found 1107.3540

IR (ATR, neat, cm⁻¹) 3317 (w), 2953 (w), 2176 (w), 1732 (m), 1665 (s), 1494 (s), 1216 (m), 1045 (w).



Western dipeptide **2.175**:

Methyl ester **2.174** (2.72 g, 3.72 mmol, 1.0 equiv.) was dissolved in THF/water (3:1, 40 mL total, 0.1 M) and cooled to 0 °C. To this was added a 1 M aqueous solution of LiOH (222 mg, 9.29 mmol, 9.29 mL, 2.5 equiv.) dropwise. The reaction was allowed to stir at 0 °C until complete (about 1 hour, monitored by TLC). The reaction was quenched by addition of 1 M aqueous HCl (until pH ~ 4) and diluted with EtOAc (80 mL). The layers were separated and the aqueous layer was extracted with EtOAc (2 x 80 mL). The combined organic layers were combined, washed with brine, dried over MgSO₄, filtered and concentrated. The crude acid **2.175** was used without further purification.



Protected sidechain **2.241**:

Boc-*L*-Ser(OBn)-OH **2.164** (2.00 g, 6.77 mmol, 1.0 equiv.) and H-Phe-OBn•TsOH **2.240** (2.90 g, 6.77 mmol, 1.0 equiv.) were dissolved in DMF (34 mL). The solution was cooled to 0 °C, followed by sequential addition of DIPEA (1.77 mL, 10 mmol, 1.5 equiv.) and HATU (2.57 g, 6.77 mmol, 1.0 equiv.). The mixture was left to slowly warm up to room temperature and stir for 5 hours. The reaction was quenched by the addition of 1 M aqueous HCl (150 mL). The obtained mixture was transferred to a separation funnel and extracted with EtOAc (3 x 150 mL). The organic layers were combined, washed with saturated aqueous NaHCO₃ (150 mL), H₂O (150 mL) and brine (150 mL), dried over MgSO₄, filtered and concentrated. The crude product was purified by flash column chromatography (SiO₂, Hex/EtOAc = 3:1) to afford the dipeptide **2.241** (3.25 g, 6.77 mmol, 90%) as a clear oil that solidified upon standing.

$$[\alpha]_D^{23} = 15.0^\circ \text{ (c = 3.0, CHCl}_3\text{)}$$

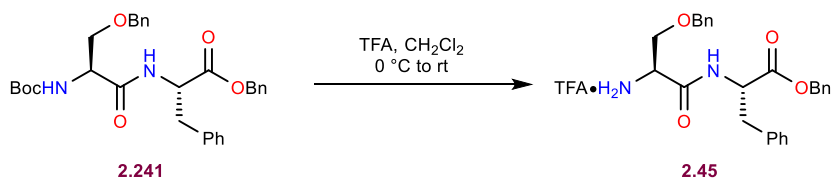
$$R_f = 0.5 \text{ (SiO}_2\text{, hexanes : EtOAc = 3:1)}$$

¹H NMR (600 MHz, CDCl₃) δ 7.38 – 7.30 (m, 6H), 7.30 – 7.25 (m, 4H), 7.18 (t, *J* = 7.4 Hz, 1H), 7.13 (dd, *J* = 8.2, 6.7 Hz, 2H), 7.08 (s, 1H), 6.99 – 6.94 (m, 2H), 5.36 (d, *J* = 6.8 Hz, 1H), 5.14 (d, *J* = 12.1 Hz, 1H), 5.10 (d, *J* = 12.1 Hz, 1H), 4.89 (q, *J* = 6.4 Hz, 1H), 4.51 (d, *J* = 11.9 Hz, 1H), 4.46 (d, *J* = 11.6 Hz, 1H), 4.29 (s, 1H), 3.93 – 3.88 (m, 1H), 3.52 (dd, *J* = 9.2, 6.7 Hz, 1H), 3.13 (dd, *J* = 13.9, 5.8 Hz, 1H), 3.06 (dd, *J* = 13.9, 5.8 Hz, 1H), 1.43 (s, 9H).

¹³C{¹H} NMR (151 MHz, CDCl₃) δ 171.0, 170.1, 155.5, 137.4, 135.7, 135.2, 129.4, 128.7, 128.6, 128.6, 128.0, 128.0, 127.1, 80.3, 73.5, 69.9, 67.3, 53.8, 53.6, 37.8, 28.4.

HRMS: (ES+) *m/z*: [M+H]⁺ calcd. for C₃₁H₃₇N₂O₆, 533.2652; found 533.2646

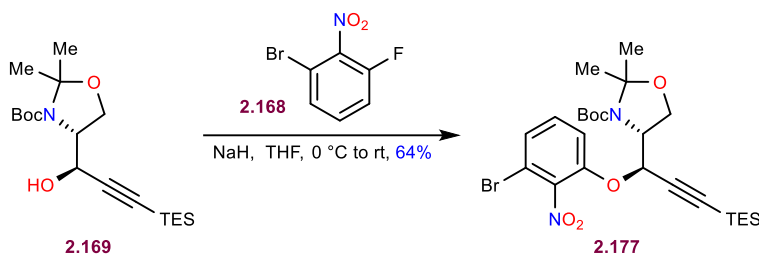
IR (ATR, neat, cm⁻¹) 3320 (w), 2977 (w), 2176 (w), 1674 (s), 1497 (s), 1167 (s), 1111 (m).



Ammonium salt **2.45**:

Boc protected dipeptide **2.241** (3.25 g, 6.77 mmol, 1.0 equiv.) was dissolved in DCM (30 mL, 0.2 M) and cooled to 0 °C. To this was added TFA (9.40 mL, 122 mmol, 20 equiv.). The reaction was allowed to warm to room temperature and stirred until complete (about 4 hours). The solvent was

removed on a rotary evaporator and the residue was redissolved in toluene. The toluene was removed *in vacuo*, and this process was repeated two more times to remove residual TFA. The ammonium salt **2.45**•TFA was isolated as a white solid (assumed quantitative yield, 3.24 g, 6.10 mmol) that was used without further purification.



Alkyne **2.177**:

Alcohol **2.169** (4.85 g, 13.1 mmol, 1 equiv.) was dissolved in THF (260 mL). The obtained solution was cooled to 0 °C, followed by portionwise addition of NaH (0.63 g, 15.7 mmol, 1.2 equiv, 60% in mineral oil). After 15 minutes of stirring at 0 °C, 1-bromo-3-fluoro-2-nitrobenzene **2.168** (3.46 g, 15.7 mmol, 1.2 equiv.) was added in one portion. The reaction mixture was cooled to 0 °C and quenched carefully with saturated aqueous NaHCO₃ (200 mL). The obtained solution was transferred to a separation funnel and extracted with ether (3 x 200 mL). The organic extracts were combined, washed with brine (200 mL), dried over MgSO₄, filtered and concentrated. Flash column chromatography (SiO₂, hexanes : EtOAc = 10:1 to 9:1) afforded the product **2.177** as a yellow oil (4.80 g, 8.43 mmol, 64%).

$[\alpha]_D^{23} = 57.9^\circ$ (c = 30.5 mg/mL, CHCl₃)

$R_f = 0.3$ (SiO₂, hexanes : EtOAc = 8:1)

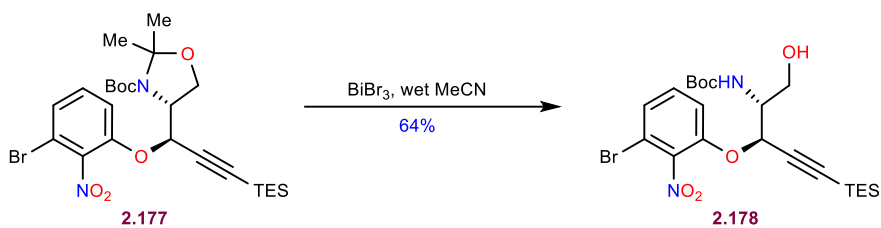
¹H NMR (500 MHz, DMSO-*d*₆, 75 °C) δ 7.50 (d, *J* = 4.4 Hz, 2H), 7.47 (dd, *J* = 5.3, 4.9 Hz, 1H), 5.52 (br, 1H), 4.18 (br, 1H), 4.07 – 4.01 (m, 2H), 1.57 (s, 3H), 1.45 (s, 12H), 0.88 (t, *J* = 7.9 Hz, 9H), 0.52 (q, *J* = 7.8 Hz, 6H).

¹³C{¹H} NMR (126 MHz, DMSO-*d*₆, 75 °C) δ 148.3, 142.6, 131.8, 126.0, 116.5, 112.0, 99.9, 93.8, 92.3, 79.8, 78.8, 63.4, 58.1, 27.6, 6.5, 3.3.

HRMS: (ES⁺, *m/z*) [M+Na]⁺ calcd. for C₂₅H₃₇⁷⁹BrN₂O₆SiNa, 591.1502; found 591.1501.

IR (ATR, neat, cm⁻¹): 2936 (w), 2913 (w), 1707 (m), 1687 (m), 1591 (m), 1544 (m), 1459 (m), 1390 (m), 1364 (s), 1168 (m), 1102 (m), 797 (m).

NMR were taken at 75 °C due to rotamerism.



Alcohol **2.178**:

To a solution of cyclic *N,O*-aminal **2.177** (4.80 g, 8.43 mmol, 1 equiv.) in wet MeCN (85 mL) was added bismuth(III)-bromide (756 mg, 1.69 mmol, 0.2 equiv.) at room temperature. The reaction mixture was stirred for 3 hours, when all starting material had disappeared by TLC analysis. The reaction mixture was then quenched by adding saturated aqueous NaHCO_3 (150 mL) and filtered through celite (celite was washed with EtOAc). The filtrate was transferred to a separation funnel and extracted with EtOAc (3 x 150 mL). The organic extracts were combined, washed with brine (150 mL), dried over MgSO_4 , filtered and concentrated. Flash column chromatography (SiO_2 , hexanes : EtOAc = 2:1) afforded the product **2.178** as a foamy colorless oil (3.46 g, 6.53 mmol, 78%).

$[\alpha]_{\text{D}}^{23} = 26.9^\circ$ (c = 18.5 mg/mL, CHCl_3)

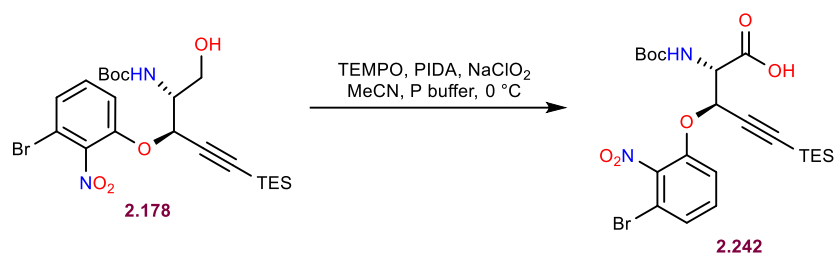
$R_f = 0.3$ (SiO_2 , hexanes : EtOAc = 2:1)

$^1\text{H NMR}$ (500 MHz, CDCl_3) δ 7.32 – 7.26 (m, 3H), 5.17 (s, 1H), 5.09 (d, $J = 6.6$ Hz, 1H), 4.02 (ddd, $J = 10.8, 8.7, 4.9$ Hz, 1H), 3.91 (dd, $J = 11.5, 4.8$ Hz, 1H), 3.72 (ddd, $J = 11.4, 6.0, 2.5$ Hz, 1H), 2.33 (br, 1H), 1.45 (s, 9H), 0.92 (t, $J = 7.9$ Hz, 9H), 0.57 (q, $J = 7.9$ Hz, 6H).

$^{13}\text{C}\{^1\text{H}\}$ NMR (126 MHz, CDCl_3) δ 155.9, 149.6, 143.0, 131.3, 126.2, 115.1, 113.7, 100.3, 93.9, 80.3, 69.5, 61.5, 55.1, 28.4, 7.5, 4.1.

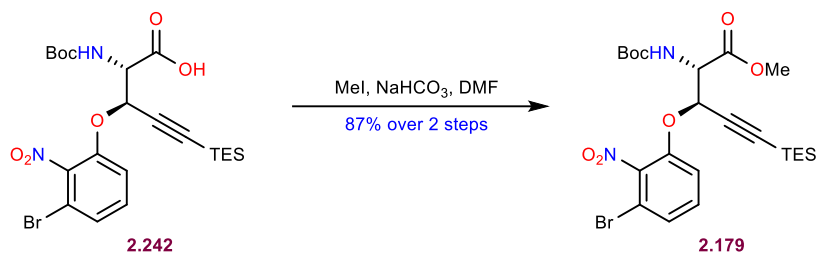
HRMS: (ES+, m/z) $[\text{M}+\text{Na}]^+$ calcd. for $\text{C}_{22}\text{H}_{33}^{79}\text{BrN}_2\text{O}_6\text{SiNa}$, 551.1189; found 551.1190.

IR (ATR, neat, cm^{-1}): 3444 (br), 2956 (w), 2876 (w), 1698 (m), 1592 (m), 1541 (s), 1459 (s), 1367 (s), 1163 (s), 1008 (s), 727 (s).



Acid **2.242**:

To a solution of alcohol **2.178** (3.46 g, 6.53 mmol, 1 equiv.) in MeCN (25 mL)/phosphate buffer (30 mL, pH=6.4) were added PIDA (210 mg, 0.65 mmol, 0.1 equiv.) and TEMPO (204 mg, 1.31 mmol, 0.2 equiv.) at room temperature. The obtained mixture was cooled to 0 °C, followed by the addition of NaClO₂ (1.95 g, 21.6 mmol, 3.3 equiv.) in one portion. The resulting solution was warmed to room temperature and left to stir overnight. Saturated aqueous NH₄Cl (100 mL) was added and the obtained mixture was transferred to a separation funnel and extracted with EtOAc (3 x 100 mL). The organic extracts were combined, washed with brine (100 mL), dried over MgSO₄, filtered and concentrated. The obtained crude product **2.242** was taken into the next step without further purification (assumed quantitative yield, 3.55 g).



Methyl ester **2.179**:

To a solution of the crude acid **2.242** (3.55 g, 6.53 mmol, 1 equiv.) in DMF (33 mL) were added NaHCO₃ (1.37 g, 16.3 mmol, 2.5 equiv.) and MeI (1.0 mL, 16.3 mmol, 2.5 equiv.) at room temperature. After 12 hours, water (100 mL) was added and the obtained mixture was transferred to a separation funnel and extracted with EtOAc (3 x 100 mL). The organic extracts were combined, washed with water (3 x 100 mL) brine (100 mL), dried over MgSO₄, filtered and concentrated. Flash column chromatography (SiO₂, hexanes : EtOAc = 5:1 to 4:1) afforded the ester **2.179** as a yellow oil (3.18 g, 6.53 mmol, 87%).

$[\alpha]_D^{23} = 22.8^\circ$ ($c = 28.5$ mg/mL, CHCl_3)

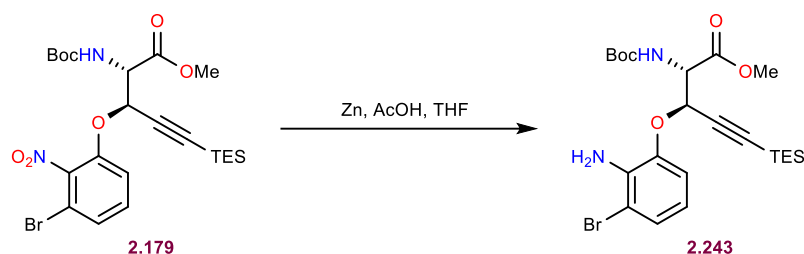
$R_f = 0.3$ (SiO_2 , hexanes : EtOAc = 4:1)

$^1\text{H NMR}$ (500 MHz, Chloroform- d) δ 7.33 – 7.27 (m, 3H), 5.34 (d, $J = 3.1$ Hz, 1H), 5.31 (d, $J = 9.6$ Hz, 1H), 4.82 (dd, $J = 9.7, 3.0$ Hz, 1H), 3.78 (s, 3H), 1.46 (s, 9H), 0.92 (t, $J = 7.9$ Hz, 9H), 0.56 (q, $J = 7.8$ Hz, 6H).

$^{13}\text{C}\{^1\text{H}\}$ NMR (126 MHz, CDCl_3) δ 169.0, 155.5, 149.2, 143.0, 131.3, 126.5, 115.2, 113.7, 98.5, 94.6, 80.5, 71.6, 57.2, 53.2, 28.4, 7.4, 4.1.

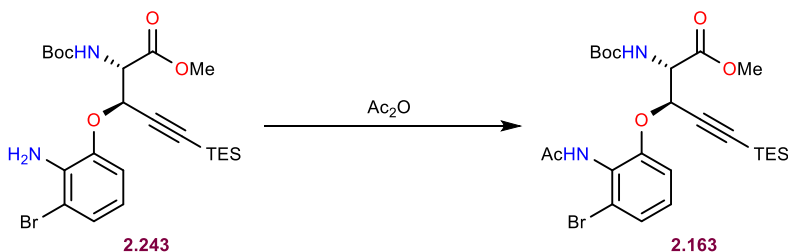
HRMS: (ES+, m/z) $[\text{M}+\text{Na}]^+$ calcd. for $\text{C}_{23}\text{H}_{33}^{79}\text{BrN}_2\text{O}_7\text{SiNa}$, 579.1138; found 579.1137.

IR (ATR, neat, cm^{-1}): 3445 (br), 2956 (w), 2876 (w), 1720 (s), 1592 (m), 1543 (s), 1501 (m), 1458 (s), 1366 (s), 1160 (s), 727 (s).



Aniline **2.243**:

To a solution of the nitroarene **2.179** (2.62 g, 4.70 mmol, 1 equiv.) in THF (45 mL) were added Zn (6.15 g, 94.0 mmol, 20 equiv, non-activated) and glacial AcOH (9 mL) at room temperature. After 1 hour of stirring (monitored by HPLC until completion), the reaction mixture was filtered through celite. Water (150 mL) was added to the filtrate which was followed by neutralization with solid Na_2CO_3 until effervescence ceased. The obtained mixture was transferred to a separation funnel and extracted with EtOAc (3 x 100 mL). The organic extracts were combined, washed with brine (150 mL), dried over MgSO_4 , filtered and concentrated. The crude aniline **2.243** was taken into the next step without further purification (assumed quantitative yield, 2.48 g).



Acetanilide **2.163**:

Aniline **2.243** (2.48 g, 4.70 mmol, 1 equiv.) was dissolved in acetic anhydride (47 mL). After stirring for 4 hours at room temperature the reaction was complete (monitored by HPLC). Acetic anhydride was removed in vacuo. The obtained crude was subjected to flash column chromatography (SiO₂, hexanes : EtOAc = 2:1) to afford the product **2.163** as a foamy colorless oil (2.49 g, 4.37 mmol, 93%).

$[\alpha]_D^{24} = 13.7^\circ$ (c = 13.0 mg/mL, CHCl₃)

R_f = 0.2 (SiO₂, hexanes : EtOAc = 2:1)

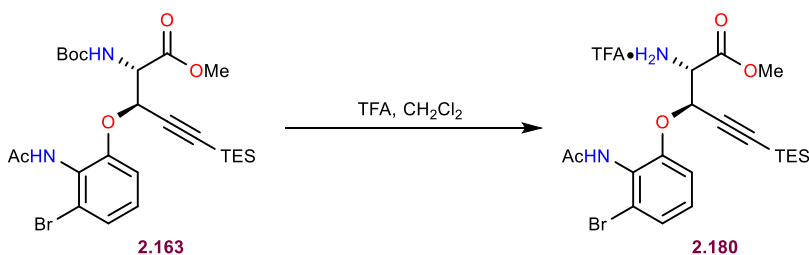
¹H NMR (500 MHz, DMSO-*d*₆) δ 9.29 (s, 1H), 7.28 – 7.11 (m, 4H), 5.39 (d, *J* = 3.4 Hz, 1H), 4.72 (dd, *J* = 9.9, 3.4 Hz, 1H), 3.58 (s, 3H), 2.00 (s, 3H), 1.43 (s, 9H), 0.88 (t, *J* = 7.9 Hz, 9H), 0.51 (q, *J* = 7.9 Hz, 6H).

¹³C{¹H} NMR (126 MHz, DMSO-*d*₆) δ 169.0, 168.2, 155.3, 152.2, 127.7, 126.8, 125.2, 123.0, 113.2, 100.7, 91.3, 78.9, 69.2, 57.3, 52.4, 28.1, 22.6, 7.2, 3.6.

HRMS: (ES⁺, *m/z*) [M+Na]⁺ calcd. for C₂₅H₃₇⁷⁹BrN₂O₆SiNa, 591.1502; found 591.1494.

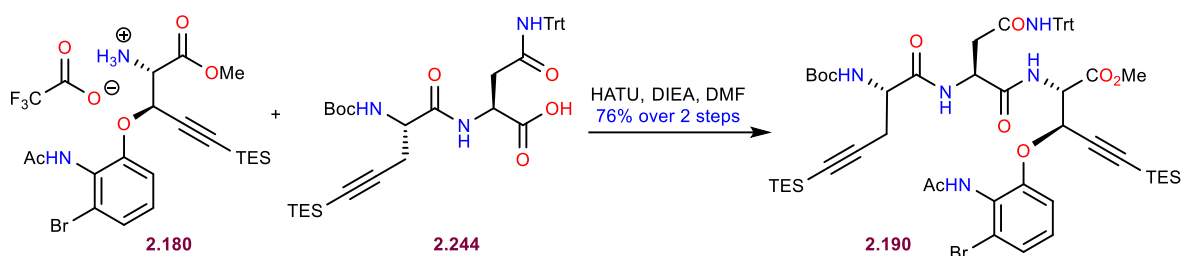
IR (ATR, neat, cm⁻¹): 3277 (br), 2956 (m), 2876 (w), 1760 (m), 1721 (s), 1666 (m), 1509 (s), 1165 (s), 727 (m).

NMR were taken in DMSO-*d*₆ due to rotamerism in CDCl₃.



Ammonium salt **2.180**:

The Boc-protected amino acid **2.163** (780 mg, 1.37 mmol, 1 equiv.) was dissolved in CH₂Cl₂/TFA = 2/1 (14 mL total volume) at room temperature. The mixture was stirred for 1 hour. CH₂Cl₂ and TFA were removed in vacuo. The obtained crude ammonium salt **2.180** was used in the next step without further purification (assumed quantitative yield, 800 mg of TFA salt).



Tripeptide **2.190**:

Boc protected dipeptide **2.244** (1.06 g, 1.55 mmol, 1.1 equiv.), which was obtained in the same way as **2.175**, and ammonium salt **2.180** (800 mg, 1.41 mmol, 1 equiv.) were dissolved in DMF (14 mL). The solution was cooled down to 0 °C, followed by sequential addition of DIEA (0.54 mL, 3.10 mmol, 2.2 equiv.), HOAt (211 mg, 1.55 mmol, 1.1 equiv.) and EDC (297 mg, 1.55 mmol, 1.1 equiv.). The mixture was left to slowly warm up to room temperature and stir for 5 hours. The reaction was quenched with the addition of 1 M aqueous HCl (80 mL). The obtained mixture was transferred to a separation funnel and extracted with EtOAc (3 x 80 mL). The organic layers were combined, washed with saturated NaHCO₃ (80 mL), H₂O (80 mL) and brine (80 mL), dried over MgSO₄, filtered and concentrated. The crude was purified by flash column chromatography (SiO₂, hexanes : EtOAc = 1:1) to afford the product **2.190** (1.20 g, 1.07 mmol, 76%) as a colorless oil.

$[\alpha]_D^{24} = -0.1^\circ$ (c = 21.0 mg/mL, CHCl₃)

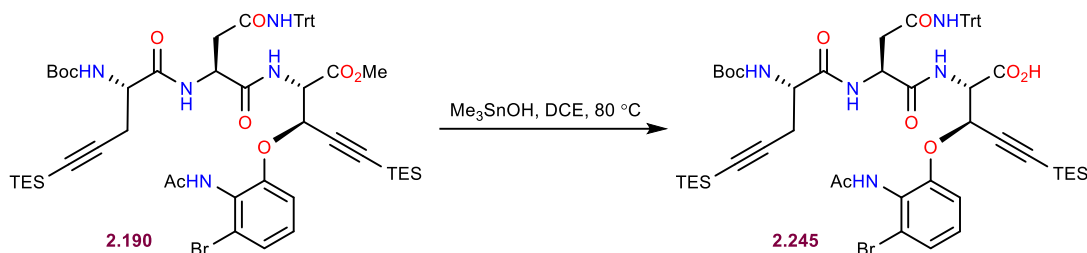
$R_f = 0.3$ (SiO₂, hexanes : EtOAc = 1:1)

¹H NMR (500 MHz, Chloroform-*d*) δ 8.45 (d, $J = 9.6$ Hz, 1H), 7.92 (s, 1H), 7.72 (d, $J = 4.4$ Hz, 1H), 7.41 (s, 1H), 7.23 – 7.15 (m, 13H), 7.12 – 7.04 (m, 5H), 5.25 (d, $J = 2.2$ Hz, 1H), 5.21 (d, $J = 7.8$ Hz, 1H), 5.11 (dd, $J = 9.5, 2.2$ Hz, 1H), 4.59 (ddd, $J = 8.9, 4.5, 1.8$ Hz, 1H), 4.33 – 4.25 (m, 1H), 3.67 (s, 3H), 2.96 (dd, $J = 13.7, 1.8$ Hz, 1H), 2.85 (dd, $J = 17.1, 5.7$ Hz, 1H), 2.77 (dd, $J = 13.8, 8.8$ Hz, 1H), 2.69 (dd, $J = 17.1, 5.5$ Hz, 1H), 1.65 (s, 3H), 1.45 (s, 9H), 0.96 (t, $J = 7.9$ Hz, 9H), 0.92 (t, $J = 7.9$ Hz, 9H), 0.57 (q, $J = 8.0$ Hz, 6H), 0.55 (q, $J = 8.0$ Hz, 6H).

¹³C{¹H} NMR (126 MHz, CDCl₃) δ 171.8, 171.1, 170.1, 169.9, 168.2, 155.3, 152.4, 144.1, 128.5, 128.2, 127.8, 127.2, 126.7, 126.1, 124.5, 112.2, 102.1, 99.6, 93.0, 86.4, 80.8, 70.9, 69.0, 56.9, 53.3, 53.0, 51.3, 40.8, 28.3, 23.7, 22.7, 7.6, 7.4, 4.5, 4.1.

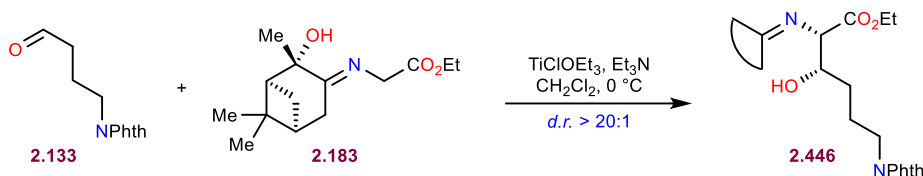
HRMS: (ES⁺, m/z) [M+H]⁺ calcd. for C₅₉H₇₆⁷⁹BrN₅O₉Si₂, 1134.4443; found 1134.4424.

IR (ATR, neat, cm^{-1}): 3318 (br), 2955 (m), 2875 (w), 2176 (w), 1751 (m), 1663 (s), 1492 (s), 1447 (s), 1254 (s), 739 (s).



Acid **2.245**:

The methyl ester **2.190** (185 mg, 0.163 mmol, 1 equiv.) was dissolved in DCE (1.6 mL), which was followed by the addition of Me_3SnOH (147 mg, 0.815 mmol, 5 equiv.). The mixture was heated to $80\text{ }^\circ\text{C}$ and stirred for 6 hours. The solvent was removed in vacuo and the obtained residue was suspended in EtOAc (1 mL), followed by the addition of aqueous 2 M HCl (1 mL). The mixture was stirred for 15 min. The layers were separated and the aqueous layer was extracted with EtOAc (2 x 1 mL). The organic extracts were combined, washed with brine (1 mL), dried over MgSO_4 , filtered and concentrated to provide the crude acid **2.245** that was used in the next step without further purification (assumed quantitative yield, 183 mg).



Aldol **2.446**:

To a solution of $\text{Ti}(\text{OEt})_4$ (6.34 mL, 30.2 mmol, 0.9 equiv.) in DCM (73 mL) at $0\text{ }^\circ\text{C}$ was added TiCl_4 (1.11 mL, 10.1 mmol, 0.3 equiv.). The solution was stirred for 15 minutes at $0\text{ }^\circ\text{C}$ before being cannulated into a solution of iminoglycinate **2.183** (9.37 g, 37 mmol, 1.1 equiv.) in DCM (256 mL) at $0\text{ }^\circ\text{C}$. A fine powder of 4-phthalimidobutanal **2.133** (7.30 g, 33.6 mmol, 1.0 equiv.) was added to the mixture at the same temperature. Triethylamine (9.37 mL, 67.2 mmol, 2.0 equiv.) was subsequently added, and the reaction was stirred at $0\text{ }^\circ\text{C}$. After consumption of 4-phthalimidobutanal **2.133** (about 3 hours, followed by TLC), brine (300 mL) was added and the obtained mixture was let to stir until it warmed up to room temperature. The resulting bilayer

suspension was filtered through celite. The organic layer was separated, and the aqueous layer was extracted with dichloromethane (2 × 250 mL). The combined organic layers were dried over anhydrous magnesium sulfate, filtered and concentrated under reduced pressure. The obtained residue **2.446** was taken into the next step without further purification (99% by mass, 15.6g).

For characterization, the crude product was purified by flash column chromatography, to yield the desired product analytically pure, as a single diastereomer (*d.r.* > 20:1).

$[\alpha]_D^{22} = -31.3^\circ$ (c = 7.4 mg/mL, CDCl₃)

R_f = 0.25 (SiO₂, hexanes : EtOAc = 1:2 + 5% Et₃N)

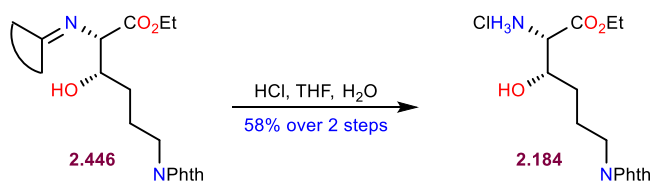
¹H NMR (500 MHz, CDCl₃) δ 7.82 (dd, *J* = 5.4, 3.1 Hz, 2H), 7.68 (dd, *J* = 5.5, 3.0 Hz, 2H), 4.13 (m, 4H), 3.81 (dt, *J* = 14.3, 7.3 Hz, 1H), 3.77 – 3.70 (dt, *J* = 14.3, 7.3 Hz, 1H), 3.48 (br, 1H), 3.00 (s, 1H), 2.55 (dd, *J* = 18.0, 2.9 Hz, 1H), 2.47 (dt, *J* = 17.6, 2.7 Hz, 1H), 2.31 (dtd, *J* = 10.7, 6.0, 2.4 Hz, 1H), 2.05 (t, *J* = 5.9 Hz, 1H), 2.01 (dd, *J* = 5.9, 3.0 Hz, 1H), 1.86 (m, 2H), 1.67 – 1.53 (m, 2H), 1.53 – 1.47 (m, 1H), 1.44 (s, 3H), 1.30 (s, 3H), 1.20 (t, *J* = 7.2 Hz, 3H), 0.84 (s, 3H).

¹³C{¹H} NMR (126 MHz, CDCl₃) δ 180.8, 170.5, 168.9, 134.1, 132.2, 123.4, 72.8, 67.1, 61.3, 50.4, 38.8, 38.6, 38.1, 34.2, 28.8, 28.4, 28.1, 27.4, 25.2, 22.9, 14.3.

HRMS: (ES⁺, *m/z*) [M+H]⁺ calcd. for C₂₆H₃₅N₂O₆, 471.2495; found 471.2491.

IR (ATR, neat, cm⁻¹): 3464 (br), 2980 (w), 2927 (w), 1772 (w), 1712 (s), 1397 (m), 1369 (m), 721 (m).

E-geometry of the imine was confirmed through NOE (2.56/2.47 with 4.14).



Ammonium salt **2.184**:

To a solution of hydroxylysine **2.446** (15.6 g, 33.2 mmol, 1.0 equiv.) in THF (166 mL) was added 2 M aqueous HCl (166 mL). The reaction mixture was stirred at room temperature for 2 days. The mixture was concentrated in vacuo. The obtained residue was triturated with ether and filtered. The solid was washed with additional ether to provide the pure ammonium salt **2.184** as a white solid (6.90 g, 17.2 mmol, 58%).

$[\alpha]_D^{23} = 15.8^\circ$ (c = 10.5 mg/mL, MeOH)

T_{melt.} 220-222 °C

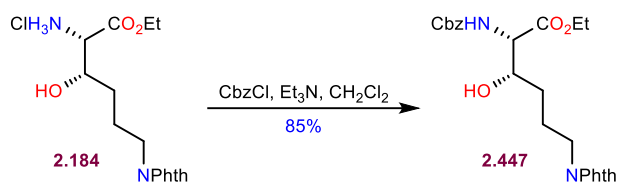
R_f = 0.4 (SiO₂, DCM : MeOH = 10:1)

¹H NMR (500 MHz, DMSO) δ 8.52 (s, 3H), 7.91 – 7.80 (m, 4H), 5.68 (d, J = 5.5 Hz, 1H), 4.20 – 4.05 (m, 2H), 3.94 – 3.92 (m, 1H), 3.90 (dt, J = 8.5, 4.3 Hz, 1H), 3.59 (t, J = 6.6 Hz, 2H), 1.85 – 1.71 (m, 1H), 1.66 – 1.43 (m, 1H), 1.14 (t, J = 7.1 Hz, 3H).

¹³C{¹H} NMR (126 MHz, DMSO) δ 167.94, 167.15, 134.43, 131.59, 123.00, 69.04, 61.51, 56.92, 37.25, 30.03, 24.69, 13.80.

HRMS: (ES⁺, *m/z*) [M+H]⁺ calcd. for C₁₆H₂₁N₂O₅, 321.1450; found 321.1449

IR (ATR, neat, cm⁻¹): 3220 (br), 2939 (w), 1771 (w), 1742 (m), 1709 (s), 1398 (m), 721 (m).



Hydrolysine **2.447**:

To a suspension of ammonium salt **2.184** (8.7 g, 24 mmol, 1.0 equiv.) in CH₂Cl₂ (240 mL) at 0 °C were added triethylamine (8.50 mL, 61 mmol, 2.5 equiv.) and CbzCl (4.2 mL, 29 mmol, 1.2 equiv.). Upon consumption (about 6 hours, monitored by HPLC), the reaction mixture was quenched with 1 M HCl (200 mL). The organic layer was separated, and the aqueous layer was extracted with dichloromethane (2 × 150 mL). The combined organic layers were dried over anhydrous magnesium sulfate, filtered and concentrated under reduced pressure. The obtained residue was purified by flash column chromatography (SiO₂, hexanes:EtOAc = 1:1) to afford the product **2.447** as a white foam (9.42 g, 20.7 mmol, 85%).

[α]_D²³ = 15.0° (c = 9.1 mg/mL, CDCl₃)

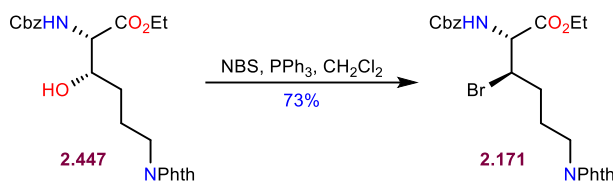
R_f = 0.4 (SiO₂, hexanes : EtOAc = 1:1)

¹H NMR (500 MHz, CDCl₃) δ 7.82 (qd, J = 5.3, 2.5 Hz, 2H), 7.70 (td, J = 5.4, 3.4 Hz, 2H), 7.39 – 7.27 (m, 5H), 5.73 (d, J = 6.8 Hz, 1H), 5.09 (s, 2H), 4.40 (dd, J = 7.8, 3.7 Hz, 1H), 4.21 (q, J = 7.2 Hz, 2H), 3.99 (tt, J = 8.5, 4.0 Hz, 1H), 3.72 (t, J = 7.0 Hz, 2H), 2.91 (q, J = 7.3 Hz, 1H), 1.90 (m, J = 13.9, 7.9, 7.1 Hz, 1H), 1.79 (dp, J = 14.4, 7.3 Hz, 1H), 1.53 (m, 2H), 1.27 (t, J = 7.1 Hz, 3H).

$^{13}\text{C}\{^1\text{H}\}$ NMR (126 MHz, CDCl_3) δ 170.29, 168.60, 156.57, 136.14, 134.10, 132.19, 128.69, 128.40, 128.30, 123.37, 72.75, 67.44, 62.05, 58.94, 37.65, 30.22, 25.26, 14.21.

HRMS: (ES+, m/z) $[\text{M}+\text{H}]^+$ calcd. for $\text{C}_{24}\text{H}_{27}\text{N}_2\text{O}_7$, 455.1818; found 455.1817.

IR (ATR, neat, cm^{-1}): 3374 (br), 2940 (w), 1771 (w), 1706 (s), 1397 (m), 1194 (m), 1052 (m), 1027 (m), 721 (m).



Bromolysine **2.171**:

To a solution of triphenylphosphine (10.9 g, 41.5 mmol, 2 equiv.) in CH_2Cl_2 (207 mL) at 0 °C was added freshly recrystallized NBS (7.38 g, 41.5 mmol, 2 equiv.) portionwise. The solution was stirred for 15 min at 0 °C, followed by the dropwise addition of a solution of alcohol **2.447** (9.42 g, 20.7 mmol, 1 equiv.) in CH_2Cl_2 (104 mL). The mixture was left to warm up to room temperature and continued to stir for 36 hours. Upon completion, CH_2Cl_2 was removed by reduced pressure and the crude mixture was purified by flash column chromatography (SiO_2 , hexanes:EtOAc = 3:1 to 2:1) to the bromide **2.171** as a white foam (7.8 g, 20.7 mmol, 73%).

$[\alpha]_{\text{D}}^{23} = 25.9^\circ$ ($c = 13.0$ mg/mL, CDCl_3)

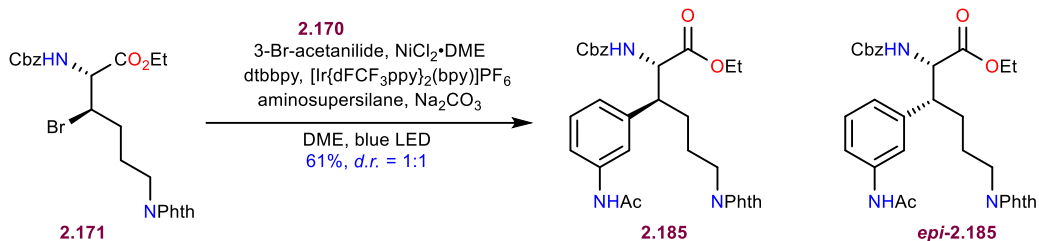
$R_f = 0.4$ (SiO_2 , hexanes : EtOAc = 2:1)

^1H NMR - (500 MHz, CDCl_3) δ 7.84 (dd, $J = 5.3, 3.1$ Hz, 2H), 7.70 (dd, $J = 5.5, 3.1$ Hz, 2H), 7.40 – 7.27 (m, 5H), 5.52 (d, $J = 9.5$ Hz, 1H), 5.07 (q, $J = 12.2$ Hz, 2H), 4.70 (dd, $J = 9.6, 2.4$ Hz, 1H), 4.62 – 4.52 (m, 1H), 4.32 – 4.16 (m, 2H), 3.71 (t, $J = 6.5$ Hz, 2H), 1.99 – 1.84 (m, 4H), 1.28 (t, $J = 7.1$ Hz, 3H).

$^{13}\text{C}\{^1\text{H}\}$ NMR (126 MHz, CDCl_3) δ 169.23, 168.40, 156.52, 136.05, 134.06, 132.17, 128.67, 128.37, 128.21, 123.38, 70.31, 67.46, 62.38, 58.18, 55.67, 36.96, 33.14, 26.88, 21.82, 21.73, 14.23.

HRMS: (ES+, m/z) $[\text{M}+\text{H}]^+$ calcd. for $\text{C}_{24}\text{H}_{26}\text{N}_2\text{O}_6\text{Br}$, 517.0974; found 517.0979.

IR (ATR, neat, cm^{-1}): 3343 (br), 2948 (w), 1771 (w), 1709 (s), 1511 (w), 1397 (m), 7.21 (m)



β-Aryl lysine **2.185**:

To a flame-dried 8 mL vial was added *N*-(3-bromophenyl)acetamide **2.170** (74.5 mg, 348 μmol, 1.2 equiv.) and aminosupersilane (115 mg, 290 μmol, 1 equiv.). The reaction vessel was taken into a nitrogen-filled glovebox where NiCl₂·DME (6.37 mg, 29.0 μmol, 0.1 equiv.), sodium carbonate (61.5 mg, 580 μmol, 2 equiv.), 4,4'-di-tert-butyl-2,2'-bipyridine (7.78 mg, 29.0 μmol, 0.1 equiv.), and (Ir[dF(CF₃)ppy]₂(dtbbpy))PF₆ (3.25 mg, 2.90 μmol, 0.01 equiv.) were added. The vial was removed from the glovebox and placed under nitrogen atmosphere. Bromide **2.171** (150 mg, 290 μmol, 1 equiv.) as a 0.125 M solution in freshly distilled and degassed DME (2.5 mL) was added. Three additional reaction vials were set up in the same way. The mixtures were stirred for 5 minutes until the color changed from yellow to blue. The four vials were removed from nitrogen, sealed with parafilm, and irradiated with four 456 nM Kessil lamps (cooled with a fan) overnight. The reaction mixture was then directly loaded onto celite and solvent was removed. The crude mixture was purified by column chromatography (2:1 to 1:2, hexanes : EtOAc) to yield acetanilide **2.185** as a 1:1 mixture of diastereomers (416 mg total yield, 61%). For characterization, the diastereomers were separated by chiral preparatory HPLC (Lux Cellulose-1 20x250mm, 30% *i*PrOH in Hexanes).

Desired diastereomer **2.185**:

$[\alpha]_D^{23} = 51.7^\circ$ (c = 0.55, CHCl₃)

$R_f = 0.2$ (SiO₂, hexanes : EtOAc = 1:2)

¹H NMR (600 MHz, DMSO) δ 9.85 (s, 1H), 7.86 – 7.79 (m, 5H), 7.51 (d, *J* = 8.1 Hz, 1H), 7.47 (d, *J* = 8.6 Hz, 1H), 7.37 (t, *J* = 1.9 Hz, 1H), 7.34 – 7.24 (m, 4H), 7.20 – 7.14 (m, 3H), 6.88 (d, *J* = 7.6 Hz, 1H), 4.90 (d, *J* = 2.0 Hz, 2H), 4.24 (t, *J* = 8.7 Hz, 1H), 4.04 (q, *J* = 7.1 Hz, 2H), 3.48 (t, *J* = 6.9 Hz, 2H), 2.92 (q, *J* = 8.0 Hz, 1H), 2.00 (s, 3H), 1.55 (q, *J* = 7.8 Hz, 2H), 1.46 – 1.26 (m, 2H), 1.13 (t, *J* = 7.1 Hz, 3H).

$^{13}\text{C}\{^1\text{H}\}$ NMR (151 MHz, DMSO) δ 171.51, 168.18, 167.87, 155.81, 140.67, 139.38, 136.80, 134.34, 131.56, 128.28, 127.71, 127.46, 123.15, 122.96, 118.30, 117.44, 65.37, 60.58, 58.84, 46.35, 37.24, 28.88, 25.88, 24.04, 13.89.

HRMS: (ES+, m/z) $[\text{M}+\text{H}]^+$ calcd. for $\text{C}_{32}\text{H}_{34}\text{N}_3\text{O}_7$, 572.2397; found 572.2402

IR (ATR, neat, cm^{-1}): 3340 (br), 1709 (s), 1547 (w), 1189 (w).

Undesired Diastereomer *epi*-2.185:

$[\alpha]_{\text{D}}^{23} = 52.0^\circ$ ($c = 1.10$, CHCl_3)

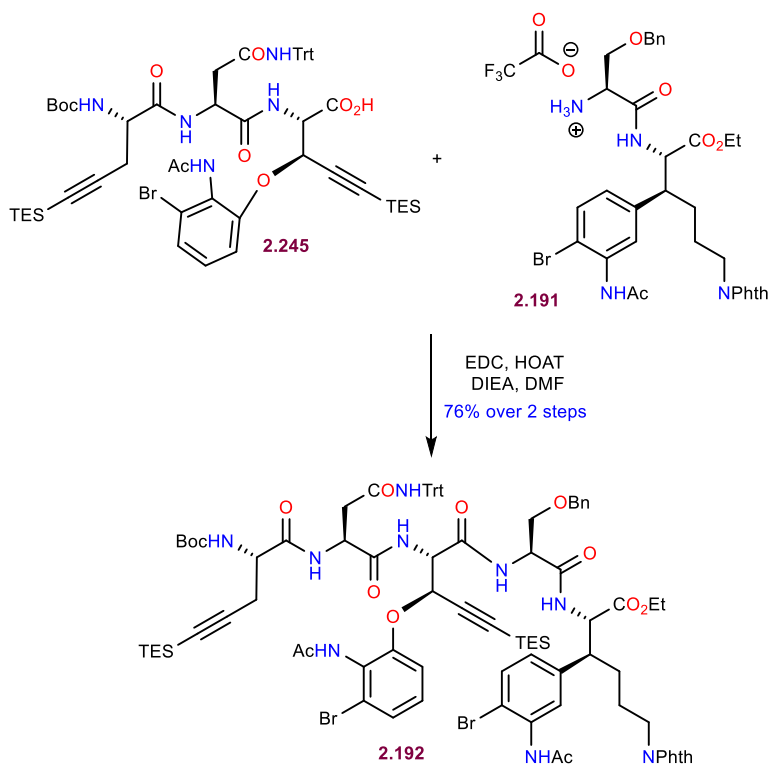
$R_f = 0.2$ (SiO_2 , hexanes : EtOAc = 1:2)

^1H NMR (500 MHz, CDCl_3) δ 7.80 (dd, $J = 5.5, 3.0$ Hz, 2H), 7.68 (dd, $J = 5.5, 3.0$ Hz, 2H), 7.45 (dd, $J = 8.0, 2.2$ Hz, 1H), 7.36 – 7.28 (m, 7H), 7.25 – 7.17 (m, 2H), 6.84 (d, $J = 7.8$ Hz, 1H), 5.12 (d, $J = 9.2$ Hz, 1H), 5.00 (q, $J = 12.2$ Hz, 2H), 4.64 (dd, $J = 9.2, 4.8$ Hz, 1H), 4.12 (qt, $J = 6.6, 3.3$ Hz, 2H), 3.65 (t, $J = 7.0$ Hz, 2H), 3.26 – 3.18 (m, 1H), 2.13 (s, 3H), 1.79 (td, $J = 8.8, 5.2$ Hz, 2H), 1.68 (dp, $J = 9.8, 6.6$ Hz, 1H), 1.58 (tdd, $J = 17.0, 10.0, 6.1$ Hz, 1H), 1.25 – 1.20 (m, 3H).

$^{13}\text{C}\{^1\text{H}\}$ NMR (126 MHz, CDCl_3) δ 171.16, 168.37, 168.19, 156.28, 139.52, 138.34, 136.17, 133.88, 132.14, 129.36, 128.54, 128.21, 128.13, 123.88, 123.18, 119.27, 118.83, 67.07, 61.60, 57.80, 47.50, 37.65, 28.69, 26.43, 24.67, 14.14.

HRMS: (ES+, m/z) $[\text{M}+\text{H}]^+$ calcd. for $\text{C}_{32}\text{H}_{34}\text{N}_3\text{O}_7$, 572.2397; found 572.2380

IR (ATR, neat, cm^{-1}): 3342 (br), 1706 (s), 1547 (w), 1201 (w)



Pentapeptide **2.192**:

Acid **2.245** (183 mg, 0.163 mmol, 1.1 equiv.) and ammonium salt **2.191** (120 mg, 0.149 mmol, 1 equiv.) were dissolved in DMF (1.5 mL). The solution was cooled down to 0 °C, followed by sequential addition of DIEA (78 μ L, 0.446 mmol, 3 equiv.), HOAt (24 mg, 0.178 mmol, 1.2 equiv.) and EDC (31 mg, 0.163 mmol, 1.1 equiv.). The mixture was left to slowly warm up to room temperature and stir for 5 hours. The reaction was quenched with the addition of 1 M aqueous HCl (1 mL). The obtained mixture was transferred to a separation funnel and extracted with EtOAc (3 x 1 mL). The organic layers were combined, washed with saturated NaHCO₃ (1 mL), H₂O (1 mL) and brine (1 mL), dried over MgSO₄, filtered and concentrated. The crude was purified by flash column chromatography (SiO₂, hexanes : EtOAc = 1:2) to afford the product **2.192** (180 mg, 0.149 mmol, 67%) as a colorless foamy oil.

$[\alpha]_D^{22} = 22.5^\circ$ (c = 25.0 mg/mL, CHCl₃)

$R_f = 0.3$ (SiO₂, hexanes : EtOAc = 1:2)

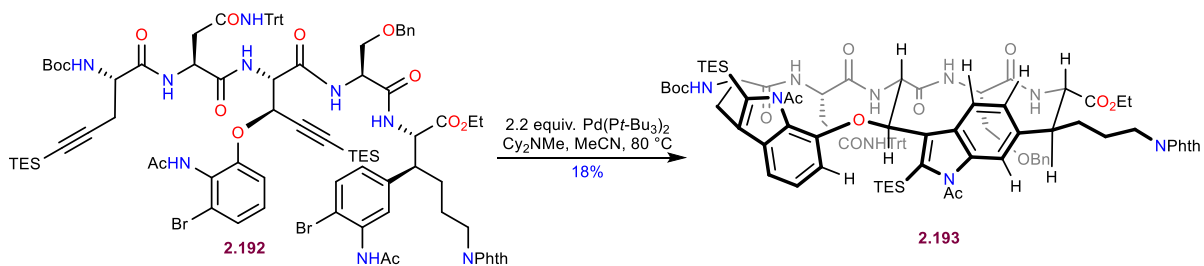
¹H NMR (500 MHz, Chloroform-*d*) δ 8.22 (d, *J* = 8.3 Hz, 1H), 8.03 (s, 1H), 7.78 (dd, *J* = 5.5, 3.0 Hz, 2H), 7.78 (s, 1H), 7.70 (s, 1H), 7.67 (dd, *J* = 5.5, 3.1 Hz, 2H), 7.45 (s, 1H), 7.25 – 7.14 (m,

21H), 7.10 – 7.05 (m, 3H) 7.01 (d, $J = 8.7$ Hz, 1H), 6.94 (t, $J = 8.1$ Hz, 1H), 6.90 (d, $J = 8.4$ Hz, 1H), 6.62 (d, $J = 8.2$ Hz, 1H), 5.29 (s, 1H), 5.26 – 5.21 (m, 1H), 4.99 (d, $J = 8.6$ Hz, 1H), 4.85 (dd, $J = 8.9, 4.3$ Hz, 1H), 4.66 (d, $J = 6.8$ Hz, 1H), 4.54 – 4.49 (m, 1H), 4.45 (q, $J = 11.4$ Hz, 2H), 4.31 – 4.22 (m, 1H), 4.03 (tp, $J = 7.2, 3.6$ Hz, 2H), 3.86 (dd, $J = 9.8, 3.8$ Hz 1H), 3.57 (q, $J = 6.2$ Hz, 2H), 3.45 (t, $J = 8.4$ Hz, 1H), 3.20 (dt, $J = 10.1, 5.2$ Hz, 1H), 3.00 (d, $J = 14.4$ Hz, 1H), 2.89 (dd, $J = 14.7, 7.9$ Hz, 1H), 2.71 (d, $J = 6.1$ Hz, 2H), 2.14 (s, 3H), 1.79 – 1.70 (m, 2H), 1.64 (s, 3H), 1.60 – 1.48 (m, 2H), 1.42 (s, 9H), 1.18 (t, $J = 7.1$ Hz, 3H), 0.96 (t, $J = 7.9$ Hz, 9H), 0.87 (t, $J = 7.9$ Hz, 9H), 0.56 (q, $J = 8.0$ Hz, 6H), 0.51 (q, $J = 8.0$ Hz, 6H).

$^{13}\text{C}\{^1\text{H}\}$ NMR (126 MHz, CDCl_3) δ 171.3, 171.0, 170.7, 170.2, 170.1, 169.3, 168.4, 168.4, 167.7, 155.4, 152.1, 144.0, 139.3, 137.7, 135.6, 134.0, 132.4, 132.2, 128.6, 128.4, 128.2, 128.0, 127.8, 127.5, 127.1, 126.8, 126.2, 125.4, 123.8, 123.3, 122.0, 113.3, 112.6, 102.4, 100.3, 92.2, 85.9, 80.5, 73.5, 71.0, 69.7, 68.6, 61.8, 57.9, 56.0, 53.3, 53.0, 51.0, 47.3, 40.1, 37.6, 28.6, 28.3, 26.4, 24.8, 23.7, 23.0, 14.3, 7.6, 7.4, 4.5, 4.1.

HRMS: (ES+, m/z) $[\text{M}+\text{H}]^+$ calcd. for $\text{C}_{92}\text{H}_{110}^{79}\text{Br}_2\text{N}_9\text{O}_{15}\text{Si}_2$, 1794.6027; found 1794.6008.

IR (ATR, neat, cm^{-1}): 3311 (br), 2955 (m), 2874 (w), 2176 (w), 1771 (w), 1711 (s), 1671 (s), 1512 (s), 1253 (m), 1019 (m), 699 (s).



Bismacrocycle **2.193**:

$\text{Pd}(t\text{-Bu}_3\text{P})_2$ (43 mg, 0.083 mmol, 2.2 equiv.) was measured inside a GB into a flask containing linear precursor **2.192** (68 mg, 0.038 mmol, 1 equiv.). The flask was taken out of the GB and dry and degassed MeCN (38 mL, 1 mM corresponding to the substrate) was added via cannula. To the obtained solution, dry and degassed Cy_2NMe (81 μL , 0.38 mmol, 10 equiv.) was added and the mixture was heated to 80 °C. After 2 hours, the reaction mixture was cooled to room temperature and the solvent was removed in vacuo. The obtained residue was redissolved in EtOAc (2 mL) and washed with 1 M aqueous HCl (1 mL). The obtained solution was dried over MgSO_4 , filtered and

concentrated. The crude was purified by flash column chromatography (SiO₂, hexanes : EtOAc = 3:1 to 3:2) to afford the product **2.193** (11 mg, 6.7 μmol, 18%) as a yellow foamy oil.

$[\alpha]_D^{22} = -49.0^\circ$ (c = 3.0 mg/mL, CHCl₃)

R_f = 0.3 (SiO₂, hexanes : EtOAc = 3:2)

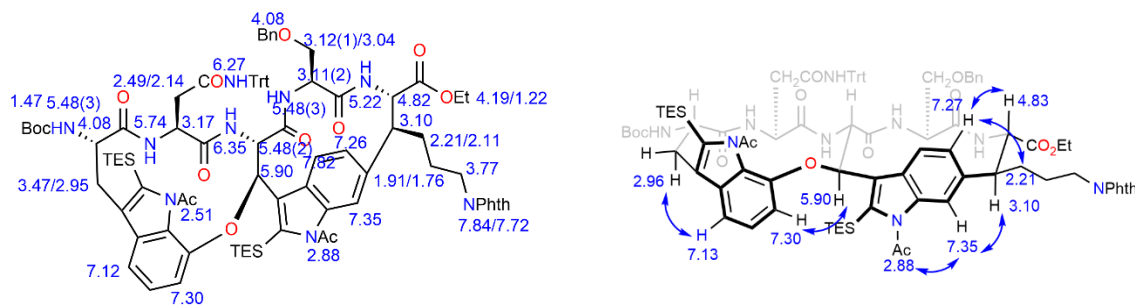
¹H NMR (600 MHz, Chloroform-*d*) δ 7.84 (dd, *J* = 5.4, 3.1 Hz, 2H), 7.82 (d, *J* = 8.5 Hz, 1H), 7.72 (dd, *J* = 5.5, 3.0 Hz, 2H), 7.35 (s, 1H), 7.30 (d, *J* = 7.8 Hz, 1H), 7.27 (d, 1H), 7.25 – 7.23 (m, 5H), 7.22 – 7.15 (m, 8H), 7.13 (d, *J* = 7.8 Hz, 1H), 7.01 (dd, *J* = 7.0, 2.3 Hz, 2H), 6.97 – 6.94 (m, 6H), 6.36 (d, *J* = 9.6 Hz, 1H), 6.27 (s, 1H), 5.90 (d, *J* = 7.7 Hz, 1H), 5.75 (d, *J* = 5.4 Hz, 1H), 5.50 – 5.42 (m, 3H), 5.23 (d, *J* = 9.5 Hz, 1H), 4.83 (t, *J* = 9.9 Hz, 1H), 4.20 (dtt, *J* = 18.0, 10.9, 7.1 Hz, 2H), 4.12 – 4.05 (m, 3H), 3.81 – 3.76 (m, 2H), 3.48 (dd, *J* = 14.1, 5.9 Hz, 1H), 3.17 (dd, *J* = 10.3, 4.8 Hz, 1H), 3.15 – 3.08 (m, 3H), 3.05 (dd, *J* = 7.4, 3.1 Hz, 1H), 2.96 (t, *J* = 12.8 Hz, 1H), 2.88 (s, 3H), 2.52 – 2.49 (m, 4H), 2.21 (td, *J* = 13.8, 12.6, 5.4 Hz, 1H), 2.18 – 2.08 (m, 2H), 1.92 (tq, *J* = 13.8, 8.0 Hz, 1H), 1.77 (dt, *J* = 14.4, 7.3 Hz, 1H), 1.48 (s, 9H), 1.22 (t, *J* = 7.1 Hz, 3H), 1.14 – 1.08 (m, 15H), 1.14 – 1.08 (m, 15H).

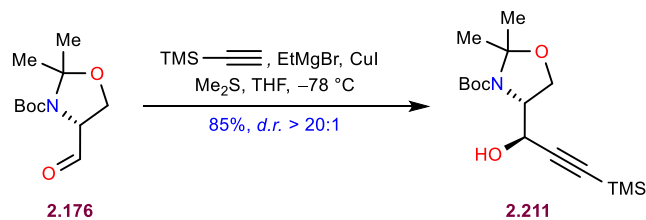
¹³C{¹H} NMR (151 MHz, CDCl₃) δ 174.7, 171.3, 170.7, 169.9, 169.4, 168.8, 168.5, 166.0, 155.5, 145.9, 144.5, 141.7, 138.4, 137.9, 136.3, 135.9, 134.6, 134.15, 132.2, 130.1, 129.6, 129.4, 128.7, 128.4, 128.3, 127.7, 127.3, 126.4, 123.4, 122.4, 121.8, 117.3, 114.2, 112.8, 80.4, 79.72, 73.1, 71.3, 69.5, 62.0, 60.5, 57.3, 57.0, 53.9, 53.6, 50.7, 48.9, 40.4, 37.4, 36.8, 30.9, 29.9, 29.5, 28.5, 27.2, 26.9, 24.8, 14.2, 8.4, 6.3, 4.5.

HRMS: (ES⁺, *m/z*) [M+H]⁺ calcd. for C₉₂H₁₀₈N₉O₁₅Si₂, 1634.7503; found 1634.7506.

IR (ATR, neat, cm⁻¹): 3347 (br), 2929 (m), 2854 (w), 1771 (w), 1714 (s), 1677 (m), 1492 (m), 1368 (m), 1221 (m), 701 (w).

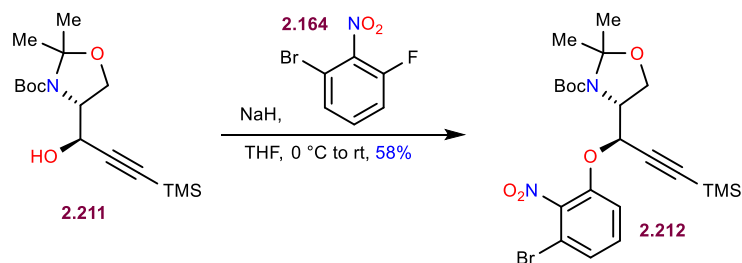
The eastern macrocycle formed as the undesired atropisomer according to ROESY correlations.





Alcohol **2.211**:

TMS-acetylene (13.0 mL, 91.6 mmol, 1.75 equiv.) was dissolved in THF (200 mL). The obtained solution was cooled to 0 °C, followed by dropwise addition of EtMgBr (26.2 mL, 3.0 M in ether, 28.3 mmol, 1.5 equiv.) at the same temperature. The mixture was heated to reflux and stirred for 1 hour. The solution was then cooled down to room temperature and cannulated into a solution of CuI (21.9 g, 115 mmol, 2.2 equiv.) in THF/DMS = 5:1 (300 mL total volume) at -78 °C. The obtained mixture was warmed to -30 °C, stirred for 30 min at this temperature then cooled back to -78 °C. To this solution was added dropwise D-Garner's aldehyde (**2.176**) (12.0 g, 52.3 mmol, 1.0 equiv.) as a solution in THF (50 mL). The reaction mixture was left to stir overnight, slowly warming up to room temperature. Saturated aqueous NH₄Cl (300 mL) was added to quench the reaction. After stirring for 30 min, the reaction mixture was transferred to a separatory funnel and extracted with Et₂O (3 x 200 mL). The organic extracts were combined, washed with brine (300 mL), dried over MgSO₄, filtered and concentrated. Flash column chromatography (SiO₂, hexanes : EtOAc = 5:1 to 4:1) afforded alcohol **2.211** as a yellow oil (14.5 g, 52.3 mmol, 85%, >20:1 d.r.). Characterization data matched previously reported values.⁷⁷



Ether **2.212**

Alcohol **2.211** (14.25 g, 43.5 mmol, 1.0 equiv.) was dissolved in THF (870 mL, 0.05 M). The obtained solution was cooled to 0 °C, followed by portionwise addition of NaH (2.20 g, 54.4 mmol, 1.25 equiv., 60% in mineral oil). After 15 minutes of stirring at 0 °C, 1-bromo-3-fluoro-2-

nitrobenzene **2.164** (11.5 g, 52.2 mmol, 1.2 equiv.) was added in one portion. The reaction was allowed to slowly warm to room temperature and stir overnight. Upon completion (monitored by HPLC), the reaction mixture was cooled to 0 °C and quenched carefully with saturated aqueous NaHCO₃ (400 mL). The obtained solution was transferred to a separatory funnel and extracted with Et₂O (3 x 400 mL). The organic extracts were combined, washed with brine (400 mL), dried over MgSO₄, filtered and concentrated. Flash column chromatography (Biotage Isolera, C₁₈-SiO₂, MeCN/H₂O = 60% to 90%) afforded the ether **2.212** as a clear oil (13.0 g, 24.6 mmol, 58%).

$[\alpha]_D^{23} = 75.1^\circ$ (c = 0.19, CHCl₃)

$R_f = 0.3$ (SiO₂, hexanes : EtOAc = 8:1)

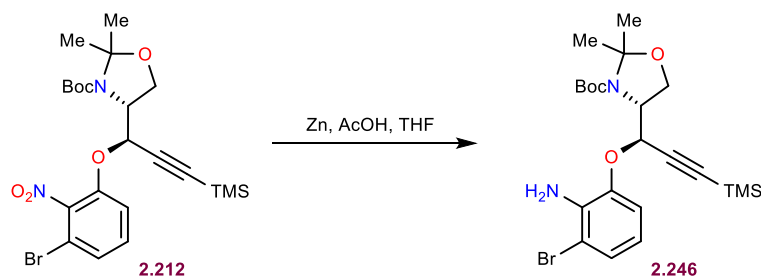
¹H NMR (600 MHz, DMSO-*d*₆, 80 °C) δ 7.56 – 7.46 (m, 3H), 5.47 (s, 1H), 4.17 (s, 1H), 4.09 – 3.97 (m, 2H), 1.57 (s, 3H), 1.46 (s, 12H), 0.12 (s, 9H).

¹³C{¹H} NMR (151 MHz, DMSO-*d*₆) δ 148.4, 142.5, 132.0, 126.1, 116.4, 111.9, 98.9, 94.7, 93.8, 79.9, 70.3, 63.4, 58.0, 27.6, 25.7, -1.1.

HRMS: (ES+) *m/z*: [M+H]⁺ calcd. for C₂₂H₃₃N₂O₆⁷⁹BrSi 527.1213; found 527.1196

IR (ATR, neat, cm⁻¹) 2975 (w), 2936 (w), 1688 (m), 1545 (m), 1390 (m), 1366 (s), 1251 (m), 1169 (m), 1007 (w), 846 (s), 762 (m)

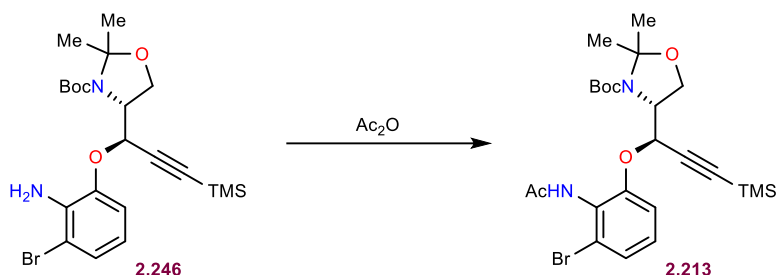
*Due to rotamerism at room temperature, NMR spectra used for assignment were taken at 80 °C in DMSO-*d*₆*



Aniline 2.246:

To a solution of ether **2.212** (3.85 g, 7.30 mmol 1.0 equiv.) in THF (73 mL) was added Zn (9.54 g, 146 mmol, 20 equiv., non-activated) and glacial AcOH (8.0 mL) at room temperature. After 1 hour of stirring (monitored by HPLC), the reaction mixture was filtered through celite. Water (200 mL) was added to the filtrate which was followed by neutralization with solid Na₂CO₃ until effervescence ceased. The obtained mixture was transferred to a separatory funnel and extracted

with EtOAc (3 x 150 mL). The organic extracts were combined, washed with brine (150 mL), dried over MgSO₄, filtered, and concentrated to afford **2.246** as an off-white foam that was taken forward without purification (quantitative yield was assumed, 3.63 g, 7.30 mmol).



Acetanilide **2.213**:

2.246 (3.63 g, 7.30 mmol, 1.0 equiv.) was dissolved in acetic anhydride (40 mL) and left to stir overnight. After full consumption of the starting material, acetic anhydride was removed at room temperature under high vacuum (heating the reaction mixture during concentration on the rotovap led to decomposition). The crude material was purified by flash column chromatography (SiO₂ hexanes : EtOAc = 2:1) to afford acetanilide **2.213** (2.74 g, 5.08 mmol, 70% over 2 steps) as a white foam.

$$[\alpha]_D^{23} = 38.8^\circ \text{ (} c = 0.49, \text{CHCl}_3 \text{)}$$

R_f = 0.3 (SiO₂, hexanes : EtOAc = 2:1)

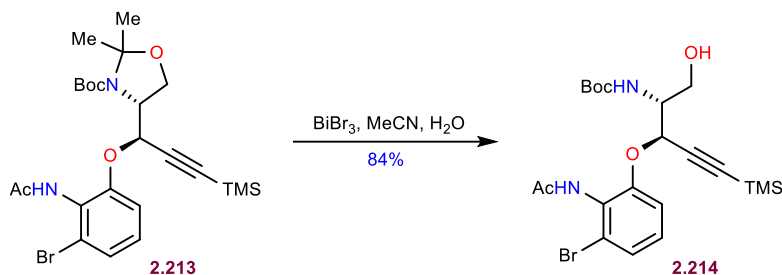
¹H NMR (600 MHz, DMSO-*d*₆, 80 °C) δ 9.05 (s, 1H), 7.31 (dd, *J* = 7.8, 1.5 Hz, 1H), 7.21 (t, *J* = 8.1 Hz, 1H), 7.18 (dd, *J* = 8.3, 1.5 Hz, 1H), 5.30 (s, 1H), 4.17 (dd, *J* = 9.0, 3.3 Hz, 1H), 4.15 – 4.12 (m, 1H), 4.08 (dd, *J* = 9.0, 6.5 Hz, 1H), 2.02 – 1.97 (s, 3H), 1.59 (s, 3H), 1.47 (s, 3H), 1.43 (s, 9H), 0.14 (s, 9H).

¹³C{¹H} NMR (151 MHz, DMSO-*d*₆, 80 °C) δ 167.7, 154.0, 128.2, 127.3, 125.3, 123.3, 114.5, 100.4, 93.8, 93.1, 79.7, 68.9, 63.6, 58.1, 27.6, 25.4, 21.8, -0.9.

HRMS: (ES+) *m/z*: [M+H]⁺ calcd. for C₂₄H₃₆N₂O₅⁷⁹BrSi 539.1577; found 539.1583

IR (ATR, neat, cm⁻¹): 3255 (br), 2976 (s), 1689 (s), 1473 (m), 1446 (m), 1392 (m), 1366 (m), 1251 (m), 1167 (m), 1062 (m), 1018 (m), 843 (m), 763 (m).

*Due to rotamerism at room temperature, NMR spectra used for assignment were taken at 80 °C in DMSO-*d*₆. The carbons at 68.9 ppm and 167.7 ppm didn't resolve at this temperature.*



Alcohol **2.214**:

To a solution of acetanilide **2.213** (2.74 g, 5.08 mmol, 1.0 equiv.) in MeCN (50 mL, 0.10 M) was added bismuth (III) bromide (456 mg, 1.02 mmol, 0.20 equiv.) at room temperature. Subsequently, 0.50 mL of water were added, and the reaction mixture was left to stir for 3 hours (monitored by HPLC until complete). The reaction mixture was then quenched by addition of saturated aqueous NaHCO₃ (150 mL) and filtered through celite (celite was washed with 150 mL of EtOAc). The filtrate was transferred to a separatory funnel, the layers were separated, and the organic layer was further extracted with EtOAc (2 x 100 mL). The combined organic extracts were washed with brine (150 mL), dried over MgSO₄, filtered and concentrated. Flash column chromatography (SiO₂, hexanes : EtOAc = 1:2) delivered alcohol **2.214** (2.14 g, 4.28 mmol, 84%) as a white foam. $[\alpha]_D^{23} = 7.2^\circ$ (c = 0.27, CHCl₃)

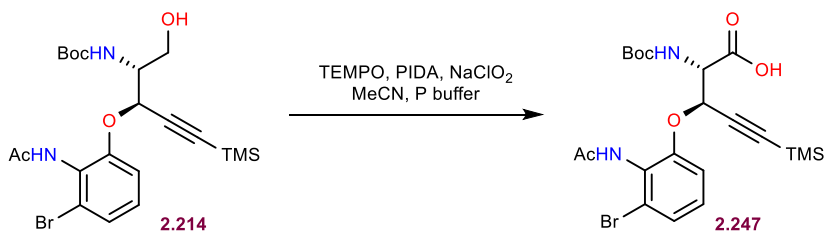
R_f = 0.3 (SiO₂, hexanes : EtOAc = 1:2)

¹H NMR (500 MHz, CDCl₃) δ 9.37 (s, 1H), 7.26 (dd, J = 7.5, 2.0 Hz, 1H), 7.20 – 7.12 (m, 2H), 6.61 (d, J = 9.2 Hz, 1H), 5.02 (d, J = 3.4 Hz, 1H), 4.84 (s, 1H), 3.97 – 3.85 (m, 1H), 3.55 – 3.40 (m, 2H), 2.03 (s, 3H), 1.42 (s, 9H), 0.10 (s, 9H).

¹³C{¹H} NMR (126 MHz, DMSO-*d*₆) δ 168.03, 155.37, 153.23, 128.02, 126.76, 124.95, 123.07, 113.44, 101.74, 92.27, 78.10, 67.76, 59.79, 55.80, 28.24, 22.73, -0.41.

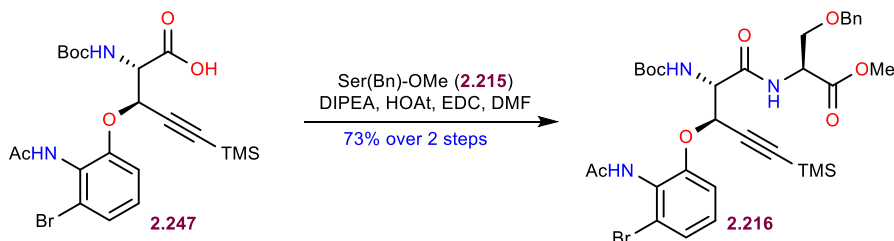
HRMS: (ES⁺) *m/z*: [M+H]⁺ calcd. for C₂₁H₃₂N₂O₅Si⁷⁹Br 499.1264; found 499.1269

IR (ATR, neat, cm⁻¹): 3280 (br), 2966 (s), 2177 (s), 1693 (m), 1669 (m), 1580 (s), 1510 (m), 1472 (m), 1446 (m), 1250 (m), 1168 (m), 843 (m), 762 (m)



Acid **2.247**:

To a solution of alcohol **2.214** (2.14 g, 4.28 mmol, 1.0 equiv.) in MeCN (55 mL) and phosphate buffer (30 mL, pH = 6.4, 0.10 M) were added PIDA (276 mg, 0.857 mmol, 0.2 equiv.) and TEMPO (268 mg, 1.71 mmol, 0.4 equiv.) at room temperature. The obtained mixture was cooled to 0 °C, followed by the addition of NaClO₂ (1.28 g, 14.1 mmol, 3.3 equiv.) in one portion. The resulting solution was warmed to room temperature and left to stir overnight. Saturated aqueous NH₄Cl (120 mL) was added, and the obtained mixture was transferred to a separatory funnel and extracted with EtOAc (4 x 100 mL). The organic extracts were combined, washed with brine (100 mL), dried over MgSO₄, filtered and concentrated. The obtained crude acid **2.247** was taken into the next step without further purification (assumed quantitative yield, 2.20 g, 4.28 mmol).



Dipeptide **2.216**:

Crude acid **2.247** (2.20 g, 4.28 mmol, 1.0 equiv.) and *O*-benzyl serine methyl ester **2.215** (1.66 g, 5.14 mmol, 1.2 equiv.) were dissolved in DMF (43 mL, 0.1 M). The solution was cooled to 0 °C before DIPEA (2.24 mL, 12.9 mmol, 3 equiv.) and HATU (1.96 g, 5.14 mmol, 1.2 equiv.) were added. The reaction was allowed to slowly warm to room temperature and stir at this temperature until complete (5 hours in total). The reaction was quenched with 1 M aqueous HCl (80 mL) and diluted with EtOAc (100 mL). The mixture was transferred to a separatory funnel, and the layers were separated. The aqueous layer was extracted with EtOAc (2 x 100 mL). The combined organic layers were washed with saturated aqueous NaHCO₃ (60 mL), water (60 mL) and brine (60 mL), dried over MgSO₄ and concentrated. The crude product was purified by flash column

chromatography (SiO₂, hexanes : EtOAc = 1:1) to yield dipeptide **2.216** (2.21 g, 3.14 mmol, 73% over two steps) as a white foam.

$[\alpha]_D^{23} = 62.3^\circ$ (c = 4.0, CHCl₃)

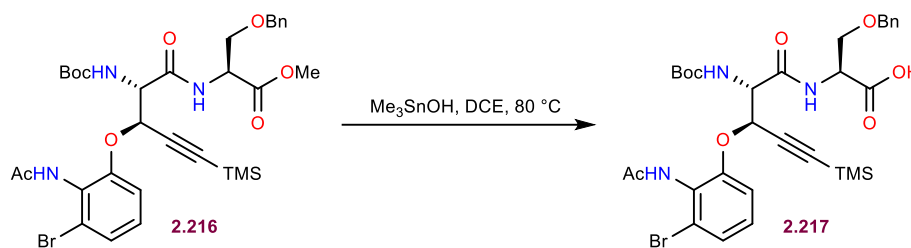
R_f = 0.4 (SiO₂, hexanes : EtOAc = 1:1)

¹H NMR (600 MHz, DMSO-*d*₆) δ 9.21 (s, 1H), 8.39 (d, *J* = 7.9 Hz, 1H), 7.36 – 7.31 (m, 2H), 7.30 – 7.23 (m, 4H), 7.16 (t, *J* = 8.1 Hz, 1H), 7.11 (d, *J* = 8.5 Hz, 1H), 7.06 (d, *J* = 10.0 Hz, 1H), 5.29 (d, *J* = 3.0 Hz, 1H), 4.69 (dd, *J* = 9.9, 3.0 Hz, 1H), 4.52 (dt, *J* = 8.5, 4.5 Hz, 1H), 4.50 – 4.40 (m, 2H), 3.71 (dd, *J* = 9.8, 4.9 Hz, 1H), 3.59 (dd, *J* = 9.9, 4.2 Hz, 1H), 3.42 (s, 3H), 2.00 (s, 3H), 1.44 (s, 9H), 0.09 (s, 9H).

¹³C{¹H} NMR (151 MHz, DMSO-*d*₆) δ 170.1, 168.0, 167.7, 155.3, 152.6, 137.8, 128.2, 127.7, 127.5, 127.5, 127.3, 125.4, 122.8, 113.5, 100.4, 92.8, 78.8, 72.1, 70.3, 69.1, 57.4, 52.4, 52.0, 28.2, 22.9, -0.5.

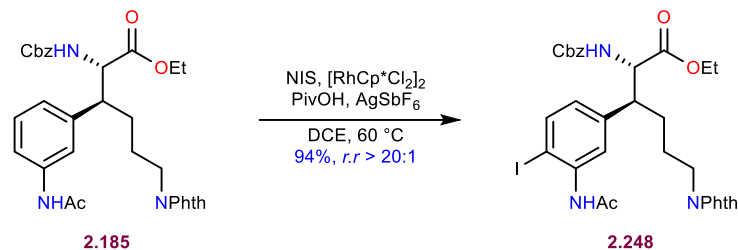
HRMS: (ES⁺) *m/z*: [M+H]⁺ calcd. for C₃₂H₄₃N₃O₈Si⁷⁹Br 704.2003; found 704.2008

IR (ATR, neat, cm⁻¹): 3299 (w), 2958 (w), 2180 (w), 1672 (s), 1497 (s), 1366 (m), 1162 (s)



Acid **2.217**:

Dipeptide **2.216** (1.81 g, 2.57 mmol, 1.0 equiv.) was dissolved in DCE (26 mL, 0.1 M). To the obtained solution was added Me₃SnOH (1.39 g, 6.77 mmol, 3.0 equiv.). The reaction was heated to 80 °C and left to stir overnight at this temperature. After cooling to room temperature, the solvent was removed *in vacuo*, and the residue was redissolved in 1:1 EtOAc/1 M aqueous HCl (20 mL) and stirred vigorously for 5 minutes. The mixture was transferred to a separatory funnel, the layers were separated and the aqueous layer was extracted with EtOAc (3 x 20 mL). The organic layers were combined, washed with brine (30 mL), dried over MgSO₄, filtered and concentrated. Crude acid **2.217** was taken forward without further purification (quantitative yield was assumed, 1.77 g, 2.57 mmol).



Iodoacetanilide **2.248**:

β -aryl lysine **2.185** (2.47 g, 4.32 mmol, 1.0 equiv.) was dissolved in DCE (43 mL, 0.1 M). To this was added pivalic acid (485 mg, 4.75 mmol, 1.1 equiv.), silver hexafluoroantimonate (371 mg, 1.08 mmol, 0.25 equiv.), and $[\text{RhCp}^*\text{Cl}_2]_2$ (267 mg, 432 μmol , 0.1 equiv.). Lastly, NIS (1.02 g, 4.54 mmol, 1.05 equiv.) was added and the reaction was heated to 60 $^\circ\text{C}$ for 6 hours. Upon completion, the reaction was cooled to room temperature and filtered through celite. The filter pad was washed with DCM (20 mL) and the solvent was removed on the rotary evaporator. The crude material was purified by column chromatography (SiO_2 , hexanes : EtOAc = 3:1 to 1:1) to produce iodide **2.248** (2.82 g, 4.04 mmol, 94%) as a light-brown foam.

$[\alpha]_{\text{D}}^{23} = 56.7^\circ$ ($c = 0.71$, CHCl_3)

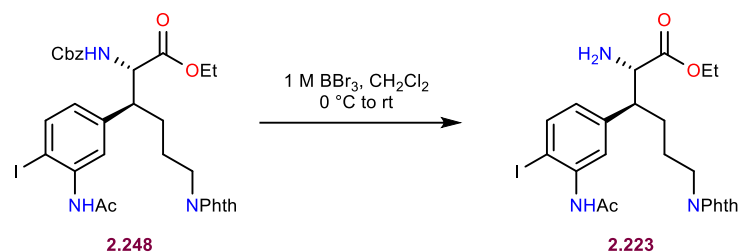
$R_f = 0.4$ (SiO_2 , hexanes : EtOAc = 1:2)

$^1\text{H NMR}$ (600 MHz, $\text{DMSO-}d_6$) δ 9.35 (s, 1H), 7.88 – 7.77 (m, 4H), 7.73 (d, $J = 8.1$ Hz, 1H), 7.53 (d, $J = 8.5$ Hz, 1H), 7.35 – 7.26 (m, 4H), 7.22 (d, $J = 7.4$ Hz, 2H), 6.86 (d, $J = 8.2$ Hz, 1H), 4.97 – 4.84 (m, 2H), 4.23 (t, $J = 8.6$ Hz, 1H), 4.03 (q, $J = 7.1$ Hz, 2H), 3.48 (t, $J = 6.8$ Hz, 2H), 2.95 (td, $J = 9.2, 4.8$ Hz, 1H), 2.02 (s, 3H), 1.66 – 1.48 (m, 2H), 1.35 (dh, $J = 17.7, 6.8$ Hz, 2H), 1.12 (t, $J = 7.1$ Hz, 3H).

$^{13}\text{C}\{^1\text{H}\}$ NMR (151 MHz, $\text{DMSO-}d_6$) δ 179.4, 171.3, 168.1, 167.9, 155.9, 141.0, 139.5, 138.6, 136.8, 134.4, 131.6, 128.3, 127.8, 127.6, 127.2, 123.0, 94.4, 65.5, 60.6, 58.6, 45.7, 39.9, 39.8, 39.7, 39.5, 39.4, 39.2, 39.1, 37.2, 28.5, 25.8, 13.9.

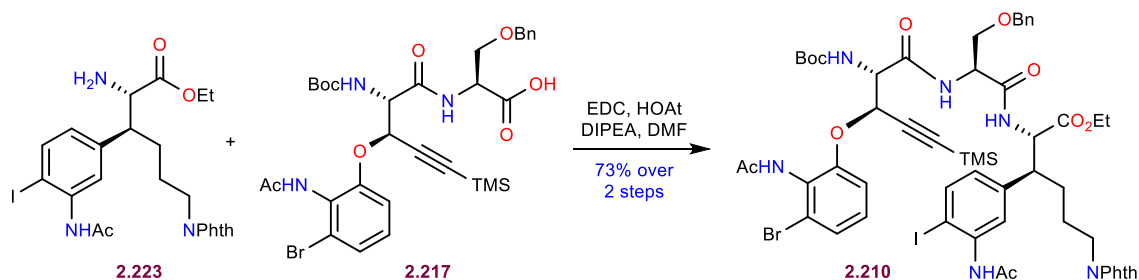
HRMS: (ES+) m/z : $[\text{M}+\text{H}]^+$ calcd. for $\text{C}_{32}\text{H}_{33}\text{N}_3\text{O}_7\text{I}$, 698.1363; found 698.1367

IR (ATR, neat, cm^{-1}) 3333 (w), 2940 (w), 1771 (w), 1708 (s), 1518 (w), 1397 (w), 1184 (w)



Amine 2.223:

Iodide **2.248** (1.78 g, 2.55 mmol, 1.0 equiv.) was dissolved in DCM (32 mL, 0.08 M) and cooled to 0 °C. To this was added 1 M BBr₃ in DCM (2.81 mL, 2.81 mmol, 1.1 equiv.) dropwise. The ice bath was removed and the reaction was left to stir until complete (about 1 hour). The mixture was cooled to 0 °C and quenched by dropwise addition of methanol (3 mL). The obtained solution was concentrated and the residue was triturated with hexanes and dried under vacuum to yield amine **2.223** as a light orange foam that was taken forward without further purification (quantitative yield was assumed, 1.44 g, 2.55 mmol).



Tripeptide 2.210:

Acid **2.217** (1.77 g, 2.56 mmol, 1.0 equiv.) and amine **2.223** (1.44 g, 2.56 mmol, 1.0 equiv.) were dissolved in DMF (26 mL, 0.1 M). To the obtained solution was added DIPEA (1.34 mL, 7.67 mmol, 3 equiv.). The solution was cooled to 0 °C before HOAt (417 mg, 3.07 mmol, 1.2 equiv.) was added. Subsequently EDC (588 mg, 3.07 mmol, 1.2 equiv.) was added. The mixture was allowed to warm to room temperature and stir overnight. The reaction was quenched with 1 M aqueous HCl (60 mL) and diluted with EtOAc (80 mL). The mixture was transferred to a separatory funnel and the layers were separated. The aqueous layer was extracted with EtOAc (2 x 80 mL). The combined organic layers were washed with saturated aqueous NaHCO₃ (60 mL), water (60 mL) and brine (60 mL), dried over MgSO₄ and concentrated. The crude product was

purified by flash column chromatography (SiO₂, hexanes : EtOAc = 1:1 to 1:2) to yield tripeptide **2.210** (2.35 g, 1.92 mmol, 75% yield over 2 steps) as a white foam.

$[\alpha]_D^{23} = 26.7^\circ$ (c = 2.0, CHCl₃)

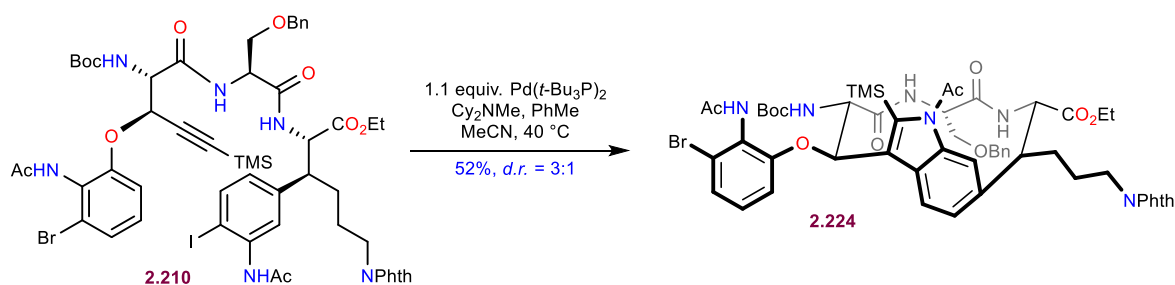
R_f = 0.3 (SiO₂, hexanes : EtOAc = 1:2)

¹H NMR (600 MHz, DMSO-*d*₆) δ 9.34 (s, 1H), 9.23 (s, 1H), 7.99 (s, 1H), 7.89 (d, *J* = 7.1 Hz, 1H), 7.82 (dt, *J* = 9.0, 6.5, 3.3 Hz, 4H), 7.68 (d, *J* = 8.2 Hz, 1H), 7.31 – 7.20 (m, 7H), 7.16 (t, *J* = 7.6 Hz, 1H), 7.12 – 7.02 (m, 2H), 6.77 (d, *J* = 8.2 Hz, 1H), 5.31 (d, *J* = 3.0 Hz, 1H), 4.57 (ddd, *J* = 17.8, 12.3, 7.0 Hz, 3H), 4.38 (s, 2H), 3.94 (qt, *J* = 10.9, 5.0 Hz, 2H), 3.54 – 3.49 (m, 1H), 3.46 (dt, *J* = 14.1, 6.5 Hz, 3H), 3.08 (dd, *J* = 9.4, 5.6 Hz, 1H), 2.04 (s, 3H), 1.99 (s, 3H), 1.60 (dq, *J* = 19.3, 8.7 Hz, 2H), 1.43 (s, 9H), 1.37 (s, 2H), 1.05 (t, *J* = 7.2 Hz, 3H), 0.07 (s, 9H).

¹³C{¹H} NMR (151 MHz, DMSO-*d*₆) δ 170.1, 169.3, 168.3, 168.0, 167.9, 167.6, 155.4, 152.5, 140.0, 139.4, 138.7, 137.9, 134.4, 131.6, 128.2, 127.7, 127.44, 127.41, 127.37, 127.30, 127.05, 125.6, 123.0, 122.8, 114.3, 100.4, 94.2, 92.8, 78.9, 72.2, 69.8, 60.7, 57.9, 56.1, 52.4, 45.7, 37.0, 28.2, 27.8, 25.7, 23.3, 22.9, 13.8, -0.5.

HRMS: (ES⁺) *m/z*: [M+H]⁺ calcd. for C₅₅H₆₅N₅O₁₂Si⁷⁹BrI, 1235.2658; found 1235.2629

IR (ATR, neat, cm⁻¹) 3261 (w), 2176 (w), 1771 (w), 1710 (s), 1520 (m), 1367 (m), 1026 (m).



Eastern macrocycle **2.224**:

The following reaction was set up under argon atmosphere

To a flask containing tripeptide **2.210** (200 mg, 162 μmol, 1.0 equiv.) was added Pd(*t*-Bu₃P)₂ (91 mg, 178 μmol, 1.1 equiv.). Dry and degassed MeCN (100 mL) was cannulated into the flask. Subsequent addition of Cy₂NMe (45 μL, 210 μmol, 1.3 equiv.) was followed by cannulation of dry and degassed PhMe (50 mL) into the flask. The resulting solution was sonicated for 1 minute to dissolve Pd(*t*-Bu₃P)₂ and Cy₂NMe and obtain a homogeneous solution. The reaction mixture was heated to 40 °C and left to stir for 5 hours at this temperature. Upon completion (determined

by HPLC analysis, atropisomeric ratio 3.3:1), the crude reaction mixture was frozen using a liquid nitrogen bath and the solvent was removed on the lyophilizer (solvent removal on a rotary evaporator led to some product decomposition as the crude mixture was concentrated). The residue was redissolved in DCM (20 mL) and the resulting solution was washed with saturated aqueous sodium thiosulfate (10 mL) and 1 M aqueous HCl (10 mL). The organic layer was transferred to a flask and stirred with an aqueous solution of *N*-Ac-Cys-OH (264 mg, 1.62 mmol, 10 equiv. in 10 mL of water) for 1 hour. The mixture was transferred to a separation funnel and the organic layer was separated and washed with brine (10 mL). Upon drying with MgSO₄ and removal of the solvent *in vacuo*, the obtained residue was purified by flash column chromatography (SiO₂, PhMe/acetone/MeOH = 7:1:0.1, this fraction contains the undesired atropisomer, then 6:1:0.1, this fraction contains the desired atropisomer).

The fraction containing the desired atropisomer was further purified with preparative TLC (SiO₂, PhMe/acetone/MeOH = 3:1:0.1) to afford a white solid (**2.224**) (70 mg, 63 μmol, 39% yield).

The fraction containing the undesired atropisomer was further purified with preparative TLC (SiO₂, Hex/EtOAc = 1:1) to afford a white solid (*atrop*-**2.224**) (23 mg, 21 μmol, 13% yield).

The total yield is 52%, *d.r.* = 3:1.

Desired atropisomer **2.224**:

$[\alpha]_D^{23} = -35.8^\circ$ (*c* = 1.40, CHCl₃)

R_f = 0.4 (SiO₂, PhMe/Acetone/MeOH = 3:1:0.1)

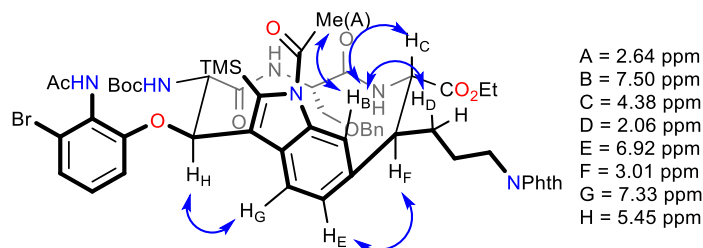
¹H NMR (600 MHz, CDCl₃) δ 7.96 (s, 1H), 7.80 (dd, *J* = 5.4, 3.1 Hz, 2H), 7.71 (dd, *J* = 5.5, 3.0 Hz, 2H), 7.50 (s, 1H), 7.33 (d, *J* = 8.0 Hz, 1H), 7.24 – 7.19 (m, 3H), 7.15 (d, *J* = 8.1 Hz, 1H), 7.11 – 7.09 (m, 2H), 6.91 (d, *J* = 8.0 Hz, 1H), 6.81 (t, *J* = 8.2 Hz, 1H), 6.61 (d, *J* = 8.4 Hz, 1H), 6.51 (s, 1H), 5.45 (d, *J* = 9.9 Hz, 1H), 5.27 (d, *J* = 8.6 Hz, 1H), 4.57 – 4.51 (m, 1H), 4.43 (m, 1H), 4.38 (t, *J* = 10.6 Hz, 1H), 4.35 (d, *J* = 12.3 Hz, 1H), 4.30 (d, *J* = 12.3 Hz, 1H), 4.28 – 4.18 (m, 2H), 3.72 (t, *J* = 6.9 Hz, 2H), 3.19 (d, *J* = 7.2 Hz, 2H), 3.00 (td, *J* = 11.3, 3.8 Hz, 1H), 2.64 (s, 3H), 2.27 (s, 3H), 2.11 – 2.02 (m, 1H), 1.97 (ddt, *J* = 18.1, 12.5, 6.5 Hz, 1H), 1.83 (ddt, *J* = 12.8, 9.8, 5.0 Hz, 1H), 1.72 (ddd, *J* = 13.2, 10.6, 6.2 Hz, 1H), 1.46 (s, 9H), 1.27 (t, *J* = 7.1 Hz, 3H), 0.31 (s, 9H).

¹³C{¹H} NMR (151 MHz, CDCl₃) δ 171.0, 169.8, 168.4, 168.2, 167.3, 156.5, 153.7, 142.8, 139.5, 137.6, 135.9, 134.2, 132.0, 130.2, 129.7, 129.1, 128.4, 127.8, 127.7, 127.5, 126.5, 126.0, 123.4, 122.1, 117.2, 113.8, 112.2, 80.3, 73.2, 70.1, 62.0, 61.0, 59.3, 52.9, 50.2, 37.6, 28.7, 27.0, 26.7, 26.2, 23.7, 14.2, 2.3.

HRMS: (ES+) m/z : $[M+H]^+$ calcd. for $C_{55}H_{64}N_6O_{12}Si^{79}Br$, 1107.3535; found 1107.3540

IR (ATR, neat, cm^{-1}) 3319 (br), 2978 (w), 2935 (w), 1771 (w), 1708 (s), 1663 (s), 1499 (m), 1255 (m), 1172 (m), 851 (m)

Key NOE correlations in the desired atropisomer:



Undesired atropisomer *atrop-2.224*:

$[\alpha]_D^{23} = 16.0^\circ$ (c = 0.61, $CHCl_3$)

$R_f = 0.3$ (SiO_2 , PhMe/Acetone/MeOH = 5:1:0.1)

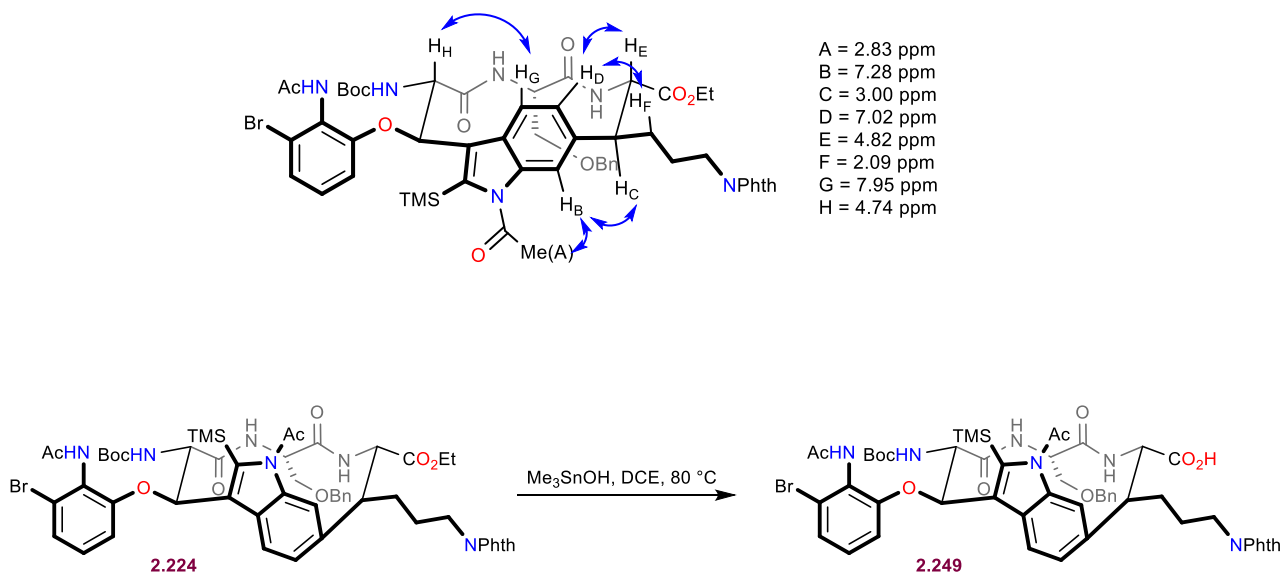
1H NMR (800 MHz, $CDCl_3$) δ 7.96 (d, $J = 8.4$ Hz, 1H), 7.85 (s, 1H), 7.82 (td, $J = 5.4, 2.9$ Hz, 1H), 7.79 (dd, $J = 5.4, 3.0$ Hz, 2H), 7.70 (ddt, $J = 7.9, 5.3, 2.6$ Hz, 1H), 7.67 (dd, $J = 5.5, 3.0$ Hz, 2H), 7.32 (d, $J = 7.8$ Hz, 1H), 7.29 – 7.26 (m, 2H), 7.25 – 7.20 (m, 3H), 7.15 – 7.13 (m, 2H), 7.09 (t, $J = 8.2$ Hz, 1H), 7.02 (d, $J = 8.4$ Hz, 1H), 6.64 (s, 1H), 5.84 (s, 1H), 5.50 (s, 1H), 4.83 (t, $J = 10.2$ Hz, 1H), 4.74 (s, 1H), 4.36 (d, $J = 11.9$ Hz, 1H), 4.32 (d, $J = 12.0$ Hz, 1H), 4.22 – 4.16 (m, 2H), 3.72 (t, $J = 7.3$ Hz, 2H), 3.51– 3.48 (m, 1H), 3.42 (t, $J = 9.1$ Hz, 1H), 3.36 (dd, $J = 9.1, 5.6$ Hz, 1H), 3.01 (td, $J = 10.0, 4.9$ Hz, 1H), 2.84 (s, 3H), 2.46 (s, 3H), 2.11 – 2.08 (m, 1H), 1.86 (dt, $J = 14.0, 6.9$ Hz, 1H), 1.76 (d, $J = 18.9$ Hz, 1H), 1.45 (d, $J = 8.0$ Hz, 9H), 1.22 (t, $J = 7.2$ Hz, 3H), 0.41 (s, 9H).

$^{13}C\{^1H\}$ NMR (151 MHz, $CDCl_3$) δ 171.2, 167.0, 169.3, 168.4, 168.3, 167.4, 155.2, 154.5, 137.9, 137.5, 136.9, 134.2, 132.1, 132.1, 130.5, 128.5, 128.4, 127.8, 127.6, 126.8, 126.3, 123.5, 123.3, 122.7, 122.6, 122.0, 116.8, 114.7, 81.4, 80.8, 73.4, 69.5, 62.0, 57.1, 53.8, 50.9, 37.5, 29.7, 28.5, 28.4, 27.1, 26.4, 23.7, 14.2, 3.0.

HRMS: (ES+) m/z : $[M+H]^+$ calcd. for $C_{55}H_{64}N_6O_{12}Si^{79}Br$, 1107.3535; found 1107.3527

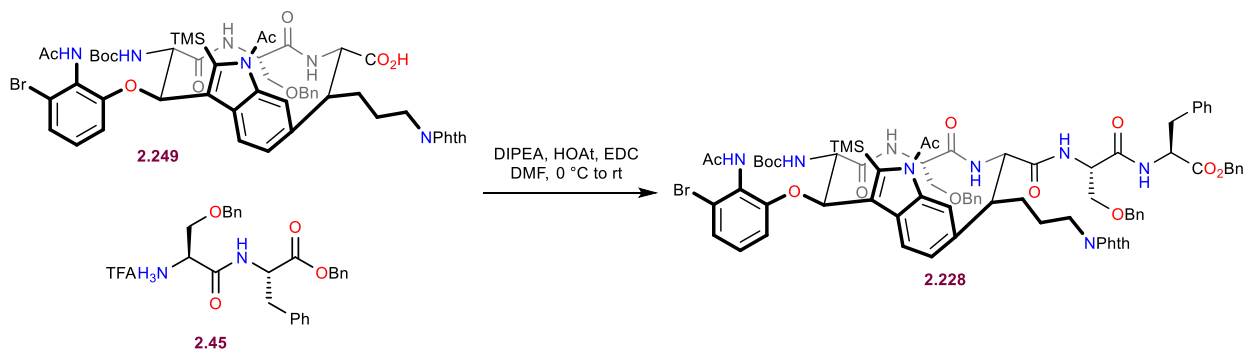
IR (ATR, neat, cm^{-1}) 3345 (br), 2977 (w), 2932 (w), 1771 (w), 1707 (s), 1665 (s), 1444 (m), 1396 (m), 1248 (m), 847 (m)

Key NOE correlations in the undesired atropisomer:



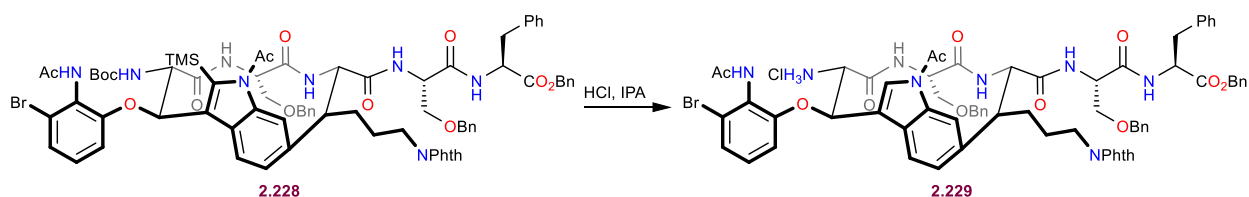
Adic 2.249:

Macrocycle **2.224** (70 mg, 63 μmol , 1.0 equiv.) was dissolved in DCE (0.63 mL, 0.1 M). To the obtained solution was added trimethyl tin hydroxide (57 mg, 0.32 mmol, 5.0 equiv.) and the mixture was heated to 80 $^\circ\text{C}$. After stirring for 12 hours at this temperature, the reaction was completed (monitored by HPLC) and the solvent was removed *in vacuo*. The obtained residue was redissolved in EtOAc (0.40 mL) and 1 M aqueous HCl (0.40 mL) was added. After vigorous stirring for 5 minutes, the layers were separated, and the aqueous layer was extracted with EtOAc (2 x 0.40 mL). The combined organic layers were washed with brine, dried over MgSO_4 , and concentrated *in vacuo* to provide the crude carboxylic acid **2.249**. Quantitative yield was assumed (68 mg, 63 μmol).



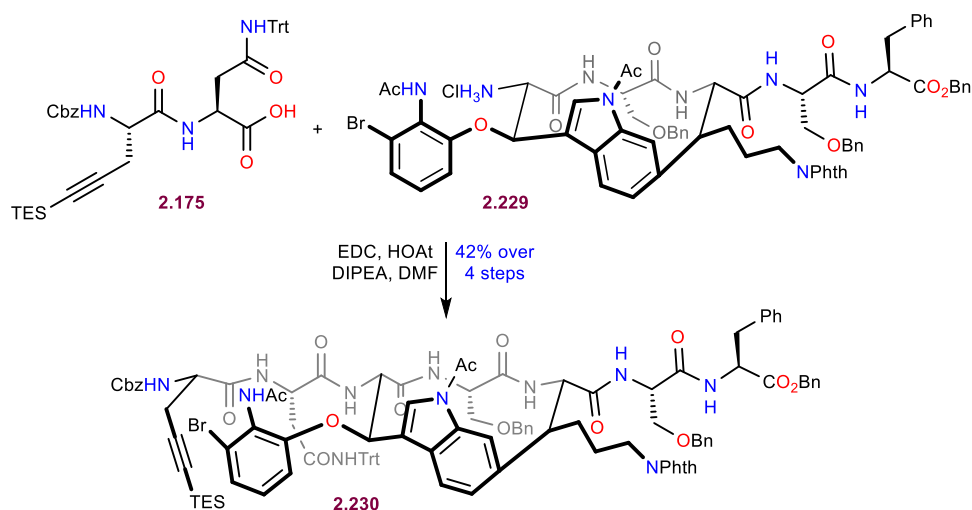
Pentapeptide 2.228:

Acid **2.249** (68 mg, 63 μmol , 1.0 equiv.) and ammonium salt **2.45**•TFA (41 mg, 76 μmol , 1.2 equiv.) were dissolved in DMF (0.63 mL, 0.10 M). To this was added DIPEA (26 μL , 0.15 mmol, 2.4 equiv.). The solution was cooled to 0 °C and HOAt (10 mg, 76 μmol , 1.2 equiv.) and EDC (14 mg, 76 μmol , 1.2 equiv.) were added successively. The mixture was allowed to slowly warm to room temperature and stir for 5 hours in total. Upon completion, the solution was transferred to a separation funnel and diluted with EtOAc (40 mL). This was washed with 1 M aqueous HCl (5 mL), saturated aqueous NaHCO₃ (5 mL), water (5 mL) and brine (5 mL), dried over MgSO₄ and concentrated *in vacuo*. Due to poor solubility, the crude product **2.228** was carried into the next step without additional purification (quantitative yield was assumed, 94 mg, 63 μmol).



Hydrochloride salt 2.229:

Pentapeptide **2.228** (94 mg, 63 μmol , 1.0 equiv.) was suspended in DCM (3 mL), which was followed by the addition of HCl in IPA (0.5 mL, 5.5–6 M) at 0 °C. After stirring for 90 minutes at 0 °C, the solvents were removed *in vacuo*. The residue was suspended in toluene (3 mL) and concentrated again. The obtained hydrochloride salt **2.229** was used in the next step without additional purification (assumed quantitative yield, 85 mg, 63 μmol).



Heptapeptide 2.230:

Ammonium salt **2.229** (85 mg, 63 μmol , 1.0 equiv.) and acid **2.175** (54 mg, 75 μmol , 1.2 equiv.) were dissolved in DMF (0.63 mL, 0.10 M). To the obtained solution was added DIPEA (33 μL , 0.19 mmol, 3.0 equiv.). The solution was cooled to 0 °C and HOAt (10 mg, 75 μmol , 1.2 equiv.) and EDC (14 mg, 75 μmol , 1.2 equiv.) were added successively. The mixture was allowed to slowly warm to room temperature and stir for 5 hours in total. Upon completion, the reaction was diluted with EtOAc (1.0 mL) and quenched with 1 M aqueous HCl (1.0 mL). The layers were separated, and the aqueous phase was extracted with EtOAc (2 x 1.0 mL). The combined organic layers were washed with saturated aqueous NaHCO_3 (1.0 mL), water (1.0 mL) and brine (1.0 mL), dried over MgSO_4 and concentrated *in vacuo*. The obtained residue was purified by flash column chromatography (SiO_2 , PhMe/acetone/MeOH = 7/1/0.1 to 3/1/0.1) to provide heptapeptide **2.230** (53 mg, 26 μmol , 42% over 4 steps) as a white solid.

$$[\alpha]_{\text{D}}^{23} = 10.5^\circ \text{ (c = 1.05, CHCl}_3\text{)}$$

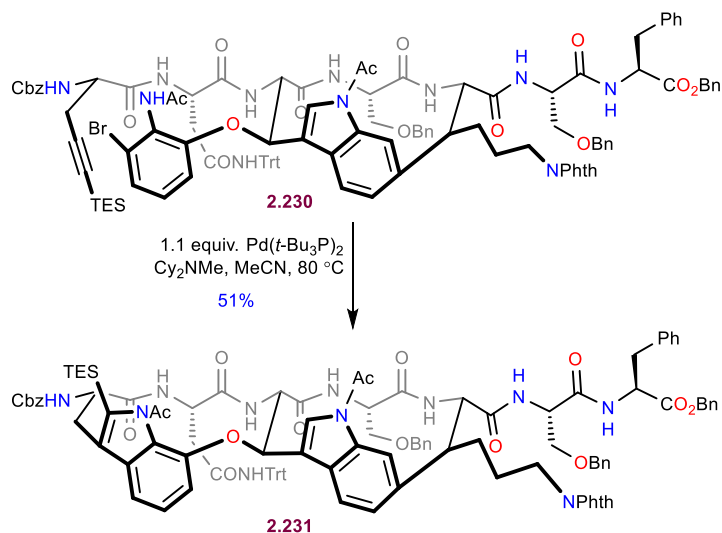
$$R_f = 0.3 \text{ (SiO}_2\text{, PhMe/acetone/MeOH = 3:1:0.1)}$$

$^1\text{H NMR}$ (600 MHz, $\text{DMSO-}d_6$) δ 8.67 (s, 1H), 8.57 (d, $J = 7.8$ Hz, 1H), 8.45 (s, 1H), 8.41 (d, $J = 7.4$ Hz, 1H), 8.32 (s, 1H), 8.17 (s, 1H), 7.81 – 7.74 (m, 5H), 7.72 (s, 1H), 7.54 (t, $J = 8.7$ Hz, 2H), 7.37 – 7.08 (m, 45H), 7.02 (t, $J = 8.2$ Hz, 1H), 6.79 (d, $J = 8.4$ Hz, 1H), 5.36 (d, $J = 9.3$ Hz, 1H), 5.06 (d, $J = 5.5$ Hz, 2H), 5.02 (d, $J = 3.1$ Hz, 2H), 4.71 – 4.65 (m, 1H), 4.60 (dq, $J = 12.0, 7.0, 6.2$ Hz, 1H), 4.55 (q, $J = 7.3$ Hz, 1H), 4.42 – 4.34 (m, 2H), 4.33 – 4.22 (m, 5H), 3.54 – 3.46 (m, 5H), 3.08 – 2.98 (m, 4H), 2.93 – 2.82 (m, 1H), 2.49 (s, 3H), 2.15 (s, 3H), 2.03 – 1.94 (m, 1H), 1.92 – 1.85 (m, 1H), 1.77 – 1.69 (m, 1H), 1.57 – 1.50 (m, 1H), 0.92 (t, $J = 7.9$ Hz, 9H), 0.50 (q, $J = 7.9$ Hz, 6H).

$^{13}\text{C}\{^1\text{H}\}$ NMR (151 MHz, $\text{DMSO-}d_6$) δ 171.0, 170.7, 169.9, 169.7, 169.5, 169.2, 168.9, 168.7, 168.0, 167.8, 166.9, 166.8, 155.8, 154.2, 144.7, 138.1, 138.0, 137.5, 136.9, 136.7, 136.1, 135.6, 134.4, 134.2, 131.7, 131.6, 129.2, 129.0, 128.7, 128.6, 128.4, 128.31, 128.27, 128.2, 128.1, 128.07, 128.01, 127.93, 127.90, 127.8, 127.63, 127.61, 127.53, 127.47, 127.37, 127.34, 127.30, 127.26, 127.18, 127.11, 126.6, 126.4, 126.3, 126.2, 124.8, 124.1, 123.5, 123.0, 122.9, 118.0, 116.7, 114.5, 112.4, 105.0, 82.3, 79.2, 73.7, 72.0, 71.5, 70.2, 69.8, 69.3, 66.1, 65.5, 59.7, 53.6, 53.4, 53.0, 51.5, 50.0, 49.2, 40.1, 37.4, 36.8, 26.9, 25.6, 23.5, 23.4, 22.9, 7.3, 4.0.

HRMS: (ES+) m/z : $[\text{M}+2\text{H}]^{2+}$ calcd. for $(\text{C}_{113}\text{H}_{116}^{79}\text{BrN}_{11}\text{O}_{18}\text{Si})/2$, 1010.8726; found 1010.8707.

IR (ATR, neat, cm^{-1}) 3299 (br), 3061 (w), 3031 (w), 2953 (w), 2177 (w), 1718 (s), 1679 (m), 1643 (s), 1516 (m), 698 (m).



Bismacrocyclic **2.231**:

The following reaction was set up under argon atmosphere

To a flask containing heptapeptide **2.230** (37 mg, 18 μmol , 1.0 equiv.) was added $\text{Pd}(t\text{-Bu}_3\text{P})_2$ (10 mg, 20 μmol , 1.1 equiv.). Dry and degassed MeCN (18 mL, 1.0 mM) was cannulated into the flask. Cy_2NMe (12 μL , 55 μmol , 3.0 equiv.) was added and the resulting solution was heated to $80\text{ }^\circ\text{C}$ and left to stir for 2 hours at this temperature. Upon completion (determined by TLC analysis), MeCN was removed *in vacuo* and the obtained residue was redissolved in DCM (10 mL) and transferred to a separation funnel. The DCM solution was washed with 1 M aqueous HCl (3 mL). The organic layer was transferred to a flask and stirred with an aqueous solution of *N*-Ac-Cys-OH (42 mg, 0.26 mmol, 10 equiv. in 5 mL of water) for 1 hour. The mixture was transferred to a separation funnel and the organic layer was separated and washed with brine (5 mL). Upon drying with MgSO_4 and removal of the solvent *in vacuo*, the obtained residue was purified by flash column chromatography (SiO_2 , PhMe/acetone/MeOH = 6/1/0.1, then 5/1/0.1) to afford protected darobactin **2.231** (18 mg, 9.3 μmol , 51%) as a white foamy solid.

$[\alpha]_{\text{D}}^{23} = -27.4^\circ$ ($c = 0.35$, CHCl_3),

$R_f = 0.3$ (SiO_2 , PhMe/Acetone/MeOH = 5:1:0.1)

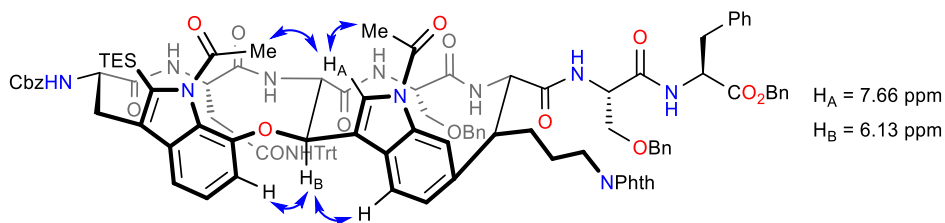
^1H NMR (600 MHz, $\text{DMSO}-d_6$) δ 8.57 (d, $J = 7.8$ Hz, 1H), 8.44 – 8.39 (m, 2H), 8.22 (s, 1H), 7.82 (d, $J = 7.6$ Hz, 0H), 7.81 – 7.76 (m, 4H), 7.66 (s, 1H), 7.48 (d, $J = 8.3$ Hz, 1H), 7.41 – 7.36 (m, 5H), 7.34 – 7.30 (m, 4H), 7.28 – 7.18 (m, 22H), 7.16 – 7.10 (m, 8H), 7.09 – 7.07 (m, 1H), 7.06 (d, $J = 7.5$ Hz, 1H), 7.03 (d, $J = 7.1$ Hz, 1H), 6.99 (d, $J = 8.0$ Hz, 1H), 6.95 – 6.92 (m, 2H), 6.13 (d, $J = 8.6$ Hz, 1H), 5.57 (d, $J = 5.6$ Hz, 1H), 5.10 – 5.04 (m, 3H), 4.99 (d, $J = 12.6$ Hz, 1H), 4.76 (t, $J = 9.3$ Hz, 1H), 4.60 (q, $J = 6.8$ Hz, 1H), 4.55 (q, $J = 7.3$ Hz, 1H), 4.38 (d, $J = 1.8$ Hz, 2H), 4.35 – 4.25 (m, 2H), 4.08 (s, 2H), 3.88 (q, $J = 8.2$ Hz, 1H), 3.55 – 3.48 (m, 4H), 3.15 – 3.09 (m, 2H), 3.04 – 3.01 (m, 2H), 2.95 (dd, $J = 10.0, 6.6$ Hz, 1H), 2.88 (dd, $J = 10.1, 6.8$ Hz, 1H), 2.77 (s, 3H), 2.73 (s, 3H), 2.03 – 1.98 (m, 1H), 1.91 – 1.85 (m, 1H), 1.80 – 1.71 (m, 1H), 1.57 (dd, $J = 20.2, 11.7$ Hz, 2H), 1.17 (m, 9H), 1.02 (m, 6H).

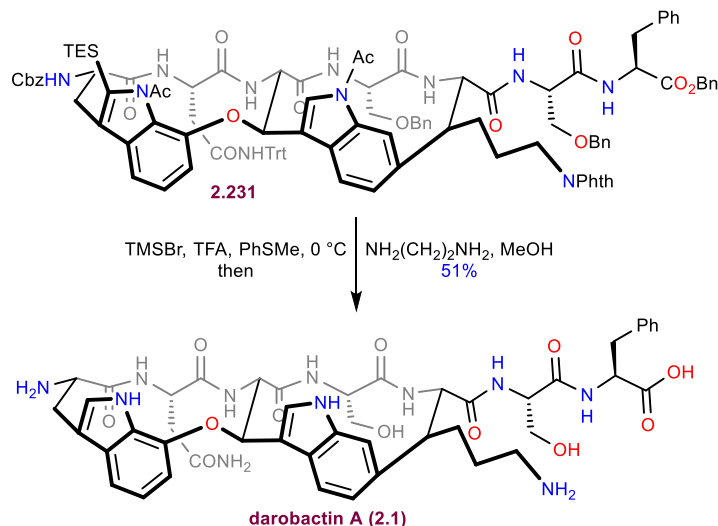
$^{13}\text{C}\{^1\text{H}\}$ NMR (151 MHz, DMSO) δ 173.0, 171.0, 170.03, 169.95, 169.3, 168.6, 168.5, 168.4, 168.0, 167.8, 166.7, 165.8, 155.35, 145.6, 145.0, 144.8, 138.0, 137.9, 137.7, 136.9, 136.7, 135.9, 135.6, 134.4, 134.2, 133.5, 133.3, 131.7, 131.6, 129.2, 129.1, 128.6, 128.4, 128.3, 128.1, 128.1, 128.03, 127.93, 127.9, 127.8, 127.53, 127.46, 127.37, 127.34, 127.2, 127.13, 127.09, 127.03, 126.95, 126.6, 126.2, 124.4, 123.0, 122.9, 122.6, 118.6, 117.5, 114.6, 112.4, 110.9, 79.2, 76.0, 72.0, 71.4, 70.4, 69.8, 69.6, 66.1, 65.6, 61.1, 59.6, 59.0, 53.6, 52.9, 51.1, 49.3, 48.8, 40.1, 38.6, 38.3, 37.5, 36.8, 28.6, 28.3, 27.0, 26.0, 23.9, 8.0.

HRMS: (ES+) m/z : $[\text{M}+2\text{H}]^{2+}$ calcd. for $(\text{C}_{113}\text{H}_{115}\text{N}_{11}\text{O}_{18}\text{Si})/2$, 970.9095; found 970.9082.

IR (ATR, neat, cm^{-1}) 3295 (br), 2931 (w), 2872 (w), 1714 (s), 1640 (s), 1496 (m), 1718 (s), 1224 (m), 698 (m).

Key NOE correlations in the bismacrocycle:





Darobactin (2.1):

To protected darobactin **2.231** (20 mg, 10 μmol , 1.0 equiv.) and thioanisole (61 μL , 0.52 mmol, 50 equiv.) were added TFA (1.0 mL) and TMSBr (68 μL , 0.52 mmol, 50 equiv.) dropwise in succession at 0 $^\circ\text{C}$. After stirring for 2 hours at this temperature, the mixture was concentrated under a stream of nitrogen. The obtained residue was concentrated three more times from PhMe (3 x 0.4 mL), then triturated with hexanes (3 x 0.4 mL). The crude was redissolved in MeOH (1.0 mL) and treated with ethylenediamine (69 μL , 1.0 mmol, 100 equiv.) at room temperature. After stirring for 2 hours, the mixture was concentrated under a stream of nitrogen. The crude mixture (20 mg scale) was taken up in 1.5 mL of 1:1 MeCN:H₂O + 3 drops of DMSO + 5 drops TFA to homogenize the resulting mixture, then purified by semi-preparative reverse-phase HPLC (Gilson GX-281 liquid handler w/ 333,334 pumps and UV/VIS-155 detector Gilson equipped with a Waters SunFire C₁₈ OBD Prep Column, 100 \AA , 5 μm , 30 mm X 150 mm). H₂O (A; +0.1 % TFA) and MeCN (B; +0.1% TFA) were used as the mobile phase with a gradient of 0-30% B over 17 minutes, holding at 26% for 3.5 minutes, 20 mL/min, $t_{\text{R}} = 14.45\text{-}15.13$ min) to afford **2.1**•TFA (5.5 mg, 5.1 μmol , 51%) as a fluffy white solid.

$[\alpha]_{\text{D}}^{23} = 7.20^\circ$ (c = 0.055, 0.1% aqueous formic acid),

¹H NMR (2.1•TFA), (800 MHz, H₂O/D₂O/Formic Acid-*d*₂ 94:4:2) δ 10.63 (d, $J = 2.6$ Hz, 1H), 10.44 (d, $J = 2.7$ Hz, 1H), 8.62 (d, $J = 7.3$ Hz, 1H), 8.32 (d, $J = 7.7$ Hz, 1H), 7.88 (d, $J = 10.6$ Hz, 1H), 7.86 – 7.81 (m, 2H), 7.50 (s, 2H), 7.47 (s, 1H), 7.46 – 7.40 (m, 3H), 7.39 – 7.30 (m, 5H), 7.23 (t, $J = 8.5$ Hz, 2H), 7.18 (t, $J = 7.7$ Hz, 1H), 6.95 (d, $J = 9.1$ Hz, 2H), 6.92 (d, $J = 8.1$ Hz, 1H), 6.65 (s, 1H), 6.18 (d, $J = 9.0$ Hz, 1H), 4.47 (d, $J = 6.8$ Hz, 1H), 4.25 (t, $J = 10.9$ Hz, 1H), 4.03 (dd, $J =$

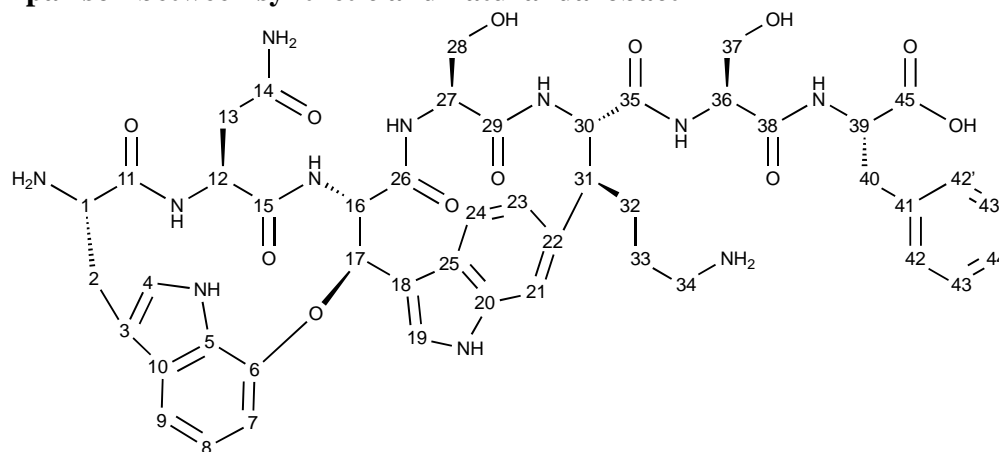
11.5, 7.7 Hz, 1H), 3.96 (q, $J = 7.5$ Hz, 1H), 3.80 (h, $J = 6.5$ Hz, 2H), 3.55 (dd, $J = 14.3, 7.6$ Hz, 1H), 3.35 – 3.27 (m, 2H), 3.23 (td, $J = 12.5, 6.2$ Hz, 2H), 3.18 – 3.09 (m, 2H), 3.01 (ddd, $J = 23.8, 12.2, 5.4$ Hz, 3H), 2.22 – 2.03 (m, 4H), 1.88 (tdd, $J = 16.5, 11.4, 6.9$ Hz, 1H), 1.74 (qdd, $J = 13.8, 9.9, 6.4$ Hz, 1H). *Note: due to water suppression in the ^1H NMR, signals corresponding to H-16 (4.68 ppm), H-36 (4.46 ppm), and H-39 (4.72 ppm) are hidden.*

$^{13}\text{C}\{^1\text{H}\}$ NMR (2.1•TFA), (200 MHz, $\text{H}_2\text{O}/\text{D}_2\text{O}/\text{Formic Acid-}d_2$ 94:4:2) δ 177.5, 176.6, 174.5, 173.7, 171.2, 171.1, 170.8, 170.7, 147.9, 139.9, 139.3, 135.7, 132.2, 131.8, 131.7, 131.5, 130.0, 127.8, 127.7, 127.6, 127.3, 122.9, 120.9, 116.4, 114.4, 113.3, 111.6, 110.9, 79.5, 66.1, 64.7, 64.0, 63.0, 58.4, 57.6, 57.2, 56.9, 53.6, 51.0, 42.4, 41.8, 39.5, 29.1, 28.42, 28.38.

HRMS: (ES+) m/z : $[\text{M}+\text{H}]^+$ calcd. for $\text{C}_{47}\text{H}_{56}\text{N}_{11}\text{O}_{12}$, 966.4104; found 966.4105.

Using the above protocol, synthetic darobactin A (2.1) was isolated as a TFA salt.

NMR comparison between synthetic and natural darobactin A



^1H NMR Comparison of TFA Salt (2.1•TFA) (Taken in $\text{H}_2\text{O}/\text{D}_2\text{O}/\text{Formic acid-}d_2$, 94:4:2)

#	Synthetic	Isolated ²	$\Delta^1\text{H}$
1	4.03	4.04	-0.01
1-NH ₂			
2'	3.55	3.55	0
2''	3.30	3.3	0
4	7.35	7.35	0
4-NH	10.63	10.63	0
7	7.24	7.24	0
8	7.18	7.18	0
9	7.23	7.22	0.01
11-NH	6.92	6.92	0

#	<i>Synthetic</i>	<i>Isolated²</i>	Δ^1H
12	3.32	3.33	-0.01
13'	2.17	2.19	-0.02
13''	2.12	2.13	-0.01
14-NH ₂ '	7.31	7.31	0
14-NH ₂ ''	6.65	6.64	0.01
15-NH	7.83	7.83	0
16	4.68	4.69	-0.01
17	6.18	6.18	0
19	7.85	7.85	0
20-NH	10.44	10.44	0
21	7.48	7.48	0
23	6.96	6.96	0
24	7.44	7.45	-0.01
26-NH	6.96	6.95	0.01
27	3.96	3.95	0.01
28'	3.22	3.22	0
28''	3.13	3.14	-0.01
29-NH	7.88	7.88	0
30	4.24	4.25	-0.01
31	3.02	3.03	-0.01
32	2.08	2.08	0
33'	1.88	1.88	0
33''	1.74	1.74	0
34	2.99	2.99	0
34-NH ₂	7.5	7.51	-0.01
35-NH	8.62	8.62	0
36	4.46	4.46	0
37	3.8	3.8	0
38-NH	8.32	8.14	0.18
39	4.72	4.64	0.08
40'	3.14	3.11	0.03
40''	3.24	3.22	0.02
42, 42'	7.32	7.32	0
43, 43'	7.42	7.42	0
44	7.37	7.37	0

$^{13}\text{C}\{^1\text{H}\}$ NMR Comparison of TFA salt (**2.1**•TFA) (Taken in $\text{H}_2\text{O}/\text{D}_2\text{O}/\text{Formic acid-}d_2$, 94:4:2)

#	Synthetic	Isolated ²	$\Delta^{13}\text{C}$
1	57.6	57.6	0.0
2'	29.1	29.2	-0.1
3	110.9	111	-0.1
4	127.5	127.6	-0.1
5	131.7	131.8	-0.1
6	148.0	147.9	0.1
7	111.6	111.6	0.0
8	122.9	123	-0.1
9	116.4	116.5	-0.1
10	131.8	131.8	0.0
11	171.1	171.1	0.0
12	53.6	53.7	-0.1
13'	41.8	41.9	-0.1
14	176.6	176.6	0.0
15	171.2	171.3	-0.1
16	66.1	66.1	0.0
17	79.5	79.5	0.0
18	114.4	114.5	-0.1
19	127.3	127.4	-0.1
20	139.9	139.9	0.0
21	113.3	113.3	0.0
22	135.7	135.7	0.0
23	127.7	127.7	0.0
24	120.0	120.0	0.0
25	127.8	127.8	0.0
26	170.7	170.7	0.0
27	56.9	56.9	0.0
28'	64.7	64.8	-0.1
29	170.8	170.9	-0.1
30	63.0	63	0.0
31	51.0	51	0.0
32	28.4	28.5	-0.1
33'	28.4	28.5	-0.1
34	42.4	42.4	0.0
35	174.5	174.6	-0.1
36	58.6	58.5	0.0

#	<i>Synthetic</i>	<i>Isolated²</i>	Δ^1H
37	64.0	64	0.0
38	173.8	173.5	0.3
39	57.2	57.9	-0.7
40'	39.5	39.8	-0.3
41	139.3	139.6	-0.3
42, 42'	132.2	132.3	-0.1
43, 43'	131.5	131.5	0.0
44	129.9	129.9	0.0
45	177.5	178.4	-0.9

2.9 References

1. Arnison, P. G.; Bibb, M. J.; Bierbaum, G.; Bowers, A. A.; Bugni, T. S.; Bulaj, G.; Camarero, J. A.; Campopiano, D. J.; Challis, G. L.; Clardy, J.; Cotter, P. D.; Craik, D. J.; Dawson, M.; Dittmann, E.; Donadio, S.; Dorrestein, P. C.; Entian, K.-D.; Fischbach, M. A.; Garavelli, J. S.; Göransson, U.; Gruber, C. W.; Haft, D. H.; Hemscheidt, T. K.; Hertweck, C.; Hill, C.; Horswill, A. R.; Jaspars, M.; Kelly, W. L.; Klinman, J. P.; Kuipers, O. P.; Link, A. J.; Liu, W.; Marahiel, M. A.; Mitchell, D. A.; Moll, G. N.; Moore, B. S.; Müller, R.; Nair, S. K.; Nes, I. F.; Norris, G. E.; Olivera, B. M.; Onaka, H.; Patchett, M. L.; Piel, J.; Reaney, M. J. T.; Rebuffat, S.; Ross, R. P.; Sahl, H.-G.; Schmidt, E. W.; Selsted, M. E.; Severinov, K.; Shen, B.; Sivonen, K.; Smith, L.; Stein, T.; Süßmuth, R. D.; Tagg, J. R.; Tang, G.-L.; Truman, A. W.; Vederas, J. C.; Walsh, C. T.; Walton, J. D.; Wenzel, S. C.; Willey, J. M.; van der Donk, W. A. *Nat. Prod. Rep.* **2013**, *30*, 108–160.
2. Montalbán-López, M.; Scott, T. A.; Ramesh, S.; Rahman, I. R.; van Heel, A. J.; Viel, J. H.; Bandarian, V.; Dittmann, E.; Genilloud, O.; Goto, Y.; Grande Burgos, M. J.; Hill, C.; Kim, S.; Koehnke, J.; Latham, J. A.; Link, A. J.; Martínez, B.; Nair, S. K.; Nicolet, Y.; Rebuffat, S.; Sahl, H.-G.; Sareen, D.; Schmidt, E. W.; Schmitt, L.; Severinov, K.; Süßmuth, R. D.; Truman, A. W.; Wang, H.; Weng, J.-K.; van Wezel, G. P.; Zhang, Q.; Zhong, J.; Piel, J.; Mitchell, D. A.; Kuipers, O. P.; van der Donk, W. *Nat. Prod. Rep.* **2021**, *38*, 130–239.
3. Zhong, G.; Wang, Z.-J.; Yan, F.; Zhang, Y.; Huo, L. *ACS Bio. & Med. Chem. Au* **2022**, <https://doi.org/10.1021/acsbiochemau.2c00062>.

4. Aslam, B.; Wang, W.; Arshad, M. I.; Khurshid, M.; Muzammil, S.; Rasool, M. H.; Nisar, M. A.; Alvi, R. F.; Aslam, M. A.; Qamar, M. U.; Salamat, M. K. F.; Baloch, Z. *Infect. Drug Resist.* **2018**, *11*, 1645–1658.
5. Tacconelli, E.; Carrara, E.; Savoldi, A.; Harbarth, S.; Mendelson, M.; Monnet, D. L.; Pulcini, C.; Kahlmeter, G.; Kluytmans, J.; Carmeli, Y.; Ouellette, M.; Outterson, K.; Patel, J.; Cavalieri, M.; Cox, E. M.; Houchens, C. R.; Grayson, M. L.; Hansen, P.; Singh, N.; Theuretzbacher, U.; Magrini, N.; Aboderin, A. O.; Al-Abri, S. S.; Awang Jalil, N.; Benzonana, N.; Bhattacharya, S.; Brink, A. J.; Burkert, F. R.; Cars, O.; Cornaglia, G.; Dyar, O. J.; Friedrich, A. W.; Gales, A. C.; Gandra, S.; Giske, C. G.; Goff, D. A.; Goossens, H.; Gottlieb, T.; Guzman Blanco, M.; Hryniewicz, W.; Kattula, D.; Jinks, T.; Kanj, S. S.; Kerr, L.; Kieny, M.-P.; Kim, Y. S.; Kozlov, R. S.; Labarca, J.; Laxminarayan, R.; Leder, K.; Leibovici, L.; Levy-Hara, G.; Littman, J.; Malhotra-Kumar, S.; Manchanda, V.; Moja, L.; Ndoye, B.; Pan, A.; Paterson, D. L.; Paul, M.; Qiu, H.; Ramon-Pardo, P.; Rodríguez-Baño, J.; Sanguinetti, M.; Sengupta, S.; Sharland, M.; Si-Mehand, M.; Silver, L. L.; Song, W.; Steinbakk, M.; Thomsen, J.; Thwaites, G. E.; van der Meer, J. W.; Van Kinh, N.; Vega, S.; Villegas, M. V.; Wechsler-Fördös, A.; Wertheim, H. F. L.; Wesangula, E.; Woodford, N.; Yilmaz, F. O.; Zorzet, A. *Lancet Infect. Dis.* **2018**, *18*, 318–327.
6. Coates, A. R. M.; Halls, G.; Hu, Y. B. *J. Pharmacol.* **2011**, *163*, 184–194.
7. Lewis, K. *Cell* **2020**, *181*, 29–45.
8. Imai, Y.; Meyer, K. J.; Iinishi, A.; Favre-Godal, Q.; Green, R.; Manuse, S.; Caboni, M.; Mori, M.; Niles, S.; Ghiglieri, M.; Honrao, C.; Ma, X.; Guo, J. J.; Makriyannis, A.; Linares-Otoya, L.; Böhringer, N.; Wuisan, Z. G.; Kaur, H.; Wu, R.; Mateus, A.; Typas, A.; Savitski, M. M.; Espinoza, J. L.; O'Rourke, A.; Nelson, K. E.; Hiller, S.; Noinaj, N.; Schäberle, T. F.; D'Onofrio, A.; Lewis, K. *Nature* **2019**, *576*, 459–464.
9. Schramma, K. R.; Bushin, L. B.; Seyedsayamdost, M. R. *Nature Chem.* **2015**, *7*, 431–437.
10. Kaur, H.; Jakob, R. P.; Marzinek, J. K.; Green, R.; Imai, Y.; Bolla, J. R.; Agustoni, E.; Robinson, C. V.; Bond, P. J.; Lewis, K.; Maier, T.; Hiller, S. *Nature* **2021**, *593*, 125–129.
11. Ritzmann, N.; Manioglu, S.; Hiller, S.; Muller, D. J. *Structure* **2022**, *30*, 350–359.
12. Balo Aidin R.; Caruso Alessio; Tao Lizhi; Tantillo Dean J.; Seyedsayamdost Mohammad R.; Britt R. David. *Proc. Natl. Acad. Sci.* **2021**, *118*, e2101571118.
13. Guo, S.; Wang, S.; Ma, S.; Deng, Z.; Ding, W.; Zhang, Q. *Nat. Commun.* **2022**, *13*, 2361.

14. Nguyen, H.; Made Kresna, I. D.; Böhringer, N.; Ruel, J.; Mora, E. de la; Kramer, J.-C.; Lewis, K.; Nicolet, Y.; Schäberle, T. F.; Yokoyama, K. *J. Am. Chem. Soc.* **2022**, *144*, 18875–18886.
15. Broderick, J. B.; Duffus, B. R.; Duschene, K. S.; Spehard, E. M. *Chem. Rev.* **2014**, *114*, 4229–4317.
16. Groß, S.; Panter, F.; Pogorevc, D.; Seyfert, C. E.; Deckarm, S.; Bader, C. D.; Herrmann, J.; Müller, R. *Chem. Sci.* **2021**, *12*, 11882–11893.
17. Böhringer, N.; Green, R.; Liu, Y.; Mettal, U.; Marnier M.; Modaresi, S.M.; Jakob, R.P.; Wuisan, Z.G.; Maier, T.; Iinishi, A.; Hiller, S.; Lewis, K.; Schäberle, T.F. *Microbiol. Spectr.* **2021**, *9*, e01535-21.
18. Seyfert, C. E.; Porten, C.; Yuan, B.; Deckarm, S.; Panter, F.; Bader, C. D.; Coetzee, J.; Deschner, F.; Tehrani, K. H. M. E.; Higgins, P. G.; Seifert, H.; Marlovits, T. C.; Herrmann, J.; Müller, R. *Angew. Chem. Int. Ed.* **2023**, *62*, e202214094.
<https://doi.org/10.1002/anie.202214094>.
19. Yudin, A. K.; Nenajdenko, V. G. *Chem. Rev.* **2019**, *119*, 10032–10240.
20. Swain, J. A.; Walker, S. R.; Calvert, M. B.; Brimble, M. A. *Nat. Prod. Rep.* **2022**, *39*, 410–443.
21. Laws III, D.; Plouch, E. V.; Blakey, S. B. *J. Nat. Prod.* **2022**, *85*, 2519–2539.
22. Leung, T.-W. C.; Williams, D. H.; Barna, J. C. J.; Foti, S.; Oelrichs, P. B. *Tetrahedron* **1986**, *42*, 3333–3348.
23. Bentley, D. J.; Slawin, A. M. Z.; Moody, C. J. *Org. Lett.* **2006**, *8*, 1975–1978.
24. Michaux, J.; Retailleau, P.; Campagne, J.-M. *Synlett* **2008**, *10*, 1532–1536.
25. Ma, B.; Litvinov, D. N.; He, L.; Banerjee, B.; Castle, S. L. *Angew. Chem., Int. Ed.* **2009**, *48*, 6104–6107.
26. Ma, B.; Banerjee, B.; Litvinov, D. N.; He, L.; Castle, S. L. *J. Am. Chem. Soc.* **2010**, *132*, 1159–1171.
27. Hu, W.; Zhang, F.; Xu, Z.; Liu, Q.; Cui, Y.; Jia, Y. *Org. Lett.* **2010**, *12*, 956–959.
28. Feng, Y.; Chen, G. *Angew. Chem., Int. Ed.* **2010**, *49*, 958–961.
29. Isley, N. A.; Endo, Y.; Wu, Z.-C.; Covington, B. C.; Bushin, L. B.; Seyedsayamdost, M. R.; Boger, D. L. *J. Am. Chem. Soc.* **2019**, *141*, 17361–17369.
30. Garfunkle, J.; Kimball, F. S.; Trzuppek, J. D.; Takizawa, S.; Shimamura, H.; Tomishima, M.; Boger, D. L. *J. Am. Chem. Soc.* **2009**, *131*, 16036–16038.

31. Shimamura, H.; Breazzano, S. P.; Garfinkle, J.; Kimball, F. S.; Boger, D. L. *J. Am. Chem. Soc.* **2010**, *132*, 7776–7783.
32. Breazzano, S. P.; Poudel, Y. M.; Boger, D. L. *J. Am. Chem. Soc.* **2013**, *135*, 1600–1606.
33. Wyche, T. P.; Ruzzini, A. C.; Schwab, L. *J. Am. Chem. Soc.* **2017**, *139*, 12899–12902.
34. Reisberg, S.; Gao, Y.; Helfrich, E. J. N.; Clardy, J.; Baran, P. S. *Science* **2020**, *367*, 458–463.
35. Subba Reddy, B. V.; Corey, E. J. *Org. Lett.* **2006**, *8*, 3391–3394.
36. Crich, D.; Banerjee, A. *J. Org. Chem.* **2006**, *71*, 7106–7109.
37. Loach, R. P.; Fenton, O. S.; Kazuma, A.; Siegel, D. S.; Ozkal, E.; Movassaghi, M. *J. Org. Chem.* **2014**, *79*, 11254–11263.
38. Chen, J.-Q.; Li, J.-H.; Dong, Z.-B. *Adv. Synth. Catal.* **2020**, *362*, 3311–3331.
39. Khatib, M. E.; Molander, G. A. *Org. Lett.* **2014**, *16*, 4944–4947.
40. Sambhiagio, C.; Marsden, S. P.; Blacker, A. J.; McGowan, P. C. *Chem. Soc. Rev.* **2014**, *43*, 3525–3550.
41. Cai, Q.; Zhou, W. *Chin. J. Chem.* **2020**, *38*, 879–893.
42. Chen, Z.; Jiang, Y.; Zhang, L.; Guo, Y.; Ma, D. *J. Am. Chem. Soc.* **2019**, *141*, 3541–3549.
43. Terret, J. A.; Cuthbertson, J. D.; Shurtleff, V. W.; MacMillan, D. W. C. *Nature* **2015**, *524*, 330–334.
44. Lee, H.; Boyer, N. C.; Deng, Q.; Kim, H.-Y.; Sawyer, T. K.; Sciammetta, N. *Chem. Sci.* **2019**, *10*, 5073–5079.
45. Teruaki, M.; Naoto, S.; Kazuhiro, I. *Chemistry Letters* **2006**, *35*, 1140–1141.
46. Ooi, T.; Goto, R.; Maruoka, K. *J. Am. Chem. Soc.* **2003**, *125*, 10494–10495.
47. Jurrat, M.; Maggi, L.; Lewis, W.; Ball, L. T. *Nature Chemistry*, **2020**, *12*, 260–269.
48. Swamy, K. C. K.; Kumar, N. N.; Balaraman, E.; Kumar, V. P. P. *Chem. Rev.* **2009**, *109*, 2551–2651.
49. Solladiè-Cavallo, A.; Simon, M. C. *Tetrahedron Letters*, **1989**, *30*, 6011–6014.
50. Solladiè-Cavallo, A.; Simon, M. C.; Schwarz, J. *Organometallics* **1993**, *12*, 3743–3747.
51. Coste, A.; Kim, J.; Adams, T. C.; Movassaghi, M. *Chem. Sci.* **2013**, *4*, 3191–3197.
52. The reaction was optimized by Merck collaborators, who have utilized this process for the synthesis of the alkyl–aryl ether between the two tryptophans of darobactin.
53. Robbins, D. W.; Boebel, T. A.; Hartwig, J. F. *J. Am. Chem. Soc.* **2010**, *132*, 4068–4069.

54. Feng, Y.; Holte, D.; Zoller, J.; Umemiya, S.; Simke, L. R.; Baran, P. S. *J. Am. Chem. Soc.* **2015**, *137*, 10160–10163.
55. Eastabrook, A. S.; Sperry, J. *Synthesis* **2017**, *49*, 4731–4737.
56. Wang, B.; Nack, W. A.; He, G.; Znang, S-Y.; Chen, G. *Chem. Sci.* **2014**, *5*, 3952–3957.
57. Chen, K.; Shi, B-F. *Angew. Chem. Int. Ed.* **2014**, *53*, 11950–11954.
58. Gong, W.; Zhang, G. Liu, T.; Giri, R.; Yu, J-Q. *J. Am. Chem. Soc.* **2014**, *136*, 16940–16946.
59. Wolff, M. E. *Chem. Rev.* **1963**, *63*, 55–64.
60. Thullen, S. M.; Treacy, S. M.; Rovis, T. *J. Am. Chem. Soc.* **2019**, *141*, 14062–14067.
61. Zhang, Z.; Stateman, L. M.; Nagib, D. A. *Chem. Sci.* **2019**, *10*, 1207–1211.
62. Wilson, I.; Jackson, R. F. W. *J. Chem. Soc. Perkin Trans. 1*, **2002**, 2845–2850.
63. Everson, D. A.; Jones, B. A.; Weix, D. J. *J. Am. Chem. Soc.* **2012**, *134*, 6146–6159.
64. Zhang, P.; Le, C.; MacMillan, D. W. C. *J. Am. Chem. Soc.* **2016**, *138*, 8084–8087.
65. Sakai, H. A.; Wei, L.; Le, C.; MacMillan, D. W. C. *J. Am. Chem. Soc.* **2020**, *142*, 11691–11697.
66. Faraggi, T. M.; Rouget-Virbel, C.; Rincon, J. A.; Barberis, M.; Mateos, C.; Garcia-Cerrada, S.; Agejas, J.; de Frutos O.; MacMillan, D. W. C. *Org. Process Res. Dev.* **2021**, *25*, 1966–1973.
67. Kim, J.; Movassaghi, M. *J. Am. Chem. Soc.* **2011**, *133*, 14940–14943.
68. Carlson, R. G.; Pierce, J. K. *J. Org. Chem.* **1971**, *36*, 2319–2324.
69. Smith, R. T.; Zhang, X.; Rincon, J. A.; Agejas, J.; Mateos, C.; Barberis, M.; Garcia-Cerrada, S.; de Frutos, O.; MacMillan, D. W. C. *J. Am. Chem. Soc.* **2018**, *140*, 17433–17438.
70. Gao, X.; Wu, Bo.; Huang, W.-X.; Chen, M.-W.; Zhou, Y.-G. *Angew. Chem. Int. Ed.* **2015**, *54*, 11956–11960.
71. Nicolaou, K. C.; Estrada, A. A.; Zak, M.; Lee, S. H.; Safina, B. S. *Angew. Chem. Int. Ed.* **2005**, *44*, 1378–1382.
72. Zhang, X.; King-Smith, E.; Renata, H. *Angew. Chem. Int. Ed.* **2018**, *57*, 5037–5041.
73. Yudin, A. K. *Chem. Sci.* **2015**, *6*, 30–49.
74. Jsselstijn, M. I.; Kaiser, J.; van Delft, F. L.; Schoemaker, H. E.; Rutjes, F. P. J. T. *Amino Acids* **2003**, *24*, 263–266.
75. Newhouse, T.; Lewis, C. A.; Baran, P. S. *J. Am. Chem. Soc.* **2009**, *131*, 6360–6361.

76. Hattori, Y.; Asano, T.; Kirihata, M.; Yamaguchi, Y.; Wakamiya, T. *Tetrahedron Letters* **2008**, *49*, 4977–4980.
77. Zhang, X.; van der Donk, W. A. *J. Am. Chem. Soc.* **2007**, *129*, 2212–2213.
78. Cong, X.; Hu, F.; Liu, K.-G.; Liao, Q.-J.; Yao, Z.-J. *J. Org. Chem.* **2005**, *70*, 4514–4516.
79. Zhao, M.; Li, J.; Mano, E.; Song, Z.; Tschäen, D. M.; Grabowski, E. J. J.; Reider, P. J. *J. Org. Chem.* **1999**, *64*, 2564–2566.
80. Wakimoto, T.; Asakawa, T.; Akahoshi, S.; Suzuki, T.; Nagai, K.; Kawagishi, H.; Kan, T. *Angew. Chem. Int. Ed.* **2011**, *50*, 1168–1170.
81. Chuang, K. V.; Kieffer, M. E.; Reisman, S. E. *Org. Lett.* **2016**, *18*, 4750–4753.
82. Schroder, N.; Wencel-Delord, J.; Glorius, F. *J. Am. Chem. Soc.* **2012**, *134*, 8298–8301.
83. Felix, A. M. *J. Org. Chem.* **1974**, *39*, 1427–1429.
84. Dobrounig, P.; Trobe, M.; Breinbauer, R. *Monatshefte Für Chem. - Chem. Mon.* **2017**, *148*, 3–35.
85. Chan, C.; Heid, R.; Zheng, S.; Guo, J.; Zhou, B.; Furuuchi, T.; Danishefsky, S. J. *J. Am. Chem. Soc.* **2005**, *127*, 4596–4598.
86. Coleman, R. S.; Carpenter, A. J. *J. Org. Chem.* **1993**, *58*, 4452–4461.
87. Burk, M. J.; Feaster, J. E.; Nugent, W. A.; Harlow, R. L. *J. Am. Chem. Soc.* **1993**, *115*, 10125–10138.
88. Burk, M. J.; Gross, M. F.; Martinez, J. P. *J. Am. Chem. Soc.* **1995**, *117*, 9375–9376.
89. Molinaro, C.; Scott, J. P.; Shevlin, M.; Wise, C.; Ménard, A.; Gibb, A.; Junker, E. M.; Lieberman, D. *J. Am. Chem. Soc.* **2015**, *137*, 999–1006.
90. Kraft, S.; Ryan, K.; Kargbo, R. B. *J. Am. Chem. Soc.* **2017**, *139*, 11630–11641.
91. Fujii, N.; Otaka, A.; Sugiyama, N.; Hatano, M.; Yajima, H. *Chem. Pharm. Bull.* **1987**, *35*, 3880–3883.
92. Soon after the disclosure of our synthesis, the Baran lab has published their synthesis: Lin, Y.-C.; Schneider, F.; Eberle, K. J.; Chiodi, D.; Nakamura, H.; Reisberg, S. H.; Chen, J.; Saito, M.; Baran, P. S. *J. Am. Chem. Soc.* **2022**, *144*, 14458–14462.
93. Miller, R. D.; Iinishi, A.; Modaresi, S. M.; Yoo, B.-K.; Curtis, T. D.; Lariviere, P. J.; Liang, L.; Son, S.; Nicolau, S.; Bargabos, R.; Morrissette, M.; Gates, M. F.; Pitt, N.; Jakob, R. P.; Rath, P.; Maier, T. Malyutin, A. G.; Kaiser, J. T.; Niles, S.; Karavas, B.; Ghiglieri, M.; Bowman, S. E. J.; Rees, D. C.; Hiller, S.; Lewis, K. *Nat. Microbiol.* **2022**, *7*, 1661–1672.

94. Okitsu, T.; Nakahigashi, H.; Sugihara, R.; Fukuda, I.; Tsuji, S.; In, Y.; Wada, A. *Chemistry – A European Journal* **2018**, *24*, 18638–18642.

2.10 Acknowledgements and Contributions

D. L. Olson and L. Zhu are acknowledged for NMR spectroscopic assistance. F. Sun is acknowledged for assistance with mass spectrometry. J. Ngai performed scale-up for **2.120** (Scheme 2.18). J. Maturano performed scale-ups for **2.171** (Scheme 2.27) and **2.214** (Scheme 2.32) and has explored the diastereoselectivity of the photoredox coupling (Figure 2.3 and Scheme 2.20). D. B. Ryffel has explored ether formation between the two tryptophans (Schemes 2.9-2.11), scaled-up and optimized the sequence for **2.122** (Scheme 2.17), scaled-up **2.143** (Scheme 2.21), **2.175** (Scheme 2.24), **2.165** (Scheme 2.27), **2.217** (Scheme 2.32), has performed final scale-ups for **2.225** (Scheme 2.34), has synthesized **2.237** (Scheme 2.37) and performed data analysis. Merck collaborators: D. Petrone, N. R. Patel, M. Shevlin, S. R. Pollack, D. R. Gauthier, P. Trigo-Mourino, L.-K. Zhang, D. Schultz, J. McCabe Dunn, L.-C. Campeau have: discovered and optimized the Mitsunobu reaction in Scheme 12; developed and scaled-up the hydrogenation route for making **2.185** (Scheme 2.33); helped in the purification and characterization of **2.145**, **atrop-2.224** and **2.1**; and explored alternative macrocyclization strategies that weren't shown here. The rest of the chemistry, including: synthesis planning, forward synthesis with initial scale-ups, optimizations, frontline exploration and data analysis were performed by M. Nestic.